CENTRE FOR MINERALS RESEARCH

# An investigation into the role of DTP as a co-collector in the flotation of a South African PGM ore

A thesis submitted to the University of Cape Town in fulfillment of the requirements for the degree of Master of Science in Engineering


By:

**Jacques Bezuidenhout**

B.Sc. Eng. (Materials), University of Cape Town




Feb 2011

# Declaration

I declare that this thesis, submitted for the degree of Master of Science in Engineering at the University of Cape Town, is my own work and has not been submitted prior to this for any degree at this university or any other institution. I know the meaning of plagiarism and declare that all the work in the document, save for that which is properly acknowledged, is my own.

Jacques Collin Bezuidenhout

# Acknowledgements

I would like to, firstly, thank my supervisors Dr. Kirsten Corin and Professor Cyril O'Connor for their outstanding supervision and invaluable general and technical assistance throughout my time at UCT. This thesis would not have been completed without their continued insight, patience and encouragement. Secondly, I would also like to thank Dr. Natalie Shackleton for her help with the ToF-SIMS experiments and Professor Peter Harris for his very useful insight and advice. Special thanks must also go to Malibongwe Manono for his help with bubble sizing experiments as well as the staff in the analytical laboratory who managed to do chemical assays on hundreds of samples from the batch flotation experiments. Finally, I would like to thank my wife Anja for her patience, love and motivation.



"*language is never innocent*"

Roland Barthes

# Synopsis

The primary aim of this study was to investigate, using a combination of batch flotation and ToF-SIMS experimental techniques, whether a collector-collector synergistic interaction between SIBX and diethyl DTP will result in significantly enhanced copper, nickel, platinum and/or palladium recoveries and grades in a PGM containing ore from South Africa. Synergism is defined as the effect of the interaction of the actions of two agents such that the result of the combined action is greater than a simple additive combination of the two agents acting separately (http://thinkexist.com/dictionary/meaning/synergy).

The ore used in this study comes from the Platreef section of the Bushveld Igneous Complex and contained approximately 0.2 % copper, 0.4 % nickel and 0.6 % sulphur. The sizing tests on the flotation feed revealed that approximately two-thirds of the copper, nickel and sulphur minerals were present in the minus 25 µm fraction. The copper was present as chalcopyrite in the ore whilst the nickel was present as pentlandite. The main gangue minerals present in the ore were the enstatites, feldspars and diopsides whilst the talc content of the ore was minimal. The mineralogy work (Chapman, 2010) showed that the PGMs were mostly present as tellurides and arsenides.

This investigation focused on the collectors SIBX and diethyl DTP, which were added simultaneously to the flotation pulp, at a total collector dosage 4.09E-04 mole/kg and in the mole ratio [76 % SIBX, 24 % diethyl DTP]. Further batch flotation tests were however completed whereby the effect of varying mole ratios, increasing or decreasing total collector dosage, the effect of sequence of addition of collectors as well as the effect of collector chain length on flotation performance was investigated. In addition, the particle size distribution of the various flotation streams from selected batch flotation tests was established. This was done in order to establish the effect of collector type on the mass recovery of different particle size fractions. Copper and nickel assaying of the different size fractions for each flotation stream then made it possible to complete a copper/nickel recovery as a function of particle size calculation. This was important because increased copper or nickel recovery may occur as a

consequence of increased fine and/or coarse particle recovery and therefore not due to a collector-collector interaction on the mineral surface, i.e. increased recovery may not necessarily mean collector-collector synergism has occurred. Finally, the effect of collector type, i.e. SIBX, diethyl DTP and their mixtures, on entrained gangue recovery was investigated using the procedure developed by Wiese (2009). The batch flotation experiments were completed at the natural pH of the ore and in the absence of activators such as copper sulphate. Furthermore, all the reagents were added to the flotation cell only, i.e. the effect of points of addition of reagents on flotation performance was not investigated.

With respect to the single collectors, the batch flotation tests showed that pure diethyl DTP is a good chalcopyrite collector but a poor pentlandite collector. Similarly, the platinum and palladium recoveries obtained with pure diethyl DTP, at a dosage of 4.09E-04 mole/kg, were significantly lower than that which was obtained with an equivalent molar dosage of pure SIBX. The pure diethyl DTP flotation results also showed that nickel recovery was directly proportional to water recovery. This suggests that diethyl DTP is unable to form the surface compounds necessary to create a hydrophobic pentlandite surface and that nickel recovery was attained through an entrainment mechanism. The batch flotation experiments however showed that nickel recovery increased from approximately 6 %, in the case of a collectorless test, to approximately 28 % when a dosage of 3.07E-04 mole/kg diethyl DTP was used. The nickel recovery in fact increased further to approximately 46 % when the diethyl DTP dosage was increased from 3.07E-04 mole/kg to 4.09E-04 mole/kg. A nickel recovery as a function of particle size investigation revealed however that the increased recovery obtained with increasing diethyl DTP collector dosage occurred because of increased fines recovery. The nickel recovery in the coarser size fractions was however not significantly different to that which was obtained with the frother only test. This demonstrates that the increased nickel recovery obtained at higher diethyl DTP dosages was not achieved through a true flotation effect because true flotation extends to all particle sizes. In contrast to diethyl DTP, the longer chain collector, di-iso-butyl DTP, was able to achieve a significantly higher nickel recovery. This was an interesting find which suggested that the effect of chain length on flotation performance is appreciably more complicated in the case of DTP compared to xanthates.

With respect to the xanthates, the work completed with pure SIBX and pure SEX showed that the xanthates are, compared to diethyl DTP at least, good chalcopyrite and pentlandite collectors. Furthermore, the copper and nickel recovery as a function of particle size investigations revealed that the recovery in the case of SIBX was significantly higher in all size fractions compared to that which was obtained with pure frother. It was concluded therefore that the xanthates are able to recover the valuable sulphides by a true flotation mechanism. It is interesting to note also that the work with pure SIBX suggested that high dosages of collector may actually reduce the floatability of the valuable minerals.

The batch flotation results presented in this thesis showed that classical collector-collector synergism did not occur for copper, nickel or platinum when mixtures of collectors, viz. SIBX and diethyl DTP, were used in the study of the ore used in this investigation, i.e. the copper, nickel or platinum recoveries obtained with collector mixtures were not significantly different to that which was obtained with pure SIBX. In addition, the batch flotation experiments done using collectors of equivalent chain lengths also showed that the apparent lack of collector-collector synergism in the case of SIBX and diethyl DTP collector mixtures cannot be attributed to a dominant or even overpowering effect of the more powerful xanthate collector (SIBX). Similarly, batch flotation tests done using various molar ratios of SIBX and diethyl DTP as well as different sequences of collector addition showed that the lack of collector-collector synergism cannot be attributed to the particular mole ratio of SIBX and diethyl DTP, viz. [76 % SIBX, 24 % diethyl DTP], used in this study or the effect of sequence of collector addition. It is concluded therefore that the use of mixtures of diethyl DTP and SIBX, added in different molar mixtures as well as in different sequences, did not result in significantly enhanced copper, nickel or platinum recovery.

In contrast to the base metal sulphides and platinum recoveries, palladium recovery was significantly increased when mixtures of SIBX and diethyl DTP were added simultaneously compared to that which was obtained with the single collectors. Palladium recovery was however not enhanced when the collectors were added sequentially. Significantly, the enhanced recovery obtained with simultaneous addition of collectors was also accompanied by a significant increase in concentrate grade. This

suggests that collector-collector synergism may have occurred in the case of palladium. The recovery by particle size work has however also shown that the use of diethyl DTP resulted in a significant increase in the recovery of the finely (<25 μm) and ultra-finely (< 10 μm) sized particles. It is thus plausible that the increase in palladium flotation performance attained with the mixture of collectors may have occurred as a consequence of the ability of the froth phase to selectively recover finely sized and liberated palladium particles. This needs to be investigated further using a microflotation device and synthetic palladium-containing minerals.

With regard to gangue recovery, the use of [SIBX + diethyl DTP] mixtures, compared to pure SIBX, resulted in increased recovery of gangue via entrainment. The increased gangue recovery was accompanied by an increase in water recovery. Furthermore, an analysis of the particle size distributions of the feed, concentrate and tailings samples showed that the use of diethyl DTP resulted in a significant increase in recovery of the finely sized particles (< 25 μm).

It is concluded therefore that the role of diethyl DTP in a [SIBX + diethyl DTP] collector mixture in the case of flotation of this PGM containing ore is to:

i. Significantly enhance froth stability which is deteriorated considerably by the presence of highly hydrophobic chalcopyrite particles when the optimum SIBX dosage, viz. 3.07E-04 mole/kg, is used. Similarly, the ore contains a fair amount of serpentine minerals which are known to cause sticky, immobile and highly unstable froths. In the case of diethyl DTP, increased froth stability may have occurred through a frother-collector interaction mechanism.
ii. Increase the mass recovery of especially finely and ultra-finely sized particles. This is a significant result because it showed that the use of DTP may result in increased recovery of finely sized PGM minerals which are not responsive to SIBX or any other collector.

# Nomenclature

| | |
|---|---|
| α | the dosage, in g/t, of guar used in a particular test |
| $e_g$ | entrainability factor |
| EG | entrained gangue |
| FG | floating gangue |
| $H$ | froth height |
| $H_f$ | final froth height |
| $H_i$ | initial froth height |
| $k$ | first order rate constant |
| $R$ | cumulative recovery |
| $R_{max}$ | maximum theoretical recovery |
| $R_f$ | froth recovery |
| $R_g$ | gangue recovery |
| $R_w$ | water recovery |
| SM | sulphide mass |
| $t$ | time |
| TG | total gangue |

# Abbreviations

| | |
|---|---|
| BMS | base metal sulphides |
| Cu | copper |
| di-E-DTP | diethyl dithiophosphate |
| di-iso-B-DTP | di-iso-butyl dithiophosphate |
| DTP | dithiophosphate class of collectors |
| DTC | dithiocarbamate class of collectors |
| g/mol | grams per mole |
| g/t | grams per tonne |
| Hz | Hertz |
| LED | light emitting device |
| l/min | litres per min |
| KCl | potassium chloride |
| kg | kilogram |
| MIBC | methyl isobutyl carbinol |
| ml | millilitre |
| mm | millimetre |
| MS | metal sulphide |
| $MX_2$ | metal xanthate |
| Ni | nickel |
| PAX | potassium amyl xantahte |
| Pd | palladium |
| Pd-Bi-Te | palladium bismuth telluride |

| | |
|---|---|
| $Pd_2As$ | palladoarsenide |
| PEX | potassium ethyl xanthate |
| PGE | platinum group element |
| PGM | platinum group mineral |
| ppm | parts per million |
| Pt | platinum |
| $PtAs_2$ | sperrylite |
| rpm | revolutions per minute |
| S | sulphur |
| SEX | sodium ethyl xanthate |
| SIBX | sodium iso-butyl xantahte |
| SIPX | sodium iso-propyl xanthate |
| TDS | total dissolved solids |
| ToF-SIMS | time of flight secondary ion mass spectroscopy |
| UV | ultraviolet |
| wt | weight |
| w/v | weight over volume |
| $X^-$ | xanthate ion |
| $X_2$ | dixanthogen |
| XRF | x-ray fluorescence (analysis technique) |
| µm | micron |

Table of Contents

# List of Figures

# List of Tables

# Chapter 1: Introduction

## 1.1 Background

The Bushveld Complex in South Africa is the world's largest deposit of platinum group elements (PGE) and hosts approximately 75 % of the world's resources of platinum, 54 % of the world's resources of palladium and 82 % of the world's resources of Rhodium (Naldrett et al., 2008). It is divided into the following three main zones: the UG2 chromitite, the Merensky reef and the Platreef (Vermaak, 2005). As can be seen from Figure 1.1, the Bushveld Complex is massive and covers approximately 66 000 km$^2$ in surface area. The outcrops are approximately 450 km east-west and 300 km north-south apart (Newell, 2008).



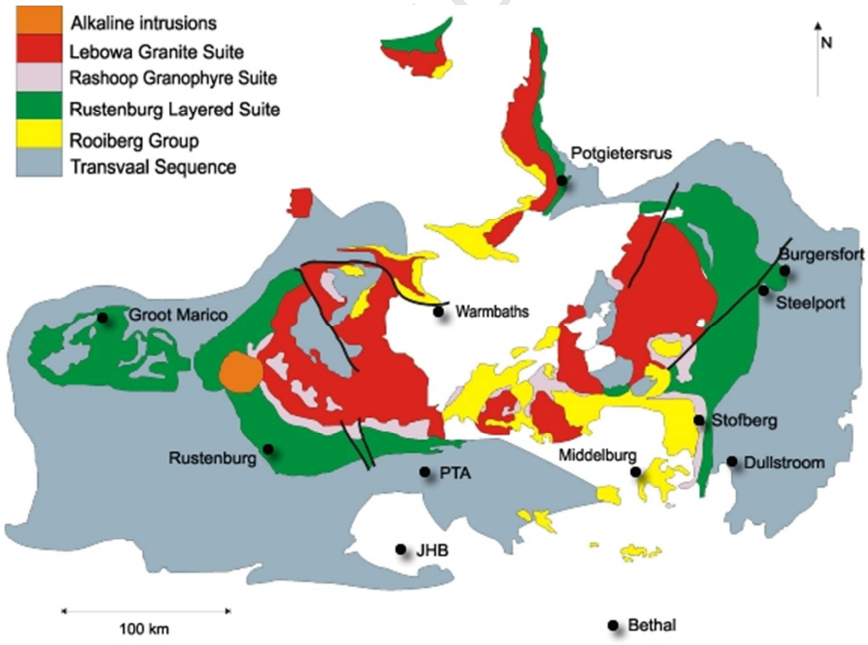


**Figure 1.1: The Bushveld Igneous Complex (University of Witwatersrand, School of Geosciences, 2009)**

The Merensky deposit, which was discovered by Dr. Hans Merensky in 1924, was the first section of the greater Bushveld Complex which was mined. Commercial exploitation of the reef was possible because the PGMs were hosted by relatively coarse-grained base metal sulphide minerals which allowed the valuable minerals to be separated from gangue by using the readily available conventional sulphide flotation process (Vermaak, 2005). Today there are at least twelve operating mines on the Merensky Reef which, collectively, produce over 127 tonnes of platinum each year. In contrast to Merensky ores, the UG2 ores were first processed in the 1980s (Newell, 2008).

Platreef was declared an economically viable ore deposit in the early 1990s (Merkle and Harney, 1990). This was attributed to, amongst many reasons, the fact that deep level mining on the eastern limb has become particularly problematic because of the inadequate thickness of the reef which results in massive head grade dilution [(Vermaak, 2005); (Newell, 2008)], whilst, on the other hand, Platreef could be accessed by the conventional open pit mining method. Holwell and McDonald (2007) conducted a full mineralogical analysis of two Platreef ore drill core samples and concluded that a good proportion of the PGMs are physically associated with the BMS. It has however also been established that significant volumes of minerals such as [Pt, Pd]-bismuthotellurides and PGE sulpharsenides, which are mostly enclosed in siliceous gangue, are present [(Vermaak, 2005), (Holwell et al., 2006a) and (Newell, 2008)]. Non-sulphide gangue minerals consist mainly of pyroxene, feldspar, serpentine and chlorites with minor quantities of talc and mica.



The Pt and Pd tellurides, provided they are not too finely grained (< 5 micron), respond well to flotation once they are liberated from their silicate host (Vermaak, 2005). Therefore, as is the case with Merensky and UG2 ores, the flotation process is used to separate the valuable sulphide and PGM minerals from the siliceous gangue for Platreef. Shackleton (2003) reported that the typical process flow sheet usually involves two- or even three-stage milling units, each followed by a flotation unit as shown in Figure 1.2. The flotation circuit reagent strategy in South Africa was to use a single collector, usually SIBX, in order to render the BMS and PGMs hydrophobic. This operating philosophy changed when, in the early 1970s, sodium di-iso-butyl DTP was added as a co-collector. The reason for adding the co-collector to the existing reagent suite was reported to be for purely economic reasons as it was expected that the addition of the second collector would lead to a direct decrease in frother

consumption because the di-iso-butyl DTP collector exhibited frothing properties (Lotter and Bradshaw, 2009); (Lotter, 2010). However, a significant increase in metallurgical performance, with respect to PGE recovery, was reported post-introduction of the secondary collector (Lotter and Bradshaw, 2009) and the use of DTPs as co-collectors consequently became a standard in the reagent suites for many PGM concentrators in South Africa. Furthermore, Mingione (1984) investigated the effect of various mixtures of the collectors di-iso-butyl DTP and SIPX on an ore that contained PGMs and reported that the optimum PGM recovery was obtained with an approximately 70 % di-iso-butyl DTP/30 % SIPX. The author attributed the increase in PGM recovery obtained with the collector mixture over that which was obtained with either pure SIPX or pure di-iso-butyl DTP to a classical collector-collector synergistic interaction. Despite much anecdotal information however the role of the collector in PGM flotation is still unclear and controversial. The aim of this investigation therefore is to attempt to examine and clarify the role of DTP collectors in PGM froth flotation applications.

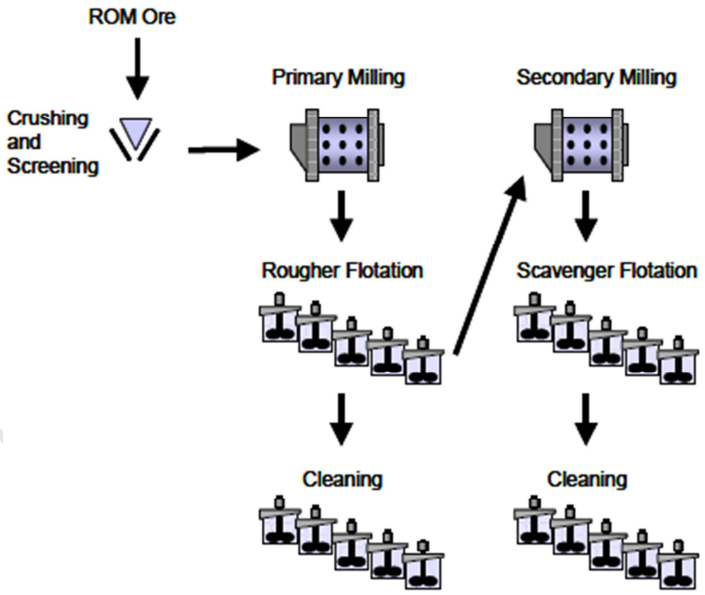


**Figure 1.2: A typical concentrator flow sheet (Shackleton, 2003)**

## 1.2 Research Objectives

The objectives of this thesis are to:

1. Ascertain whether collector synergism as shown by copper, nickel, PGE recoveries and grades is observed when mixtures of SIBX and diethyl DTP are used in the flotation of a PGM ore.
2. Ascertain whether the synergistic effects, if they are observed, occur as a result of froth phase effects or pulp phase effects.
3. Establish whether metallurgical performance, as indicated by metal recoveries and grades, is influenced by the sequence of collector addition.
4. Establish, using the procedure developed by (Wiese, 2009) whereby the total gangue recovered can be separated into entrained gangue and floating gangue, whether the use of DTP as a co-collector results in an increase in entrained gangue recovery.
5. Establish whether the use of DTP results in the selective flotation of coarse and/or fine particles.
6. Establish whether DTP enhances flotation rate kinetics.
7. Investigate the frothability of DTP in a two-phase froth column and compare with three-phase batch flotation test results to:
    a. Establish whether DTP enhances froth stability in the absence of solids and compare the performance to typical flotation frothers
    b. Establish whether DTP enhances froth stability in the presence of solids as is indicated by water recovery in batch flotation test results
8. Establish, using an appropriate surface analytical technique, whether DTP co-adsorbs with xanthate onto sulphide mineral surfaces.

## 1.3 Project Scope

This thesis primarily investigates whether mixtures of collectors result in a synergistic improvement in metal recoveries and grades by conducting batch flotation tests on a Platreef ore sample. The batch flotation tests were supported by frothability work using a two phase froth column, a froth camera and

ToF-SIMS tests. The purpose of doing a number of tests in addition to the batch flotation tests was to separate the froth phase effects from the pulp phase effects and to determine the relative adsorption of xanthate and DTP molecules onto the surface of the BMS minerals when both the collectors are added to the flotation pulp compared to when the collectors are added individually. The reagents used in this investigation were limited to collectors and frothers, i.e. no activators and/or pH modifiers were used in this study; a high molecular weight guar was however used in some tests in order to quantify gangue recovery via entrainment. The collectors used in the batch flotation tests were butyl xanthate (SIBX), ethyl xanthate (SEX), diethyl DTP (di-E-DTP) and di-iso-butyl DTP (di-iso-B-DTP) whilst the frother used was Dowfroth 200 (D200). The collectors SEX and di-iso-butyl DTP were used in order to investigate the effect of chain length on performance, i.e. combinations of butyl xanthate plus butyl DTP and ethyl xanthate plus diethyl DTP. The reagents were in all cases added to the flotation cell, i.e. the effect of changing the reagent addition point was not investigated. A number of tests were however conducted in order to investigate the effect of sequence of addition of the collectors SIBX and diethyl DTP on metal recoveries and grades.



The scope of this thesis therefore is:

1. To evaluate the effect of combinations of collectors on flotation performance in a PGM ore. The performance measurement to be used is metal recovery and concentrate grade which is obtained by conducting batch flotation tests.
2. To relate performance obtained in (1) to pulp phase effects by establishing if DTP co-adsorbs with SIBX onto the valuable particle surfaces and thus modifies collector surface adsorption characteristics.
3. To relate performance obtained in (1) to froth phase effects by quantifying entrainment with and without DTP as well as by using a froth camera to gain insight into the behaviour of the froth phase
4. To evaluate and determine the frothability of DTP in a two-phase system and relate this to (2) and (3).
5. To establish whether there is a direct relationship between particle size recovery and collector reagent suite.

6. To gain insight into the importance of DTP as a froth modifier and to thus establish whether its interaction with the frother is as significant, or perhaps more so, than its interaction with the collector.

## 1.4 Overview of Layout

Chapter 1 provides the background to the project and begins with a brief historical overview of PGM flotation in the South African context. In this chapter, it is explained how and why the South African PGM flotation practice has changed from a single collector to multiple collector reagent suites and why this practice has generated debate in the industry in recent times. The chapter then continues to list the aims and objectives of this work and ends with a summary of the scope of work. Chapter 2 provides the literature reviewed for the work presented in this thesis which begins with an overview of the general geology and mineralogy of the ore used in this study and is followed by discussing, in detail, the important parameters in froth flotation. Next the structures of two- and three-phase froths are discussed which are then related to froth stability. Finally, the chapter ends with a detailed review of collectors used in PGM flotation. Chapter 3 discusses the numerous experimental procedures used in this work. It begins by detailing sample preparation, ore characterisation and batch flotation techniques. The batch flotation technique, which is the primary experimental technique employed in this investigation, is discussed with respect to both the experimental method and is followed by the procedures used to analyse the data. The batch flotation procedure was complimented by a number of other experimental procedures and these are all listed and discussed in this chapter. In Chapter 4 the results obtained from the experimental test work are presented and discussed in the next chapter. In Chapter 6 the concluding remarks are given which is followed by a list of recommended future work. This thesis concludes with a full list of references.

# Chapter 2: Literature Review

## 2.1 General Geology & Mineralogy of Platreef Ore

In 1924 Dr. Hans Merensky discovered what is today called the Merensky reef. Upon realising the enormity of his discovery he began to trace the outcrop and in 1925 he discovered a new PGE orebody near the town of Potgietersrus, which is known as Mokopane today, and called it "Platreef" (Cawthorn, 1999). The area was systematically explored until 1930 after which all exploration activities were abruptly stopped because metal prices slumped dramatically following the onset of the Great Depression in 1929 (Holwell et al., 2005). More than 60 years then passed before mining activity recommenced in this part of the Bushveld Complex. Anglo Platinum currently operates two mines in the area: Sandsloot, which opened in 1992 and Zwartfontein South pit, which was opened in 2002. The success at these two mines has led to a huge spike in exploration activity since the year 2000 and, currently, the Platreef resource is the most extensively explored PGE resource in the world [(Holwell and McDonald, 2006b), (Holwell et al., 2005)].



### 2.1.1 General Geology

Platreef, the main PGE-bearing lithology of the northern limb of the Bushveld Complex, "*occurs where the intrusion overlies quartzites, shales, ironstones, dolomites and granites*" (Maier, 2005). The reef comprises "*a complex series of medium to coarse grained pyroxenites and norites that contain xenoliths of the floor rocks*" [(Manyeruke et al., 2005) after (Gain and Mostert, 1982)]. Unlike the deposits in the western and eastern limbs, the Platreef rests directly on country rock sediments and Archaean basement (Holwell and McDonald, 2010). The Platreef is classed as a highly inhomogeneous orebody and contains many different types of rock, including pyroxenites, para-pyroxenites, feldsphatic pyroxenites, serpentines, gabbronorites and norites. Mineralisation, with respect to copper, nickel and PGE, is irregular but it has a greater modal percentage of sulphides compared to the Merensky reef

(Sharman-Harris et al., 2005). The highest grades of [platinum + palladium + gold] are found at Sandsloot mine where the Platreef overlies dolomite (Maier, 2005).

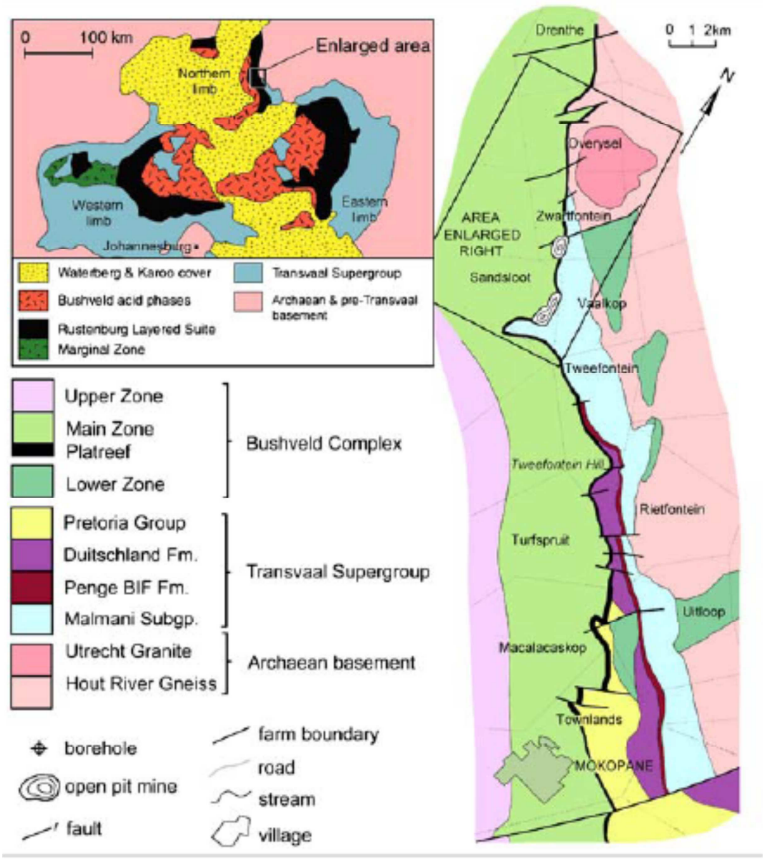


**Figure 2.1: A geological map of the Platreef (Holwell et al., 2006a)**

### 2.1.2 Platreef Mineralogy

Mineralogical investigations of the PGM minerals in ore samples taken from various parts of the Platreef ore body have recently been conducted by Armitage et al. (2002), Holwell et al. (2006) and Holwell and McDonald, (2007). Armitage et al. (2002) and Holwell et al. (2006) used drill core ore samples from Sandsloot whilst Holwell and McDonald (2007) used drill core ore samples from Overysel for their

investigations. The work completed by Holwell and McDonald (2007) on Overysel drill core samples concluded that: (i) PGE content is directly proportional to BMS content, (ii) pyrrhotite is the major carrier of osmium, iridium and ruthenium and these are present as solid-solution in the pyrrhotite, (iii) there are no appreciable amounts of palladium in pyrrhotite, (iv) pentlandite also contains significant concentrations of osmium, iridium and ruthenium but the levels are appreciably lower compared to pyrrhotite, (v) pentlandite, however, is the major carrier of rhodium and palladium, (vi) no PGEs are present in chalcopyrite although some platinum was detected in the chalcopyrite grains, and (vii) platinum appears to be present as submicron PGM inclusions. Interestingly Holwell and McDonald (2006b) also stated that the direct relationship between BMS content and PGE content at Overysel is somewhat unusual for Platreef as many other researchers have found little or no correlation between sulphur grades and PGM grades for other areas north and south of Overysel whilst Kinloch (1982) reports that only 31 %, by volume, of the platinoid minerals are associated with the BMS. The remaining platinoid minerals, which are mostly tellurides and arsenides, are in fact, according to Kinloch (1982), associated with the silicate gangue. Shamaila and O'Connor (2008) compared, as shown in Table 2.1, the bulk mineralogy and PGM distribution of the three main zones of the Bushveld Complex.



**Table 2.1: A summary of the bulk mineralogy and PGM distribution of the Platreef, Merensky and UG2 reefs of the Bushveld Igneous Complex (Shamaila and O'Connor, 2008)**

| | Platreef | Merensky | UG2 |
|---|---|---|---|
| **Bulk Mineralogy** | Pyroxene | Pyroxene | Chromite |
| | Serpentine | Feldspar | Pyroxene |
| | Calc silicates | Base metal sulphides | Feldspar |
| | Base metal sulphides | | Base metal sulphides |
| **PGM Distribution** | Tellurides ≈ 30 % | Tellurides ≈ 30 % | Tellurides < 5 % |
| | Arsenides ≈ 21 % | Arsenides ≈ 7 % | Arsenides ≈ 5 % |
| | Alloys ≈ 26 % | Alloys ≈ 7 % | Alloys ≈ 20 % |
| | Sulphides ≈ 3 % | Sulphides ≈ 36 % | Sulphides ≈ 70 % |
| | Rest ≈ 20 % | Rest ≈ 20 % | Rest ≈ 5 % |

Finally, it is important to note that the mineralogical work highlighted above was completed using geological samples and not flotation feed samples. Therefore, whilst it is generally assumed that the trends observed in geological samples extend to flotation feed samples, i.e. PGMs are physically associated with BMS, this may not be always true. Vermaak (2005) claimed that up to 50 % of PGMs may be completely liberated from their BMS hosts after milling for a typical Bushveld Complex ore. Thus it is critical that PGE assays on all relevant flotation streams be completed when batch flotation tests are conducted whose aim is to optimise reagent suites in order to enhance PGE recovery.

## 2.2 Principles of Flotation

### 2.2.1 Introduction and Process Description



Froth flotation, probably the most important processing technique in the minerals beneficiation industry today because it has permitted economic mining and treatment of low grade and complex orebodies, is a physico-chemical process that utilises differences in surface properties to separate those minerals considered valuable from those considered waste (Wills and Napier-Munn, 2006). Its greatest advantage is that it is a selective process and therefore is able to separate, for example, lead minerals from zinc minerals when treating a complex lead-zinc ore body. This would be very difficult, if not impossible, to achieve in the processes which preceded froth flotation, such as gravity separation for example, because of the fine particle sizes needed to achieve liberation today. It is estimated that close to two billion tonnes of ore are treated by froth flotation annually (Pearse, 2005).

The process, as shown in Figure 2.2, usually takes place in a rectangular or cylindrically shaped tank. The tank is fitted with a pulp stirrer for agitation and a gas or air bubble dispersion device. During normal operation air bubbles are passed through the slurry from the bottom up and are distributed equally around the cell. This results in a number of collisions between air bubbles and solid particles. Those particles that have previously been rendered hydrophobic, which is achieved by the addition of suitable chemicals called collectors, may attach to the air bubble once collision has occurred. If attachment is successful, the bubble-particle aggregate will rise to the surface of the pulp. Particle-bubble collision

and attachment takes place in what is referred to as the pulp zone. The second zone, called the froth zone, rests above the pulp zone. The function of the froth zone is to suspend the hydrophobic particles and to allow the hydrophilic particles which have reported to the froth zone by mechanisms other than true flotation time to drop back into the pulp zone. The froth phase, rich in valuable minerals, is removed from the cell by either a scraping mechanism or the froth migrates by itself over the weir (Wills and Napier-Munn, 2006).

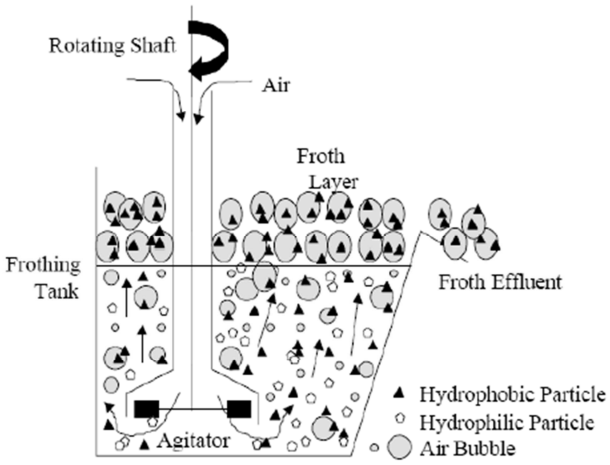


**Figure 2.2: Schematic representation of a flotation machine**



### 2.2.2 The Sub-Processes of Flotation

The overall flotation process can be divided into various consecutive sub processes which all contribute to the success of the separation of the valuable mineral from the gangue. They can be summarised as follows (Sweet, 1999):

i. The valuable mineral's surface is rendered hydrophobic by the collector(s).
ii. Air is introduced into the flotation cell causing a swarm of air bubbles to rise.

iii. As the bubbles rise up through the pulp phase, they collide with solid particles. If collision occurs with a hydrophobic particle, the particle will attach to the bubble (true flotation). The particle may also detach from the bubble.

iv. The loaded bubble is transported to the pulp-froth interface.

v. Hydrophobic particles are suspended in the froth zone. Particles which have reported to the froth zone by mechanisms other than true flotation may report back to the pulp zone.

vi. The transport and collection of the loaded bubble in the froth phase.

Each of these sub-processes may again be subdivided into micro-processes and in each a number of separate effects take place. Ahmed and Jameson (1989) report that points (iii) and (iv) are strongly influenced by the flotation rate constant.



### 2.2.3 Flotation as a Rate Process

The fundamental premise is that the flotation process can be described as a first order rate process which leads to a kinetic equation of the following form (Agar, 1985):

$$R = R_{max}[1 - exp^{-kt}] \ldots (2.1)$$

where $R$ = cumulative recovery after time $t$, $R_{max}$ = maximum theoretical flotation recovery, $k$ = flotation rate constant and $t$ = cumulative flotation time.

Klimpel (1984) proposed that the flotation process can be divided into a rate controlled regime and an ultimate recovery regime using the following equation:

$$R = R_{max}[1 - \{1/(kt)\}(1 - exp^{-kt})] \ldots (2.2)$$

## 2.3 Important Parameters in Flotation

Froth flotation plants are extremely difficult to optimise since the process, as shown in Figure 2.3, is highly interactive (Klimpel et al., 1994). Crozier (1992), in fact, listed over 25 parameters which, independently and in combination with other parameters, can influence flotation performance. Klimpel (1984) divided the main parameters into the following three major components: (i) equipment/hydrodynamic components, (ii) operational components and (iii) chemistry components. These parameters are (i) of equal importance and (ii) are interactive. Thus, for the flotation researcher especially, isolating a particular parameter in order to study its effect on flotation performance requires careful experimental design and data analysis (Bradshaw, 1997).



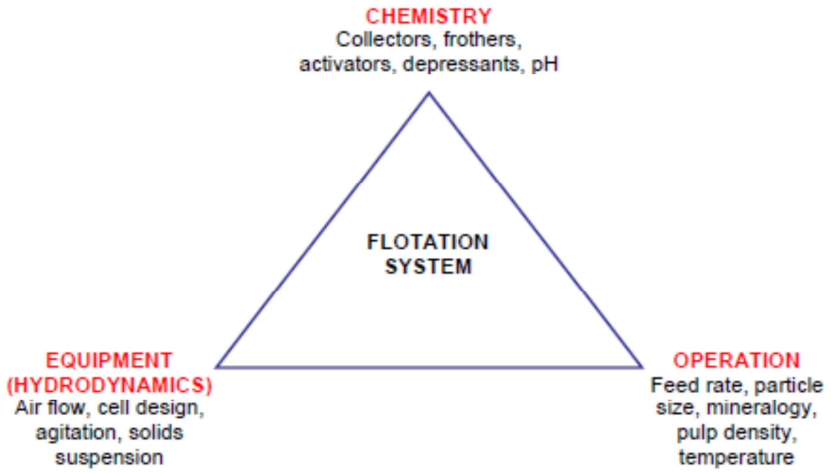


**Figure 2.3: Summary of the variables in froth flotation (Klimpel, 1984)**

### 2.3.1 Equipment Parameters

The role of hydrodynamics in froth flotation is to create and control the conditions which govern particle-bubble interaction and thus flotation performance (Finch et al., 2000). In practice cell hydrodynamics are determined by parameters such as impeller tip velocity, air inflow velocity, volume

flow rate as well as frother type and concentration (Newell and Grano, 2007). The role of hydrodynamics on froth flotation is however not the focus of this study and therefore no further details are included here.

### 2.3.2 Operational Parameters

Klimpel (1984) included factors such as ore mineralogy, particle size, circuit design, pulp density and ore throughput under the heading "operational parameters". The role of particle size in froth flotation is very complex. The traditional view is that there is a size range in which mineral recovery is optimum and recovery falls off rapidly below and above this size range (Jowett, 1979); (Trahar, 1981). This behaviour, shown graphically by Figure 2.4, is generally attributed to differences in collision, attachment and detachment efficiencies between particles and air bubbles.



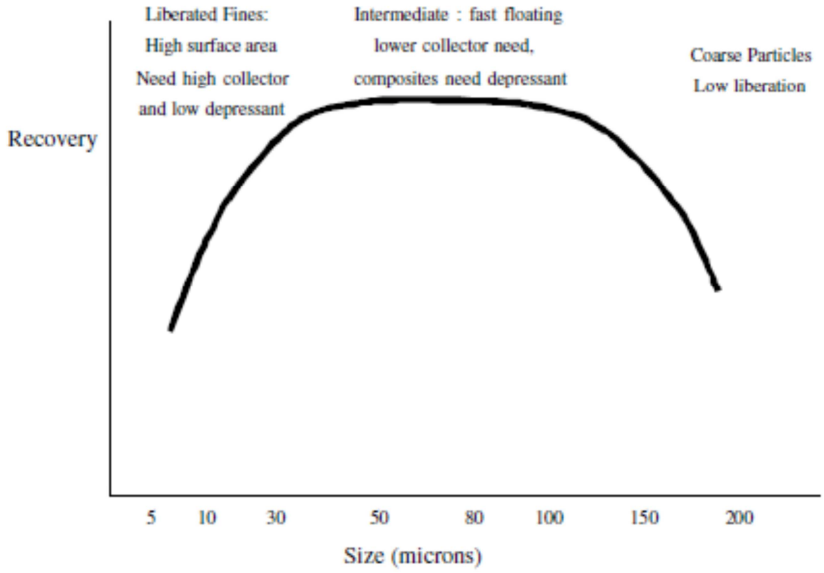


**Figure 2.4: A typical recovery as a function of particle size curve subdivided into three distinct regions (Pease et al., 2006)**

Larger particles by nature have a higher probability of contact with air bubbles compared to smaller particles and therefore larger particles have higher flotation rates compared to smaller particles (Tao,

2004). Dai et al. (1998) and Dai et al. (2000) have shown that the probability of attachment increases with increasing particle size and increasing particle hydrophobicity. The particle-bubble may detach however if the detachment forces exceed attachment forces – the detachment forces come from oscillation effects when large particles collide with a loaded bubble, from slurry turbulence and particle inertia effects (Tao, 2004). In summary therefore, the probability of detachment increases with increasing particle size.

The above explanation for particle size behaviour in froth flotation above is however an oversimplification since the effect of frothers and frothing behaviour was not considered. Schwarz (2004) noted that "*particle size plays a key role in bubble coalescence and froth stability*". This has in fact been shown to be true by Szatkowski and Freyburger (1985) who showed that fine quartz particles, i.e. small hydrophilic particles, rendered bubbles more resistant to coalescence and promoted a stable froth. This increased froth stability led to increased recovery of fine particles. Similarly, Livshits and Dudenkov (1965) suggested that coarse particles can act as a buffer between bubbles and thus increase froth stability by preventing bubble coalescence. This was however contradicted by Moudgil (1992) who claimed that coarse phosphate particles destabilised the froth.



In addition to all the parameters mentioned previously, it is also interesting to note that Pease et al. (2006) showed the recovery of finely sized hydrophobic particles was reduced in a conventional flotation system which contains a wide distribution of hydrophobic particle sizes. If however the size distribution of hydrophobic particles present was narrowed, i.e. there are more or less and equal amount of similarly sized hydrophobic particles, then fine hydrophobic particle recovery is increased to levels equivalent to the optimum range in Figure 2.4. Clearly therefore, the recovery of particles to the concentrate stream is not simply due to physical effects between particle and bubble but is a combination of many interactive variables.

### 2.3.3 Chemical Parameters

The chemical parameters involved in flotation are both numerous and highly interactive, which perhaps makes this section of the flotation engineering system particularly complex. Flotation reagents are a

major component of the chemical parameters because the process is practically impossible without them. In the most basic form of froth flotation, their function is to manipulate the flotation pulp's chemical environment so that the surfaces of those minerals considered economically valuable can be rendered sufficiently hydrophobic in order to prepare them for attachment with gas bubbles. Once attachment has taken place, the valuable mineral can be transported out of the pulp zone and into the froth zone and thus is separated from those minerals considered gangue. They are classified according to the role they fulfil in the flotation process. The main classes of flotation reagents are collectors, frothers, depressants and activators. The role of the frother is to keep air bubbles dispersed and thus prevent their coalescence into larger bubbles as well as to stabilise the bubbles that have reached the surface. The role of a collector is to induce hydrophobicity onto selected mineral surfaces in order to endow them with a propensity to attach themselves to the bubbles. The role of depressants is to prevent the recovery of those minerals considered gangue that, in the absence of such depressants, are recovered. However, as with the other parameters, the roles of the individual flotation reagents are not mutually exclusive and reagents can fulfil roles other than their original intention in different flotation systems (Bradshaw, 1997).



## 2.4 Reagents in Froth Flotation

### 2.4.1. Frothers

Frother molecules are neutral molecules made up of a hydrocarbon chain and a polar end-group (Pearse, 2005). The hydrocarbon group can be straight, branched or cyclic whilst the polar group can be a hydroxyl, carbonyl, ester, carboxyl, amine, nitrile, phosphate or sulphate. The molecule, due to its heteropolar structure, is surface-active and preferentially adsorbs at the air-water interface with the hydrocarbon chain preferring the air-side and the polar group preferring the water-side where it hydrogen bonds with water molecules (Laskowski, 1993) and thus helps to keep air bubbles dispersed as well as prevent their coalescence (Wills and Napier-Munn, 2006). The functions of the froth phase in turn are to (i) transport the mineral laden bubble from the pulp-froth interface to the concentrate launder and (ii) promote further separation of hydrophobic from hydrophilic particles by the gravity drainage of gangue bearing water back to the pulp phase (Nguyen and Schulze, 2004).

### *2.4.1.1 The Role of Frothers in Froth Flotation*

One of the most important aspects of froth flotation is the formation of a froth in which the valuable minerals are retained for further upgrading. Thus, the presence of a frothing agent is vital to the flotation process (King, 1982). In addition to the formation of froths, frothers fulfil other roles which are critically important to the process. These are:

i. Their molecules prevent or at least inhibit bubble coalescence by stabilising the liquid film surrounding the bubbles (Pugh, 1996); bubble coalescence is undesirable in froth flotation because it leads to bubble-particle detachment, an increase in pulp bubble size, a reduction in surface area flux and therefore an overall reduction in valuable mineral recovery to concentrate. Two mechanisms by which frother molecules may prevent bubble coalescence are hydrogen bonding with neighbouring molecules and Marangoni effects. In the first mechanism it is proposed that the frother molecules form hydrogen bonds with the neighbouring water molecules and thus a stabilised water film around the bubble. This water film is divided into two parts, an inner capillary film and an outer free flowing film, as shown in Figure 2.5.

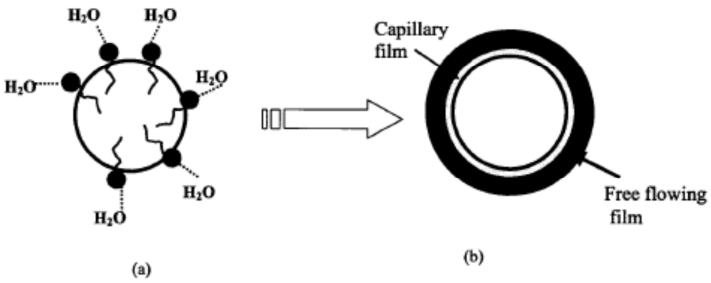


**Figure 2.5: (a) Frother molecules adsorb on bubble surface and hydrogen bond with water molecules resulting in (b) a water film around the bubble (Rodel, 1981)**

It is the capillary film which is tightly bound to the bubble and is immobile which resists drainage and therefore prevents coalescence (Rodel, 1981). The Marangoni effect proposes that, under dynamic conditions, the surface tension in a froth film is higher during extension and lower

during compression than the equilibrium values. The expanding or contracting surface therefore provides a restoring force which protects the film against local thinning (Harris, 1982).

ii. They reduce the bubble rise velocity in the pulp phase and thus create favourable conditions for bubble-particle attachment, i.e. the frother influences bubble-particle adhesion kinetics (Finch et al., 2008). The general explanation for this behaviour has its origin in how bubbles deform in the absence of any frother or any surfactant for that matter. Figure 2.6 (a) shows that when a bubble rise in a water bath, dynamic pressures across the bubble cause the bubble to flatten. This phenomenon does not occur in the presence of frother which suggests a restoring force must be present which resists deformation (cf. Figure 2.6 (b)).

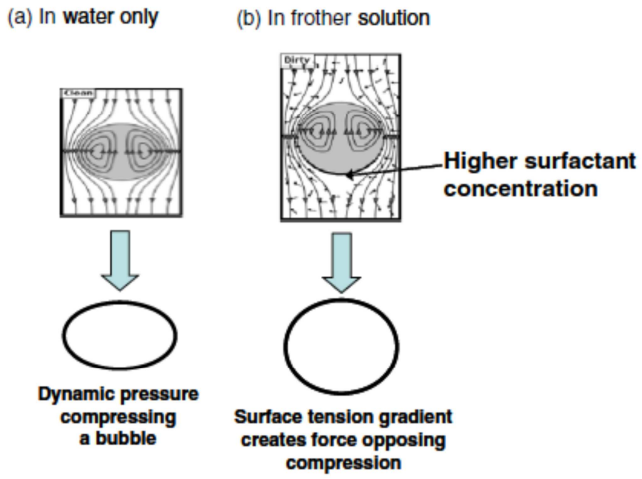


**Figure 2.6: Illustration of dynamic pressure causing bubble deformation in (a) water only case and (b) the force created by surface tension gradient that occurs in the presence of frother that resists deformation (Finch et al., 2008)**

One explanation for this restoring force is that water sweeps frother away from the top of the bubble and concentrates it at the bottom which, in turn, causes increased tension at the front of the bubble. Similarly therefore, with regard to bubble rising velocity, the surface tension force acts in the opposite direction to the flow of water and therefore increases drag causing bubble rise velocity to reduce (Finch et al., 2008).

iii. Frothers reduce bubble diameter and thus aid in the generation of fine bubbles (Finch et al., 2008); the exact explanation for this phenomenon is not yet known because, as shown by Sweet

(1999), it is not directly related to surface tension. Whatever the mechanism, bubble diameter is an important parameter in froth flotation as it influences the performance of other parameters. One such parameter is the flotation rate constant, which is linearly related to the bubble surface area flux which, in turn, is inversely related to the bubble size (Grau et al., 2005). Ahmed and Jameson (1985) investigated the role of bubble size on the rate of flotation of fine particles and reported superior results with smaller bubbles. Subrahmanyam and Forssberg (1988) consider the overall stability of the froth to be a function of bubble size.

iv. They stabilise the bubble-particle aggregate by interacting with collectors (refer to Section 2.4.1.5).

### *2.4.1.2 Description of Foam and Froth Structure*

Foams have a perfect isotropic structure where polyhedral gas bubbles are separated by thin liquid films (Garcia-Gonzales et al., 1999) and are formed by introducing gas bubbles into a liquid that contains surfactant. The planar layers separating gas/air bubbles are called *lamellae* and, as shown in Figure 2.7, one can visualise the three lamellae as three planes intersecting and abruptly stopping at a common point.



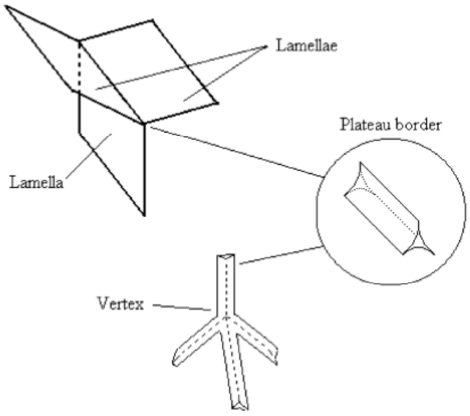


**Figure 2.7: Schematic of a foam (Ventura-Medina and Cilliers, 2002)**

At the intersection point of the three lamellae, channels called *Plateau borders* are formed (Weaire and Hutzler, 1999). These Plateau borders have cross-sections in the shape of triangles whose sides are arches of circles (the extent of curvature is determined by the liquid content of the Plateau border). When four Plateau borders intersect a *vertex* is formed. The vertices are shaped in the form of a tetrahedron and the channels are approximately $109.5^{o}$.

The processes taking place in foams are drainage, film rupture on the foam surface and coalescence (Weaire and Hutzler, 1999). Foam drainage essentially is the flow of liquid through the interstitial spaces between bubbles, i.e. lamellae, Plateau borders and vertices (Schwarz, 2004) and is driven mainly by gravity although viscous and capillary forces do also play a significant role (Pugh, 2005). Bubble coalescence occurs when significant thinning of the liquid film between two adjacent bubbles has occurred and thus usually is preceded by drainage. The coalescence of bubbles results in the disappearance of faces and the change of two bubble cell units into one (Nguyen and Schulze, 2004). Froth stability can thus be related to the ability of a froth or foam to prevent thinning of the liquid film between two bubbles, i.e. the factors that influence the thickness of the lamellae are important when froth stability is considered. These factors are related to process chemistry, the actions of particles as well as frother molecules on the lamellae (Sweet, 1999).



#### *2.4.1.3 Factors that Influence Froth Stability*

***i. Chemical Interactions between Reagents***

Sweet (1999) reported that chemical interactions between reagents can significantly enhance or reduce the stability of froth. Livshits and Dudenkov (1965) added minuscule amounts of soluble salts of copper and lead to frother solutions and then measured the dynamic and static froth stability parameters in the presence and absence of xanthate. They reported that the metal ions in solution formed visible, highly hydrophobic and dispersed precipitates with the xanthates which accelerated bubble coalescence and thus reduced froth stability. The authors argued that the precipitates must therefore be able to

penetrate the bubbles and thus burst the lamellae but that this can be prevented by adding more frother.

O'Connor et al. (1988) investigated the role of copper sulphate in pyrite flotation and found that it had a significant effect on the maximum froth height obtained in static three-phase froth tests whilst Moolman et al., (1995) used digital imaging techniques to show that the addition of copper sulphate to a pyrite flotation circuit led to the formation of a brittle froth.



***ii. Frother Concentration***

The behaviour of flotation froths is controlled by the properties of the frother molecules at the air/water interface. This interface becomes visco-elastic, more immobile and increasingly stable when increased amounts of frother molecules are adsorbed at the air/water interface. The ultimate effect is that liquid drainage from the lamellae is retarded and, hence, bubble coalescence is inhibited. The overall effect is that froth stability is increased with increasing frother concentration (Langevin, 2000). The mechanism proposed by Cho and Laskowski (2002) to account for this phenomenon is that, if the lamellae are thinned, then the concentration of frother molecules at the interface is disturbed from its equilibrium concentration. Therefore, if excess frother molecules are present in the pulp, these will migrate to the interface and thus restore the equilibrium concentration. The alternative theory which accounts for increased froth stability with increasing frother concentration is the Marangoni effect (cf. Section 2.4.1.2, point i).

***iii. Particle Properties***

As alluded to towards the end of Section 2.3.3, particles within the Plateau borders can cause them to become stable, and thus form a stable froth, or less stable, causing the froth to collapse (Exerowa and Kruglyakov, 1998). Tambe and Sharman (1993) suggested that the effectiveness of particles in

stabilising flotation froths is related to their ability to be adsorbed at the air/water interface. They reported that the air/water interface, in addition to providing steric hindrance to bubble coalescence, also increased the viscosity of the interface when high concentrations of particles were adsorbed at the interface. Ross (1991) suggested that if the bubble film thickness is less than the particle size then these finely sized particles can, provided that the films do not rupture, become entrapped between two adjacent bubbles. These entrapped particles will either enhance or reduce froth stability depending on the system properties – particle shape, particle roughness, particle concentration, particle hydrophobicity and the rate of thin film formation. Dippenaar (1982) demonstrated that, if viscosity effects can be ignored for a given froth which contains a specific mass of hydrophobic particles then, the rate of film thinning will be directly proportion to the particle size. Velikov et al. (1998) therefore concluded that the structure of the froth is affected by the presence of particles but that the froth recovery of these particles is affected by the structure of the froth.

A particular particle property, particle hydrophobicity, will be discussed further here. Ata et al. (2002) reported higher recoveries for moderately hydrophobic particles (contact angle ≈ $63^{o}$) compared to strongly hydrophobic particles (contact angle ≈ $82^{o}$). The authors attributed lower recovery to rapid bubble coalescence with consequent drop back of particles into the pulp phase from the froth phase in the presence of the strongly hydrophobic particles. They also noted that the flotation froths which contained the strongly hydrophobic particles produced lower water recoveries and ascribed it to occur as a consequences of drainage and froth destabilisation. Pugh (1996) reported that hydrophobic particles can bridge thin films – once these bridges becomes unstable, which may occur due to dewetting caused by the hydrophobic nature of the particles, film rupture may occur.



#### *2.4.1.4 Frother Interaction with Collectors*

Leja and Schulman (1954) proposed that frothers become effective only when there is a suitable degree of molecular interaction between frother and collector molecules at the air/water and solid/water interfaces. They furthermore proposed that the actual mechanism of adherence of an air bubble to a suitably collector-coated particle is due to these collector-frother molecular interactions. The

interactions will therefore increase the tenacity of mineral to bubble adhesion because of the formation of the continuous film of associated molecules.

Figures 2.8 and 2.9 illustrate the concept of frother and collector molecular interactions and their role in the dynamic attachment of air bubbles to solid particles as visualised by Leja and Schulman (1954). Prior to bubble-particle attachment, as indicated in Figure 2.8, collector and frother molecules, both associated and non-associated, are distributed at all the interfaces and in the bulk solution. As soon as the air bubble contacts the solid surface, as shown in Figure 2.9, the collector-frother molecules at the air-water interface can penetrate the diffuse monolayer on the solid, and adsorb strongly on the solid surface, thereby greatly increasing local surface concentration and local hydrophobic character of the surface. At the moment of particle-bubble attachment the mixed monolayer at the air/water interface becomes slightly more condensed and consequently stabilises the bubble.

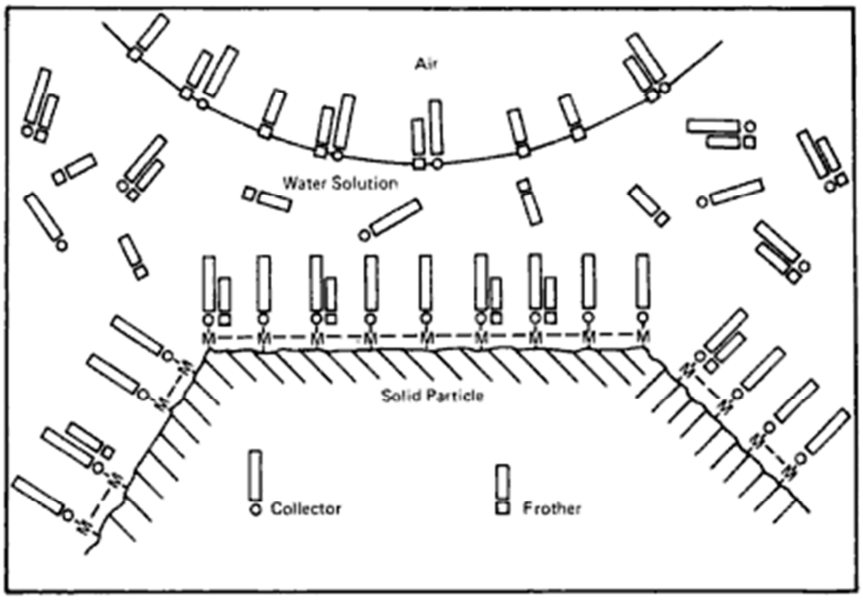


**Figure 2.8: Mechanism of bubble attachment - bubble approaching a collector coated solid surface; diffused monolayers of associated and unassociated molecules at interfaces and in solution (Leja and Schulman, 1954)**

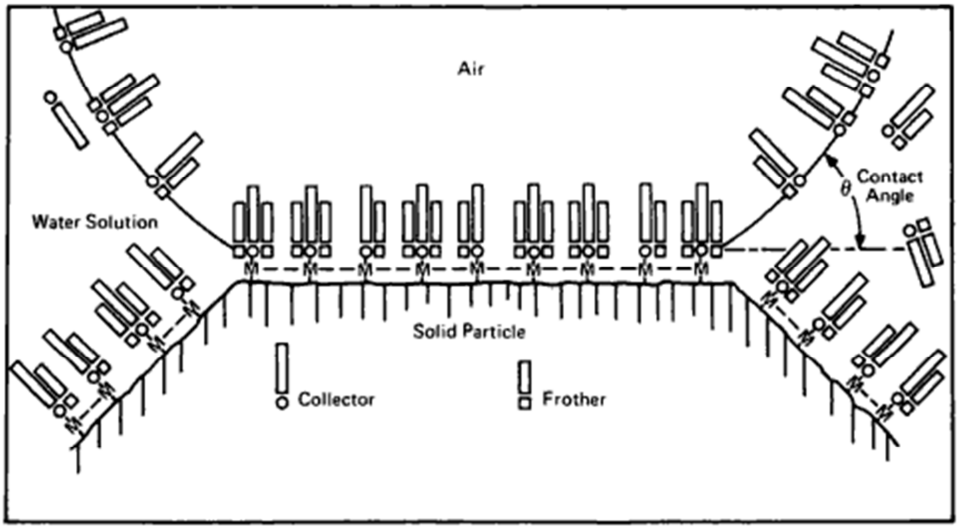


**Figure 2.9: Mechanism of bubble attachment - adherence of an air bubble established through the penetration of the monolayer at the solid/liquid interface by the monolayer at the air/liquid interface (Leja and Schulman, 1954)**



Excessive concentrations of collector and frother molecules at the interfaces are likely to be more harmful rather than beneficial because penetration will be hindered as attachment is not possible if the degree of interaction is too high (Leja and Schulman, 1954). This may happen due to the formation of multiple polar groups and/or van der Waals bonding between the collector and the frother which will result in rigid, solidified mixed films at either of the participating interfaces. Adamson (1960) therefore concluded that the primary function of the frothing agent in froth flotation is therefore to stabilise the attachment of the bubble to the particle and that it's frothing ability may be of secondary importance.

Mukai et al. (1972) investigated the interaction between alcohol and ethyl xanthate in galena flotation and reported that the best recovery was obtained with the amyl alcohol. The authors attributed the better performance to the co-adsorption of the collector-frother molecules. Laskowski (1998) studied the interaction between α-terpineol and ethyl xanthate in the chalcocite flotation and reported a significant increase in both rate kinetics and total recovery with increasing α-terpineol dosage. Since α-terpineol does not affect chalcocite wettability, this result points to the interaction of α-terpineol and

xanthate at the moment of collision and attachment of the chalcocite particle to the bubble. The importance of frother-collector interactions have thus been confirmed by several researchers.

### *2.4.1.5 Material Transportation To and In the Froth Phase*

The transport mechanisms for particles entering or exiting the froth zone are shown in Figure 2.10.

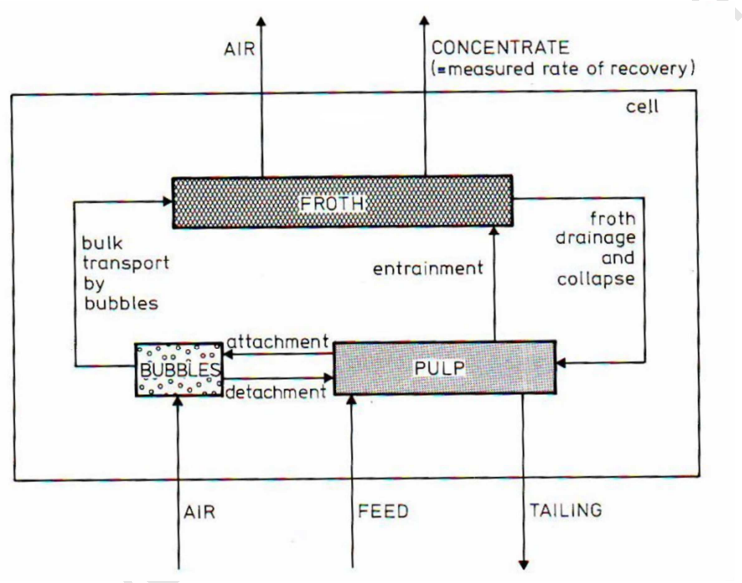


**Figure 2.10: Transport paths of materials in flotation (Subrahmanyam and Forssberg, 1998)**

In a perfect froth flotation system, i.e. one in which those particles considered gangue are completely liberated from those considered economically valuable and sliming of hydrophobic particles and air bubbles do not happen, particles can enter the froth phase by either true flotation or a mechanical mechanism, such as entrainment. In true flotation the desired particle is rendered hydrophobic and reports to the froth phase by attaching to a gas bubble, whilst for hydrophilic particles, the possible means of transportation are entrainment and entrapment [(Kirjavainen, 1996); (Savassi et al. (1998)]. In addition, all particles present in the froth, whether they are hydrophobic or hydrophilic, may drop back into the pulp zone due to liquid drainage and bubble coalescence mechanisms in the froth.

Entrainment of water and suspended particles into the froth is caused by air bubbles ascending through the pulp-froth interface as explained by the bubble swarm mechanism [(Subrahmanyam and Forssberg, 1988), (Savassi et al., 1998), (Savassi, 2005)]. This mechanism is independent of particle surface properties, i.e. it is non-selective and equally affects both hydrophilic and hydrophobic particles, and takes place alongside true flotation because the same bubbles are responsible for both processes (Savassi, 2005). Entrainment does however discriminate according to particle size, i.e. only those considered "fines and ultrafines" tend to be recovered via this mechanism. The reason for this is that the fine particles, due to their negligible mass, tend not to drop back into the pulp once they enter the froth phase. Jowett (1966), Johnson (1974) and Warren (1985) described gangue recovery as a function of water recovery using the following equation:

$$R_g = e_g R_w \ldots (2.3)$$

where $R_g$ = gangue recovery and $R_w$ = water recovery. The proportionality factor, $e_g$, defines the entrainment function and is often referred to as the entrainability factor.

### 2.4.2 Collectors

The primary requirement for successful recovery of valuable minerals by the froth flotation process is that the mineral of interest's surface must be rendered hydrophobic. This is achieved by the addition of collectors whose molecules/ions concentrate on mineral-water interfaces and thus render the mineral particle surfaces water-repellent. Collectors usually are surface active compounds that consists of a polar functional group, hydrophilic in character and through which they attach to the mineral, and a non-hydrocarbon segment which attaches to the air bubble (King, 1982). Glembotskii et al. (1972) divided collector molecules into two types: ionising and non-ionising. Ionising collectors are further subdivided using a classification system based on the type of ion that produces the water-repellent effect in water. This classification system is shown in Figure 2.11.

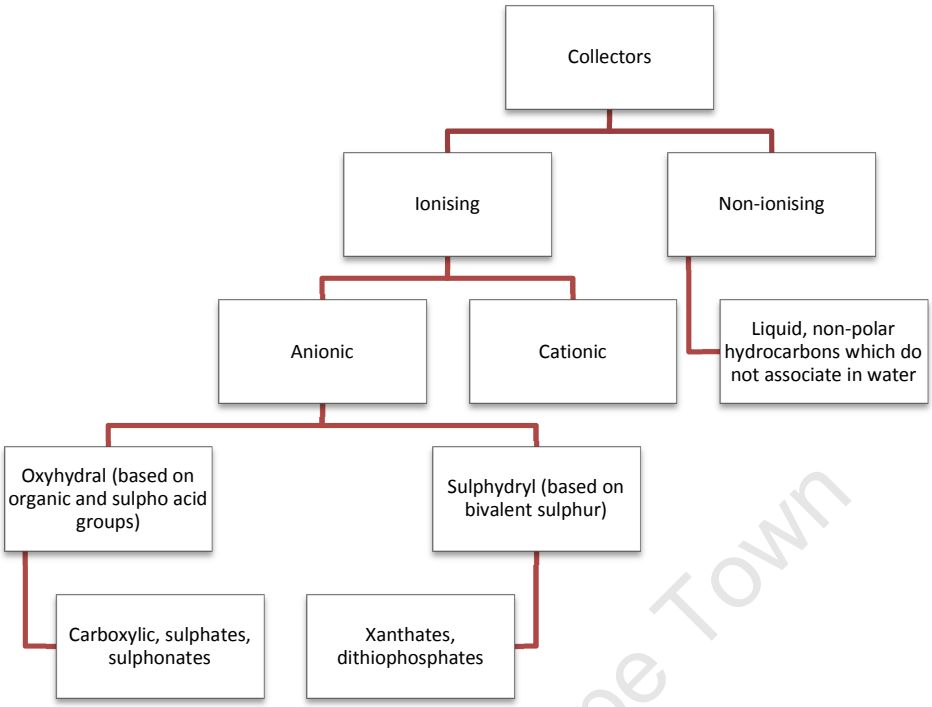


**Figure 2.11: Classification of collectors (Glembotskii et al., 1972)**



The cationic collectors are used in the flotation of oxides, carbonates, silicates and alkali earth metals such as barite and sylvite (Wills and Napier-Munn, 2006). Anionic collectors are further subdivided, based on the type and structure of their polar groups, into oxyhydral and sulphydryl collectors (Wills and Napier-Munn, 2006). It is the sulphydryl collectors that are used in the flotation of sulphide minerals. As this thesis specifically focuses on the flotation of sulphide minerals, only the collectors used in this process will be discussed further.

### *2.4.2.1 Xanthates*

Xanthates, first patented in 1925 (Sweet, 1999), are formed by reacting an alkali hydroxide with an alcohol and carbon disulphide (Wills and Napier-Munn, 2006) to give a molecule which has a complex asymmetrical structure and consists of a polar part and a non-polar part as is shown in Figure 2.12. The anion in this structure is composed of a hydrocarbon chain and a polar group whilst the metal ion acts as

the cation. The hydrocarbon group is responsible for hydrophobicity and the polar group interacts with the mineral surface but the metal cation plays no role in the reactions leading to mineral hydrophobicity.

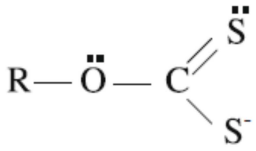

**Figure 2.12: Generic structure of a xanthate molecule, R = hydrocarbon chain group**

The length of the hydrocarbon chain is important as it determines the strength of the attachment between collector and mineral. This is due to the fact that, in addition to the chemical forces which are set-up between the collector polar group and the mineral's surface, intermolecular forces are also set-up between the hydrocarbon chains. Therefore, in order to remove the collector molecule from the mineral surface, any ion which attempts to do so will have to overcome both the chemical forces between the mineral surface and the collector polar group as well as the intermolecular forces between the collector chains – and a longer chain will have more intermolecular forces and therefore contribute to greater strength of adsorption.

Xanthates are usually added in small amounts in industrial flotation circuits as excessive concentrations, apart from reducing selectivity by increased flotation of gangue, may also lead to a reduction in valuable sulphide mineral recovery (Wills and Napier-Munn, 2006). The loss in recovery with excessive collector concentration is attributed to a decrease in hydrophobicity due to the formation of a second layer of collector on the mineral surface with the opposite orientation of the first layer. Taggart (1951), using contact angle as a measure of hydrophobicity, showed that excessive collector concentrations resulted in a decrease in hydrophobicity. Xanthate collectors are usually used in weakly alkaline pulps because they decompose rapidly in an acid medium while hydroxyl ions can displace the xanthate anions from the mineral surface in strongly alkaline pulps. The xanthates collectors are commonly supplemented in flotation circuits with other, secondary, collectors. Thus, for example, if liberated gold is present in a copper sulphide ore, then DTP collectors are usually added in conjunction with the xanthate. Xanthates

may in fact become the auxiliary collectors in applications where selectivity between various sulphide minerals is important – such as copper-molybdenum circuits.

### *2.4.2.2 Dithiophosphates*

Dithiophosphate collectors (DTP), first patented by Whitworth (1926), are widely used in sulphide mineral flotation applications (Mingione, 1984). This reagent is produced by neutralising dithiophosphoric acid with an organic or inorganic base. Dithiophosphoric acid, in turn, is produced by reacting phosphorus pentasulphide ($P_2S_5$) with phenols or alcohols. The reagent has the general molecular structure as shown in Figure 2.13.

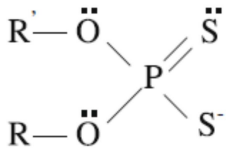

**Figure 2.13: Generic structure of a dithiophosphate molecule, where R = alkyl chain**

The difference in flotation behaviour between xanthate and DTP is commonly attributed to the differences in their respective molecular structures and consequent behaviour of the donor atoms, i.e. the oxygen and phosphorus atoms (Nagaraj, 1988). Oxygen is more electronegative and more polar than phosphorus and therefore the oxygen atom in the DTP and xanthate molecules have strong electron withdrawing effects. This, combined with the fact that phosphorus is more electropositive than carbon in the xanthate, results in DTP being a weaker but more selective collector compared to the xanthates (Nagaraj, 1988). Poling (1976) and Glembotskii et al. (1972) attributed DTPs apparent weak collecting properties, when compared to xanthates, to the high water solubility of heavy metal DTPs in comparison to the corresponding heavy metal complexes of xanthates which causes DTP to be more easily affected by depressants. Bradshaw (1997) however reported that DTP may, because it has an additional alkyl group in its structure compared to the xanthates, induce higher hydrophobicity provided that all other factors are equal and that the collectors undergo similar reactions. This comparison would

hold in the case of the collectors forming the metal thiolate but possibly not in the case of xanthate forming dithiolate.

Lovell (1982) reported that DTP, when used in conjunction with xanthates, is more selective against iron sulphides compared to when xanthates are used alone. Somasundaran and Moudgil (1988) attributed DTPs proposed selective action against iron sulphides as being due to the fact that significant quantities of soda ash are added in the manufacturing process in order to increase the chemical's shelf life; soda ash, like lime, is known to be highly selective against pyrite. In contrast to Lovell (1982), Finkelstein and Goold (1972) noted that DTP has been used in the flotation of molybdenite, pyrite and copper sulphide minerals whilst Heilbig et al. (2000) observed synergistic pyrite recovery with mixtures of xanthate and di-iso-butyl DTP at pH 9 in microfloat experiments. Laskowski (2005) reported that the DTPs are particularly efficient collectors for precious metals like silver and gold. Stamboliadis (1976) reported that, according to their floatability with DTP, minerals may be classified in the following order: chalcopyrite, galena, sphalerite, pyrite but that the nickel minerals, pentlandite and millerite, are unfloatable with commercially available DTPs.

Lovell (1982) and Mingione (1984) also reported that the long chain dialkyl DTPs, defined as those with more than four carbon atoms in their structure, exhibit both frothing and collecting properties whilst the short chain DTPs are essentially non-frothing. The frothing properties of the longer chain DTPs were attributed to the decomposition of the alcohols used in the manufacturing process (Lovell, 1982). Mingione (1984) suggested that the particular salt form of the dialkyl DTP may also influence the frothing properties. Mingione (1984) also reported that the diaryl DTPs will display light to moderate frothing properties because of the phenols from which they are made.

Two prominent features of DTP when compared to xanthate are:

(i) Higher resistance to hydrolysis and oxidation than the corresponding xanthates as shown in Figure 2.14. This means that the oxidation of DTP to its corresponding dithiolate is more

difficult for DTP compared to xanthate and therefore, if the dithiolate contributes significantly to flotation activity, the trithiocarbonates will readily produce more dithiolates on mineral surfaces at lower oxidation potentials compared to xanthates and dithiophosphates (du Plessis, 2003).

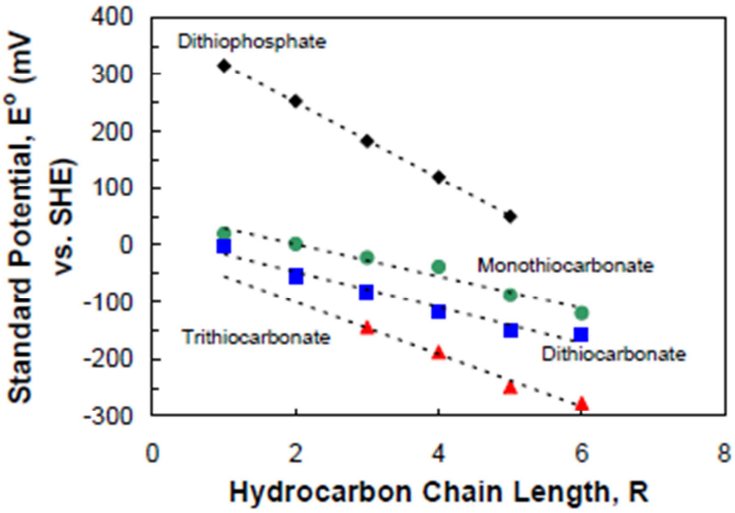


**Figure 2.14: Standard redox potentials for thiocarbonate/dithiolate couples as a function of hydrocarbon chain length (Chander, 1999)**

(ii) The solubility products for metal xanthates are much lower compared to the solubility product for metal dithiophosphate (Chander, 1999).

### *2.4.2.3 Summary of Mechanisms of Collector Adsorption on Sulphide Minerals*

It is well-established that thiol collectors adsorb onto sulphide minerals via a mixed potential mechanism involving the anodic oxidation of collectors and the cathodic reduction of oxygen (Yoon and Basilio, 1993). This statement is important as it highlights the role of oxygen in collector adsorption onto the mineral surface, i.e. collector adsorption onto the mineral surface does not take place without the previous action of oxygen and indicates that sulphide minerals are semi-conductors which facilitate

the electrochemical reactions occurring (Fuerstenau, 1982). Furthermore, the anodic processes can only occur when the pulp potential across the solid/solution interface is above the equilibrium value for that process. The equilibrium potential in turn is determined by the free energy change in the process and hence the potential across the solid/solution interface determines what reactions can occur on the surface of the sulphide mineral (Somasundaran and Moudgil, 1988). Another parameter important in the collector adsorption mechanism theory is the mineral itself, i.e. the type of interaction between the collector anion and the mineral is mineral specific (Yoon and Basilio, 1993).

The following types of electrochemical mechanisms are reported to be possible: (i) chemisorption, (ii) catalytic oxidation, and (iii) metal-thiol formation (Yoon and Basilio, 1993). Chemisorption involves the formation of a monolayer of the thiol oxidation product at potentials below the thermodynamic potential for metal-thiol compound formation (Yoon and Basilio, 1993). In chemisorption the collector interacts with the mineral surface without movement of the metal ions from their lattice sites. This interaction has a covalent character and adsorption, as stated above, is restricted to monolayer coverage. The anodic oxidation reaction involving the collector at the mineral surface can be represented by the following equation:

$$X^- \rightarrow X_{ads} + e^- \ldots (2.4)$$

Somasundaran and Moudgil (1988) reported that chemisorbed thiol species are intermediates in the formation of dithiolates or metal compounds and that this conversion, in the case of transformation to the dithiolate, proceeds via reaction (2.5). However, when reaction (2.4) is much faster than reaction (2.5), the chemisorption process can reach monolayer coverage before further processes become significant. In that case the dithiolate will not form.

$$X_{ads} + X^- \rightarrow X_2 + e^- \ldots (2.5)$$

In catalytic oxidation, the thiol compound is transformed to its dithiolate, which is a neutral molecule, via an oxidation mechanism. This transformation, which is usually slow in terms of kinetics, is catalysed by the presence of minerals. The mineral provides a passage for the transfer of electrons from the site where the collector is oxidised to the site where oxygen is reduced but does not participate in the reaction itself and its surface remains unaffected. The dithiolate product, which is dixanthogen in the case of xanthates and dithiophosphotagen in the case of DTP, is only physisorbed and therefore is weakly held to the mineral surface. This mechanism predominates where the mineral does not readily liberate metal ions to form metal-thiol compounds [(Bradshaw, 1997), (Lotter and Bradshaw, 2009), (Yoon and Basilio, 1993)]. The oxidation of the thiol ion to the corresponding dithiolate can be represented by the following equation:

$$2X^- \rightarrow X_2 + 2e^- \ldots (2.6)$$

In the metal-thiol formation mechanism, which is also called the EC-mechanism, the mineral participates in the adsorption process to form a metal-thiol compound on the mineral surface. The EC-mechanism occurs when the mineral is easily oxidised or when the formation of a metal-thiol compound is favoured and can be represented by the following equations:

electrochemical: $MS \rightarrow M^{2+} + S^0 + 2e^- \ldots (2.7)$

chemical: $M^{2+} + 2X^- \rightarrow MX_2 \ldots (2.8)$

The overall adsorption mechanism can then be presented by the reaction:

$$MS + 2X^- \rightarrow MX_2 + S^0 + 2e^- \ldots (2.9)$$

The process can also result in the formation of an oxy-sulphur ion:

$$MS + 2X^- + 4H_20 \rightarrow MX_2 + SO_4^{2-} + 8H^+ + 8e^- \ldots (2.10)$$

These equations can also occur in separate stages if, for example, the sulphide surface oxidises to sulphate before collector is added. Upon addition of the collector the oxidised surface species could exchange with the thiol ion to form dithiolate:

$$MS + 6H_2O \rightarrow M(OH)_2 + SO_4^{2-} + 10H^+ + 8e^- \ldots (2.11)$$

followed by:

$$M(OH)_2 + 2X^- \rightarrow MX_2 + 2OH^- \ldots (2.12)$$

In the EC-mechanism, mineral oxidation, and therefore the availability of metal ions, is controlled by pulp potential while the metal-xanthate reaction step, i.e. the chemical step, is controlled by the stability constant of the metal-thiol compound which determines whether the compound will be formed at specific conditions [(Bradshaw, 1997), (Lotter and Bradshaw, 2009), (Yoon and Basilio, 1993)].

### *2.4.2.4 Collector Adsorption on Chalcopyrite, Pentlandite and PGMs*

- ***Chalcopyrite***

Chalcopyrite is the most abundant copper mineral and consists of 30.43 weight % iron, 34.63 weight % copper and 34.94 weight % sulphur. It has a very brassy to honey yellow colour and displays a tetragonal crystal structure. Copper is present as Cu(I) while iron is in the form Fe(III), giving a formula of $Cu^{+}Fe^{3+}S_2$ (Pearce et al., 2006). Chalcopyrite often floats successfully without the presence of collector and this is usually attributed to surface oxidation reactions which can either lead to the formation of elemental sulphur on the mineral's surface or can cause iron atoms to migrate from the lattice thus leaving a hydrophobic metal-deficient layer on the surface (Woodcock et al., 2007). This natural floatability-like behaviour of chalcopyrite does however complicate flotation studies as it becomes difficult to isolate the effect of collectors on hydrophobicity.

In industrial flotation plants, however, a moderate amount of collector is usually required to achieve economic recovery of the mineral and this is attributed to the presence of surface precipitates and oxidation products that negate the mineral's natural floatability. The proposed mechanism of flotation has been ascribed to the formation of cuprous xanthate as well as dixanthogen (Woodcock et al., 2007). Abramov (1966) proposed that flotation of chalcopyrite is reduced significantly when dixanthogen does not form. This was confirmed by Allison et al. (1972) who determined the products of the reaction between chalcopyrite and aqueous methyl, ethyl, propyl and butyl xanthates to be dixanthogen in each case. Ackerman et al. (1987) proposed that the superior flotation of chalcopyrite over, for example pyrite (both are n-type semiconductors), reflects the relative high solubility of $Cu^{2+}$ from the mineral surface and its oxidation of X to $X_2$ in situ. In the case of pyrite, the oxidation of X to $X_2$ is more difficult because dissolved $Fe^{2+}$ must first be converted to $Fe^{3+}$ and, even once this is done, the $X_2$ formation would be less than with $Cu^{2+}$. Yoon and Basilio (1993) reported that xanthate formed dixanthogen on chalcopyrite at potentials near the reversible potential for the xanthate/dixanthogen couple. At higher potentials, however, chalcopyrite oxidised and copper ions were released. These reacted to form the metal xanthate and this in turn co-existed with the dixanthogen. Xanthate adsorption may therefore be ascribed to the catalytic oxidation mechanism.

With regard to flotation with DTP, Finkelstein and Goold (1972) reported the presence of cuprous diethyl DTP, $Cu(DTP)_2$, on chalcopyrite after reaction with potassium diethyl DTP in alkaline conditions and proposed CuDTP+$(DTP)_2$ formation in acid and neutral conditions. Woodcock et al. (2007) considers DTP to be a strong collector for chalcopyrite and stated that they are often used in sulphide copper cleaning circuits at high pH because they are believed to be more selective against iron sulphides than xanthate collectors.

- ***Pentlandite***

Pentlandite is an iron-nickel sulphide and is the main source of nickel worldwide. The mineral has the general formula $(Fe,Ni)_9S_8$, i.e. it is believed to be composed of equal amounts of nickel and iron. It has a complex structure, with a face centred cubic arrangement and the metal ions in both tetrahedral and octahedral coordination with the sulphur atoms. The difficulties in recovering pentlandite are often attributed to the effect of surface oxidation, slime coatings and the formation of passivating layers of the metal ions that occur in the process water. Hodgson and Agar (1989) reported that dixanthogen is formed from chemisorbed xanthate on the pentlandite surface according to the following reactions:

$$Ni + X^- \rightarrow NiX + e^- \ldots (2.13)$$

$$NiX + X^- \rightarrow Ni(X)_2 \rightarrow NiX_2 + e^- \ldots (2.14)$$

The formation of dixanthogen would occur concurrently with the adsorption of xanthate on the pentlandite during the oxidation process and enhance hydrophobicity.

Stamboliadis (1976) reported that pentlandite will not generally float with the use of DTP collectors; the author states that the reason for this "*apparent weakness of DTP to float the nickel minerals is*

*associated with the nature of both the polar and organic part of these compounds*." This means that the reagent is incapable of forming the insoluble nickel compounds necessary for flotation because it either has too few carbon atoms in the organic chains or the chains are branched. This is however contradicted by more recent work completed by Matveeva and Gromova (2007) who used UV spectroscopy analysis to show that 59 % of iso-propyl DTP adsorbed onto a pentlandite-pyrrhotite sample whilst 82 % of iso-butyl DTP adsorbed onto the a pentlandite-pyrrhotite sample. The authors then repeated the experiments but used a pure pyrrhotite sample and showed that the DTP collectors tested did not adsorb onto the pyrrhotite.

- ***PGMs***

Vermaak (2005) prepared synthetic palladium-bismuth-telluride (Pd-Bi-Te) and platinum-arsenide (PtAs) samples and studied the adsorption of ethyl xanthate onto these synthetic minerals using voltametry, impedance measurements and Raman spectroscopy. The author observed that (i) Pd-Bi-Te showed very strong anodic activity when polarised at potentials above 200 mV (SHE) in the presence of PEX and (ii) increased exposure times led to a decrease in capacitance values. The lowering of the capacitance value was attributed to the formation of a continuous surface layer whilst the increase in anodic activity was ascribed to the formation of dixanthogen on the surface because the cathodic and anodic polarisation curves predicted a mixed potential higher than that of the xanthate-dixanthogen couple. The author also noted that the Raman spectroscopy work not only confirmed the presence of dixanthogen but also detected molecular xanthate on the surface of the Pd-Bi-Te mineral. This suggested that (i) chemisorbed xanthate is formed at short exposure times and (ii) when exposure time is increased the chemisorbed xanthate converts to dixanthogen. However, the chemisorbed xanthate and dixanthogen can co-exist on the same surface. In conclusion, the author noted that the reported poor recovery of the Pd-Bi-Te minerals cannot be attributed to a lack of interaction of the collector with the surface and thus hypothesised that the only possible explanation for the poor Pd-Bi-Te recoveries experienced in industrial flotation plants is that those particles considered ultrafines are not recovered when the "xanthate only" collector reagent suite is used. Vermaak (2005) tested this hypothesis by taking flotation feed, concentrate and tailings samples from a flotation plant which reported poor Pd-Bi-Te recoveries. The mineralogical work done on these samples indicated that: (i) the minerals are fully

liberated from their sulphide and silicate hosts after grinding and (ii) the major proportion of the Pd-Bi-Te minerals in the tailings stream are present as fine and ultrafine particles.

Shackleton et al. (2007a) used microflotation techniques to determine the floatability of synthetic moncheite [(Pt,Pd)$(Bi,Te)_2$ and $PtTe_2$)] and merenskyite [(Pd,Pt)$(Bi,Te)_2$ and $PdTe_2$]. The microflotation results were then related to their surface properties through zeta potential, ToF-SIMS and XPS techniques. It is interesting to note that microflotation results showed that the synthetic merenskyite samples exhibited high natural floatability whilst the moncheite samples exhibited low to moderate floatability – in the case of the former, a minimum recovery of 63 % was attained in the absence of any collector whilst, in the case of the latter, a minimum recovery of only 18 % was attained. In the presence of SIBX, recovery increased to 99 % for both the merenskyite and moncheite synthetic samples. The work completed by Shackleton et al. (2007a) thus is in agreement with that which was done by Vermaak (2005) as it showed that the PGE tellurides responded well to xanthate collectors. Unlike Vermaak (2005) however Shackleton et al. (2007a) attributed the poor recoveries of merenskyite and moncheite in industrial flotation plants to the depressing effect of copper ions when copper sulphate is used as activator. The authors speculated that the negative effect of the copper ions on recovery may be due to patchy precipitation of hydrophilic $Cu(OH)_2$ on most of the active sites present on the mineral surfaces thereby limiting collector adsorption.

Shackleton et al. (2007b) also investigated the flotation behaviour of synthetic sperrylite ($PtAs_2$) and palladoarsenide ($Pd_2As$) using microflotation, zeta potential measurements, ToF-SIMS analyses and XPS. The authors reported that both sperrylite and palladoarsenide respond well to flotation in the presence of SIBX. The excellent recoveries obtained were ascribed to either the effect of xanthate being covalently bonded to the surface or because of the formation of dixanthogen.

#### *2.4.2.5 Collector Mixtures and Synergism*

The practice of utilising mixtures of various collectors is well established in the mineral processing industry [(Taggart, 1950), (Bradshaw, 1997), (Wiese et al., 2005), (Heilbig et al., 2000), (Bradshaw et al.,

1998), (Lotter and Bradshaw, 2009)]. This is perhaps not surprising because many processing plants treat poly-sulphide ores and a single-collector reagent scheme may not cover the full spectrum of sulphide minerals present in the ore (Nagaraj and Ravishankar, 2007). In such cases it can be advantageous to use a mixture of collectors because such mixtures, if designed properly, will cover the full range of sulphide minerals present in the ore and therefore will maximise total mineral recovery. Improved performance is generally ascribed to be either due to the summation of the differing contributions of the respective collectors as proposed by Mitrofanov et al. (1985) or due to collector-collector synergism, where the effect of a combination of collectors interact to produce an effect which exceeds the sum of their individual effects (Plaskin and Zaitseva, 1988). This behaviour is however not limited to polysulphide ores as mixtures of collectors have often been shown to behave with greater effectiveness than would be expected from their individual contributions in single sulphide mineral flotation studies. Bradshaw (1997), for example, studied the effect of mixtures of xanthate and DTC on pyrite flotation whilst Heilbig et al. (2000) studied the effect of mixtures of xanthate and di-iso-butyl DTP on pyrite flotation – both researchers reported enhanced performance with mixtures and attributed this to increased mineral hydrophobicity due to collector-collector synergistic effects.

Synergism will not only influence metallurgical performance, i.e. grade and recovery, but, importantly for flotation plant operators, various mixtures or blends of reagents have been shown to reduce flotation reagent costs without any significant loss in metallurgical performance (Crozier and Klimpel, 1989). In summary, the benefits of adopting a collector-collector mixture over a single-collector reagent scheme in flotation plants are (Lotter and Bradshaw, 2009):

- Higher rate of flotation (Adkins and Pearse, 1992)
- Improvement in coarse particle recovery (Plaskin et al., 1954)
- Reagent dosage reduction and/or cost saving (Bradshaw, 1997)

The study and analysis of synergism between reagents is complicated by the fact that (i) the reagents used in industrial plants are not always synthesised from pure products and synergistic behaviour may occur inadvertently due to the dissolved impurities and (ii) the roles and interactions of individual

reagents may be difficult to isolate due to the complexity of the flotation process itself. For example, frothers are added to provide a stable froth phase but they can interact with collectors and improve hydrophobicity in the pulp zone (Bradshaw et al., 1998). Furthermore, Bradshaw et al. (2005) showed that improved mineral hydrophobicity may not necessarily translate to higher mineral recovery in a real flotation system. The authors used a microflotation apparatus as a "hydrophobicity meter" and showed that hydrophobicity increased with increasing xanthate chain length when the molecule was adsorbed onto a galena sample. However, when the tests were replicated in a batch flotation cell, i.e. in the presence of froth, the expected benefits of higher mineral hydrophobicity were not observed and this was attributed to the strong froth destabilising effects of highly hydrophobic particles.

The exact mechanism(s) of synergistic enhancement of flotation performance observed when using collector mixtures is/are still a subject open to considerable debate and may be due to collector-collector interactions, collector-frother interactions or even frother-frother interactions (Bradshaw et al., 1998). Plaskin et al. (1954) studied collector-collector synergism using mixtures of ethyl and amyl xanthate in the flotation of galena and arsenopyrite and recorded recoveries that were higher than the simple summation of the individual effects by pure collectors. The authors attributed the higher recovery to improved adsorption, and therefore higher hydrophobicity, on the individual mineral surface. Bradshaw and O'Connor (1994) studied collector-collector synergism using mixtures of xanthate and DTC in the flotation of pyrite and reported that the mixtures yielded higher recoveries, higher grades and greater recovery of coarse particles. The authors hypothesised that the synergistic effect observed is due to increased mineral hydrophobicity which is due to the weakly adsorbing dixanthogen absorbing in multilayers around the strongly adsorbing dithiocarbamate which acts as an anchor on the mineral's surface (Bradshaw et al., 1998). Bagci et al. (2006) and Bradshaw et al. (1998) also proposed that synergism originates because mineral surfaces have a heterogeneous distribution of energetically different sites and therefore the weaker, but more selective, collector will preferentially adsorb onto the high energy sites and thus, in effect, forcing the stronger collector to adsorb onto the energetically weaker sites – the net effect is that overall hydrophobicity is improved.

In addition to collector-collector interactions, synergism may also occur due to collector-frother interactions. This may occur because frother molecules may accumulate at the mineral surface and, at

the time of bubble-particle collision, re-orientate and facilitate attachment. This will promote a stable froth phase and strong tenacity of the bubble-particle attachment. It is this strong attachment that results in efficient flotation and, ultimately, improved recoveries and grades (Bradshaw et al., 1998).

### 2.4.3 Depressants

Laskowski and Pugh (1992) described the function of depressants in flotation systems as being opposite to that of a collector, i.e. it is to inhibit flotation of a given mineral. This is achieved by either (i) preventing collector from adsorbing onto hydrophilic minerals or (ii) by adsorbing onto those minerals considered gangue and thus rendering them completely hydrophilic. Typical depressants which are used in the former case are the cyanide, lime and sodium sulphide while polymeric depressants are used in the latter (Fuerstenau et al., 2007). The primary requirements of depressants used in gangue depression are that they: (i) must have functional groups that exhibit preferential attraction to the gangue minerals, (ii) must have a strongly hydrophilic character by virtue of either the same or other functional groups in the molecular structure and (iii) should not possess functional groups that compete effectively with the collector for the surface of the minerals which are to be floated (Fuerstenau et al., 2007).



The polymeric depressants typically used in PGM flotation applications are either modified guar gum or carboxymethyl cellulose (CMC) (Bradshaw et al., 2005). The function of these depressants is to reduce the flotation of those minerals considered as “floating gangue” or FG into the froth (Robertson et al., 2003). The major difference between them is that CMC ionises in solution and so is negatively charged while guar is typically only slightly charged if at all (Mackenzie, 1986). CMC molecules therefore, once adsorbed onto gangue minerals, cause these minerals to become negatively charged and, particularly at high dosages, they therefore tend to repel each other. Guar gum, as is shown in Figure 2.15, is a branched polysaccharide with galactomannan forming the basic unit. The hydroxyl groups are arranged in a cis-configuration on the C-2 and C-3 atoms (Wiese, 2009).

A secondary effect of the depressants is the reduction in the stability of the froth which is (i) partly caused by the absence of froth-stabilising talc and (ii) partly caused by the nature of the polymer itself (Wiese, 2009). Polymeric depressants, particular guars, have been hypothesised to cause sulphide mineral depression when they are used at high dosage. This is because these minerals are known to adsorb onto sulphide minerals as well as the gangue (Shortridge et al., 2003). Harris et al. (1999) hypothesised that sulphide minerals can be trapped when heterogeneous agglomeration occurs. This hypothesis was based on the fact that, when the authors increased energy input to the batch flotation cell, the effect of sulphide mineral depression was reduced.

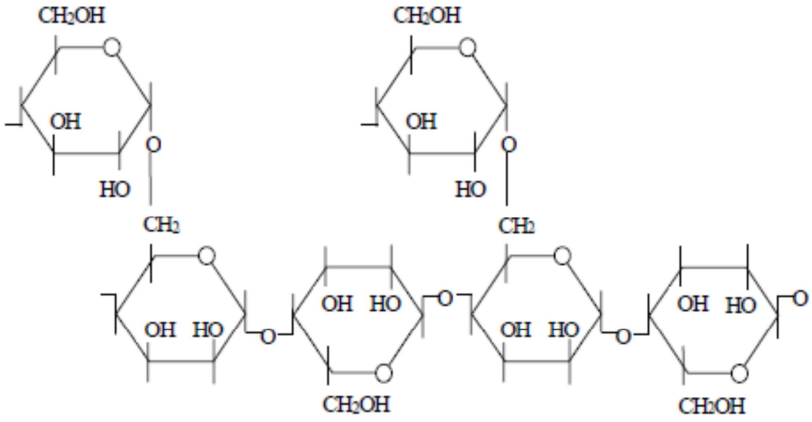


**Figure 2.15: Structure of a guar gum molecule**

## 2.5 Reagent Practice in the PGM Flotation Industry

South African platinum concentrators generally employ a mixture of collector reagents, usually xanthates and DTPs, in their reagent suites and have been doing so since the early 1970s [(Lotter, 2010), (Breytenbach et al., 2003)] when a di-iso-butyl DTP collector, also known as Aerofloat 3477, was introduced as a co-collector with SIBX. Wiese et al. (2005) investigated the role of DTP on a Merensky ore and concluded that DTP, when used in conjunction with xanthates, did not improve sulphide mineral recovery over and above the xanthate-only reagent suite. They did however show that the xanthate-

DTP collector mixture improved pyrrhotite recovery in the presence of copper sulphate activator. This was an important finding as pyrrhotite is reported to be a major carrier of PGEs for Merensky ores.

The Lac des Iles deposit in Canada contains the PGE minerals kotulskite, pallodoarsenide with lesser amounts of moncheite, sperrylite, telluropalladinite, vysotskite and stibiopalladinite. The base metal sulphides are, as is the case with the Merensky and UG 2 ores, associated with PGEs and are present in the ore as pyrite, chalcopyrite, pentlandite and pyrrhotite. The reagents used in the flotation plant are CMC for talc depression, PAX and di-iso-butyl DTP as collectors and MIBC as frother (Woodcock et al., 2007).

The Stillwater orebody in Montana (USA) contains the PGMs braggite, cooperite, moncheite, vysotskite and isoferroplatinum. The minerals braggite and cooperite hosts 67 % of the platinum while 25 % of the platinum occurs as metal alloy (isoferroplatinum). The remaining 8 % occurs as telluride (moncheite). Palladium largely occurs as solid solution in pentlandite. The main base metal sulphide minerals present are chalcopyrite and pentlandite (Xiao and Laplante, 2004). The flotation operations at Stillwater achieve a (Pt + Pd) recovery of between 93 and 95%. This recovery is attained at a concentrate grade of between 1800 and 2500 g/t (Pt + Pd). The flotation reagents used are 450 g/t CMC, 47 g/t PAX, 35 g/t di-iso-butyl DTP, NaHS (amount unspecified) and 275 g/t sulphuric acid. NaHS is used as a sulphidiser; sulphuric acid is used to reduce the pulp pH from 9.6 to 8.2 (Woodcock et al., 2007).

The Norilsk-Talnakh deposit in Russia is a high-grade nickel-copper sulphide ore deposit. The important base metal sulphides in the ore are chalcopyrite, pentlandite, cubanite and pyrrhotite. The PGEs are associated with the base metal sulphides and are present as isoferroplatinum, rustenburgite, atokite, sperrylite, cooperite, braggite, stibiopalladinite, vysotskite and sobolevskite (Xiao and Laplante, 2004). The flotation plant uses sodium di-iso-butyl DTP as collector and pine oil as frother in the copper flotation circuit whilst PEX and sodium dimethyl dithiocarbamate are used as collectors in the nickel flotation circuit (Woodcock et al., 2007).

## 2.6 Formulation of Work Strategy

The aim of this study is to investigate the role of diethyl DTP as a secondary collector in PGM flotation applications, i.e. the performance of a particular flotation reagent needed to be evaluated in a system involving at least two other flotation reagents. This system is complex as the variables are interactive and careful experimental planning and design is critical if one is to obtain meaningful experimental data. The choice of experimental system was flotation tests supplemented with two-phase froth column tests and particle surface analysis. Conducting reagent evaluation test work on a full scale flotation circuit is neither practical nor desirable because a decrease in circuit performance could result in dire financial losses. In addition, there is lack of control over the operational parameters on full plant scale which complicates data interpretation. The flotation tests were thus conducted batch-wise using a 3 litre modified Leeds flotation cell at constant air flow rate and pulp level.

It was considered to be important that the pulp effects be separated from the froth effects and therefore the batch flotation cell was fitted with froth monitoring technology. In addition, in order to determine if frothing behaviour was due to reagent chemistry effects or particle effects, tests were conducted in which the frothing behaviour of reagents in a two-phase froth column was studied and investigated. The effect of reagent type and quantity on pulp phase was studied by surface-analytical techniques (ToF-SIMS).

# Chapter 3: Experimental Details

Flotation tests were conducted using standard laboratory bench scale tests in order to investigate the effect of DTP collectors, either independently or in combination with xanthate collectors, on the recovery of copper, nickel, non-sulphide gangue, palladium and platinum from a South African PGM ore. Flotation performance was evaluated from the mass of solids and water recovered, the grades and recoveries of copper, nickel, palladium, platinum, the mass of total non-sulphide gangue recovered as well as the masses of floatable gangue and entrained gangue recovered. Furthermore, ToF-SIMS, which is an analytical technique that is used to identify the atomic or molecular species present on the surfaces of minerals, was used to measure the adsorption characteristics of DTP, either alone or in combination with SIBX, onto sulphide minerals. Finally, a two-phase froth column test rig was used to determine and compare the foam forming capabilities of DTP, SIBX and standard flotation frothers. This was carried out as it was considered important that the foam forming capabilities of the DTP collector be insignificant.



## 3.1 The Ore

A bulk Platreef ore sample, approximately 200 kg in mass, was delivered to the Centre for Minerals Research (CMR) for test work. The entire sample was screened using 3 mm and 15 mm aperture size screens. The minus 3 mm size fraction was immediately transferred to a sealable drum, the intermediate sizes cone crushed whilst the plus 15 mm pebbles were crushed in a jaw crusher in order to prepare them for cone crushing. This was followed by screening, using the 3 mm sized sieve, of the previously jaw and cone crushed products. Again, the minus 3 mm size fraction was transferred to the sealable drum, the crushing chamber diameter of the cone crusher reduced (when necessary) and the plus 3 mm fraction cone crushed. This procedure was repeated until the target particle size distribution, which was 100 % passing 3 mm, was attained. The crushed sample was then removed from the drum, blended, riffled and split into representative 1 kg portions using a rotary sample splitter.

## 3.2 Ore Milling

Milling was conducted using a 200 mm diameter Eriez stainless steel laboratory rod mill. The mill charge consisted of 20 stainless steel rods of varying diameter, as shown by Figure 3.1, a 1 kg ore sample and 500 ml synthetic plant water whilst the mill speed was set at 90 Hz. No reagents were added to the mill.

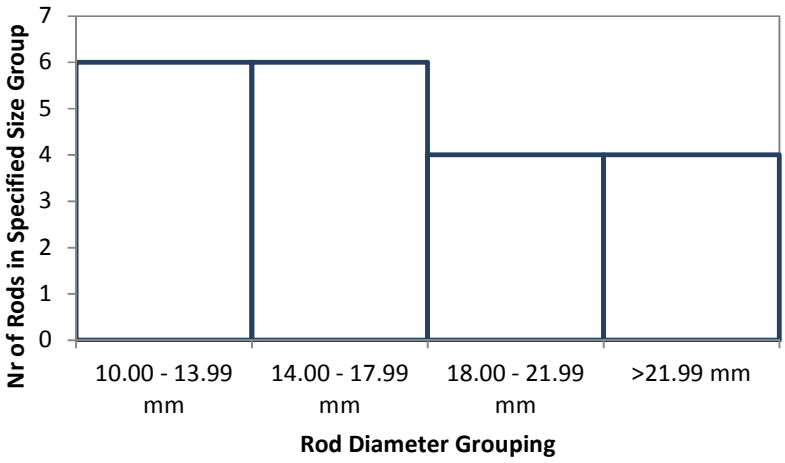


**Figure 3.1: A histogram showing the distribution of rod diameters used for milling**



Three 1 kg ore samples were wet milled for different time lengths in order to establish a milling curve (cf. Figure 3.2). The milling time required to achieve a flotation feed product with target size 85 % passing 75 µm, which was 35 minutes and 20 seconds, was then obtained from the milling curve. A fourth sample was then milled to the time required to achieve the 85 % passing 75 µm target size distribution. This sample was screened and the particle size distribution determined (cf. Figure 3.3).

Synthetic plant water was prepared by adding various chemical salts, which were all of analytical grade, to distilled water. All milling and flotation experiments were conducted using synthetic plant water. The ions present in the synthetic plant water are shown in Table 3.1.

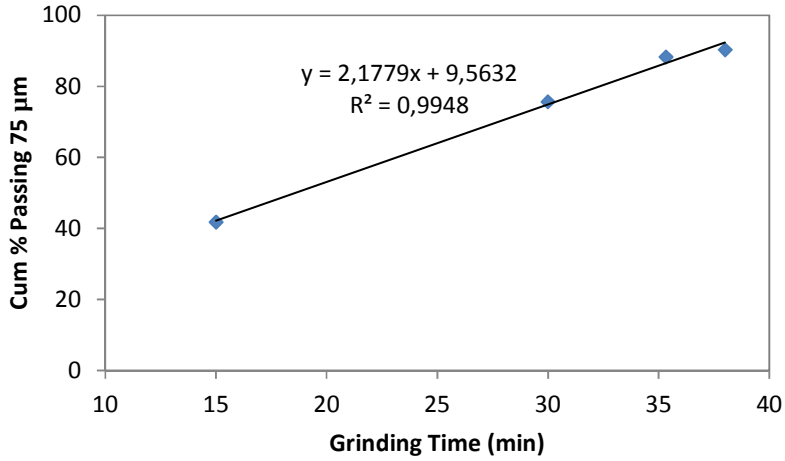


**Figure 3.2: The percentage of particles smaller than 75 µm obtained by milling to various time lengths**

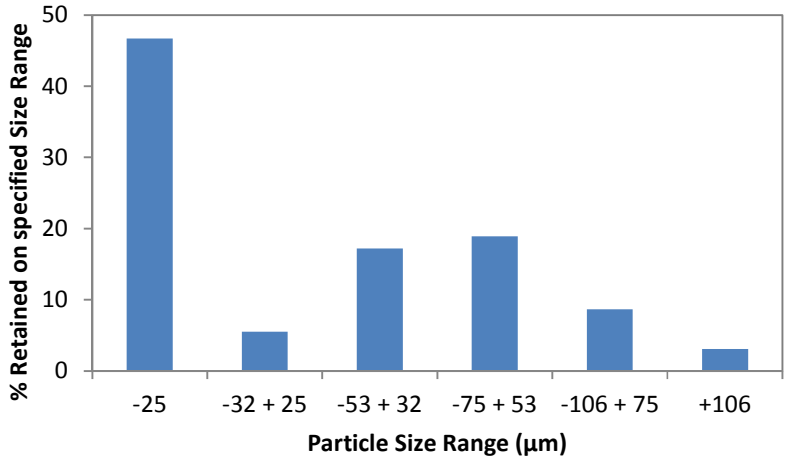


**Figure 3.3: The particle size distribution of the flotation feed**

**Table 3.1: The concentrations of ions present in the synthetic plant water**

| Ion | $Ca^{2+}$ | $Mg^{2+}$ | $Na^{+}$ | $Cl^{-}$ | $SO_4^{2-}$ | $NO_3^{-}$ | $NO_2^{-}$ | $CO_3^{2-}$ | TDS |
|---|---|---|---|---|---|---|---|---|---|
| **Concentration (ppm)** | 80 | 80 | 135 | 270 | 250 | 135 | 40 | 40 | 1030 |

## 3.3 Batch Flotation Tests

### 3.3.1 Flotation Reagents

In this study a polyglycol ether frother, Dowfroth 200, at a dosage of 40 g/t (or 2.00E-04 mole/kg), was used in the batch flotation tests. The collectors used in this study, as is shown in Table 3.2, were SEX, SIBX, diethyl DTP and di-iso-butyl DTP. All the collectors were supplied by Senmin.

**Table 3.2: List of collectors used in this study**

| Collector Name | Abbreviations used in this thesis | Molecular Weight (g/mol) | Molecular Structure |
|---|---|---|---|
| Sodium ethyl xanthate | SEX | 144 | $C_2H_5OCS_2Na$ |
| Sodium iso-butyl xanthate | SIBX | 172 | $C_4H_9OCS_2Na$ |
| Sodium diethyl dithiophosphate | diethyl DTP/di-E-DTP | 208 | $C_4H_{10}NaO_2PS_2$ |
| Sodium di-iso-butyl dithiophosphate | di-iso-butyl DTP/di-iso-B-DTP | 264 | $C_8H_{18}NaO_2PS_2$ |



The primary collectors, SEX and SIBX, were supplied as dry powders and were 88 % pure whilst the secondary collectors, diethyl DTP and di-iso-butyl-DTP, were supplied in liquid form and were 50 % pure. The collector samples were, at all times, stored in a refrigerator where the temperature was kept at approximately 5 $^{o}$C. Collector samples with solution strength 1 % (w/v) active content were freshly prepared daily using distilled water.

The depressant used in this study was Sendep 369, which is a modified guar gum supplied by Senmin. Guar gum solution was prepared on the day prior to flotation tests being conducted. The solution, which was set at 0.5 % concentration (w/v), was prepared by adding the guar very slowly to the centre of the vortex generated when water inside a glass beaker is briskly stirred by a magnetic stirrer. Stirring was maintained for four hours after which the beaker was covered with a suitable glass cover and allowed to stand for 24 hours. This allowed any insoluble compounds to settle at the bottom of the

glass beaker. The guar dosages used in the flotation experiments were 100 g/t and 500 g/t and these were calculated "as is" and thus was not corrected for active content. This depressant was characterised by the UCT Polymer Characterisation Laboratory and the results are shown in Table 3.3.

**Table 3.3: Sendep 369 depressant characterisation results**

| Sendep 369 Characterisation Results | | | |
|---|---|---|---|
| Molecular Weight (g/mol) | 383 947 | Purity, % | 89.3 |
| pH at 1.50 % concentration | 7.9 | % Insolubles | 25.0 |

### 3.3.2 General Batch Flotation Procedure and Analytical Techniques

On completion of the grinding stage, the milled slurry was transferred to a 3 litre capacity flotation cell, (cf. Figure 3.4), where the percentage solids was adjusted to approximately 35 % by adding sufficient synthetic plant water until the desired pulp level was attained.

**Figure 3.4: A photograph of a modified Leeds flotation cell (photograph by Dhliwayo, (2005))**

The parameters controlled were pulp level, impeller speed and volumetric air flow into the slurry. Pulp level was controlled manually by the addition of water when necessary to maintain a 20 mm froth height. This was possible because the sides of the flotation cell were Perspex which facilitated pulp level control. The impeller speed was adjusted to 1200 rpm once flotation began but was initially maintained at 900 rpm during the reagent conditioning stages whilst the air flow was maintained at 7 l/min throughout.

A feed sample was taken from the stirred slurry inside the flotation cell using a 60 ml capacity syringe before air or reagents were introduced into the slurry. Similarly, two tailings samples were taken using 60 ml capacity syringes at the end of each flotation test after the air to the cell was turned off. The collectors were added first and conditioned for two minutes while the frother was added last and also conditioned for two minutes. Concentrates were collected after 2, 5, 11 and 20 minutes of flotation time by scraping the froth into a collecting pan every 15 seconds. This flotation procedure is summarised in Tables 3.4 and 3.5. Table 3.4 shows the experimental procedure which was utilised when the collectors were added to the ore slurry simultaneously. This is sometimes referred to as the "pre-mixed" condition. Table 3.5, on the other hand, shows the experimental procedure which was followed when the collectors were added sequentially.



**Table 3.4: A summary of the flotation procedure followed the collectors were added simultaneously**

| Stage/Action | Start Time (min) | End Time (min) | Float Time (min) | Conditioning Time (min) | Collectors | | Frother |
|---|---|---|---|---|---|---|---|
| | | | | | Primary | Secondary | |
| Collect feed sample | - | - | - | - | - | - | - |
| Condition collectors | 0 | 2 | - | 2 | YES | YES | - |
| Condition frother | 2 | 4 | - | 2 | - | - | YES |
| Concentrate 1 | 4 | 6 | 2 | - | - | - | - |
| Concentrate 2 | 6 | 9 | 3 | - | - | - | - |
| Concentrate 3 | 9 | 15 | 6 | - | - | - | - |
| Concentrate 4 | 15 | 24 | 9 | - | - | - | - |
| Collect tailings samples | - | - | - | - | - | - | - |

**Table 3.5: A summary of the flotation procedure followed when collectors were added in sequence**

| Stage/Action | Start Time | End Time | Float Time | Conditioning Time | Collectors | | Frother |
|---|---|---|---|---|---|---|---|
| | (min) | (min) | (min) | (min) | Primary | Secondary | |
| Collect feed sample | - | - | - | - | - | - | - |
| Condition collector 1 | 0 | 1 | - | 1 | YES | - | - |
| Condition collector 2 | 1 | 2 | - | 1 | - | YES | - |
| Condition frother | 2 | 4 | - | 2 | - | - | YES |
| Concentrate 1 | 4 | 6 | 2 | - | - | - | - |
| Concentrate 2 | 6 | 9 | 3 | - | - | - | - |
| Concentrate 3 | 9 | 15 | 6 | - | - | - | - |
| Concentrate 4 | 15 | 24 | 9 | - | - | - | - |
| Collect tailings samples | | | | | | | |

The feed, concentrate and tailing samples obtained from the batch flotation tests were filtered, dried at 80 to 85 $^{o}$C oven temperature, and weighed prior to chemical analysis. All tests were done in duplicate and at the natural pH of the ore. The weighed and dried feeds, concentrates and tailings samples were analysed for copper, nickel and total sulphur. Copper and nickel assays were obtained using a Bruker S4 Explorer XRF spectrophotometer while the sulphur analyses were obtained using a Leco DR 423 sulphur analyser. PGE assays on selected samples were obtained from an external assay laboratory.



### 3.3.3 Analysis and Evaluation of Flotation Performance

#### *3.3.3.1 Concentrate Mass and Water Recovery*

Water recoveries were calculated by subtracting the mass of dry solids and water used for washing the scraper and cell lip from the mass of the slurry inside the collecting pan. The cumulative concentrate mass and water recovered relationship determines the froth phase characteristics and the extent of gangue flotation. At constant froth depth therefore, water recovery was used as an indicator of froth stability.

### *3.3.3.2 Copper and Nickel Grades and Recovery*

The most commonly presented result of a batch flotation test is the copper, nickel and PGE grade-recovery curves. The grade-recovery curves show the selectivity and efficiency of the flotation process obtained with various collector types and concentrations. The cumulative concentrate grade versus cumulative concentrate mass curves, which are equivalent to the grade-recovery curves in fact, shows whether any increased metal recovery obtained, when condition A is compared to condition B for example, occurred as a consequence of a pulp phase effect or froth phase effect. This is because any increase in recovery due to a true flotation effect, or a pulp phase effect, will be illustrated by an increase in concentrate grade per unit mass concentrate recovered. If, on the other hand, the increased recovery obtained occurred as a consequence of a froth phase effect, then concentrate grade versus concentrate mass plot for condition B will simply be an extension of the plot for condition A. This effectively means that the increased recovery obtained with condition B was achieved because of increased mass pull and therefore because of increased froth stability. The metal recovery versus water recovery plots also highlights the effect of the froth phase on recovery. Lastly, metal recovery versus flotation time plots are used as they highlight the effect of various flotation conditions on the rate of flotation.



### *3.3.3.3 Calculation of Floating (FG) and Entrained Gangue (EG)*

The procedure utilised in this study to determine the proportions of floatable and non-floatable gangue reporting to the concentrate by either true flotation or mechanical entrainment was developed by Wiese (2009). In this procedure three basic assumptions are made: (i) the sulphide minerals in the concentrate samples have an average sulphur content of 36.45 %, (ii) all or nearly all floatable gangue is depressed at 500 g/t depressant dosage and therefore the only gangue reporting to the concentrate at such a high depressant dosage is entrained gangue and (iii) all sulphide minerals are fully liberated from the gangue. The sulphide content of each sample is obtained by multiplying the sulphur assay with the mass of that particular concentrate sample and dividing this by the average assumed sulphur content. The total mass of gangue in the concentrate is then simply the mass of the concentrate minus the mass of the sulphide minerals. Finally, the gradient of the curve given by the total gangue versus water

recovery at a 500 g/t depressant dosage is used to determine the entrainment factor. This entrainment factor is used to calculate the mass of gangue reporting to the concentrate at 0 g/t depressant dosage and at the 100 g/t depressant dosage. This procedure is summarised for convenience in the form of a flow diagram in Figure 3.5.

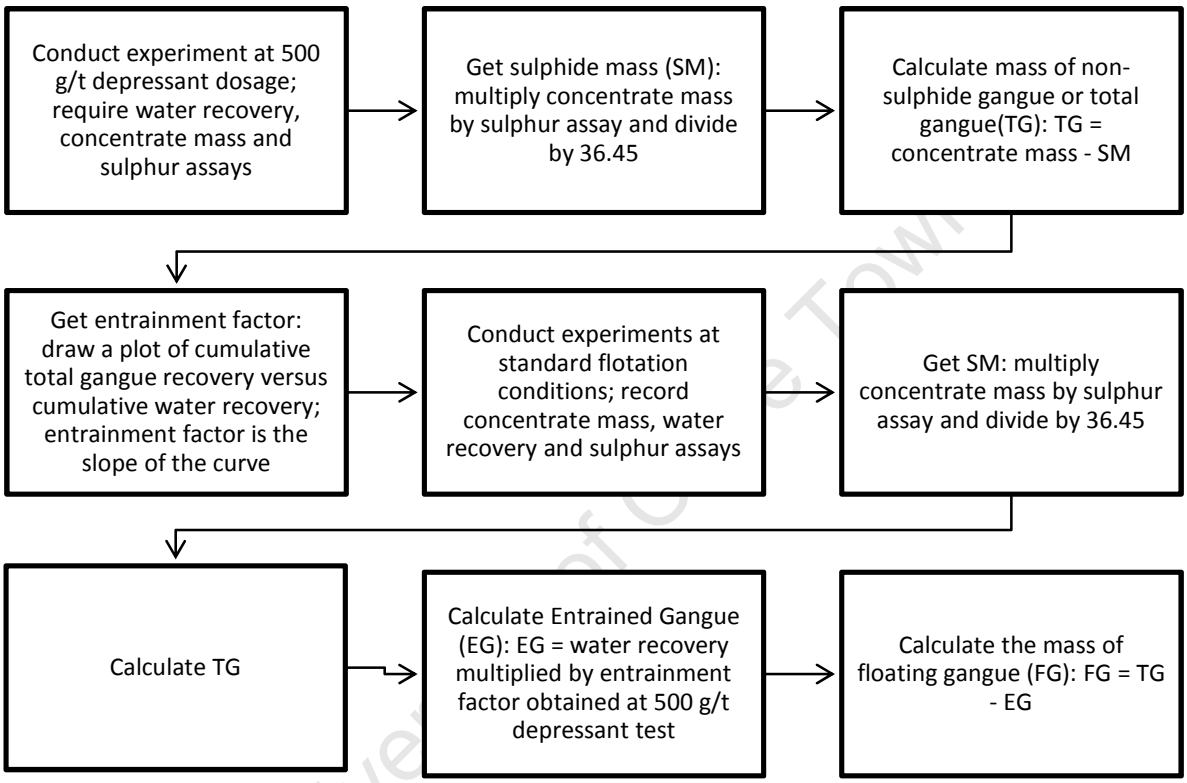


**Figure 3.5: Schematic illustrating the procedure used to calculate and separate the entrained and floating gangue**

### *3.3.3.4 Froth Surface Image Recording*

The surface of the froth for selected batch flotation tests was monitored and recorded using a froth camera. Figure 3.6 shows a schematic of the experimental set-up, i.e. it consists of a video camera to capture the image; the camera is built inside a waterproof housing and is surrounded by a ring of LEDs

to provide consistent illumination, a video recorder to save the images onto a moveable storage device and the machine vision software which is used to convert video images into meaningful numbers such as average bubble diameter.

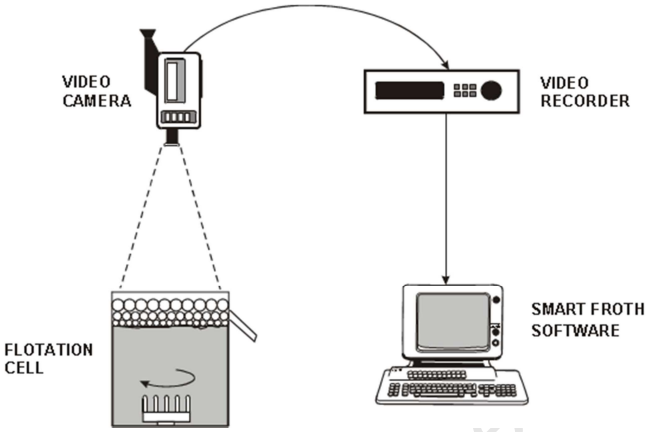


**Figure 3.6: Experimental setup for froth imaging (Oostendorp, 2003)**



## 3.4 Frothing Tests

The frothability of various collectors was investigated and compared to that which was obtained with standard frothers using a two-phase froth column test rig. The aim of these experiments was to determine the frothability of diethyl DTP. This was considered important because it was intended that the collector should not possess frothing properties.

### 3.4.1 The Test Rig

A schematic illustrating the principle of operation of the froth column is shown in Figure 3.7. The test rig used in this study was similar in design to that which is shown in Figure 3.7. The Perspex column had an internal diameter of 44 mm and total height 1700 mm. The air flow rate to the column was controlled

by a 0 – 3 l/min capacity air flow meter and the air pressure, which was set at 200 kPa, was controlled by a pressure regulator. Air passed into the froth column through a sparger of unknown pore size which was fitted to the bottom of the froth column.

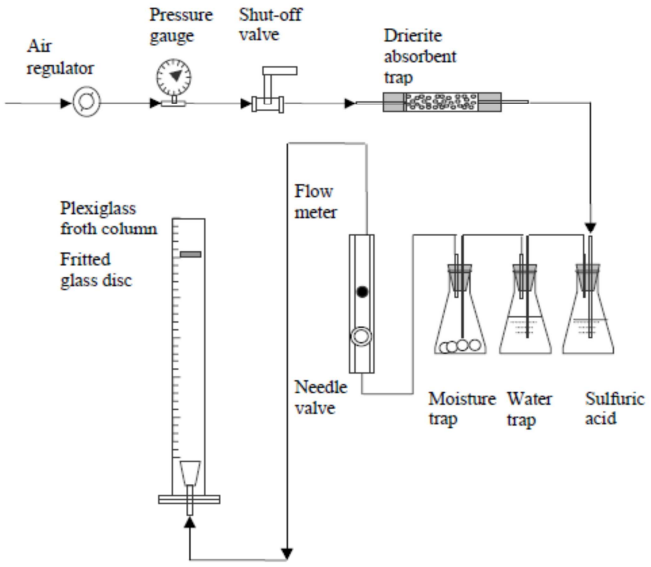


**Figure 3.7: Schematic diagram of a typical froth column (Xia, 2000)**

### 3.4.2 Experimental Procedure

A known volume of distilled water dosed with known concentration of reagent(s) was introduced into the column and the "*zero height*" or the height the liquid reached was marked (cf. Figure 3.8). Air, at a controlled flow rate, was then introduced into the column via a sparger situated at the bottom of the column. The tests were conducted at 0.5, 1.0, 1.5 and 2.0 l/min air flow rates for each condition tested. Once air was introduced into the column a froth, which increased in thickness with time until an equilibrium foam height was reached, formed at the top of the liquid. The equilibrium condition was reached when the rate of bubble collapse at the top of froth is matched by the rate at which air is supplied through the sparger. The time required to establish this equilibrium condition was three

minutes. The final froth height, which is also called the equilibrium froth height, was measured once froth equilibrium was attained.

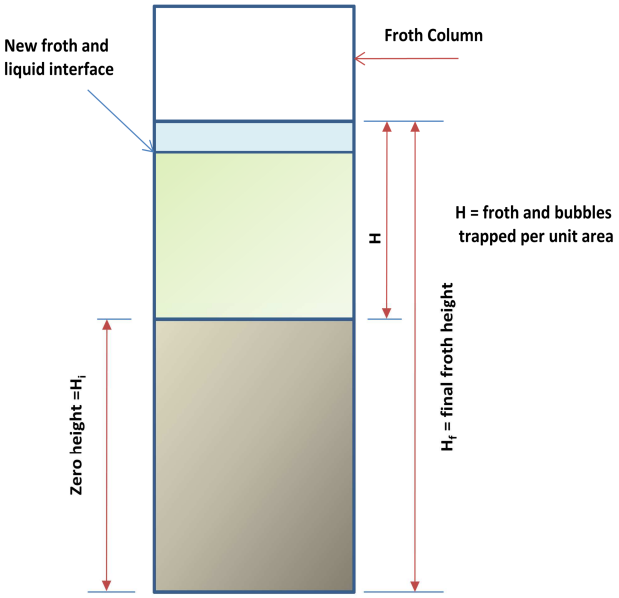


**Figure 3.8: The froth and liquid interfaces in a froth column (reproduced from Xia (2000))**

All experiments were completed at room temperature, in duplicate and in equivalent molar concentrations of the various reagents tested. In addition, all tests were conducted using distilled water. Distilled water was chosen over synthetic plant water because it was considered important that the test work be completed in the absence of any chemical species which may or may not contribute to either froth enhancement or a reduction in froth stability. The reagents tested were diethyl DTP, di-iso-butyl DTP, SIBX, Dowfroth 200, Dowfroth 250, Senfroth 7, Senfroth 20 and Betafroth 206. The test involving SIBX, since this is a collector which is known to have no frothing forming properties, was interpreted as the control experiment. The froth column was removed from the rig between experiments, cleaned with a KCl solution, and flushed with large volumes of pressurised water in order to remove any reagent solution which may have adhered onto the walls of the cylinder.

### 3.4.3 Performance Evaluation

The froth height, *H*, which is defined as the summation of the froth and bubbles trapped in the liquid per unit cross-sectional area of the column, was used as a measure of the frothability or "frothing power" of the solutions of solvents at different concentrations and aeration rates. This is expressed, as is shown in the schematic in Figure 3.8, as:

$$H = H_f - H_i$$

Curves are fitted which express froth height (*H*) as a function of air flow rate and solvent concentration.



## 3.5 Time of Flight Secondary Ion Mass Spectroscopy (ToF-SIMS)

In mineral processing terms, ToF-SIMS is an analytical technique that is used to identify the atomic or molecular species present on the surfaces of minerals (Shackleton, 2007c). The technique was used in this study in order to investigate collector adsorption onto sulphide minerals in the case of collector mixtures as opposed to the single collector reagent suite. Specifically, two key questions that needed to be answered were: (i) does diethyl DTP adsorb onto the sulphide minerals present in the ore at the standard conditions used for batch flotation tests and, if yes, (ii) does diethyl DTP adsorption onto sulphide minerals increase in the presence of SIBX?

### 3.5.1 General Technique Description

Highly energetic and pulsed primary ions, typically liquid metal ions such as $Ga^+$ and $Cs^+$, are used to bombard the surface of the sample. This results in atomic and molecular ions being dislodged and discharged from the outermost surface of the sample. The free ions (*secondary* particles), since they are

charged, are then electrostatically accelerated in a flight path towards the detector, which is a mass spectrometer. The machine is able to record the time difference between impact and detection, i.e. the *time-of-flight*. Less dense ions arrive earlier at the detector compared to heavier ions. The major limitations of ToF-SIMS are: (i) this technique can only give semi-quantitative results, (ii) a large number of grains need to be analysed for statistical reproducibility which is both costly and time consuming (Lascelles and Finch, 2005).

### 3.5.2 Experimental Procedure

Milled pulp was conditioned for two minutes with various collector reagents suites in a flotation cell, i.e. SIBX only, diethyl DTP only, or a mixture of the collectors. In the case of the mixture of collectors, the SIBX was added and conditioned for two minutes ahead of the diethyl DTP. After conditioning was completed, a sample of the conditioned pulp was taken using a 200 ml glass beaker and screened using 106 µm and 38 µm aperture size screens. When necessary, a minimal amount of synthetic plant water was used to aid the screening process. The +38-106 µm fraction was removed and transferred into a holding container, which was sealed under argon, and stored in a freezer for up to 24 hours. This was necessary because it was not possible to complete the experiments in one day. When ready, the samples were removed from the freezer and dried using argon gas after which 40 sulphide grains were picked with the aid of an optical microscope. The grains, resting on an aluminium and sticky-tape base, were then transferred to the instrument for surface analysis.



Surface analysis of the minerals was carried out using a PHI TRIFT IV ToF-SIMS instrument operating in the static SIMS regime. Throughout the study a 30kV, 100µm-$Au_1$ bunched cluster beam with charge compensation was used. The grains were imaged and analysed for K, Si, Na, Ca, Mg, Al, Fe, Ni and Cu during positive ion analysis and S, O, OH, Cl, DTP and xanthate during negative ion analysis. The data obtained were evaluated using Statistica. The intensities obtained are normalised for the elements of interest and presented as percent normalised yield.

# Chapter 4: Results

This chapter describes the results of batch flotation tests conducted to investigate the effect of collector type and dosage on the recovery of both valuable and gangue components of the ore described in Chapter 3. It begins in Section 4.1 with a description of the distribution of elemental copper, nickel and sulphur as a function of particle size in the flotation feed. Detailed mineralogical reports are then provided which show the type and quantity of minerals present in the ore. This is followed, in Section 4.2, with batch flotation test reproducibility results. In Sections 4.3 to 4.6 the results of the batch flotation tests are shown whilst in Section 4.7 recovery as a function of particle size data are provided. In the final section of this chapter, Section 4.8, the results of surface analysis (ToF-SIMS) tests are presented.

## 4.1 Feed Characterisation

As explained in Chapter 3.3, a composite flotation feed sample was screened into different particle size fractions; each fraction was then assayed for copper, nickel and sulphur. The results obtained, shown in Figure 4.1, indicated that more than two-thirds of the copper and nickel containing minerals were present in the finest size fraction, i.e. less than 25 µm. This is notable as it indicates that fine particle size recovery will be important if valuable mineral recovery is to be optimised. The chart however also emphasises that a significant proportion of valuable sulphides are also present in the coarser fraction, i.e. > 75 µm, and therefore that coarse particle recovery is still important.

Table 4.1 shows that the main gangue minerals present in the ore are the enstatites, feldspars and diopsides (Shackleton, 2009). This mineralogical report furthermore indicates that the (i) talc content of the ore was minimal, (ii) serpentine content was much higher compared to the Merensky and UG2 reefs (Shamaila and O'Connor, 2008) and (iii) the BMS content of the ore is approximately 2 % (by weight). In Table 4.2 it is shown that, with respect to PGM mineralisation, nearly 75 % (by area) of the PGMs present in the ore occur as tellurides and arsenides while the remaining 25 % consists mostly of metal

alloys and PGM-sulphides (Chapman, 2010). This is a significant result because it indicates that, if the PGMs are liberated from their sulphide and silicate hosts, then PGM recovery will not be maximised by optimising sulphide recovery only.

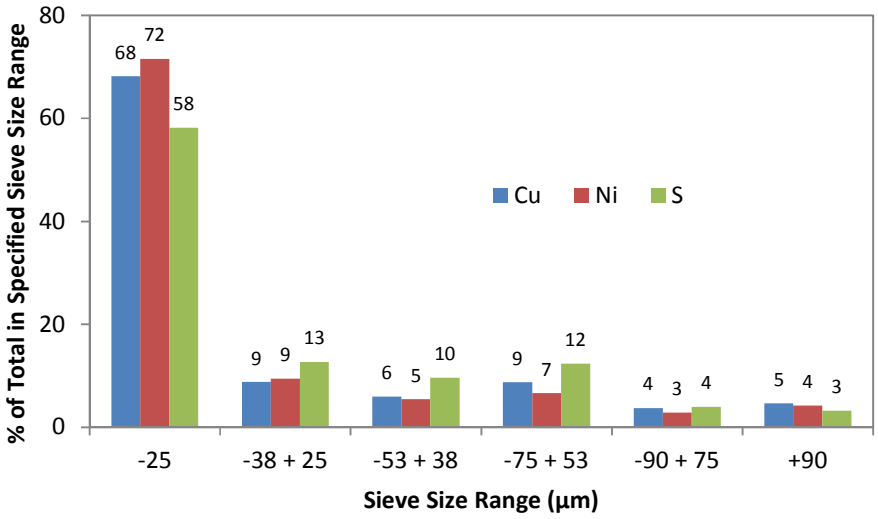


**Figure 4.1: Mass distribution of elements copper, nickel and sulphur in the various particle size fractions of the flotation feed**

**Table 4.1: Ore bulk mineralogy (Shackleton, 2009)**

| Ore Bulk Mineralogy | | | |
|---|---|---|---|
| **Mineral** | **Composition (%)** | **Mineral** | **Composition (%)** |
| Enstatite | 39.1 | Diopside | 15.1 |
| Feldspar | 18.4 | Serpentine | 6.9 |
| Chlorite | 8.2 | Amphibole | 3.0 |
| Talc | 0.8 | Mica | 0.8 |
| Iron Oxides | 0.5 | Other Silicates | 2.4 |
| BMS | 2.1 | Other | 2.7 |

**Table 4.2: The distribution of PGMs in the ore sample (Chapman, 2010)**

| Distribution of PGMs in Ore | | | |
|---|---|---|---|
| **Mineral** | **Area (%)** | **Mineral** | **Area (%)** |
| Pt-sulphide | 9.1 | Pd-arsenide | 0.0 |
| PtPd-sulphide | 3.1 | Ferroplatinum | 6.1 |
| PtRh-sulphide | 0.8 | Pt-alloys | 7.6 |
| Pt-telluride | 30.9 | Pd-alloys | 7.6 |
| Pd-telluride | 15.5 | PGE-sulparsenides | 2.4 |
| Pt-arsenide | 12.8 | Gold | 4.0 |

## 4.2 Batch Flotation Tests Reproducibility

Batch flotation tests were conducted in duplicate in order to determine the standard error associated with a particular result. The standard error, which was obtained by dividing the sample standard deviation by the square root of the sample size, was used as a guide in order to evaluate the reproducibility of the data. In other words, in order for a set of tests to be considered reproducible, the data points had to be within accepted standard error for all the parameters which were considered important. The important parameters which needed to be monitored were concentrate mass, water recovery, concentrate assay and metal recovery. In Section 4.3 it is demonstrated that the standard errors for the aforementioned parameters are minimal. It is important to remember that the confidence level of any particular standard error value was 75 % for all the standard errors reported.



### 4.2.1 Pure Xanthate Batch Flotation Tests

#### *4.2.1.1 Concentrate Mass and Water Recovery*

Table 4.3 summarises the total concentrate mass and water recoveries as well as the standard errors for the “xanthate only” tests. As a general rule of thumb, the standard error for water recovery should not exceed 50 g in batch flotation tests where a 1 kg ore sample and a 3 litre flotation cell are used.

Similarly, with respect to the concentrate mass, the standard error for concentrate mass should not exceed 5 g under the same flotation conditions. All the tests are within this error limit and the tests can therefore, from the point of view of concentrate mass recovery and water recovery at least, be regarded as reproducible and within standard error.

Figure 4.2 shows that the mass of concentrate recovered increased with an increase in SIBX collector dosage. Similarly, Figure 4.3 shows that there was an increase in water recovery when SIBX collector dosage was increased. An increase in water recovery is usually associated with an increase in froth stability and also an increase in the carrying capacity of the froth, i.e. one expects that more gangue particles will be entrained in the froth which will lead to an increase in concentrate mass. When the abovementioned figures are compared, it is noted that an increase in water recovery is associated with an increase in solids recovery. Therefore, not only are the errors minimal, but the trends are consistent with expectations, which gives further credibility to the experimental data.



**Table 4.3: A summary of concentrate mass and water recoveries as well as the standard error for these parameters for the "xanthate only" batch flotation tests**

| Reagent Suite | Total Concentrate Mass (g) | | | | Total Water Recovered (g) | | | |
|---|---|---|---|---|---|---|---|---|
| **2.00E-04 mole/kg[#] D200 + *x*** | **Test 1** | **Test 2** | **Ave** | **Std Error** | **Test 1** | **Test 2** | **Ave** | **Std Error** |
| *x* = 1.02E-04 mole/kg SIBX | 71.6 | 70.7 | 71.1 | 0.44 | 403.4 | 376.3 | 389.9 | 13.6 |
| *x* = 3.07E-04 mole/kg SIBX | 71.4 | 69.4 | 70.4 | 0.98 | 386.3 | 406.9 | 396.6 | 10.3 |
| *x* = 4.09E-04 mole/kg SIBX | 78.7 | 72.4 | 75.6 | 3.19 | 525.4 | 451.3 | 488.4 | 37.1 |
| *x* = 5.12E-04 mole/kg SIBX | 85.0 | 77.2 | 81.1 | 3.93 | 553.9 | 511.0 | 532.6 | 21.5 |
| *x* = 4.09E-04 mole/kg SEX | 92.0 | 86.4 | 89.2 | 2.81 | 571.6 | 515.0 | 543.3 | 28.3 |

[#] refers to the concentration of reagent within the flotation pulp, i.e. for frother the concentration used in these experiments was 2.00E-04 mole of frother per 1 kg of ore sample. In the case of the graphs presented from here onwards the term "MOL" is used; this refers to the molar dosage of reagent which was added to the flotation pulp; the terms effectively are equivalent.

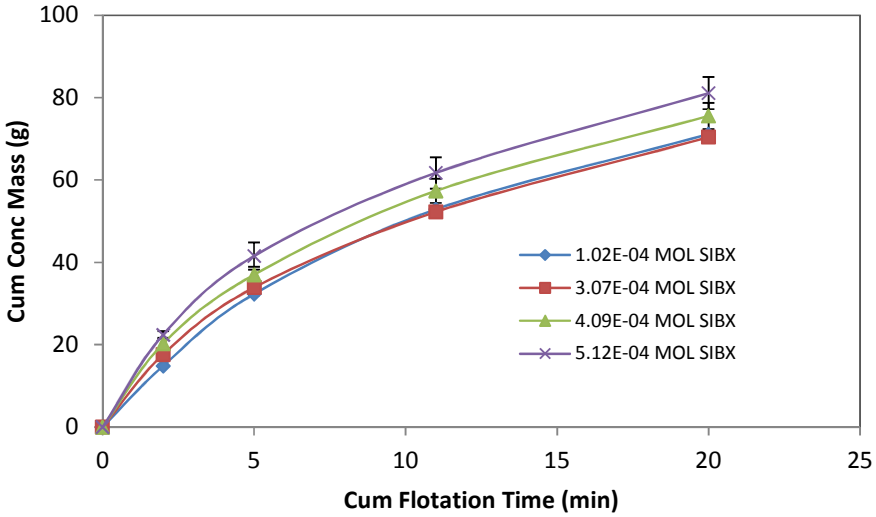


**Figure 4.2: The cumulative mass of concentrate presented as a function of cumulative flotation time for batch flotation tests with increasing SIBX collector dosage**

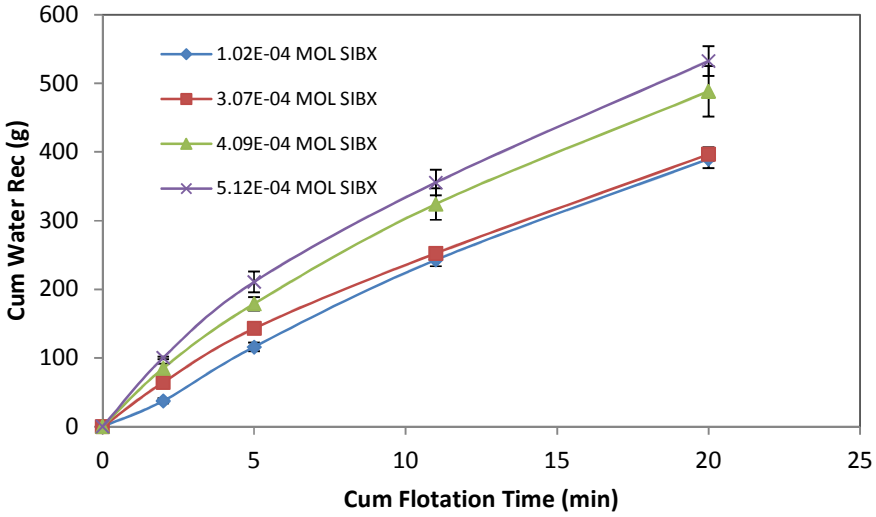


**Figure 4.3: The cumulative water recovery presented as a function of cumulative flotation time for batch flotation tests with increasing SIBX collector dosage**

### *4.2.1.2 Concentrate Copper and Nickel Assays*

Table 4.4 shows the copper and nickel final concentrate grades, standard errors and relative standard errors for the "xanthate only" batch flotation test results at different xanthate dosages. It shows that the maximum standard error of the copper grade does not exceed 0.04 whilst the maximum error of the nickel grade is 0.09. The relative standard error, which is defined as the standard error divided by the sample average, and is expressed as a percentage, is less than 5 % for both the copper and nickel assays. This is well below the generally accepted relative standard error, which is 30 % (Klein et al., 2010), above which data should not be considered reliable. The standard error and relative standard error data in Table 4.4 therefore shows that the concentrate grade results are consistent and repeatable.

**Table 4.4: A summary of the standard error associated with the copper and nickel assays for the "xanthate only" batch flotation tests**

| Reagent Suite | % Cu in Conc | | | % Ni in Conc | | |
|---|---|---|---|---|---|---|
| **2.00E-04 mole/kg D200 + *x*** | **Ave** | **Std Error** | **Rel Std Error** | **Ave** | **Std Error** | **Rel Std Error** |
| *x* = 1.02E-04 mole/kg SIBX | 1.68 | 0.03 | 1.79 % | 3.53 | 0.00 | 0.00 % |
| *x* = 3.07E-04 mole/kg SIBX | 1.92 | 0.01 | 0.52 % | 3.48 | 0.04 | 1.15 % |
| *x* = 4.09E-04 mole/kg SIBX | 1.50 | 0.04 | 2.67 % | 3.21 | 0.09 | 2.80 % |
| *x* = 5.12E-04 mole/ kg SIBX | 1.50 | 0.01 | 0.67 % | 3.15 | 0.05 | 1.59 % |



Figure 4.4 shows the cumulative copper and nickel grades as a function of cumulative concentrate mass for a particular test taken from Table 4.4. It is added here to illustrate that errors in both the copper and nickel grades were minimal for all four concentrates for this particular test. The dotted line represents the average of the two tests. Each data point for the "average plot" has an error bar which indicates the standard error for that particular data point (when the error bar is not visible then it means that the error bar is smaller than the icon). It is important to note that no data point is outside the error bar range and therefore the tests, from the point of view of assay error, are considered to be reproducible. Furthermore, it is important to note that when Tables 4.3 and 4.4 are compared, the results showed a decrease in concentrate grade with an increase in water recovery. This is the expected trend because a greater water recovery increases mass pull and therefore decreases selectivity. Therefore, not only are

the assay errors minimal, but the trends are consistent across the various tests. Thus, in summary, the results can be considered to be adequately reproducible.

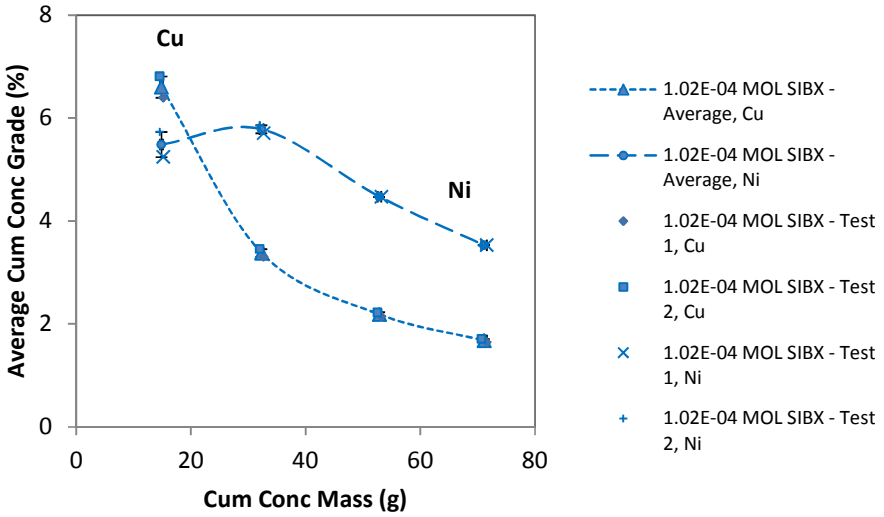


**Figure 4.4: The cumulative copper and nickel content of the concentrate for two independent tests as well as the average of the two tests when the SIBX dosage was 1.02E-04 mole/kg**



### *4.2.1.3 Copper and Nickel Recovery*

Table 4.5 shows that the recovery error was less than 1 % for both copper and nickel recovery except in the case where $x$ = 4.09E-04 mole/kg SIBX. The relative standard error was also less than 1 % for all tests except the case where $x$ = 4.09E-04 mole/kg SIBX. In that case the standard recovery errors and the relative standard error were 2.31 % and 3.79 % respectively for the nickel recovery which was still considered acceptable.

Figure 4.5 shows the cumulative copper and nickel recovery plots as a function of cumulative flotation time for a particular test from Table 4.5. The dotted line represents the average of the two tests. As was the case in Figure 4.4, each data point from the average plot has an error bar associated with it.

This error bar indicates the standard error for that particular data point. It is important to note that no data point is outside the error bar range and therefore the tests are considered reproducible.

**Table 4.5: A summary of copper and nickel recovery standard errors for the "xanthate only" batch flotation tests**

| Reagent Suite | % Cu Rec (final recovery) | | | % Ni Rec (final recovery) | | |
|---|---|---|---|---|---|---|
| **2.00E-04 mole/kg D200 + *x*** | **Ave** | **Std Error** | **Rel Std Error** | **Ave** | **Std Error** | **Rel Std Error** |
| *x* = 1.02E-04 mole/kg SIBX | 73.2 | 0.30 | 0.41 % | 59.9 | 0.00 | 0.00 % |
| *x* = 3.07E-04 mole/kg SIBX | 75.8 | 0.07 | 0.09 % | 59.6 | 0.28 | 0.47 % |
| *x* = 4.09E-04 mole/kg SIBX | 72.0 | 0.06 | 0.08 % | 61.00 | 2.31 | 3.79 % |
| *x* = 5.12E-04 mole/ kg SIBX | 73.3 | 0.67 | 0.91 % | 63.2 | 0.16 | 0.25 % |

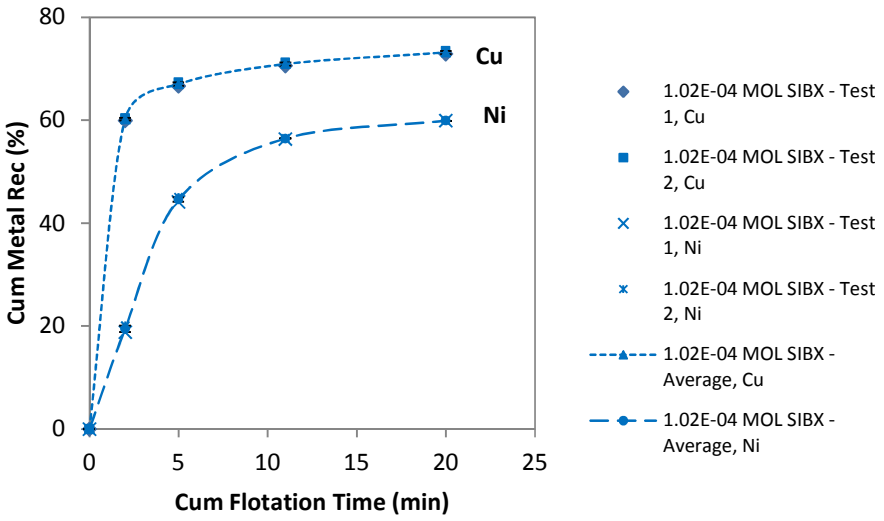


**Figure 4.5: Cumulative recovery of copper and nickel as a function of cumulative flotation time showing test repeatability and error bars for a particular test taken from Table 4.5**

### 4.2.2 Pure DTP Batch Flotation Tests

#### *4.2.2.1 Concentrate Mass and Water Recovery*

Table 4.6 summarises the average concentrate mass and water recoveries as well as the standard errors for the tests completed using only diethyl DTP as a collector. All the tests were within the recommended water and concentrate recovery error limits (cf. Section 4.3.2.1) and it was therefore concluded that the data was adequately reproducible. A comparison of the standard errors in Tables 4.3 and 4.6 reveals that the concentrate mass error for the "diethyl DTP" tests was larger when compared to the "xanthate only" tests. This is to be expected however since a significant amount of additional water was recovered here.

**Table 4.6: A summary of concentrate mass and water recoveries as well as the standard error for "diethyl DTP only" batch flotation tests**

| Reagent Suite | Concentrate Mass (g) | | Water Recovery (g) | |
|---|---|---|---|---|
| **2.00E-04 mole/kg D200 + *y*** | **Ave** | **Std Error** | **Ave** | **Std Error** |
| *y* = 9.62E-05 mole/kg di-E-DTP | 85.5 | 1.16 | 706.9 | 3.33 |
| *y* = 3.07E-04 mole/kg di-E-DTP | 105.6 | 2.07 | 939.6 | 32.94 |
| *y* = 4.09E-04 mole/kg di-E-DTP | 105.3 | 2.00 | 936.5 | 16.56 |



#### *4.2.2.2 Concentrate Copper and Nickel Assays*

Table 4.7 lists the copper and nickel concentrate grade errors for the "diethyl DTP only" batch flotation test results and shows that the maximum copper standard error did not exceed 0.04 whilst the maximum nickel error was higher – this was consistent with the "xanthate only tests". Furthermore, as can be seen from Figure 4.6, which shows the cumulative copper and nickel grades as a function of cumulative concentrate mass for a particular test taken from Table 4.7, the data points for the average plots are within standard error. In summary therefore, the assay results are consistent and repeatable.

**Table 4.7: A summary of standard errors associated with copper and nickel assays for the "diethyl DTP only" batch flotation tests**

| Reagent Suite | % Cu in Conc | | | % Ni in Conc | | |
|---|---|---|---|---|---|---|
| **2.00E-04 mole/kg D200 + *y*** | **Ave** | **Std Error** | **Rel Std Error** | **Ave** | **Std Error** | **Rel Std Error** |
| *y* = 9.62E-05 mole/kg di-E-DTP | 1.51 | 0.04 | 2.65 % | 1.38 | 0.10 | 7.25 % |
| *y* = 3.07E-04 mole/kg di-E-DTP | 1.23 | 0.02 | 1.63 % | 1.83 | 0.02 | 1.09 % |
| *y* = 4.09E-04 mole/kg di-E-DTP | 1.26 | 0.04 | 3.17 % | 1.80 | 0.05 | 2.78 % |

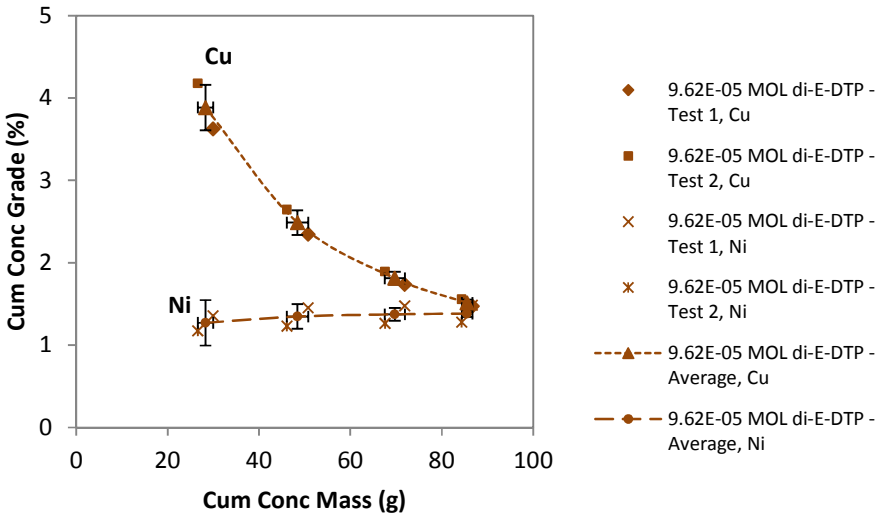


**Figure 4.6: The cumulative copper and nickel content of the concentrate for two independent tests as well as the average of the two tests when the diethyl DTP dosage was 9.62E-05 mole/kg**

### *4.2.2.3 Copper and Nickel Recovery*

Table 4.8 shows that the recovery standard error was less than 1 % for the copper recovery tests and less than 2 % for the nickel recovery tests. The cumulative copper and nickel recovery plots represented as a function of cumulative time for the test condition where *y* = 9.62E-05 mole/kg di-E-DTP is shown in Figure 4.7. This figure indicates that both the copper and nickel recovery errors were minimal for all four concentrates for this particular test.

**Table 4.8: A summary of standard errors associated with copper and nickel recovery for the "diethyl DTP only" batch flotation tests**

| Reagent Suite | % Cu Rec (final recovery) | | | % Ni Rec (final recovery) | | |
|---|---|---|---|---|---|---|
| **2.00E-04 mole/kg D200 + *y*** | **Ave** | **Std Error** | **Rel Std Error** | **Ave** | **Std Error** | **Rel Std Error** |
| *y* = 9.62E-05 mole/kg di-E-DTP | 75.0 | 0.61 | 0.81 % | 28.6 | 1.62 | 5.66 % |
| *y* = 3.07E-04 mole/kg di-E-DTP | 75.7 | 0.28 | 0.37 % | 46.2 | 0.65 | 1.41 % |
| *y* = 4.09E-04 mole/kg di-E-DTP | 76.2 | 0.44 | 0.58 % | 46.3 | 1.93 | 4.17 % |

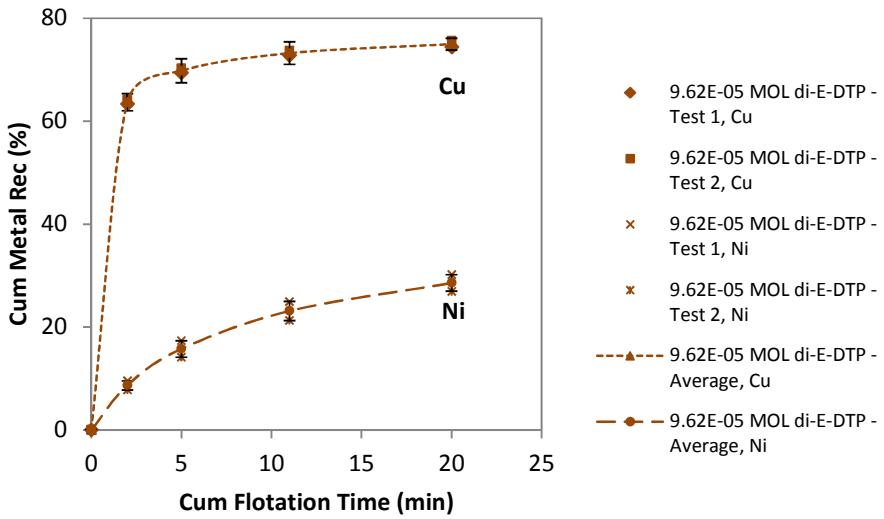


**Figure 4.7: Cumulative recovery of copper and nickel as a function of cumulative flotation time showing test repeatability and error bars for a particular test taken from Table 4.8**

### 4.2.3 Collector Mixtures

#### *4.2.3.1 Concentrate Mass and Water Recovery*

Table 4.9 summarises the total concentrate mass and water recoveries as well as the standard errors for the "collector mixtures" tests. The table indicates that the water error was relatively large for the test where *z* = {4.09E-04 mole/kg [90 % SIBX + 10 % di-E-DTP]} whilst the mass error was relatively large for

test where *z* = {3.49E-04 mole/kg [59 % SIBX + 41 % di-E-DTP]}. Therefore, even though the water recovery error was less than 50 g for these tests, the concentrate grade and recovery errors need to be considered before these tests can be classified adequately reproducible.

**Table 4.9: A summary of concentrate mass and water recoveries as well as the standard error for these parameters for the "collector mixture" batch flotation tests**

| Reagent Suite | Total Concentrate Mass (g) | | | | Total Water Recovered (g) | | | |
|---|---|---|---|---|---|---|---|---|
| 2.00E-04 mole/kg D200 + *z* | Test 1 | Test 2 | Ave | Std Error | Test 1 | Test 2 | Ave | Std Error |
| *z* = 4.09E-04 mole/kg, 76 % SIBX, 24 % di-E-DTP | 86.2 | 86.5 | 86.3 | 0.13 | 581.8 | 608.1 | 595.0 | 13.2 |
| *z* = 4.09E-04 mole/kg, 90 % SIBX, 10 % di-E-DTP | 72.0 | 66.7 | 69.4 | 2.64 | 449.7 | 369.3 | 409.5 | 40.2 |
| *z* = 4.57E-04 mole/kg, 89 % SIBX, 11 % di-E-DTP | 74.4 | 77.1 | 75.7 | 2.53 | 440.4 | 486.3 | 463.4 | 7.00 |
| *z* = 3.49E-04 mole/kg, 59 % SIBX, 41 % di-E-DTP | 85.8 | 77.3 | 81.6 | 4.25 | 551.5 | 486.8 | 519.2 | 32.4 |

### *4.2.3.2 Concentrate Copper and Nickel Assays*

Table 4.10 shows the copper and nickel grade errors for the "collector mixture" series of batch flotation tests. The table shows that the maximum copper grade standard error was equal to 0.10 % whilst the maximum nickel grade error was somewhat higher but still less than 0.2 %.

**Table 4.10: A summary of standard errors associated with copper and nickel concentrate grades for the "collector mixture" batch flotation tests**

| Reagent Suite | % Cu in Conc | | | % Ni in Conc | | |
|---|---|---|---|---|---|---|
| 2.00E-04 mole/kg D200 + *z* | Ave | Std Error | Rel Std Error | Ave | Std Error | Rel Std Error |
| *z* = 4.09E-04 mole/kg, 76 % SIBX, 24 % di-E-DTP | 1.37 | 0.02 | 1.46 % | 2.86 | 0.04 | 1.40 % |
| *z* = 4.09E-04 mole/kg, 90 % SIBX, 10 % di-E-DTP | 1.79 | 0.07 | 3.91 % | 3.48 | 0.16 | 4.60 % |
| *z* = 4.57E-04 mole/kg, 89 % SIBX, 11 % di-E-DTP | 1.62 | 0.10 | 6.17 % | 3.24 | 0.17 | 5.25 % |
| *z* = 3.49E-04 mole/kg, 59 % SIBX, 41 % di-E-DTP | 1.60 | 0.02 | 1.25 % | 3.01 | 0.02 | 0.66 % |

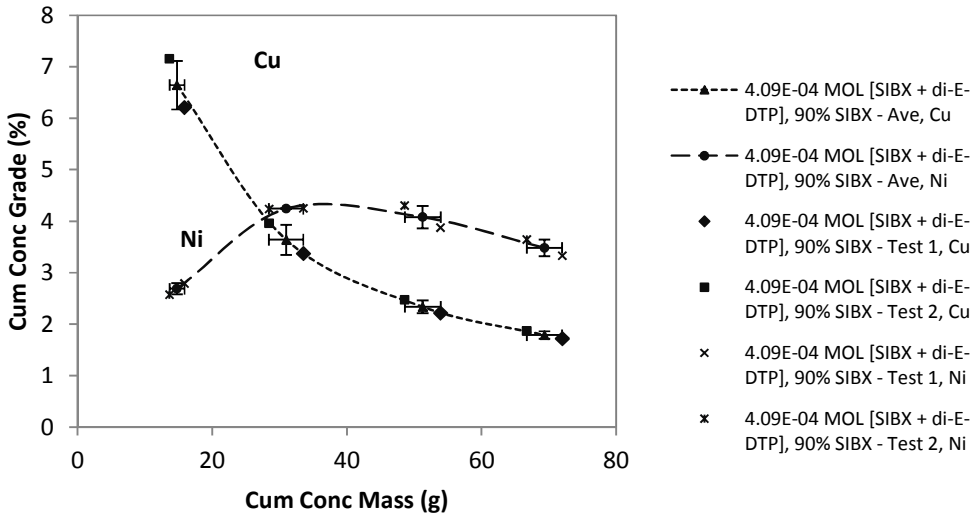


**Figure 4.8: The cumulative copper and nickel content of the concentrate for the test with highest water recovery error**

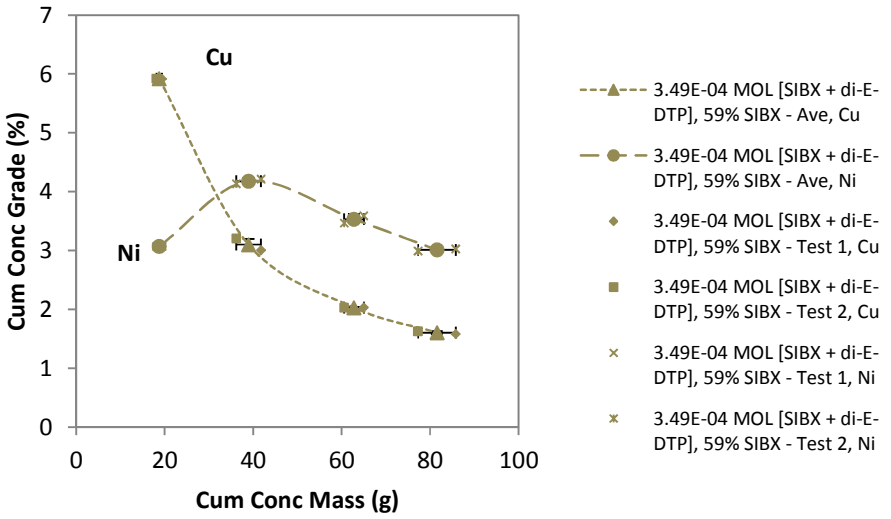


**Figure 4.9: The cumulative copper and nickel content of the concentrate for the test with highest concentrate mass error**

Figure 4.8, which shows a graph of cumulative concentrate grade as a function of cumulative mass pull for the test where *z* = {4.09E-04 mole/kg [76 % SIBX + 24 % di-E-DTP]}, indicates that even though the water error was relatively large for this test, the assay data points were within the standard error bars and the test can thus be considered reproducible. A similar argument can be made in Figure 4.9 which shows a plot of cumulative concentrate grade as a function of cumulative mass for the test where *z* = {3.49E-04 MOL [59 % SIBX + 41 % di-E-DTP]}. Figure 4.9 shows that all assay points are within standard error of the average data point and thus this test, even though it has a relatively large concentrate mass error, can also be considered reproducible.

### *4.2.3.3 Copper and Nickel Recovery*

**Table 4.11: A summary of standard errors associated with copper and nickel recovery for the "collector mixture" batch flotation tests**

| Reagent Suite | % Cu Rec (final recovery) | | | % Ni Rec (final recovery) | | |
|---|---|---|---|---|---|---|
| **2.00E-04 mole/kg D200 + *z* (in mole/kg)** | **Ave** | **Std Error** | **Rel Std Error** | **Ave** | **Std Error** | **Rel Std Error** |
| *z* = 4.09E-04, 76 % SIBX, 24 % di-E-DTP | 74.1 | 0.39 | 0.53 % | 61.0 | 0.02 | 0.03 % |
| *z* = 4.09E-04, 90 % SIBX, 10 % di-E-DTP | 73.7 | 0.01 | 0.01% | 57.9 | 0.28 | 0.48 % |
| *z* = 4.57E-04, 89 % SIBX, 11 % di-E-DTP | 73.7 | 0.45 | 0.61 % | 59.1 | 0.08 | 0.14 % |
| *z* = 3.49E-04, 59 % SIBX, 41 % di-E-DTP | 76.0 | 0.75 | 0.99 % | 59.7 | 1.43 | 2.40 % |



Table 4.11 shows that the copper recovery standard error was less than 1 % and the nickel recovery standard error less than 2 %. The cumulative copper and nickel recovery plots represented as a function of cumulative time for the test condition where *z* = {4.09E-04 mole/kg, [90 % SIBX + 10 % di-E-DTP]} are shown in Figure 4.10. This graph indicates that even though the water recovery error was relatively high for this test, the copper and nickel recovery data points for two independent tests were within standard error of the average. Similarly, Figure 4.11 shows that the recovery data points were within standard error of the average for the test where *z* = {3.49E-04 mole/kg [59 % SIBX + 41 % di-E-DTP]}. Thus, even though the concentrate mass error was relatively large for this specific test, the recovery plots of two independent tests are within standard error of the average and this test can thus be considered "reproducible".

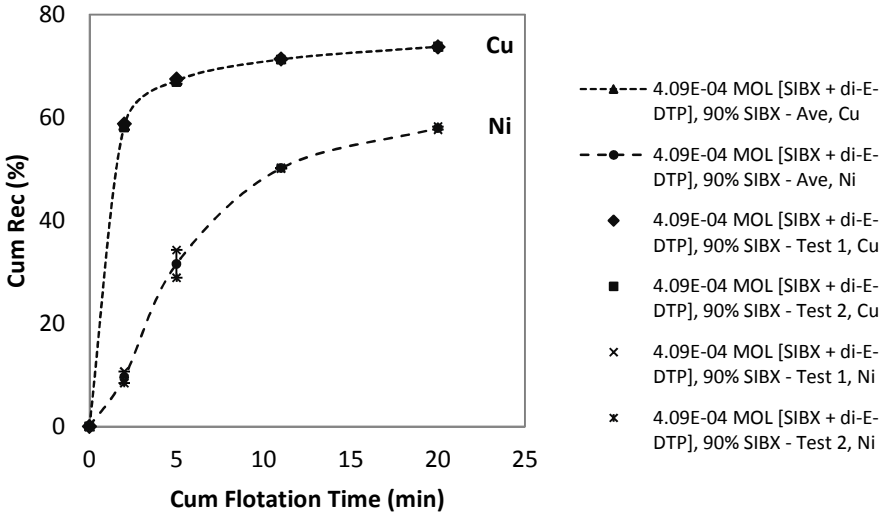


**Figure 4.10: Test repeatability represented as cumulative copper & nickel recovery plots for test where *z* = 4.09E-04 mole/kg [90 % SIBX + 10 % di-E-DTP]**

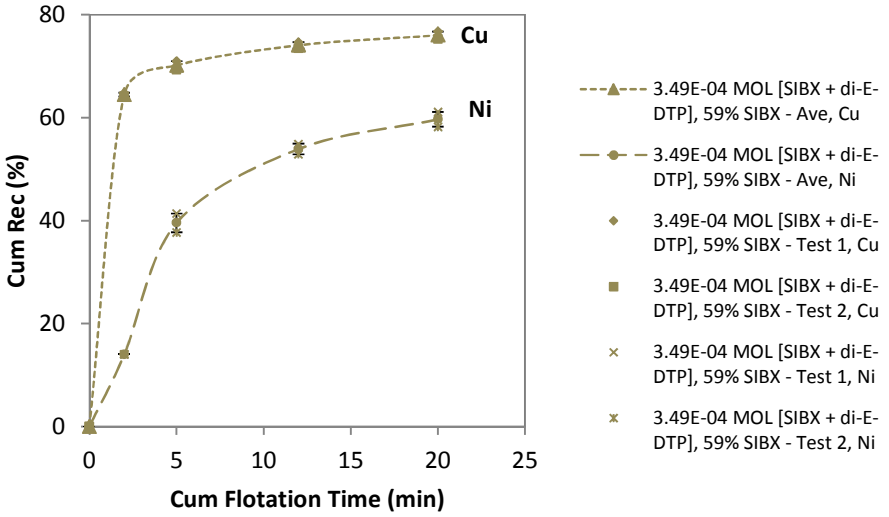


**Figure 4.11: Test repeatability represented as cumulative copper and nickel recovery plots for test where *z* = 3.49E-04 mole/kg [59 % SIBX + 41 % di-E-DTP];**

## 4.3 Frother Comparison Batch Flotation Test Results

A number of tests were completed using two different frothers, in the absence of any other reagents, in order to ascertain whether the frother which was to be used in this investigation, Dowfroth 200, possessed collecting properties. The other frothing agent used was MIBC. These two frothers were selected using molecular weight, molecular structure, purity, and availability as criteria. The second aim of these experiments was to establish whether the ultimate copper and nickel recovery values were different with the different frothers in the presence of collector, i.e. to establish if the frothers interacted with the collectors. This was considered an important criterion because the focus of this investigation was to establish whether the collectors SIBX and DTP interacted to produce enhanced metal recoveries and therefore the role of the frother needed to be one which, as far as possible, only provided a stable froth phase.



### 4.3.1 Mass and Water Recovery

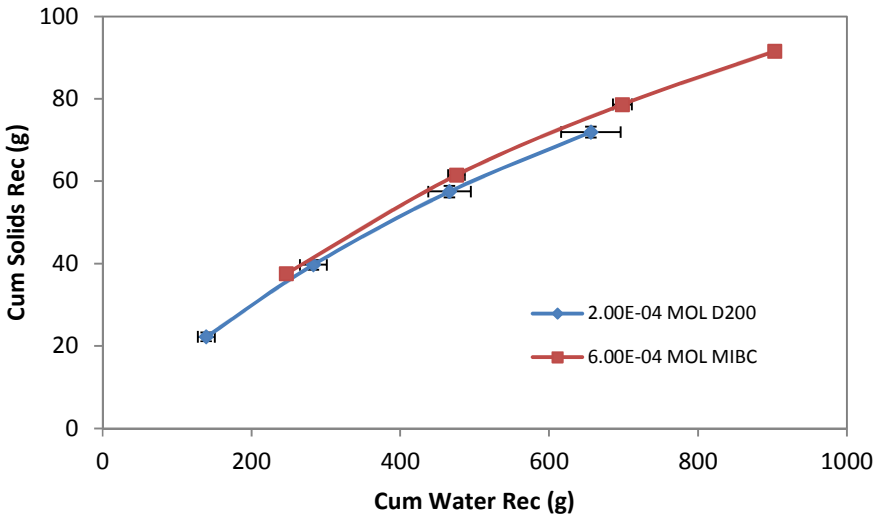


**Figure 4.12: Cumulative concentrate mass as a function of water recovery for collectorless batch flotation tests**

Figure 4.12, a plot of concentrate mass versus water recovery, shows there was essentially no difference in the slope of the mass versus water plots but significantly larger amounts of water were recovered with MIBC as compared to with Dowfroth 200.

### 4.3.2 Copper and Nickel Recovery in the Absence of Collector

Figure 4.13 shows the effect of frother type on copper and nickel recoveries. This figure shows that any differences in the final reported copper and nickel recoveries were due to the differences in water recovery. It is noted that the plots in Figure 4.13 show two interesting patterns – nickel recovery was directly proportional to water recovery whilst the copper recovery pattern was one that is typically associated with true flotation. This was further investigated by determining the copper and nickel recoveries by particle size and the results obtained are shown in Figure 4.14.



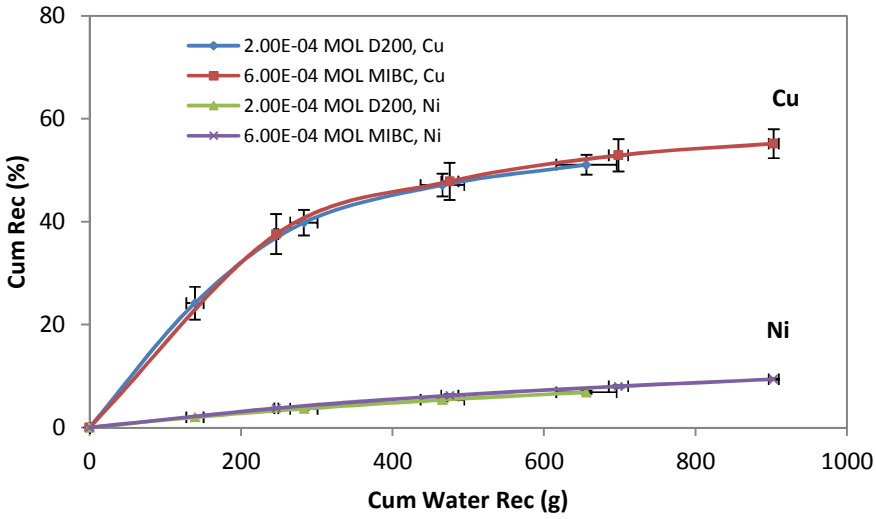


**Figure 4.13: Copper and nickel recovery as a function of water recovery for the collectorless batch flotation tests**

Figure 4.14 shows the recovery of copper and nickel by size fraction for the "Dowfroth 200 only" test. This figure demonstrates that the copper recovery generally increased with a decrease in particle size and peaks at 80 % recovery of the copper-containing minerals in the ultrafine fractions (-10 µm). Figure 4.14 also shows that the nickel recovery averaged more or less 5 % for the particles larger than 25 µm but increased to approximately 20 % for the -10 µm particles.

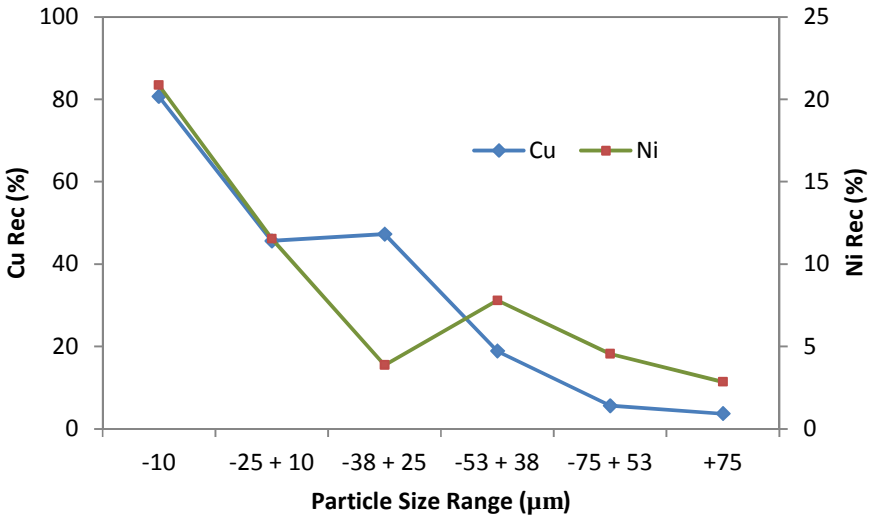


**Figure 4.14: Copper and nickel recovery per size fraction for the "frother only" test**



### 4.3.3 Copper and Nickel Recovery in the Presence of Collector

Figure 4.15 shows the effect of frother type, in the presence of both SIBX and diethyl DTP, on the recovery of copper and nickel as a function of water recovery. This figure clearly shows that the choice of frother was not significant with regard to copper or nickel recoveries when mixtures of SIBX and diethyl DTP were compared. Figure 4.16, on the other hand, shows the effect of frother type, in the presence of SIBX, on the recovery of copper and nickel as a function of water recovery. Figure 4.16 shows that there was a difference in the copper recovery patterns obtained when Dowfroth 200 was used as frother and SIBX as collector compared to when MIBC was used as frother and SIBX as collector.

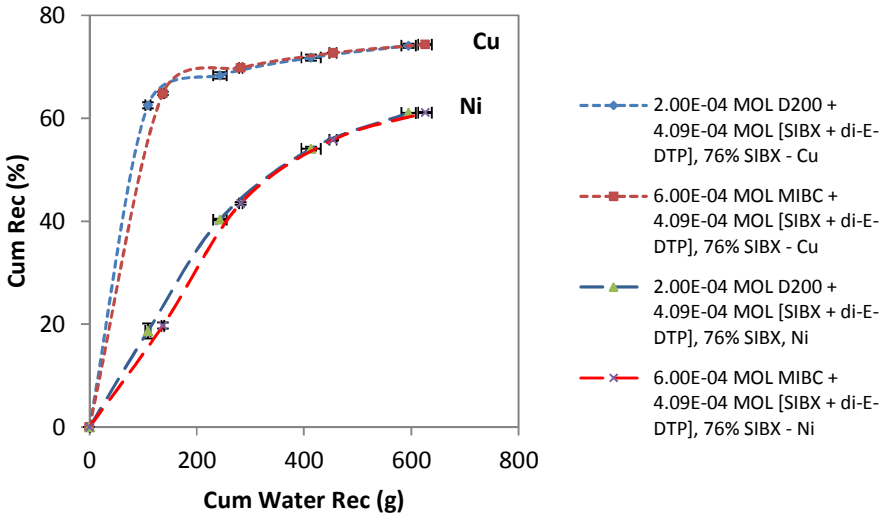


**Figure 4.15: Copper and nickel recovery as a function of water recovery – Dowfroth 200 compared to MIBC in presence of SIBX and diethyl DTP**

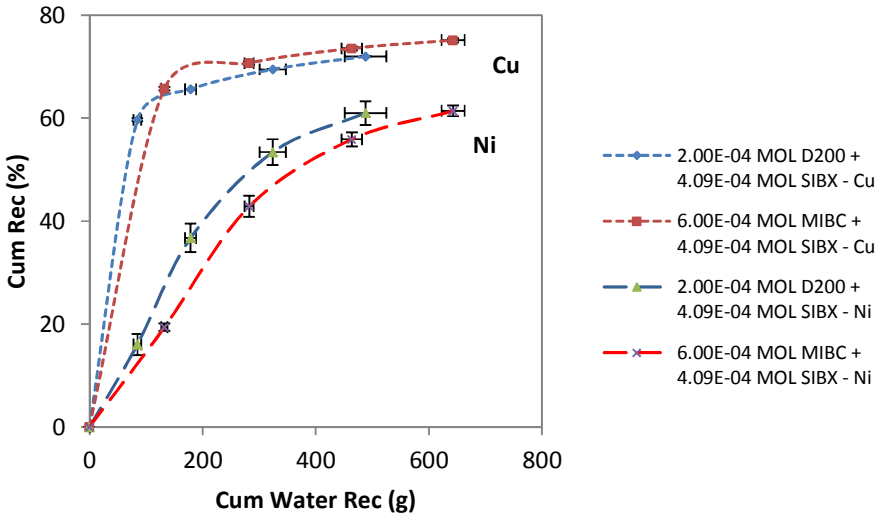


**Figure 4.16: Copper and nickel recovery as a function of water recovery – Dowfroth 200 compared to MIBC in the presence of SIBX**

### 4.3.4 Froth Imagining for Collectorless Batch Flotation Tests

The Smartfroth™ froth monitoring system was used to capture images of the froth phase when necessary. Randomly selected images of the froth phase are shown in Figures 4.17 to 4.20. Table 4.12 on the other hand shows the mass of water recovered for each of the concentrates collected in batch flotation tests where froth imaging was also done. This table complements the images in Section 4.4.5, 4.5.5 and 4.6.6 as water recovery can be related to the images.

**Table 4.12: Water recovered for each concentrate during batch flotation tests**

| Reagent Suite: 2.00E-04 mole/kg D200 + ξ | Conc 1 | Conc 2 | Conc 3 | Conc 4 |
|---|---|---|---|---|
| | Ave Water Rec (g) | Ave Water Rec (g) | Ave Water Rec (g) | Ave Water Rec (g) |
| ξ = 0 | 139 | 144 | 183 | 190 |
| ξ = 3.07E-04 mole/kg SIBX | 64 | 79 | 109 | 144 |
| ξ = 4.09E-04 mole/kg SIBX | 85 | 94 | 145 | 164 |
| ξ = 4.09E-04 mole/kg di-E-DTP | 229 | 232 | 249 | 227 |
| ξ = 4.09E-04 mole/kg [76 % SIBX + 24 % di-E-DTP] | 109 | 134 | 170 | 182 |



Figure 4.17 shows images of the froth which were obtained during the first two minutes of flotation whilst Figure 4.18 shows the images of the froth which were obtained when the second concentrate was collected. Similarly, Figure 4.19 shows images of the froth which were obtained when the third concentrate was collected and Figure 4.20 shows images of the froth which were obtained when the fourth and last concentrate was collected. Figure 4.17 also indicates that the froth was, as can be seen from the greenish appearance of the first picture on the left, initially highly mineralised but quickly became less so as can be seen from the more whitish appearance of the image on the right. The bubbles were mostly spherical in shape and the distribution of bubble diameters appeared to be consistent. In addition the froth also appeared to be very watery and highly mobile – these are characteristics which are consistent with a highly stabilised froth with significant entrainment of gangue. There are a few larger diameter bubbles present in Figure 4.17 which indicates that some bubble coalescence did take place during this time.

The froth, more or less, maintained its basic appearance until the end of the test, i.e. bubble shape remained circular and the froth was watery and mobile throughout the experiment. The images however also show that, by the time the flotation test have proceeded to the third and fourth concentrates, as is shown by Figures 4.19 and 4.20, there was no indication of large diameter bubbles forming anymore and the froth was less mobile compared to the froth obtained from the first two concentrates. Finally, it is also important to note that the froth from the third and fourth concentrates appear very white in colour. This may indicate mineral recovery effectively ceased after the second concentrate.

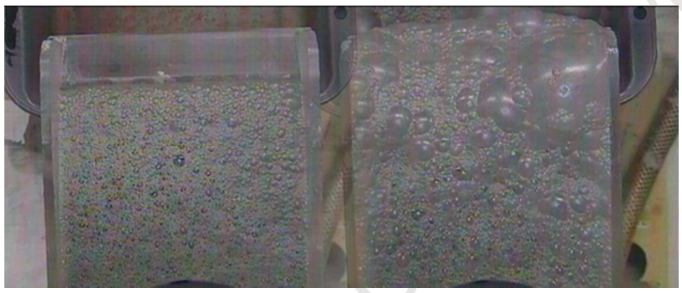

**Figure 4.17: Images of the froth from the first concentrate from the test where only Dowfroth 200, at a dosage of 2.00E-04 mole/kg, was added to the flotation pulp**

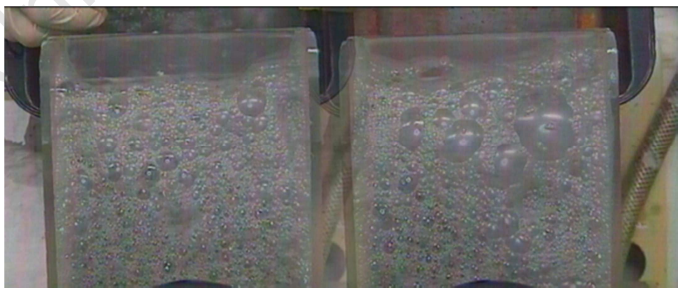

**Figure 4.18: Images of the froth from the second concentrate from the test where only Dowfroth 200, at a dosage of 2.00E-04 mole/kg, was added to the flotation pulp**

**Figure 4.19: Images of the froth from the third concentrate from the test where only Dowfroth 200, at a dosage of 2.00E-04 mole/kg, was added to the flotation pulp**

**Figure 4.20: Images of the froth from the fourth concentrate from the test where only Dowfroth 200, at a dosage of 2.00E-04 mole/kg, was added to the flotation pulp**

## 4.4 Batch Flotation Test Results using Pure Xanthate as Collector

This section describes the results of batch flotation tests conducted to investigate the effect of varying SIBX collector dosage on the recoveries and grades of copper, nickel and gangue. Further test work was conducted where, in addition to SIBX, a high molecular weight guar gum was added in order to depress the floating gangue. Flotation performance was evaluated from copper and nickel recovery, copper and nickel concentrate grades, water recovery, and the mass of both entrained and floating gangue in the concentrate. An additional test was conducted using SEX in the place of SIBX in order to compare the effect of chain length on the performance of xanthate collectors.



### 4.4.1 Mass and Water Recovery

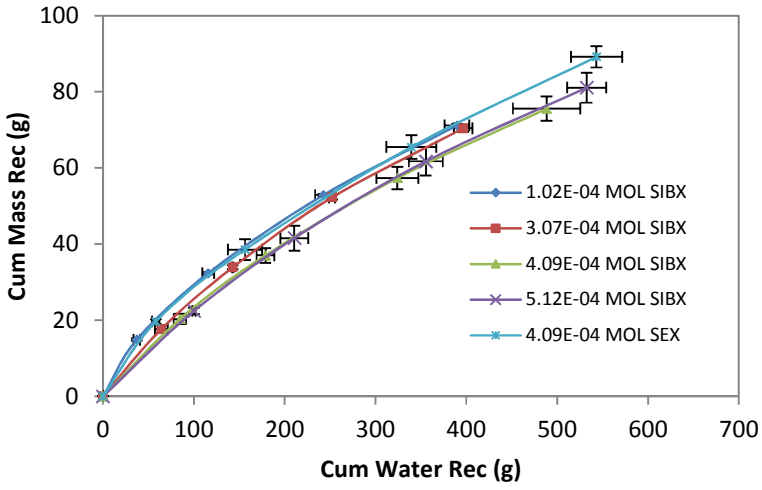


**Figure 4.21: Cumulative concentrate mass recovered as a function of cumulative water recovered for different dosages and type of xanthate collector**

Figure 4.21, a plot of the cumulative mass of concentrate versus the cumulative mass of water recovered for batch flotation tests using SIBX and SEX as collectors, shows that increasing collector dosage was accompanied by a slight increase in water recovery. It is interesting to note that a high

concentration of SEX had essentially the same effect as a low concentration of SIBX but with increased water recovery and thus increased froth stability.

### 4.4.2 Grade and Recovery

The grade-recovery curves obtained for copper and nickel are shown in Figures 4.22 and 4.23. They indicate that the highest copper grade and recovery was obtained at an SIBX dosage of 3.07E-04 mole/kg whilst, in the case of nickel, the final concentrate grades and recoveries were largely invariant with respect to the collector dosage. Increasing the concentration of SIBX in the flotation pulp beyond 3.07E-04 mole/kg resulted in a decrease in both copper recovery and grade. Hence, the lower SIBX dosage produced the best combination of copper and nickel grades and recoveries.

Table 4.13, which highlights overall performance rather than indicating performance with respect to flotation time, shows that the concentrate upgrade ratio, viz. average % nickel in concentrate divided by the average % nickel in feed, decreased with increasing SIBX concentration. Table 4.13 also indicates that the copper recovery obtained at 3.07E-04 mole/kg SIBX dosage was significantly higher than the copper recovery obtained at any other xanthate concentration and that this difference in recovery was statistically significant. Table 4.13 furthermore indicates that SIBX, at the dosage tested in this investigation, performed better than SEX with respect to concentrate grade. However, as is shown in Figure 4.23, SEX produced greater initial nickel grades and recoveries. This indicates that a mixture of SIBX and SEX may be beneficial with respect to nickel. In Table 4.13 the symbol (*****) indicates the statistically significant difference in copper recovery, at 95 % confidence level, between the instance where *x* = 3.07E-04 mole/kg SIBX and any other SIBX or SEX concentration. Thus, for example, it can be noted that the copper recovery obtained when *x* = 3.07E-04 mole/kg SIBX is 3.53 % higher than the condition when *x* = 4.09E-04 mole/kg SIBX, i.e. this difference was statistically significant. Similarly, the symbol (**+**) indicates the statistically significant difference in copper grade, at 95 % confidence level, between the instance where *x* = 3.07E-04 mole/kg SIBX and any other SIBX or SEX concentration. Thus, for example, it can be noted that the difference in copper grade between *x* = 3.07E-04 mole/kg SIBX and *x* = 4.09E-04 mole/kg SEX was more than 0.50 % and this difference was statistically significant. The term “N/S” in Table 4.13 implies that the difference was not significant.

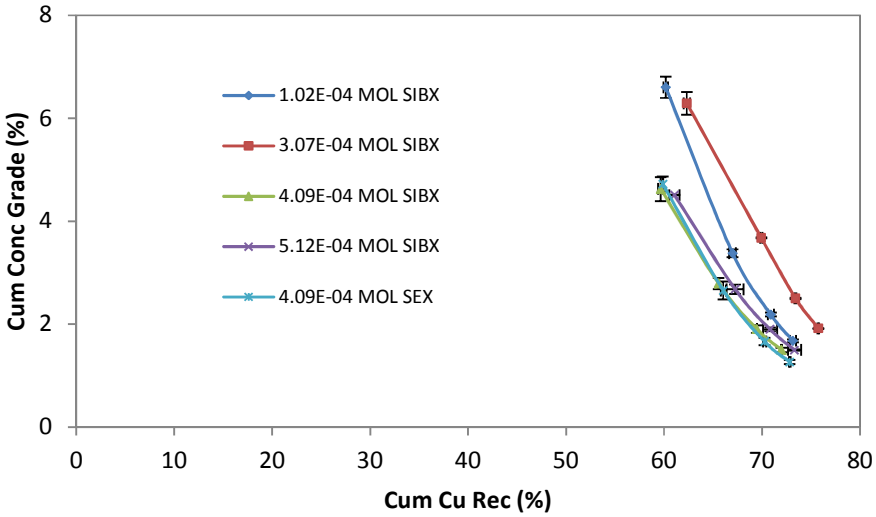


**Figure 4.22: The copper grade-recovery curves for the tests using only xanthate, at varying dosage, as collector**

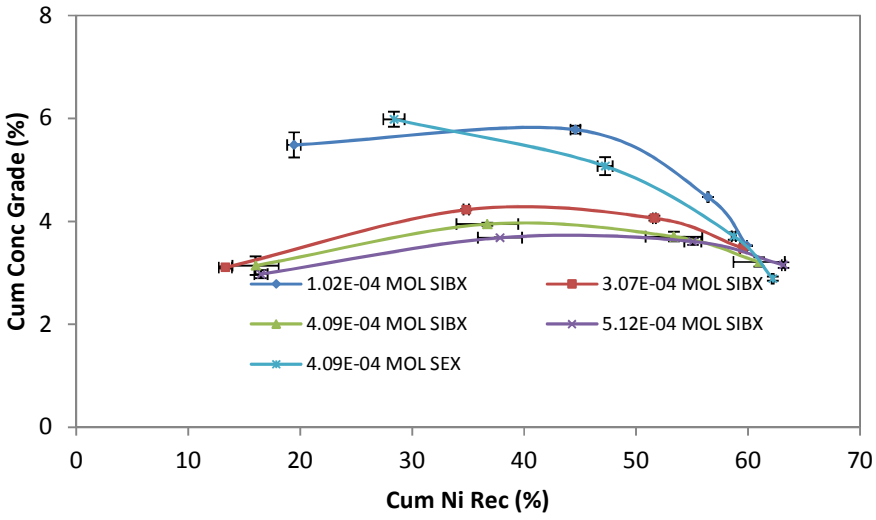


**Figure 4.23: The nickel grade-recovery curves for the tests using only xanthate, at varying dosage, as collector**

**Table 4.13: A summary of the copper and nickel grades and recoveries which was obtained with pure xanthate as collector**

| Reagent Suite | Copper | | | | | Nickel | | | | |
|---|---|---|---|---|---|---|---|---|---|---|
| 2.00E-04 mole/kg D200 + *x* | Rec | Grade | Statistically Significant Difference | | Upgrade Ratio | Rec | Grade | Statistically Significant Difference | | Upgrade Ratio |
| | | | Rec* | Grade+ | | | | Rec** | Grade++ | |
| *x* = 1.02E-04 mole/kg SIBX | 73.2 ± 0.3 | 1.68 ± 0.03 | 1.87 | 0.16 | 10.0 | 59.9 ± 0.0 | 3.53 ± 0.00 | 0.00 | 0.00 | 8.2 |
| *x* = 3.07E-04 mole/kg SIBX | 75.6 ± 0.1 | 1.92 ± 0.01 | 0.00 | 0.00 | 10.9 | 59.6 ± 0.3 | 3.48 ± 0.05 | N/S | N/S | 8.2 |
| *x* = 4.09E-04 mole/kg SIBX | 72.0 ± 0.1 | 1.50 ± 0.04 | 3.53 | 0.32 | 9.1 | 61.0 ± 2.3 | 3.21 ± 0.09 | N/S | 0.14 | 7.8 |
| *x* = 5.12E-04 mole/kg SIBX | 73.3 ± 0.7 | 1.50 ± 0.01 | 1.00 | 0.38 | 8.7 | 63.2 ± 0.2 | 3.15 ± 0.05 | N/S | 0.28 | 7.4 |
| *x* = 4.09E-04 mole/kg SEX | 72.8 ± 0.1 | 1.26 ± 0.04 | 2.63 | 0.56 | 8.0 | 62.2 ± 0.1 | 2.89 ± 0.09 | N/S | 0.46 | 6.8 |

### 4.4.3 Kinetic Analysis of Flotation Results

Figure 4.24 shows that the use of SEX, as compared to SIBX at the same molar collector dosage, led to a higher rate of nickel recovery. The figure furthermore shows that, generally, at dosages where copper rate was highest the rate of nickel recovery was lowest. The data from Figure 4.24 was used to obtain the first order rate constants ($k$) and infinite time recoveries ($R_{inf}$) using the Klimpel model (Agar, 1985). These results are shown in Table 4.14. The data in Table 4.14 also shows that, in the case of nickel, increased flotation residence time could have resulted in a considerably higher final recovery. In the case of copper however, Table 4.14 shows that the host mineral was fast-floating and maximum recovery was attained at short flotation times.

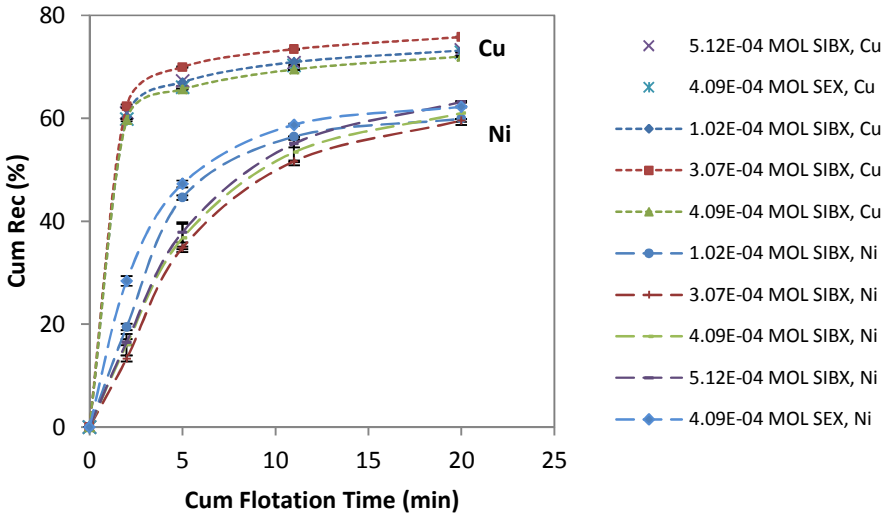


**Figure 4.24: The effect of xanthate collector dosage and type on the recovery of copper and nickel as a function of flotation time**

**Table 4.14: The calculated first order rate constants and infinite time recovery values for the batch flotation tests where SIBX and SEX were flotation collectors**

| Reagent Suite | Max Cu Rec (%) | | Max Ni Rec (%) | | Rate Constant ($min^{-1}$) | |
|---|---|---|---|---|---|---|
| 2.00E-04 mole/kg D200 + *x* | Actual | $R_{inf}$ | Actual | $R_{inf}$ | Cu, *k* | Ni, *k* |
| *x* = 1.02E-04 mole/kg SIBX | 73.2 ± 0.3 | 73.7 ± 0.3 | 59.9 ± 0.0 | 69.5 ± 0.4 | 2.64 ± 0.0 | 0.43 ± 0.0 |
| *x* = 3.07E-04 mole/kg SIBX | 75.8 ± 0.1 | 76.4 ± 0.0 | 59.6 ± 0.3 | 74.7 ± 0.2 | 2.65 ± 0.1 | 0.26 ± 0.0 |
| *x* = 4.09E-04 mole/kg SIBX | 72.0 ± 0.1 | 72.1 ± 0.1 | 61.0 ± 2.3 | 74.3 ± 1.5 | 2.77 ± 0.1 | 0.30 ± 0.0 |
| *x* = 5.12E-04 mole/kg SIBX | 73.0 ± 0.7 | 73.2 ± 0.6 | 62.9 ± 0.3 | 77.6 ± 0.8 | 2.83 ± 0.0 | 0.28 ± 0.0 |
| *x* = 4.09E-04 mole/kg SEX | 72.8 ± 0.1 | 73.0 ± 0.2 | 62.2 ± 0.1 | 68.4 ± 0.3 | 2.66 ± 0.0 | 0.61 ± 0.0 |

### 4.4.4 Effect of Depressant

This section investigates the effect of a guar gum on the flotation behaviour of non-sulphide gangue and sulphide minerals. The tests were performed at one xanthate concentration and for one xanthate type

only, viz. SIBX at a dosage of 4.09E-04 mole/kg. The aims were to: (i) determine the extent to which gangue floats with xanthate collectors and, (ii), separate entrained gangue from the floating gangue and thus relate the collector reagent suite to entrainment. The procedure used to separate entrained gangue from naturally floating gangue is explained in Chapter 3, Section 3.3.3.3.

### *4.4.4.1 Mass & Water Recovery*

Figure 4.25 shows the effect of increasing guar dosage on concentrate mass and water recovery at a specific SIBX dosage. It is important to note that, with regard to guar dosage, the unit g/t (grams per tonne) is used. It is also important to note that the g/t consumption refers to total reagent added and not active content added, i.e. the effects of impurities and insoluble species were not taken into account. The graph indicates that there was not a reduction in water recovery with an increase in guar dosage but a significant drop in concentrate mass at the higher guar dosage.



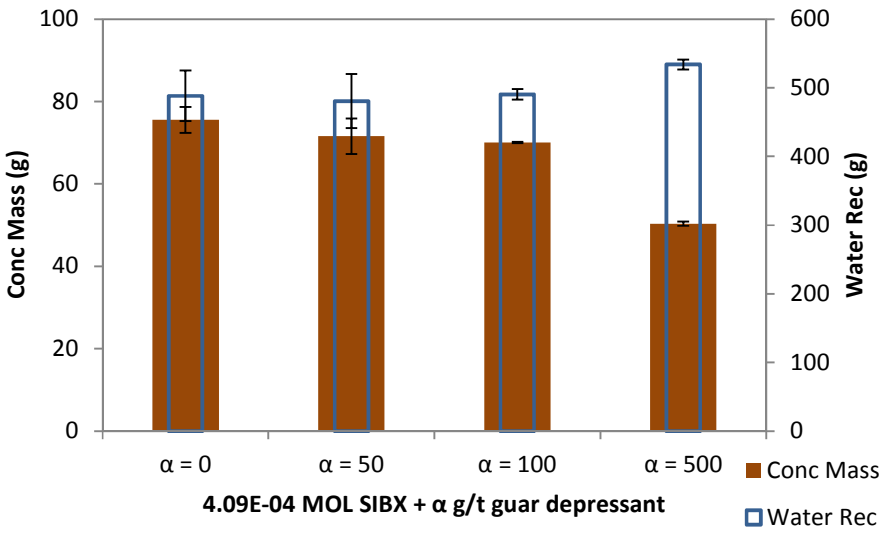


**Figure 4.25: The effect of increasing guar dosage, in the presence of a constant dosage of SIBX, on mass and water recovery**

### *4.4.4.2 Copper & Nickel Recovery*

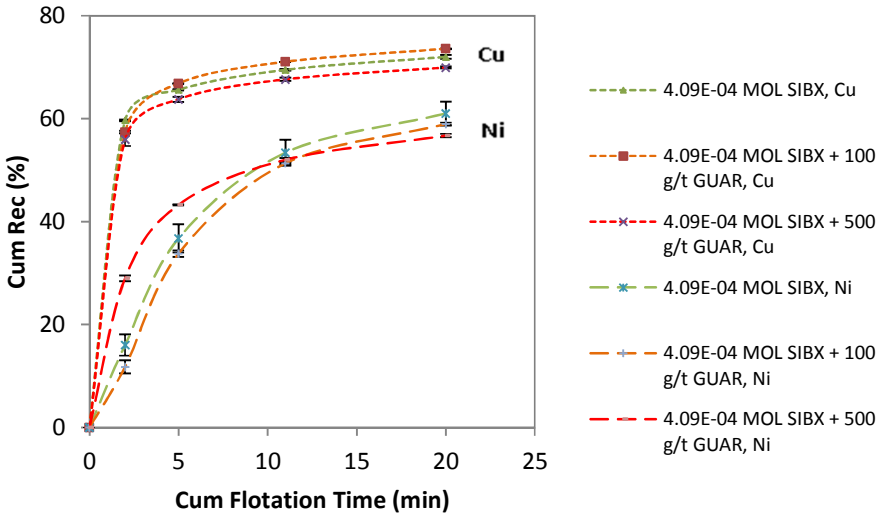


**Figure 4.26: The effect of increasing guar dosage, in the presence of a constant SIBX dosage, on copper and nickel recovery as a function of flotation time**

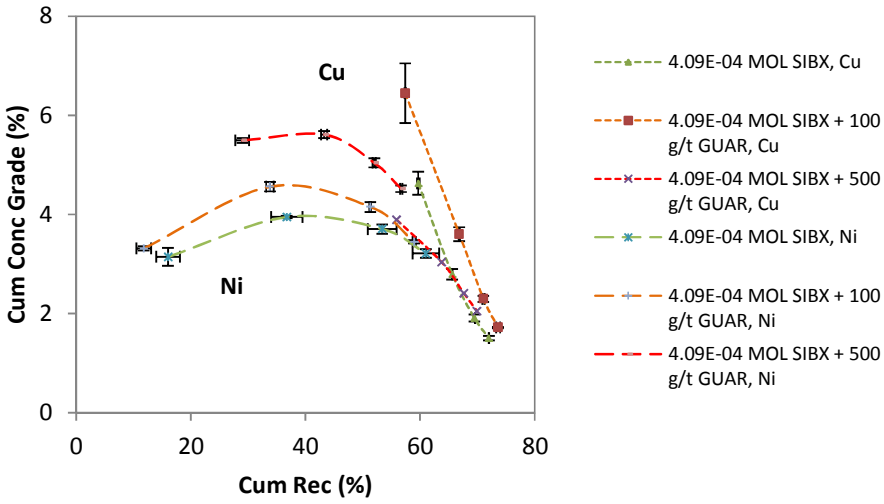


**Figure 4.27: Grade-recovery curves for copper and nickel at different dosages of guar and a constant SIBX dosage of 4.09E-04 mole/kg**

Figure 4.26 shows the effect of increasing guar dosage, in the presence of SIBX at a dosage of 4.09E-04 mole/kg ore, on the recoveries of copper and nickel as a function of time whilst Figure 4.27 shows the same effect but this time represented as copper and nickel grade-recovery curves. These figures show that final copper and nickel recoveries were compromised when very high dosages of guar (500 g/t) were added to the flotation system.

#### *4.4.4.3 Gangue Recovery*

The procedure to separate entrained gangue and floating gangue from the total non-sulphide gangue recovered in a batch flotation test, which was developed by Wiese (2009), was used in this investigation and the results obtained are shown in Table 4.15 and Figure 4.28. The basis of this procedure was discussed in detail in Chapter 3, Section 3.3.3.3. As is shown in Table 4.15 a considerable amount of gangue reported to the concentrate as floating gangue (FG). Figure 4.28 however shows that not all the floating gangue was depressed, even at 500 g/t guar dosage. This is partly perhaps because the reagent used was relatively impure as well as insoluble (cf. Table 3.3 in Chapter 3) and thus a dosage in excess of 500 g/t was perhaps needed. The fact that not all flotating gangue was depressed at a dosage of 500 g/t guar does not invalidate the procedure.



**Table 4.15: The effect of increasing guar dosage, at a constant SIBX dosage, on non-sulphide gangue recovery**

| Reagent Suite<br>2.00E-04 mole/kg D200 + 4.09E-04 mole/kg SIBX + α | Total Conc Mass (g) | Total Gangue in Conc (g) | Floating Gangue Mass in Conc (g) | Entrained Gangue Mass in Conc (g) | Proportion of Gangue Recovered by Entrainment |
|---|---|---|---|---|---|
| α = 0 g/t guar | 75.6 ± 3.2 | 61.9 ± 2.9 | 31.0 ± 0.3 | 30.9 | ≈ 50 % |
| α = 50 g/t guar | 71.6 ± 4.3 | 60.0 ± 4.5 | 29.6 ± 2.4 | 30.4 | ≈ 50 % |
| α = 100 g/t guar | 70.1 ± 0.2 | 58.2 ± 0.2 | 27.2 ± 1.0 | 31.0 | ≈ 53 % |
| α = 500 g/t guar | 50.4 ± 0.5 | 38.7 ± 0.3 | 4.9 ± 0.5 | 33.7 | ≈ 90 % |

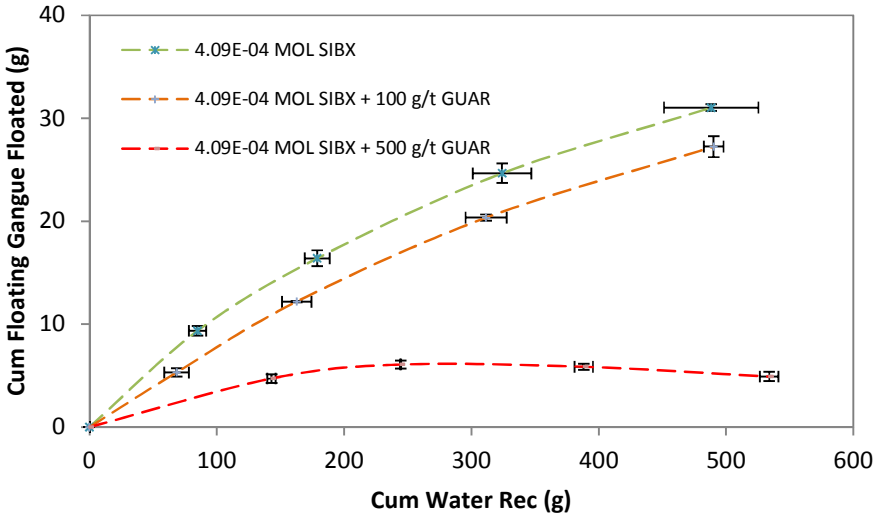


**Figure 4.28: The cumulative mass of floating gangue recovered as a function of water recovered for tests completed using a constant SIBX dosage but varying guar dosages**



### 4.4.5 Froth Imaging for Batch Flotation Tests with Varying Dosages of SIBX

#### *4.4.5.1 Froth Imaging for Batch Flotation Test with Reagent Suite 2.00E-04 mole/kg D 200 + 3.07E-04 mole/kg SIBX*

Figure 4.29 shows two randomly selected images of the first concentrate for the test where the collector type and dosage was SIBX and 3.07E-04 mole/kg. The images are in complete contrast to those which were obtained when only frother was used (cf. Figure 4.17). The average bubble diameter appears large and the froth height shallow. These features are consistent with a highly destabilised froth phase caused by rapid bubble coalescence. In addition, the bubble shape appears to be more polyhedral rather than circular but elongated bubble shapes are also present. The presence of elongated froth bubbles suggests that the froth was sticky, tough and not mobile, which, based on visual observations noted while the tests were completed, is true. The froth colour is dark grey with a yellowish/gold-like taint which indicates a highly mineralised froth.

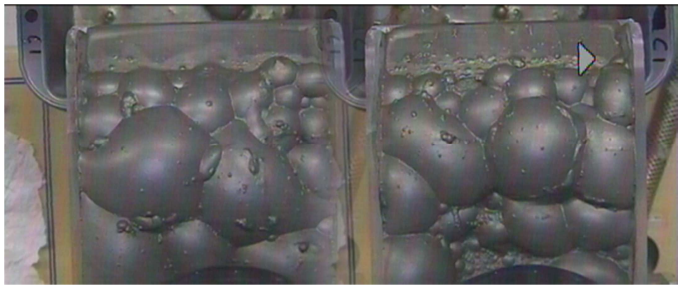

**Figure 4.29: Images of the froth from the first concentrate from the test where the collector was SIBX at a dosage of 3.07E-04 mole/kg**

Figure 4.30 shows two time-dependent images of the froth from the second concentrate, i.e. the image on the left preceded the image on the right. The average bubble diameter appears to have increased from what it was during the first concentrate. Bubble coalescence also appears to be still significant as can be seen from the fact that the image on the left contains a number of small bubbles which coalesced to form one large bubble as shown in the image on the right. The images also show a shallow froth height which is indicative of a highly destabilised froth zone. The froth still appears to be sticky and considerably less water-rich as was the case with the collectorless tests (cf. Figure 4.18).



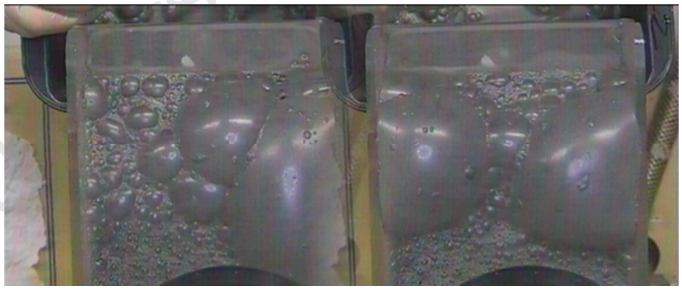

**Figure 4.30: Images of the froth from the second concentrate from the test where the collector was SIBX at a dosage of 3.07E-04 mole/kg**

In Figures 4.31 and 4.32, which shows the images of the froth obtained from the third and fourth concentrates respectively, the average bubble diameters appears to have reduced significantly from what it was in the first and second concentrates. The froth now appears more watery and less sticky

compared to the froth from the first and second concentrates but, compared to the collectorless tests (cf. Figures 4.19 and 4.20), highly immobile. A major difference between the images shown in Figures 4.20 and 4.32, which show the images of the froth from the fourth concentrate obtained in the absence and presence of SIBX respectively, is froth colour. The images of the froth in Figure 4.32 are still relatively grey-coloured when compared to the images of the froth from Figure 4.20, which in contrast, appear white. This is an indication that flotation was still proceeding even at this stage of the test compared to the collectorless test.

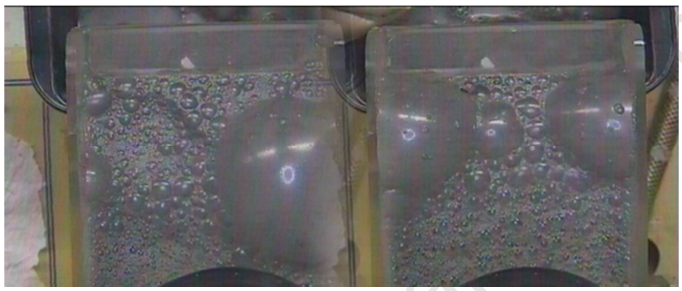

**Figure 4.31: Images of the froth from the third concentrate from the test where the collector was SIBX at a dosage of 3.07E-04 mole/kg**

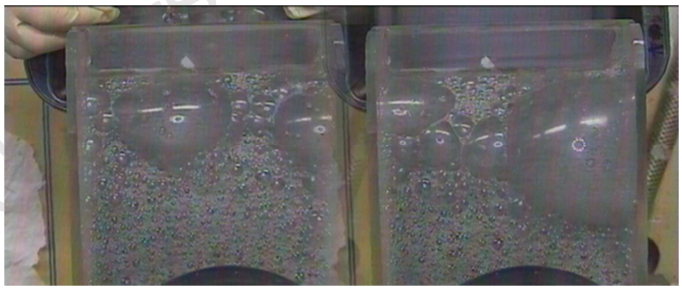

**Figure 4.32: Images of the froth from the fourth concentrate from the test where the collector was SIBX at a dosage of 3.07E-04 mole/kg**

### *4.4.5.2 Froth Imaging for Batch Flotation Test with Reagent Suite 2.00E-04 mole/kg D200 + 4.09E-04 mole/kg SIBX*

Figure 4.33 shows images of the froth from the first concentrate of the test where SIBX, at a collector dosage of 4.09E-04 mole/kg ore, was used. The average bubble diameter appears to be considerably larger than was the case for the collectorless test (cf. Figure 4.17) but not significantly different to the case when SIBX, at a dosage of 3.07E-04 mole/kg, was added (cf. Figure 4.31). This suggests that bubble coalescence occurred rapidly. The general bubble shape is more polyhedral compared to when the collector dosage was 3.07E-04 mole/kg which suggests the froth is deeper and more drained in this case. A significant difference between the images presented in Figures 4.29 and those presented in Figure 4.33 is froth colour. The images in Figure 4.29 have a yellow/gold appearance whilst the images in Figure 4.33 appear dull grey.

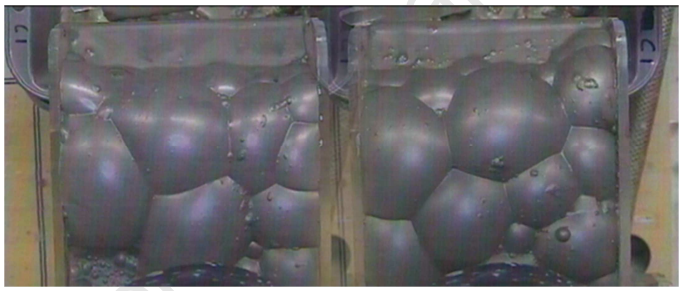

**Figure 4.33: Images of the froth from the first concentrate from the test where the collector was SIBX at a dosage of 4.09E-04 mole/kg**

Figure 4.34 shows randomly selected images of the froth from the second concentrate when the SIBX dosage was 4.09E-04 mole/kg. The froth appears to be sticky in character and somewhat immobile when compared to the images of the froth from the collectorless tests (cf. Figure 4.18). Figures 4.35 and 4.36, on the other hand, shows randomly selected images from the third and fourth concentrates. The froth from the third and fourth concentrates was considerably more watery and less sticky than those from the first and second concentrates but less watery than the froth obtained from the collectorless test (cf. Figures 4.19 and 4.20). The froths from the third and fourth concentrates from this test did not

however appear to be significantly different in bubble diameter, bubble shape, froth stickiness or froth colour from that which was obtained when the collector dosage was 3.07E-04 mole/kg.

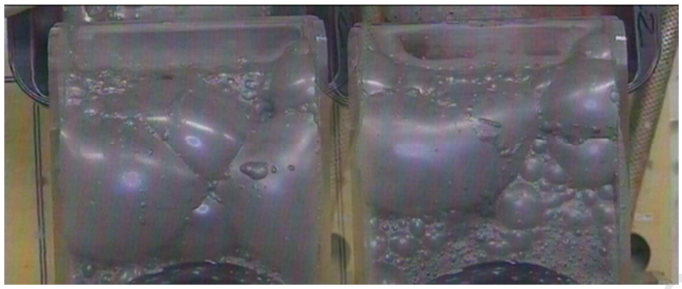

**Figure 4.34: Images of the froth from the second concentrate from the test where the collector was SIBX at a dosage of 4.09E-04 mole/kg**

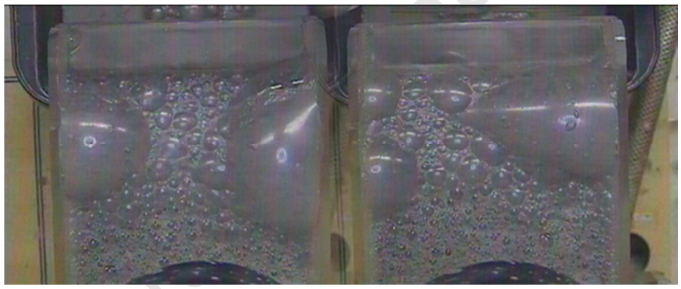

**Figure 4.35: Images of the froth from the third concentrate from the test where the collector was SIBX at a dosage of 4.09E-04 mole/kg**

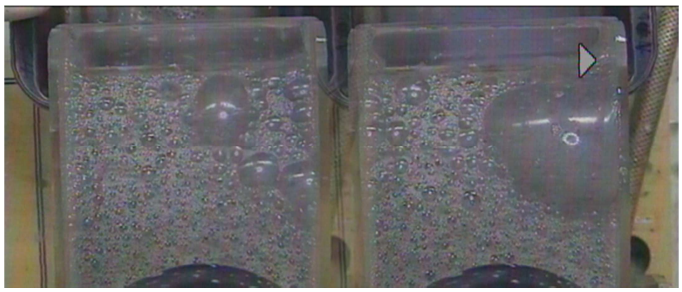

**Figure 4.36: Images of the froth from the fourth and last concentrate from the test where the collector was SIBX at a dosage of 4.09E-04 mole/kg**

## 4.5 Batch Flotation Results using Pure DTP as Collector

This section describes the results of batch flotation tests conducted to investigate the effect of varying DTP collector dosage on the recoveries and grades of copper, nickel and gangue. As was the case with the xanthate tests, further tests were conducted where, in addition to DTP, a high molecular weight guar was added in order to depress the floating gangue. Flotation performance was thus evaluated from copper and nickel recovery, copper and nickel concentrate grades, water recovery, and the mass of both entrained and floating gangue in the concentrate.

### 4.5.1 Mass and Water Recovery



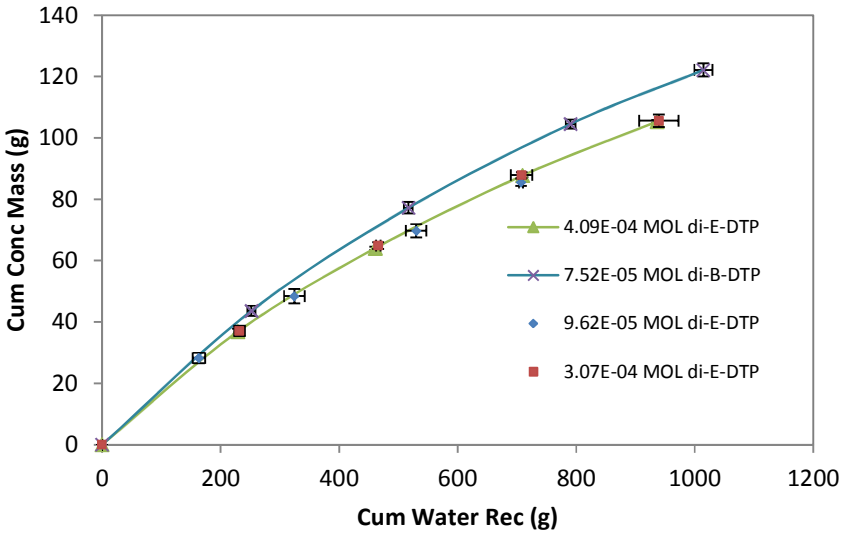


**Figure 4.37: Cumulative concentrate mass recovered versus water recovered for tests with different dosages and types of DTP**

Figure 4.37 shows the cumulative concentrate mass recovered versus water recovered for tests in which a constant frother dosage and varying amounts of DTP collector were used. The figure shows that mass of water recovered was significantly greater than was the case with the SIBX tests (cf. Figure 4.21). The

di-iso-butyl DTP result shows a marginally greater mass recovery at a given water recovery which may be indicative of increased froth stability.

### 4.5.2 Grade and Recovery

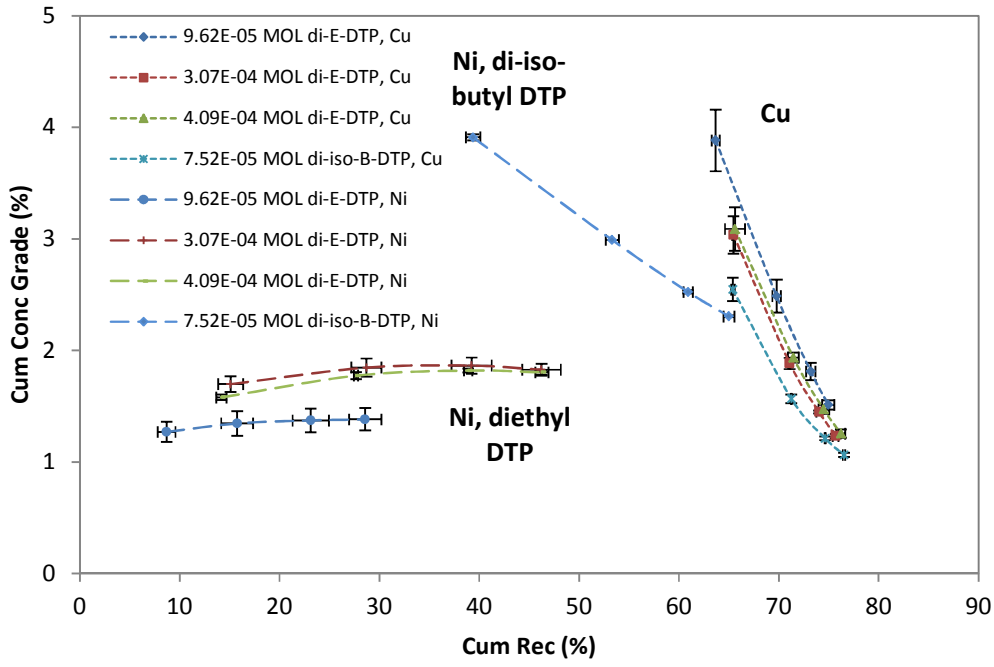


**Figure 4.38: The effect of varying DTP chain length and dosage on copper and nickel grade-recovery**

Figure 4.38 shows the grade-recovery curves for copper and nickel which were obtained when diethyl DTP and di-iso-butyl DTP were used as collectors. This figure indicates that diethyl DTP, when compared to SIBX, was a good copper collector but recovered nickel poorly. The nickel recovery did however improve appreciably when the diethyl DTP dosage was increased as is shown in Table 4.16. This increased nickel recovery obtained at the higher diethyl DTP dosages was also however accompanied by a considerable increase in water recovery as is shown in Figure 4.39 (cf. Section 4.6.3). Figure 4.38 and Table 4.16 both also show that the use of di-iso-butyl DTP resulted in a significant increase in both the copper and nickel recoveries as compared to diethyl DTP.

**Table 4.16: Final copper and nickel grade and recovery results for "DTP only" batch flotation tests**

| Reagent Suite | Copper | | | Nickel | | |
|---|---|---|---|---|---|---|
| **2.00E-04 mole/kg D200 + *y*** | **Rec (%)** | **Grade (%)** | **Upgrade Ratio** | **Rec (%)** | **Grade (%)** | **Upgrade Ratio** |
| *y* = 9.62E-05 mole/kg di-E-DTP | 75.0 ± 0.6 | 1.51 ± 0.04 | 8.52 | 28.6 ± 1.6 | 1.38 ± 0.10 | 3.25 |
| *y* = 3.07E-04 mole/kg di-E-DTP | 75.7 ± 0.3 | 1.23 ± 0.02 | 7.02 | 46.2 ± 0.7 | 1.83 ± 0.02 | 4.29 |
| *y* = 4.09E-04 mole/kg di-E-DTP | 76.2 ± 0.4 | 1.26 ± 0.04 | 7.01 | 46.3 ± 1.9 | 1.80 ± 0.05 | 4.26 |
| *y* = 7.52E-05 mole/kg di-iso-B-DTP | 76.5 ± 0.1 | 1.06 ± 0.02 | 6.12 | 65.0 ± 0.6 | 2.30 ± 0.01 | 5.19 |

### 4.5.3 The Effect of Water Recovery on Copper and Nickel Recovery

Figure 4.39 shows that, for the same mass of water recovered, significantly more nickel was recovered with di-iso-butyl DTP rather than diethyl DTP. Figure 4.39 also however shows that the use of di-iso-butyl DTP has led to more water, when compared to the diethyl version, being recovered – even at the very low concentration used in this investigation. Figure 4.39 furthermore shows that the relationship between water recovery and nickel recovery is approximately linear for the diethyl DTP tests.

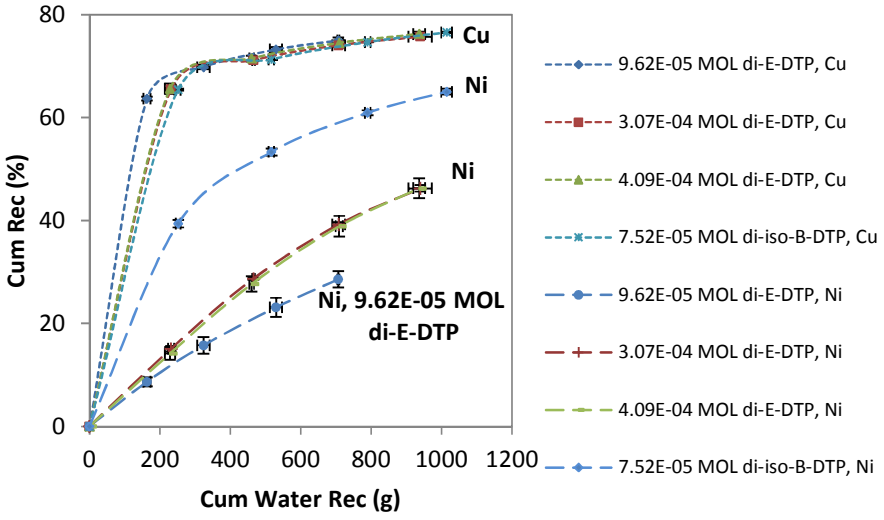


**Figure 4.39: Copper and nickel recovery as a function of water recovery for different dosages and types of DTP**

Figure 4.40 shows the concentrate grade obtained at various concentrate masses recovered when DTP was used as the collector. The figure complements Figure 4.39 because it shows that the nickel content of the concentrate did not change significantly with increasing mass pull for the tests completed with diethyl DTP as collector but that, comparatively, di-iso-butyl DTP is a good nickel collector because the concentrate contained a significantly higher percentage of nickel at any particular mass.

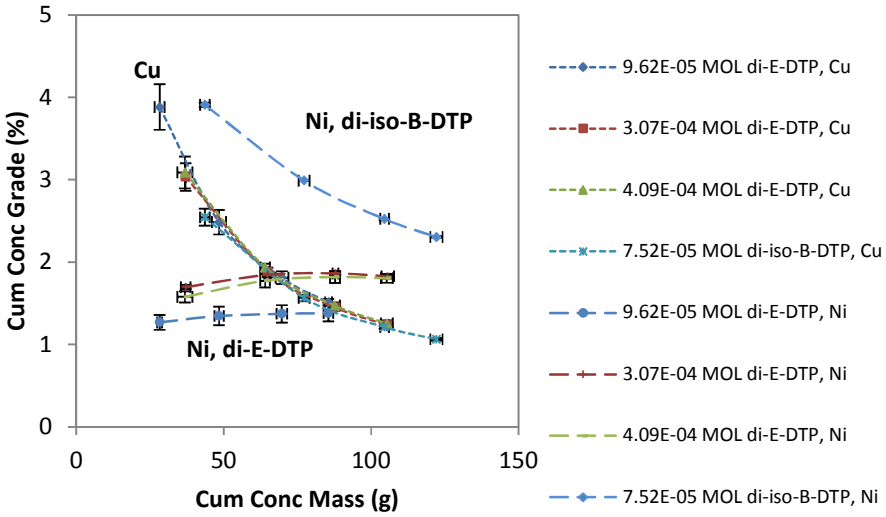


**Figure 4.40: The effect of DTP type, dosage and chain length on cumulative concentrate grades as a function of cumulative concentrate mass**



### 4.5.4 Kinetic Analysis of Flotation Results

Figure 4.41 shows the effect of DTP chain length and dosage on the recovery of copper and nickel as a function of flotation time whilst Table 4.17 shows the copper and nickel kinetic first order rate constants, which were obtained using the Klimpel model (Agar, 1985), for the specified DTP tests. Figure 4.41 and Table 4.17, in summary, also show that:

i. The longer chain collector, di-iso-butyl DTP, even at a significantly lower collector concentration, recovered nickel at a much faster rate as compared to diethyl DTP
ii. The rate of flotation of copper was unaffected by DTP chain length or concentration in the pulp

iii. The copper first order rate constants obtained with DTP as flotation collector was higher than that which was obtained with SIBX (cf. Table 4.14)

iv. The infinite time nickel recovery value was considerably higher than the actual recovery achieved. This suggests that, all other conditions being equal, increased flotation time may result in an increased nickel recovery. The expected nickel recovery increase with increased flotation time is however significantly less for diethyl DTP compared to the xanthates. For example, the calculated infinite time nickel recovery with SIBX, at a collector dosage of 3.07E-04 mole/kg, was 74.7 % (cf. Table 4.14), whilst the calculated infinite time recovery with diethyl DTP, at the same collector concentration, was 53.4 % (cf. Table 4.17). This indicates that the xanthates are better collectors for nickel compared to diethyl DTP

v. The infinite time copper recovery value was not significantly different to the actual final recovery achieved. This suggests that the copper mineral in the ore was fast floating in nature and that increased flotation time would not necessarily lead to increased recovery.



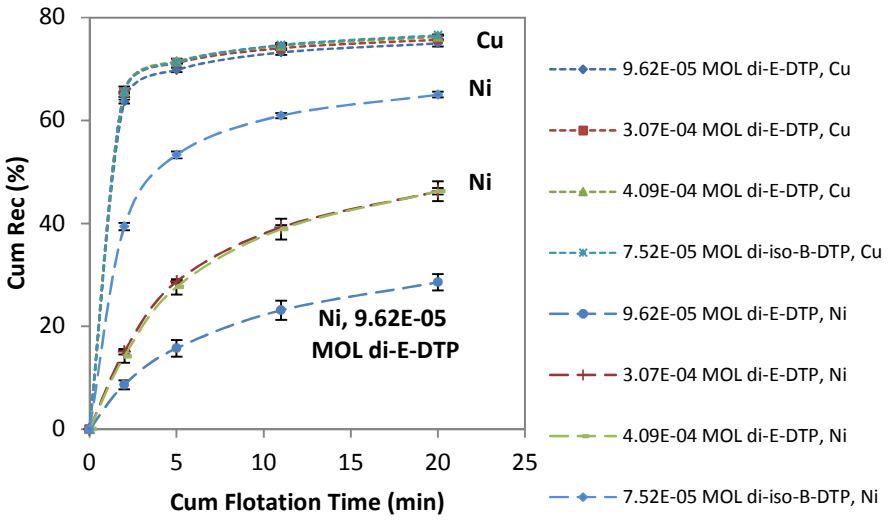


**Figure 4.41: Cumulative recoveries of copper and nickel as a function of time obtained with variations in DTP concentration in pulp and chain length**

**Table 4.17: The calculated first order rate constants and infinite time recovery values for the batch flotation tests where diethyl DTP and di-iso-butyl DTP were the collectors**

| Reagent Suite | Max Cu Rec (%) | | Max Ni Rec (%) | | Rate Constant ($min^{-1}$) | |
|---|---|---|---|---|---|---|
| 2.00E-04 mole/kg D200 + *y* | Actual | $R_{inf}$ | Actual | $R_{inf}$ | Cu | Ni |
| *y* = 0 mole/kg di-E-DTP | 51.0 ± 1.9 | 55.1 ± 2.3 | 6.9 ± 0.3 | 8.3 ± 0.3 | 0.66 ± 0.15 | 0.26 ± 0.02 |
| *y* = 9.62E-05 mole/kg di-E-DTP | 75.0 ± 0.6 | 75.5 ± 0.6 | 28.6 ± 1.6 | 34.3 ± 1.2 | 3.10 ± 0.02 | 0.28 ± 0.03 |
| *y* = 3.07E-04 mole/kg di-E-DTP | 75.7 ± 0.3 | 75.5 ± 0.2 | 46.2 ± 0.7 | 53.4 ± 2.8 | 3.47 ± 0.02 | 0.35 ± 0.10 |
| *y* = 4.09E-04 mole/kg di-E-DTP | 76.2 ± 0.4 | 76.7 ± 0.4 | 46.3 ± 1.9 | 54.5 ± 1.9 | 3.37 ± 0.08 | 0.32 ± 0.02 |
| *y* = 7.52E-05 mole/kg di-iso-B DTP | 76.5 ± 0.1 | 77.0 ± 0.1 | 65.0 ± 0.6 | 67.4 ± 0.4 | 3.23 ± 0.04 | 1.03 ± 0.03 |

## 4.5.5 Effect of Depressant

### *4.5.5.1 Mass and Water Recovery*

**Table 4.18: The effect of increasing guar and diethyl DTP dosages on concentrate mass and water recovery**

| Guar Dosage (g/t) | 9.62E-05 MOL di-E-DTP | | 3.07-04 MOL di-E-DTP | | 4.09E-04 MOL di-E-DTP | |
|---|---|---|---|---|---|---|
| | Water Rec (g) | Conc Mass (g) | Water Rec (g) | Conc Mass (g) | Water Rec (g) | Conc Mass (g) |
| 0 | 706.9 | 85.5 | 939.6 | 105.6 | 936.5 | 105.4 |
| 100 | 745.7 | 81.0 | 985.7 | 110.3 | 1137.4 | 135.6 |
| 500 | 539.3 | 39.1 | 816.6 | 64.0 | 779.1 | 64.4 |

Table 4.18 shows the effect of increasing guar and diethyl DTP dosages on concentrate mass and water recoveries. The data presented in the table indicates that there was an increase in water recovery at intermediate guar dosages (100 g/t). In addition, at an intermediate guar dosage and at a diethyl DTP dosage of 4.09E-04 mole/kg, there was a significant increase in concentrate mass as compared to the no guar case. Finally it is also noted that once the guar dosage was increased to very high levels (500 g/t), a significant reduction in especially concentrate mass was obtained. This may indicate that depression of those particles considered floating gangue had occurred.

### *4.5.5.2 Copper & Nickel Recovery*

Figure 4.42 shows the effect of increasing guar and diethyl DTP dosages on copper recovery as a function of water recovery. This figure shows that the copper recovery was significantly reduced when a high dosage of guar (500 g/t) was added to the flotation pulp.

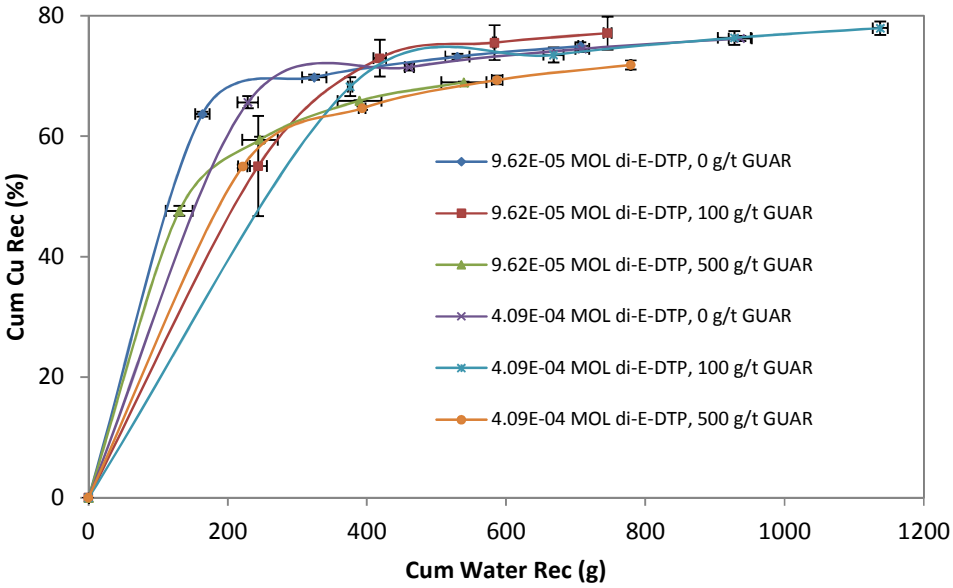


**Figure 4.42: Effect of increasing guar dosage on copper recovery for different dosages of diethyl DTP**

Figure 4.43 shows the effect of increasing guar and diethyl DTP dosages on nickel recovery as a function of water recovery. This figure shows that, as was the case with the copper recovery (cf. Figure 4.42), the nickel recovery was significantly reduced when a high dosage of guar, viz. 500 g/t, was added to the flotation pulp. Figure 4.43 also shows that nickel recovery was increased significantly in the presence of 100 g/t guar when the diethyl DTP dosage was 4.09E-04 mole/kg.

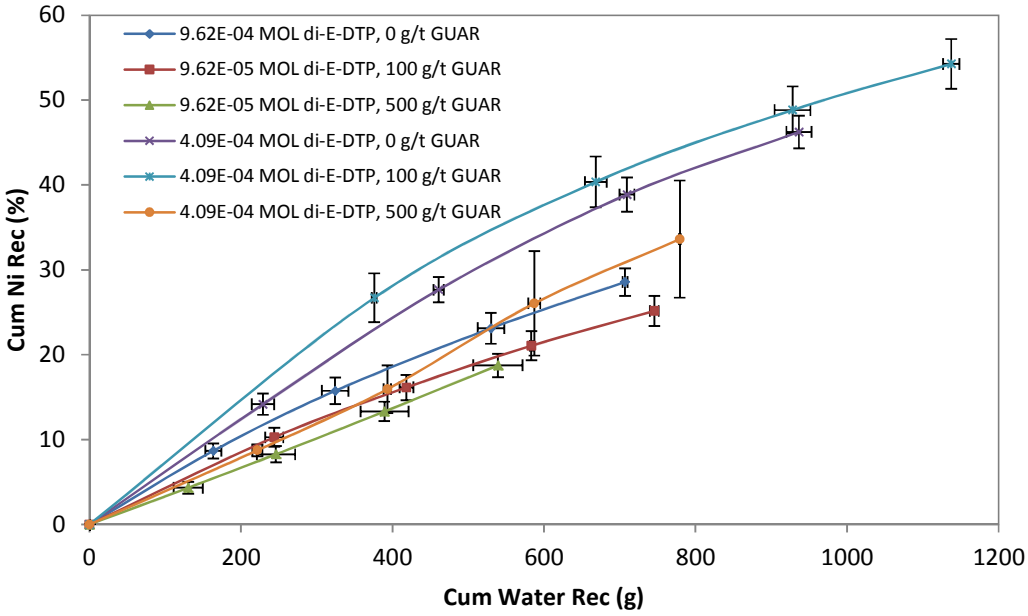


**Figure 4.43: Effect of increasing guar dosage on nickel recovery for varying dosages of diethyl DTP**

Figures 4.44 and 4.45 show the effect of increasing guar dosage on the copper and nickel grade-recovery curves obtained with diethyl DTP as collector. The figures confirm, as was expected, that the concentrate grade increased significantly when guar was added at a high dosage to the flotation system but that recovery decreased when high dosages of guar were added. Figures 4.44 and 4.45 also show however that guar dosages in excess of 100 g/t were necessary in order to make significant improvements in concentrate grade.

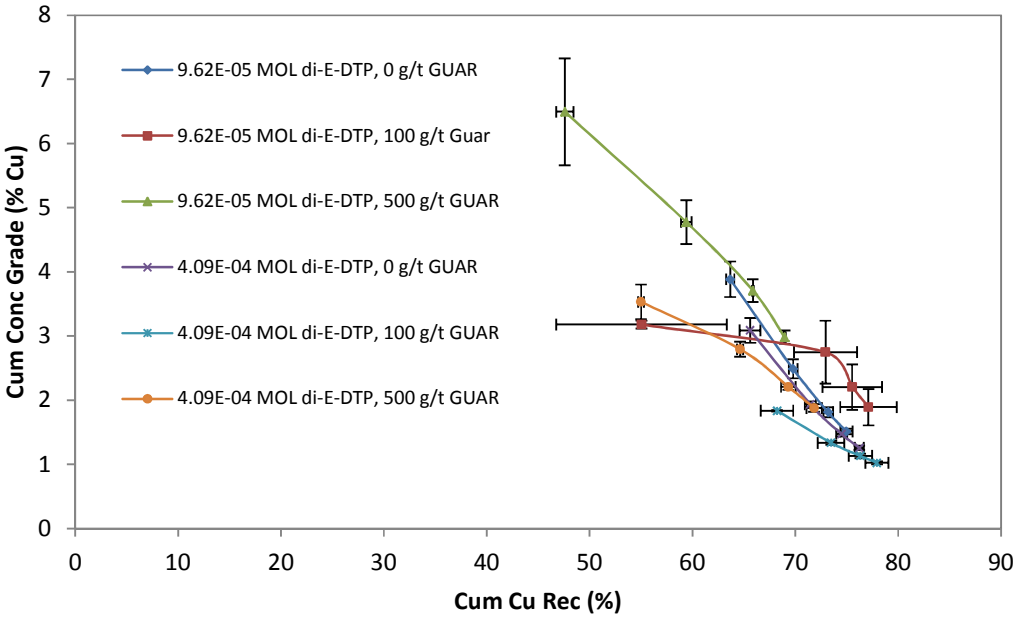


**Figure 4.44: Effect of increasing guar dosage on copper grade and recovery for different dosages of diethyl DTP**

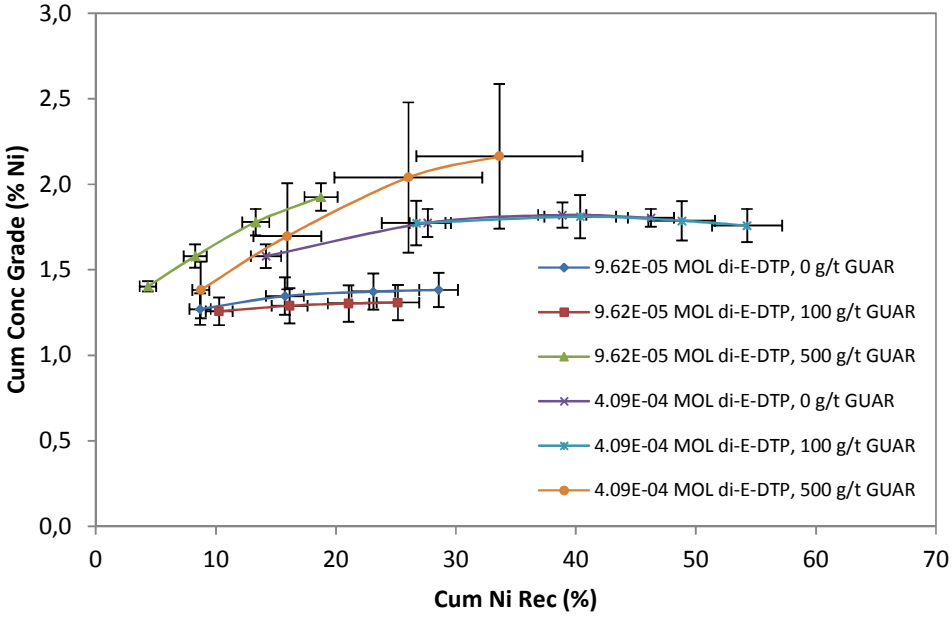


**Figure 4.45: Effect of increasing guar dosage on nickel grade and recovery for different dosages of diethyl DTP**

### *4.5.5.3 Gangue Recovery*

The amount of gangue recovered by entrainment when DTP was used compared to SIBX is shown in Table 4.19. The procedure by which the information in Table 4.19 was obtained is outlined in Chapter 3, Section 3.3.3.3. This table shows that DTP, compared to SIBX, resulted in a significantly greater gangue recovery via entrainment. In fact, at an equivalent dosage, the use of diethyl DTP has led to more than double the mass of gangue reporting to the concentrate via entrainment.

**Table 4.19: The effect of increasing guar and diethyl DTP dosages on gangue recovery**

| Reagent Suite | Total Conc Mass (g) | Total Gangue in Conc (g) | Mass of "*Floating Gangue*" in Conc (g) | Mass of "*Entrained Gangue*" in Conc (g) |
|---|---|---|---|---|
| **2.00E-04 mole/kg D200 + 9.62E-05 mole/kg di-E-DTP + α** | | | | |
| α = 0 g/t guar | 85.5 ± 1.2 | 78.7 ± 0.7 | 34.5 ± 1.0 | 44.2 |
| α = 100 g/t guar | 81.0 ± 0.7 | 75.4 ± 1.5 | 28.8 ± 2.8 | 46.6 |
| α = 500 g/t guar | 39.1 ± 1.7 | 34.0 ± 1.7 | 2.4 ± 1.0 | 31.6 |
| **2.00E-04 mole/kg D200 + 3.07E-04 mole/kg di-E-DTP + α** | | | | |
| α = 0 g/t guar | 105.6 ± 2.1 | 96.5 ± 2.0 | 31.8 ± 0.9 | 64.7 |
| α = 100 g/t guar | 110.3 ± 3.2 | 100.8 ± 2.9 | 33.8 ± 1.1 | 67.0 |
| α = 500 g/t guar | 64.0 ± 1.1 | 56.5 ± 0.9 | 4.8 ± 3.0 | 51.7 |
| **2.00E-04 mole/kg D200 + 4.09E-04 mole/kg di-E-DTP + α** | | | | |
| α = 0 g/t guar | 105.3 ± 2.0 | 96.3 ± 1.8 | 31.9 ± 0.5 | 64.4 |
| α = 100 g/t guar | 135.6 ± 3.5 | 125.9 ± 2.5 | 32.6 ± 4.5 | 93.3 |
| α = 500 g/t guar | 64.4 ± 0.4 | 57.9 ± 0.6 | 4.3 ± 1.3 | 53.6 |
| **2.00E-04 mole/kg D200 + 4.09E-04 mole/kg SIBX + α** | | | | |
| α = 0 g/t guar | 75.6 ± 3.2 | 61.9 ± 2.9 | 31.0 ± 0.3 | 30.9 |
| α = 100 g/t guar | 70.1 ± 0.2 | 58.2 ± 0.2 | 27.2 ± 1.0 | 31.0 |
| α = 500 g/t guar | 50.4 ± 0.5 | 38.7 ± 0.3 | 4.9 ± 0.5 | 33.7 |

### 4.5.6 Froth Imaging for Batch Flotation Test with Reagent Suite 2.00E-04 mole/kg Dowfroth 200 + 4.09E-04 mole/kg diethyl DTP

Figure 4.46 shows two randomly selected images of the first concentrate for the test where the collector type and dosage was diethyl DTP and 4.09E-04 mole/kg. The images are in complete contrast to those which were obtained when SIBX was used at an equivalent collector dosage (cf. Figure 4.33) but very similar to those obtained when only frother was used (cf. Figure 4.17). The froth colour is grey but less green/gold than that which was obtained with "frother only", which was probably due to heavy gangue contamination of the froth. The average bubble diameter, when compared to the "frother only" images (cf. Figure 4.17), appears slightly larger which indicates that bubble coalescence was more prevalent here. The average bubble diameter in Figure 4.46 is however significantly smaller than that which was obtained with SIBX at an equivalent collector dosage (cf. Figure 4.33). The bubble shape appears to be mostly circular which suggests a froth which contains significant amounts of water and therefore is very stable.

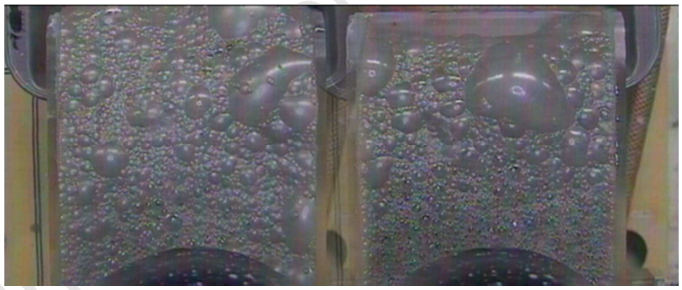

**Figure 4.46: Images of the froth from the first concentrate from the test where the collector type and dosage was diethyl DTP and 4.09E-04 mole/kg;**

The froth image from the second concentrate, shown in Figure 4.47, appears very white in colour. This is in complete contrast to the froth images obtained from the SIBX tests at the same flotation times (cf. Figure 4.30, Figure 4.34). Similarly, the images in Figure 4.48 and Figure 4.49 show that the froth from the third and fourth concentrates was significantly whiter in appearance as compared to the equivalent SIBX test (cf. Figure 4.35 and Figure 4.36).

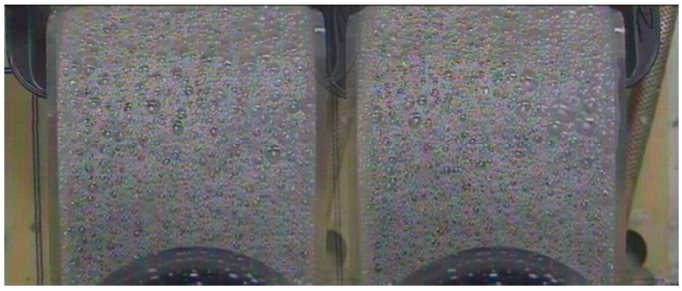

**Figure 4.47: Images of the froth from the second concentrate from the test where the collector type and dosage was diethyl DTP and 4.09E-04 mole/kg**

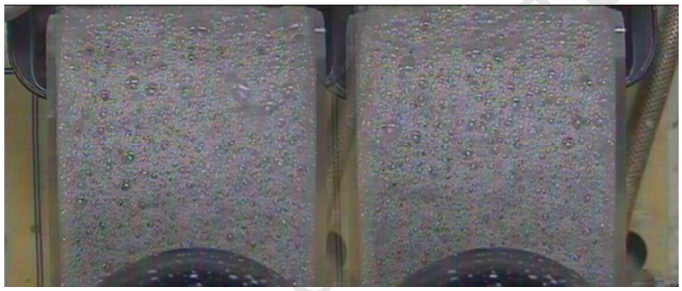

**Figure 4.48: Images of the froth from the third concentrate from the test where the collector type and dosage was diethyl DTP and 4.09E-04 mole/kg**

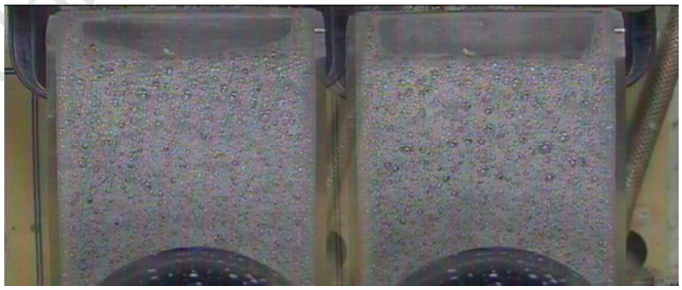

**Figure 4.49: Images of the froth from the fourth concentrate from the test where the collector type and dosage was diethyl DTP and 4.09E-04 mole/kg**

## 4.6 Batch Flotation Results Using Mixtures of Collectors

This section describes the results of batch flotation tests conducted to investigate the effect of mixtures of xanthates and DTP collectors on the recoveries and grades of copper, nickel, PGE and gangue. As was the case with the pure collector tests, further tests were conducted where, in addition to DTP, a high molecular weight guar was added in order to depress the floating gangue. Flotation performance was thus evaluated from copper and nickel recovery, copper and nickel concentrate grades, water recovery, and the mass of both entrained and floating gangue in the concentrate.

### 4.6.1 Mass and Water Recovery

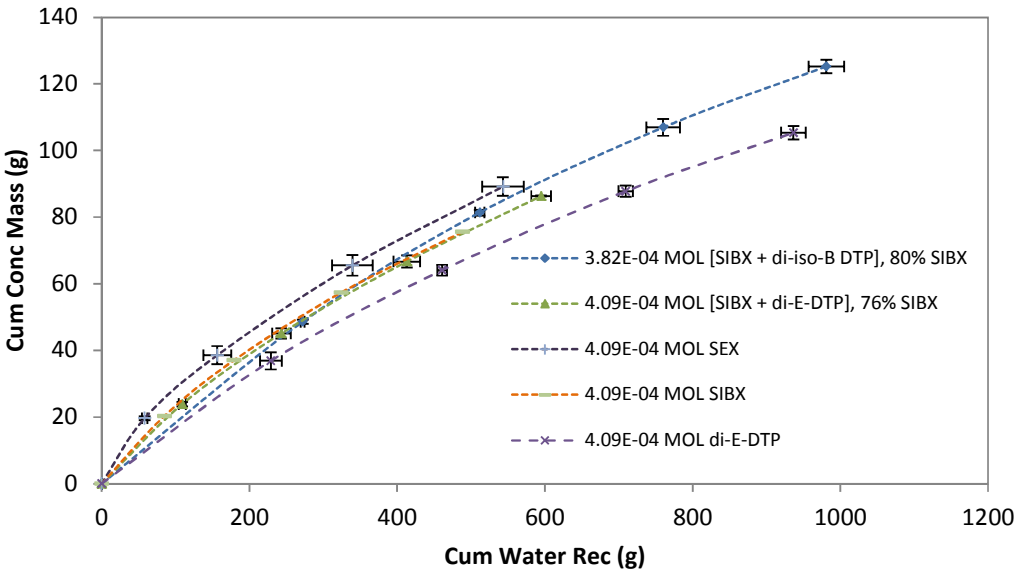


**Figure 4.50: Cumulative concentrate mass recovered versus water recovered for tests with different dosages and types of collector**

Figure 4.50 shows the cumulative concentrate mass obtained as a function of cumulative water recovered using a constant frother dosage and mixtures of xanthate and DTP collectors. The figure shows that, compared to the pure xanthate cases, a higher water recovery was obtained when diethyl DTP was used alone or when a combination of SIBX and di-iso-butyl DTP was used. The figure also

shows that the [SIBX + diethyl DTP] mixture only resulted in an extension of the concentrate mass/water recovery curve which was obtained with 4.09E-04 mole/kg SIBX as the only collector, i.e. the slope was not changed.

### 4.6.2 Grade and Recovery

The grade-recovery curves for copper and nickel obtained when mixtures of collectors were used are shown in Figures 4.51 to 4.55. Figure 4.51 shows the results obtained when batch flotation tests were completed using a lower total collector dosage (1.02E-04 mole/kg) whilst Figures 4.52 and 4.53 show the results obtained at the standard total collector dosage (4.09E-04 mole/kg). Figures 4.54 and 4.55, on the other hand, show the effect of collector chain length on copper and nickel recovery and grade, i.e. the flotation performance obtained when mixtures of SIBX and diethyl DTP are compared to that which was obtained when mixtures of SIBX and di-iso-butyl DTP or mixtures of SEX and diethyl DTP were used. Table 4.20 shows the final copper and nickel recovery and grades obtained when mixtures of SIBX and DTP were tested at a total collector dosage higher and lower than 4.09E-04 mole/kg.

Figure 4.51 shows that mixtures of xanthate and DTP, at a total dosage 1.02E-04 mole/kg, resulted in higher nickel recoveries compared to single-collector results. This additional recovery was however accompanied by a lower concentrate grade and was therefore achieved by non-selective means, i.e. increased non-selective mass pull. Figures 4.51 and 4.52 show that the highest copper grades were obtained with pure SIBX whilst the differences in nickel grade between that obtained with SIBX and those obtained when mixtures of collectors were used are within experimental error. Figure 4.53 shows that the use of SEX and combinations of SEX and diethyl DTP, as compared to SIBX and combinations of SIBX and diethyl DTP, resulted in greater initial nickel recoveries and grades. Figure 4.54 and Table 4.20 shows that the final copper recovery achieved was not significantly different for the various combinations of collectors tested whilst Figure 4.55 shows that the highest nickel recovery was obtained when a mixture of SIBX and di-iso-butyl DTP was used. This however, as can be seen from the mass recovery data in Table 4.20, had the undesirable effect of increasing total mass pull by more than 50 % which had a disastrous effect on concentrate grade.

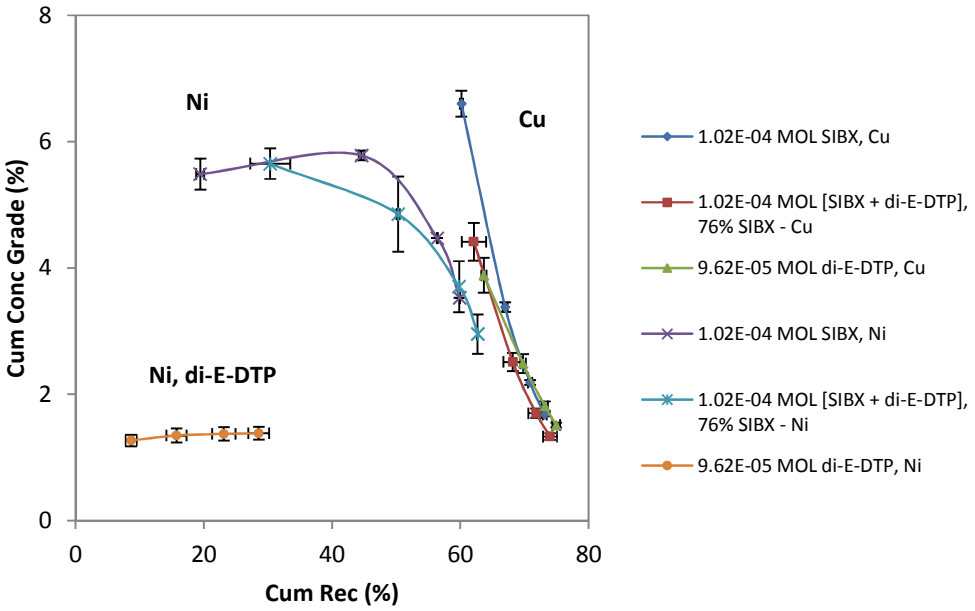


**Figure 4.51: The effect of collector mixtures, at a total dosage of 1.02E-04 mole/kg ore, on copper and nickel recoveries and grades**

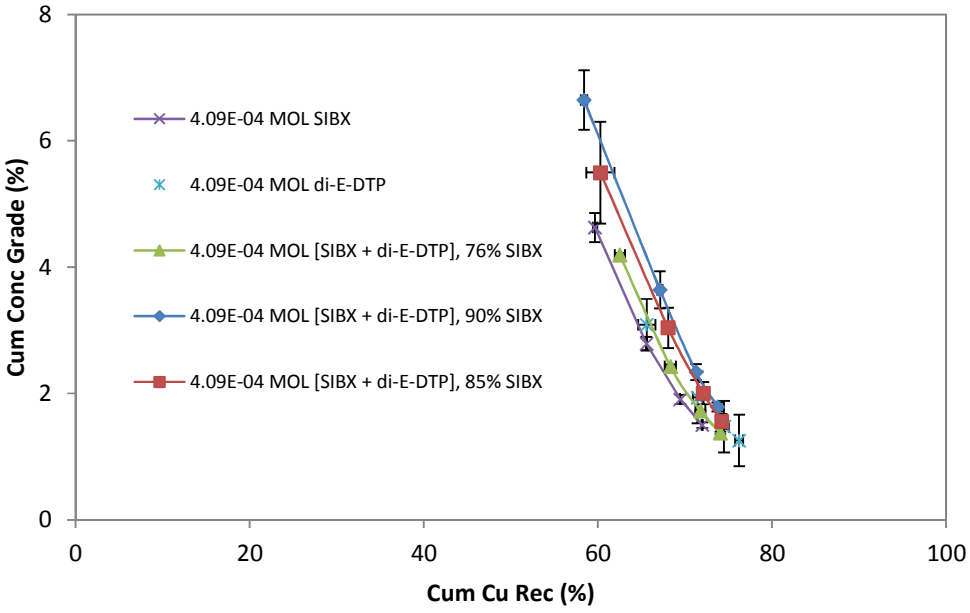


**Figure 4.52: The effect of collector mixtures, at the standard collector dosage (4.09E-04 mole/kg), on copper recovery and concentrate grade**

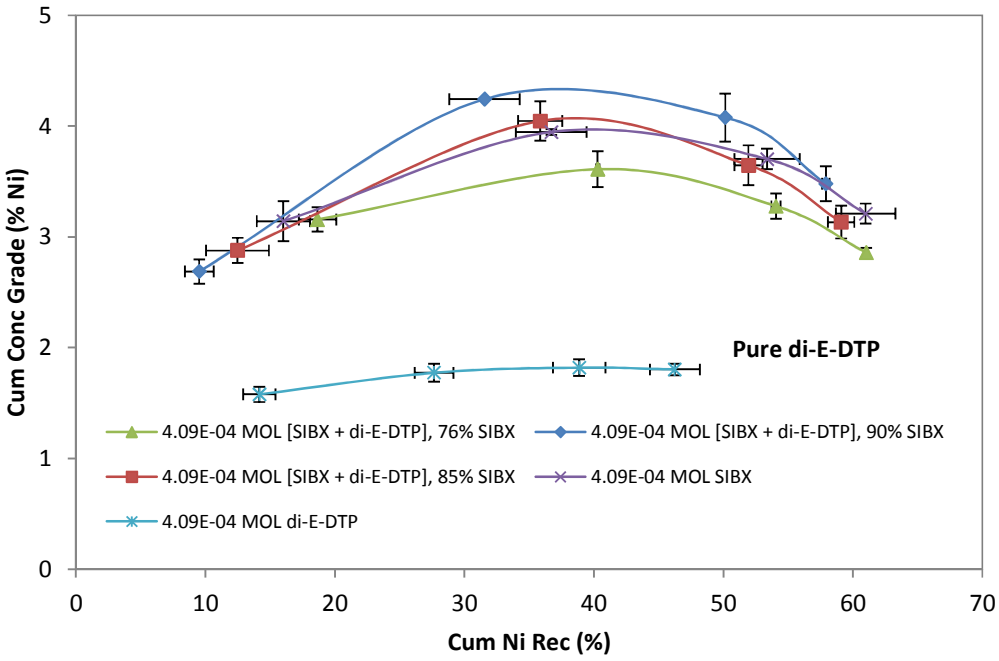


**Figure 4.53: The effect of collector mixtures, at the standard collector dosage, on nickel recovery and concentrate grade**

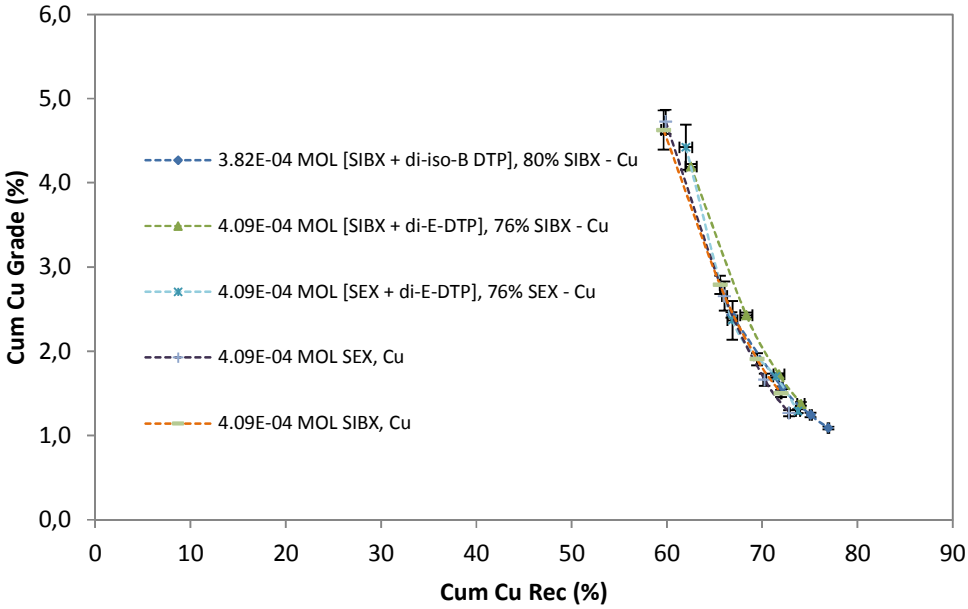


**Figure 4.54: The effect of combinations of different collectors, with different chain lengths, on copper recovery and grade**

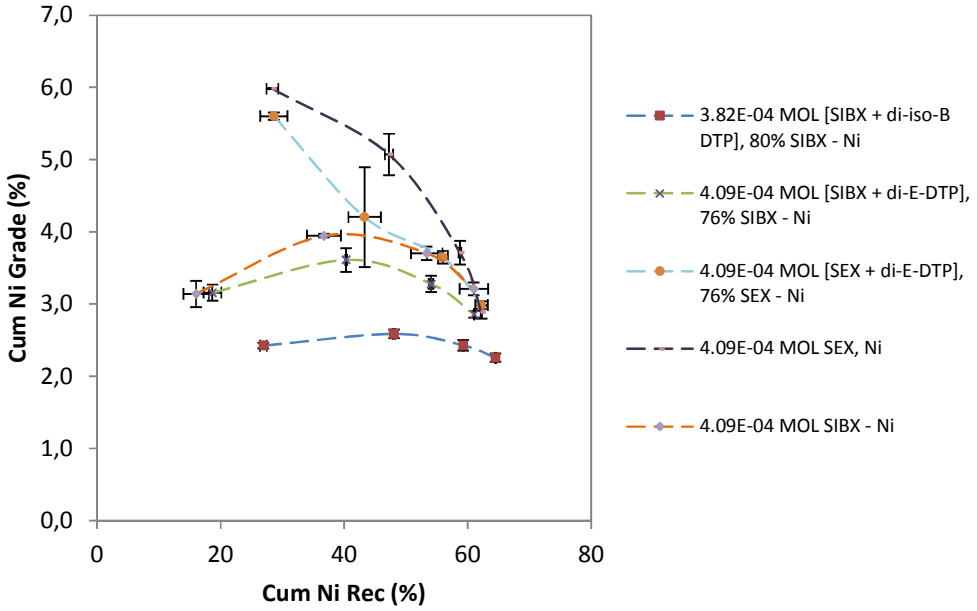


**Figure 4.55: The effect of combinations of different collectors, with different chain lengths, on nickel recovery and grade**



**Table 4.20: Results of batch flotation tests conducted using mixtures of collectors but at a total collector dosage different to the standard**

| Reagent Suite | | Cu | | Ni | | Mass of Conc (g) | Water Rec (g) |
|---|---|---|---|---|---|---|---|
| **2.00E-04 mole/kg D200 + *z* mole/kg Total Collector** | | **Rec (%)** | **Grade (%)** | **Rec (%)** | **Grade (%)** | | |
| *z* = 4.09E-04; SIBX & di-E-DTP | % SIBX = 76% | 74.1 ± 0.3 | 1.37 ± 0.02 | 61.0 ± 0.0 | 2.86 ± 0.04 | 86.3 ± 0.1 | 595.0 ± 13.2 |
| *z* = 4.57E-04; SIBX & di-E-DTP | % SIBX = 89% | 73.3 ± 0.5 | 1.62 ± 0.10 | 59.1 ± 0.1 | 3.24 ± 0.17 | 75.7 ± 1.4 | 463.4 ± 7.0 |
| *z* = 3.49E-04; SIBX & di-E-DTP | % SIBX = 59% | 75.6 ± 0.8 | 1.60 ± 0.02 | 59.7 ± 1.4 | 3.01 ± 0.02 | 81.6 ± 4.3 | 519.2 ± 32.4 |
| *z* = 3.82E-04; SIBX & di-iso-B DTP | % SIBX = 80% | 77.0 ± 0.1 | 1.09 ± 0.02 | 64.5 ± 0.1 | 2.26 ± 0.06 | 125.2 ± 2.0 | 981.0 ± 24.1 |

Table 4.20 shows that final copper and nickel recoveries were essentially unaffected by both the proportion of diethyl DTP in the SIBX-diethyl DTP collector mixtures and the total collector dosage (*z*). It is interesting to note however that the water recovery was reduced when the total collector dosage was increased or reduced from the standard dosage (*z* = 4.09E-04)

### 4.6.3 The Effect of Water Recovery on Copper and Nickel Recovery

Figure 4.56 shows the effect of collector type and dosage on copper recovery as a function of water recovery whilst Figure 4.57 shows the effect of collector type and dosage on copper grade as a function of concentrate mass. Figures 4.56 and 4.57 show that the ultimate copper recovery attained was determined by water recovery and mass pull rather than collector reagent suite. Figure 4.58 shows the effect of collector type and dosage on nickel recovery as a function of water recovery.



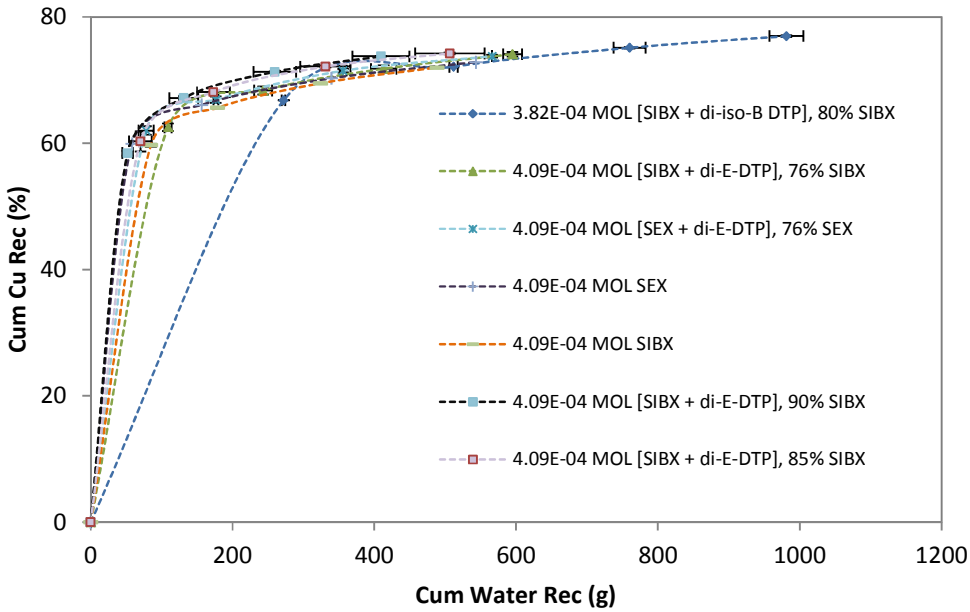


**Figure 4.56: Cumulative copper recovery as a function of water recovery obtained using mixtures of xanthates and DTP**

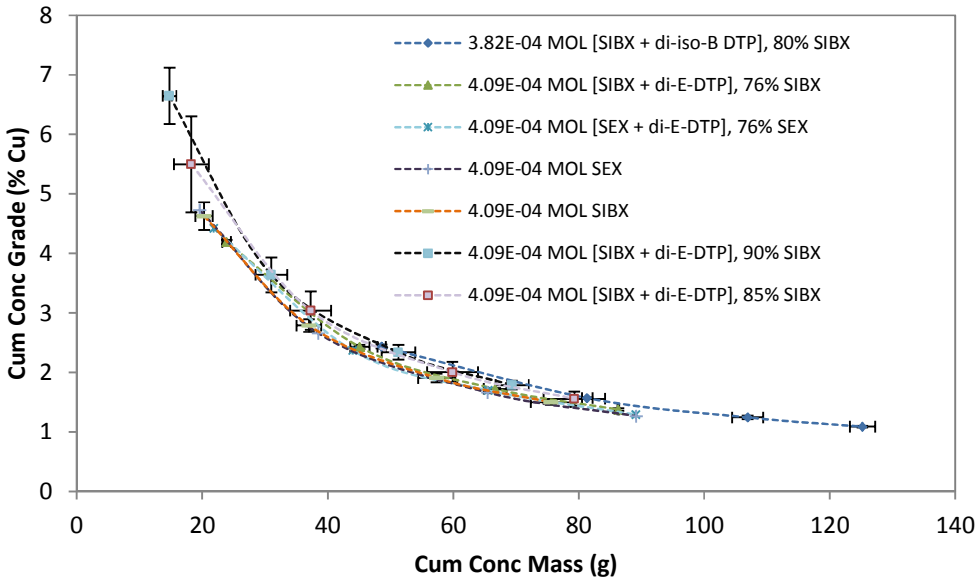


**Figure 4.57: Cumulative concentrate grade as a function of mass recovery obtained using mixtures of xanthate and DTP**

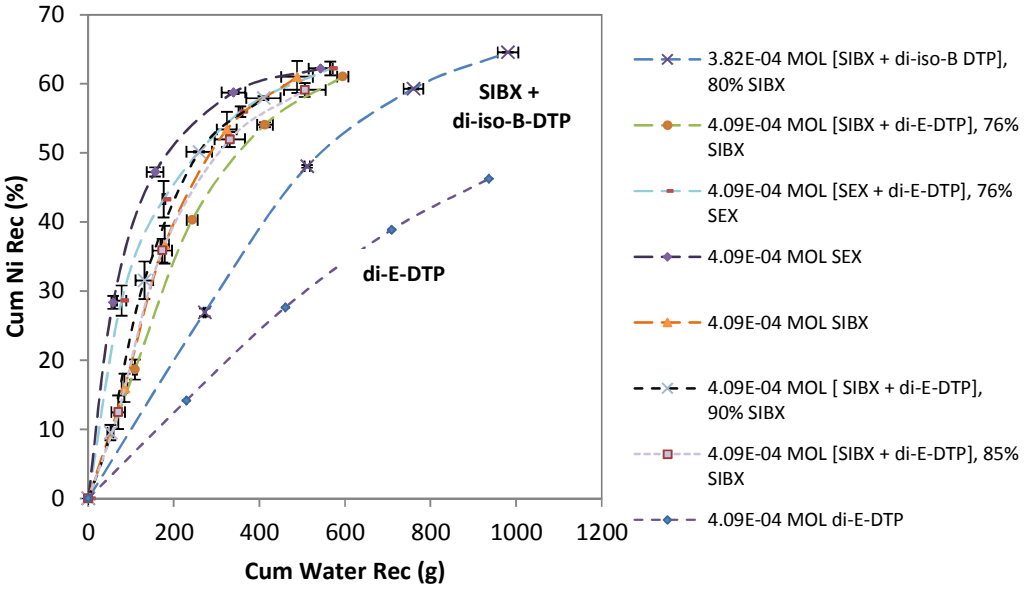


**Figure 4.58: Cumulative nickel recovery as a function of water recovery obtained using mixtures of xanthates and DTP**

Figure 4.58 shows that the nickel recovery versus water recovery curves for the various collector regimes were distinctly different to that which was obtained for copper (cf. Figure 4.56). For example, at a water recovery of 200 g, the list of reagent suites which gave nickel recoveries from best to worse are SEX, [SEX + diethyl DTP] and followed by the [SIBX + diethyl DTP] mixtures. It is interesting to note that the [SIBX + di-iso-butyl DTP] curve is far to the right when compared to the [SIBX + diethyl DTP] curves.

### 4.6.4 Kinetic Analysis of Flotation Results

Figure 4.59 shows the recovery of copper as a function of flotation time for various mixtures of collectors. This figure shows that the best copper recovery was obtained with mixtures of SIBX and di-iso-butyl DTP. Figure 4.59 also shows that approximately 60 % of the copper was recovered within the first four minutes of flotation time. This suggests that, together with the fact that the curve flattened rapidly after 4 minutes flotation time, the chalcopyrite was fast floating.



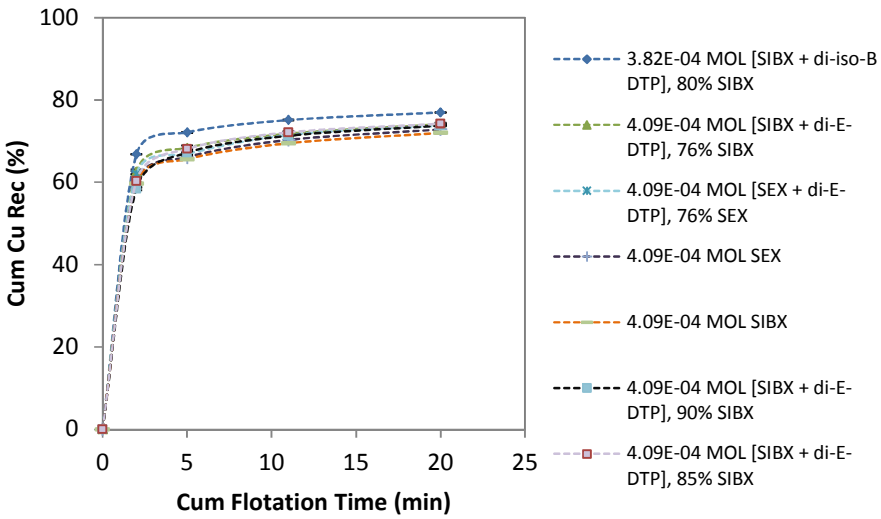


**Figure 4.59: Cumulative copper recovery as a function of flotation time obtained with variations in collector type, chain length and concentration in pulp**

Figure 4.60 show the recovery of nickel as a function of flotation time for various mixtures of collectors. This figure shows that, as was the case with copper, the best nickel recovery was obtained with mixtures of SIBX and di-iso-butyl DTP. Figure 4.59 showed that approximately 60 % of copper was recovered after 4 minutes flotation time whilst Figure 4.60 shows that between 10 and 30 % of the nickel was recovered during the same period. It can thus be concluded that the nickel-containing minerals (mostly pentlandite) were, comparatively, slow floating.

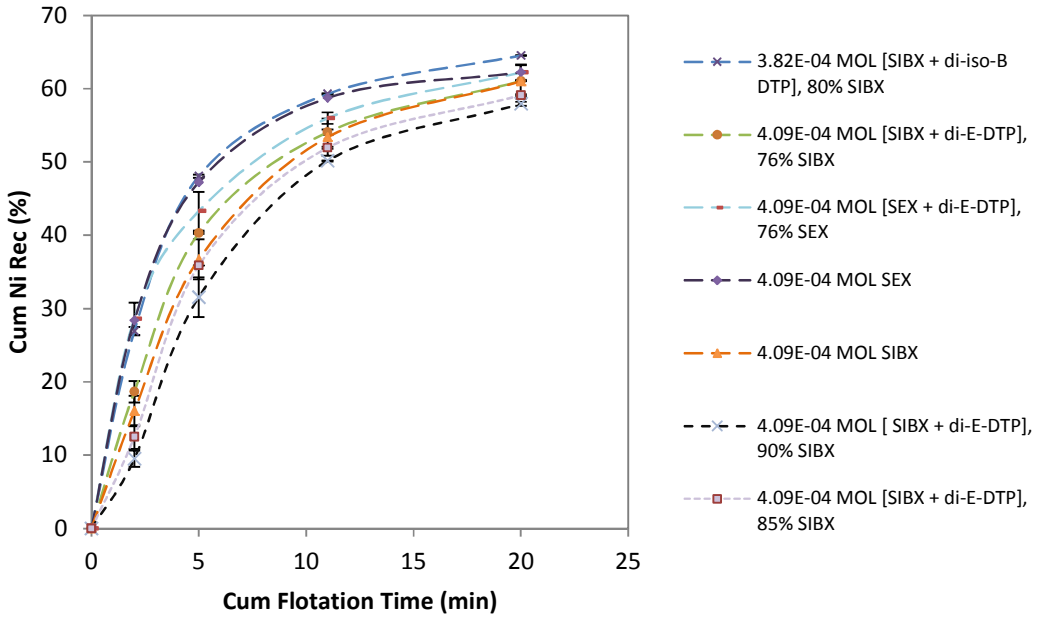


**Figure 4.60: Cumulative nickel recovery as a function of flotation time obtained with variations in collector type, chain length and concentration in pulp**

Table 4.21 shows that the infinite time copper and nickel recoveries as well as the first order rate constants attained with various collector reagent suites. The table shows that infinite time nickel recovery was always significantly greater than the actual recovery after twenty minutes flotation time. This indicates that longer residence times could increase nickel recovery irrespective of the collector regime. Combinations of SIBX and diethyl DTP predicted greater infinite time nickel recoveries than combinations of SEX and diethyl DTP although the rate constants are greater in the latter mixture. It is also interesting to note that a higher infinite time nickel recovery was predicted for the mixture [90 %

SIBX + 10 % diethyl DTP, 4.09E-04 mole/kg collector] than for the mixture [76 % SIBX + 24 % diethyl DTP, 4.09E-04 mole/kg collector]. This suggests that the predicted infinite time nickel recovery decreased with an increase in the diethyl DTP content of the [SIBX + diethyl DTP] collector mixture.

**Table 4.21: First order rate constants and infinite time recovery values obtained with the collectors SEX, SIBX, diethyl DTP and di-iso-butyl DTP and their mixtures**

| Reagent Suite | Max Cu Rec (%) | | Max Ni Rec (%) | | Rate Constant ($min^{-1}$) | |
|---|---|---|---|---|---|---|
| **2.00E-04 mole/kg D200 + *x*** | **Actual** | **$R_{inf}$** | **Actual** | **$R_{inf}$** | **Cu** | **Ni** |
| *x* = 4.09E-04 mole/kg SIBX | 72.0 ± 0.1 | 72.1 ± 0.1 | 61.0 ± 2.3 | 74.3 ± 1.5 | 2.77 ± 0.07 | 0.30 ± 0.04 |
| *x* = 4.09E-04 mole/kg [SIBX + di-E-DTP], 90 % SIBX; 10 % di-E-DTP | 73.7 ± 0.0 | 74.6 ± 0.0 | 57.9 ± 0.3 | 77.1 ± 4.0 | 2.23 ± 0.06 | 0.22 ± 0.03 |
| *x* = 4.09E-04 mole/kg [SIBX + di-E-DTP], 85 % SIBX; 15 % di-E-DTP | 74.2 ± 0.1 | 75.0 ± 0.4 | 59.1 ± 1.0 | 73.9 ± 0.9 | 2.47 ± 0.31 | 0.27 ± 0.03 |
| *x* = 4.09E-04 mole/kg [SIBX + di-E-DTP], 76 % SIBX; 24 % di-E-DTP | 74.1 ± 0.4 | 74.3 ± 1.8 | 61.0 ± 0.0 | 71.3 ± 0.4 | 3.04 ± 1.05 | 0.37 ± 0.01 |
| *x* = 3.82E-04 mole/kg [SIBX + di-iso-B-DTP], 80 % SIBX; 20 % di-iso-B-DTP | 77.0 ± 0.1 | 77.3 ± 0.1 | 64.5 ± 0.1 | 71.3 ± 0.1 | 3.58 ± 0.04 | 0.55 ± 0.01 |
| *x* = 4.09E-04 mole/kg SEX, 76 % SEX; 24 % di-E-DTP | 73.8 ± 0.2 | 73.7 ± 0.1 | 62.2 ± 1.0 | 67.2 ± 2.2 | 2.97 ± 0.13 | 0.57 ± 0.04 |



## 4.6.5 Effect of Depressant

### *4.6.5.1 Mass & Water Recovery*

Table 4.22 shows the relationship between water recovered and mass recovered as a function of guar dosage for various collector regimes tested in this investigation. It shows that the use of diethyl DTP as collector, in the presence of 100 g/t guar, resulted in an increase in water and mass recovery as compared to the case when not any guar was used. The table also shows that only a very small decrease

in concentrate mass was achieved for the "SIBX only" and "SIBX + DTP" collector regimes at the 100 g/t guar dosage. However, once the guar dosage was increased to 500 g/t, the mass of concentrate recovered decreased to approximately 50 g from a "no guar case" of 76 g with "SIBX only" collector regime or 86 g with the "SIBX + DTP" collector regime. These results suggest that fairly high dosages of guar are required if the floating gangue is to be fully depressed.

**Table 4.22: A comparison of the effect of guar dosage on mass and water recovery for either SIBX or diethyl DTP or a combination of the two collectors**

| Guar Dosage (g/t) | 4.09E-04 mole/kg SIBX | | 4.09E-04 mole/kg di-E-DTP | | 4.09E-04 mole/kg [76 % SIBX + 24 % di-E-DTP] | |
|---|---|---|---|---|---|---|
| | Water Rec (g) | Conc Mass (g) | Water Rec (g) | Conc Mass (g) | Water Rec (g) | Conc Mass (g) |
| 0 | 488.4 | 75.6 | 936.5 | 105.3 | 594.9 | 86.3 |
| 100 | 490.3 | 70.1 | 1137.4 | 135.6 | 562.1 | 77.1 |
| 500 | 533.9 | 50.4 | 779.1 | 64.4 | 507.0 | 49.8 |

### *4.6.5.2 Copper & Nickel Recovery*

Table 4.23 summarises the copper and nickel grades and recoveries obtained with increasing guar dosage using SIBX and DTP as individual collectors as well as a combination of the two. The data in Table 4.23 shows that, at a guar dosage of 500 g/t, copper recovery decreased compared to the case when guar was not added or when an intermediate dosage was added. The data in Table 4.23 also show that a slight increase in the average copper recovery was obtained when the individual collectors were used at an intermediate dosage of guar although the grades decreased in the case of DTP indicating a non-selective increase in mass pull. When both collectors as well as an intermediate dosage of guar were added, the average copper recovery decreased slightly. It is however also interesting to note that, in the case of the collector mixture, the presence of guar molecules in the flotation pulp did not seem to influence nickel recovery significantly.

**Table 4.23: A comparison of the effect of guar dosage on copper and nickel recovery and grades for either SIBX or diethyl DTP or a combination of the two collectors**

| Guar Dosage (g/t) | 4.09E-04 mole/kg SIBX | | | | 4.09E-04 mole/kg di-E-DTP | | | | 4.09E-04 mole/kg [76 % SIBX + 24 % di-E-DTP] | | | |
|---|---|---|---|---|---|---|---|---|---|---|---|---|
| | Cu Rec & Grade | | Ni Rec & Grade | | Cu Rec & Grade | | Ni Rec & Grade | | Cu Rec & Grade | | Ni Rec & Grade | |
| | Rec (%) | Grade (%) | Rec (%) | Grade (%) | Rec (%) | Grade (%) | Rec (%) | Grade (%) | Rec (%) | Grade (%) | Rec (%) | Grade (%) |
| 0 | 72.0 | 1.5 | 61.0 | 3.2 | 76.2 | 1.3 | 46.3 | 1.8 | 74.1 | 1.4 | 61.0 | 2.9 |
| 100 | 73.6 | 1.7 | 58.9 | 3.4 | 77.9 | 1.0 | 54.3 | 1.8 | 72.0 | 1.4 | 60.0 | 3.1 |
| 500 | 69.9 | 2.0 | 56.7 | 4.5 | 71.8 | 1.9 | 33.6 | 2.2 | 68.7 | 2.6 | 59.5 | 5.7 |

### *4.6.5.3 Gangue Recovery*

Table 4.24 shows the mass of non-sulphide gangue, entrained gangue and floating gangue recovered using the various collector suites employed in this investigation. The "non-sulphide gangue" is the sum of the mass of floating gangue and the mass of entrained gangue that was recovered to the concentrate. The procedure used to separate entrained gangue from floating gangue has been explained in Chapter 3, Section 3.3.3.3.



**Table 4.24: The effect of collector suite, either a single collector or a mixture of collectors, on entrained gangue recovery**

| Reagent Suite 2.00E-04 mole/kg D200 + Collector | Non-Sulphide Gangue Mass (g) | Floating Gangue Mass (g) | Entrained Gangue Mass (g) |
|---|---|---|---|
| 4.09E-04 mole/kg [76 % SIBX + 24 % di-E-DTP] | 74.1 ± 0.4 | 33.6 ± 0.7 | 39.6 |
| 4.09E-04 mole/kg [85 % SIBX + 15 % di-E-DTP] | 67.8 ± 5.0 | 34.2 ± 2.3 | 33.7 |
| 4.09E-04 mole/kg [90 % SIBX + 10 % di-E-DTP] | 57.8 ± 3.3 | 30.5 ± 0.2 | 27.2 |
| 4.09E-04 mole/kg di-E-DTP | 96.3 ± 1.8 | 31.9 ± 0.5 | 64.4 |
| 4.09E-04 mole/kg SIBX | 61.9 ± 3.0 | 31.0 ± 0.3 | 30.9 |

Table 4.24, as was established in Table 4.19, shows that DTP significantly increased gangue recovery via entrainment when compared to SIBX at equivalent collector dosages. Table 4.24 also shows that the mass of non-sulphide gangue recovered when mixtures of SIBX and diethyl DTP was used increased with increasing diethyl DTP content of the mixture.

### 4.6.6 The Effect of Sequence of Collector Addition on Cu, Ni and PGE Recoveries and Grades

A number of tests were conducted in which the order of addition of collectors was varied and the results obtained are shown in Figures 4.61 to 4.68. The aim of these tests was to ascertain if the flotation response, as is indicated by water recovery, copper recovery, nickel recovery, PGE recovery and concentrate grades, varied if the sequence of collector addition was varied.



#### *4.6.6.1 Copper & Nickel Recovery*

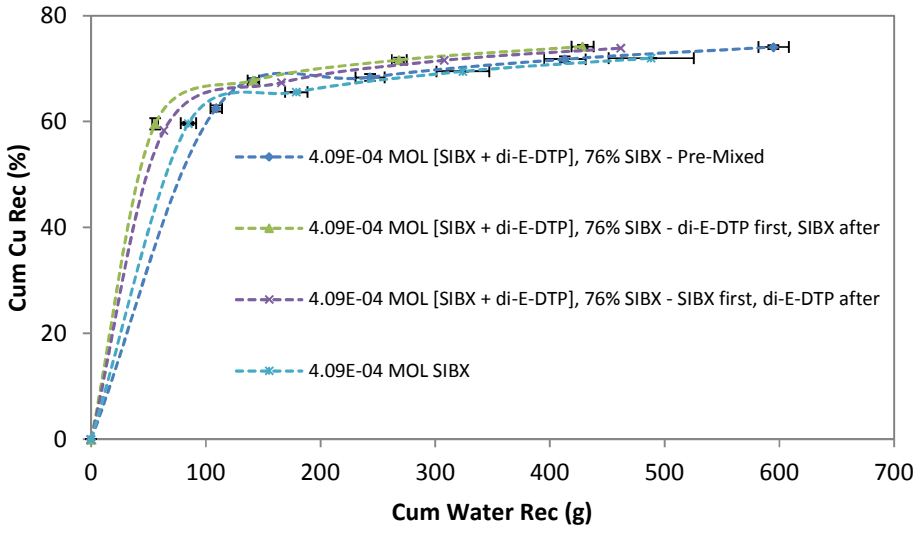


**Figure 4.61: The effect of sequence of addition of collectors on copper recovery as a function of water recovery**

Figure 4.61 and Figure 4.62 show the effect of order of addition of the different collectors on the cumulative copper and nickel recoveries as a function of water recovery respectively. The figures show that the ultimate copper or nickel recovery was unaffected by the sequence of addition of collectors but that significantly more water was recovered with the premixed test procedure.

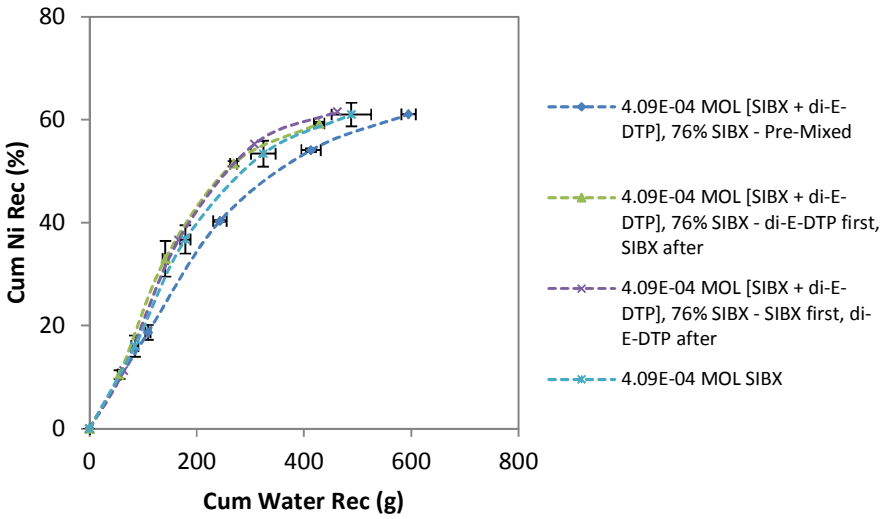


**Figure 4.62: The effect of sequence of addition of collectors on nickel recovery as a function of water recovery**



### *4.6.6.2 Palladium and Platinum Recovery*

Figure 4.63 shows the cumulative palladium grade versus cumulative concentrate mass recovered. This figure shows that the premixed condition achieved substantially higher palladium grades for the same concentrate mass compared to any other condition which, in turn, indicates that the premixed condition promoted the preferential recovery of palladium. The latter statement is supported by the palladium recovery versus time flotation plot (cf. Figure 4.64) which also shows that the ultimate palladium recovery achieved was substantially higher for the premixed configuration. Figure 4.63 also shows that the "SIBX only" result was almost identical to the "SIBX followed by diethyl DTP" collector regime which indicates that the DTP had very little effect on recovery if the mineral particles were first exposed to

SIBX. This is supported by the "diethyl DTP only" result, shown in Figures 4.63 and 4.65, which indicates that the collector, on its own, is a very poor palladium collector.

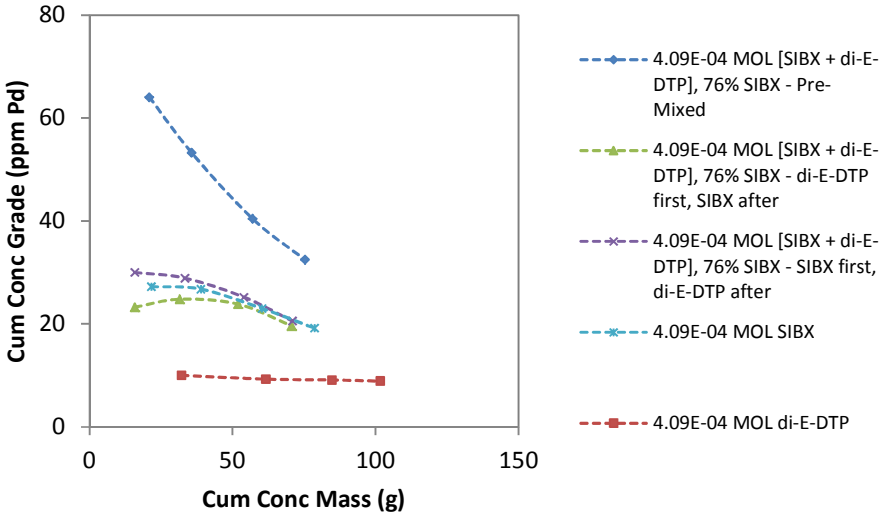


**Figure 4.63: The effect of the individual collectors SIBX and diethyl DTP as well as their mixtures added in particular sequences on palladium grade as a function of concentrate mass**

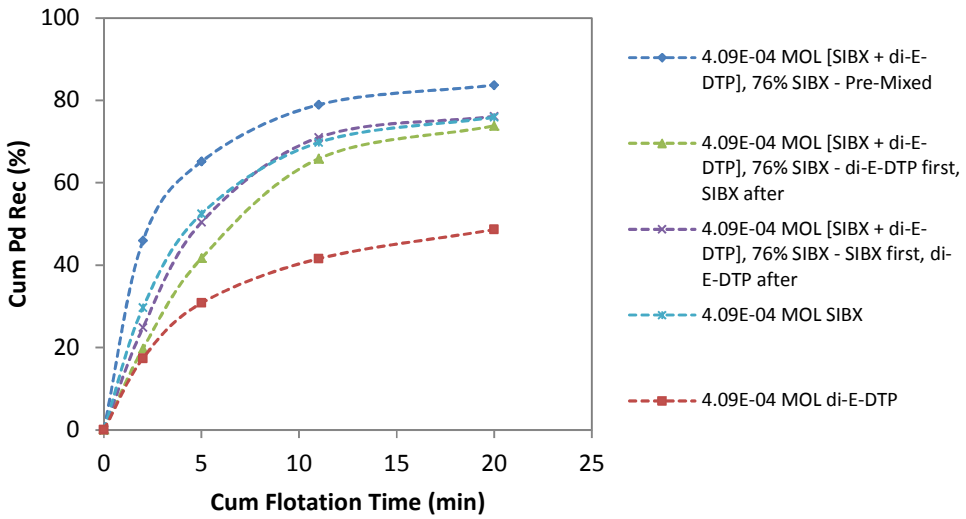


**Figure 4.64: The effect of the individual collectors SIBX and diethyl DTP as well as their mixtures added in particular sequences on palladium grade as a function of flotation time**

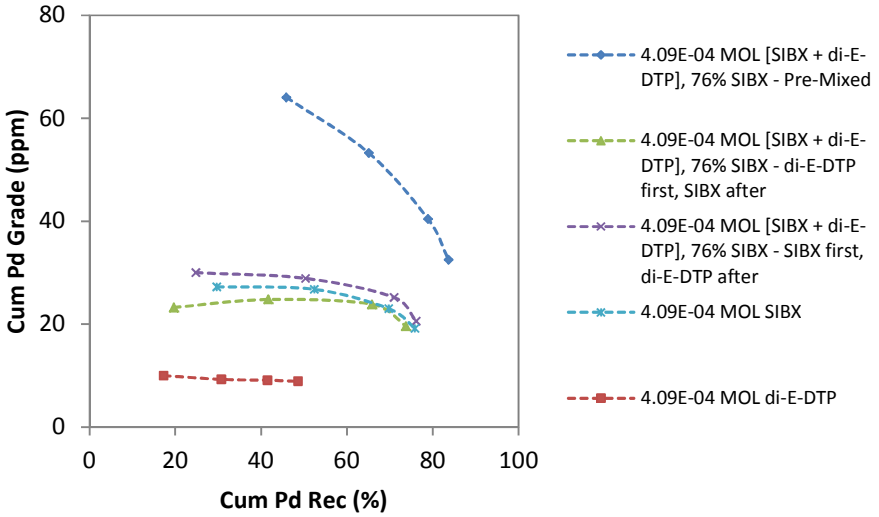


**Figure 4.65: A comparison of palladium grade-recovery curves for mixtures of SIBX and diethyl DTP in which the sequence of collector addition was varied against the grade-recovery curves for the individual collectors**

Figure 4.66 shows the effect of sequence of addition of a combination of the collectors SIBX and diethyl DTP, as well as the collectors individually, on the cumulative platinum grade versus cumulative concentrate mass recovered. This figure shows that there was no significant difference in performance between the "SIBX only" collector regime and "pre-mixed" collector regime whilst the conditions where the order of collector addition was varied resulted in slightly reduced ultimate platinum recovery values. Figure 4.67, which shows the cumulative platinum recovery as a function of cumulative flotation time, also indicates that there was no significant difference in platinum recovery between the "SIBX only" regime and the "premixed" collector regime. Finally, as was the case with palladium, the figures presented shows that diethyl DTP was a poor platinum collector.

Table 4.25 on the other hand shows the platinum and palladium first order rate constants as well as the infinite time recoveries obtained with various collector reagent suites and sequences of collector addition when more than one collector was used.

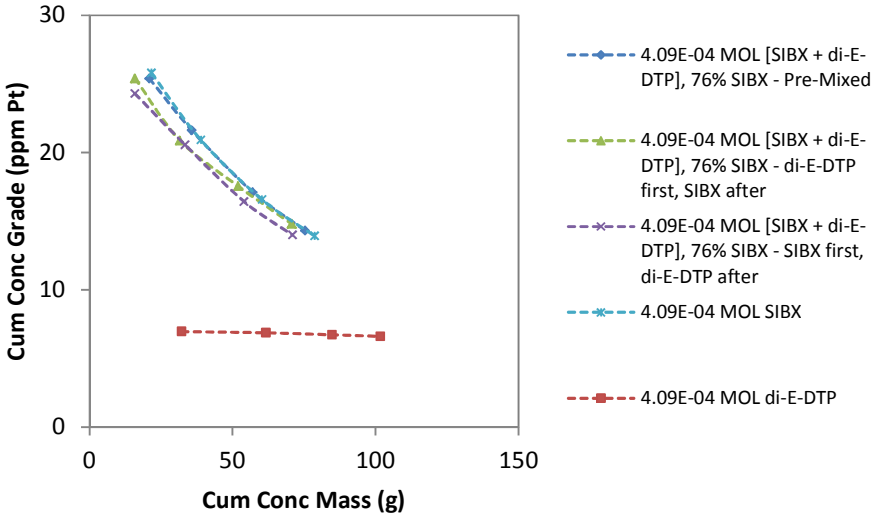


**Figure 4.66: The effect of the individual collectors SIBX and diethyl DTP as well as their mixtures added in particular sequences on platinum grade as a function of concentrate mass**

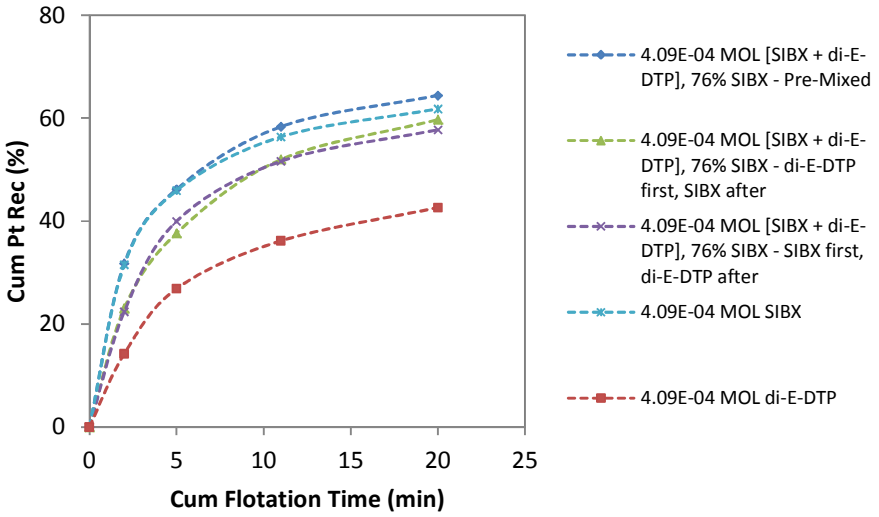


**Figure 4.67: The effect of the individual collectors SIBX and diethyl DTP as well as their mixtures added in particular sequences on platinum grade as a function of flotation time**

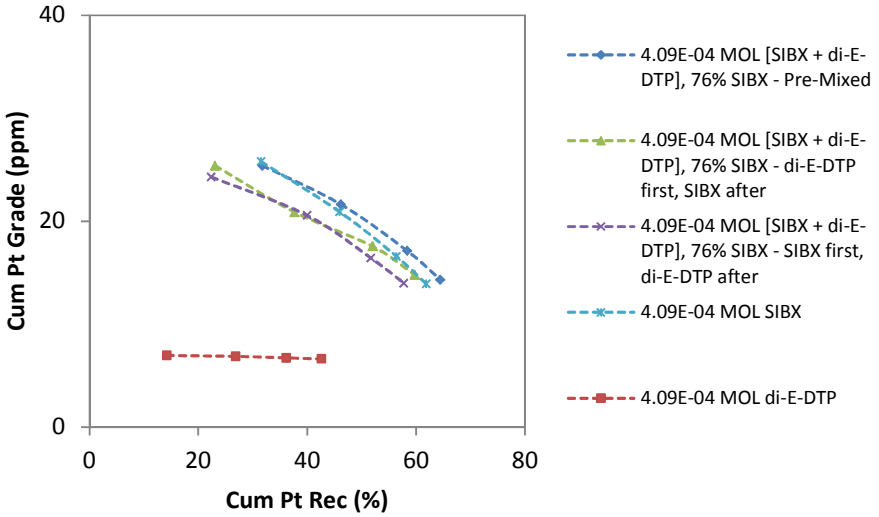


**Figure 4.68: A comparison of platinum grade-recovery curves for mixtures of SIBX and diethyl DTP in which the order of addition was varied against the grade-recovery curves for the individual collectors**

**Table 4.25: First order rate constants and infinite time recovery values obtained with the collectors pure SIBX, pure diethyl DTP and their mixtures which was added in different sequences**

| Reagent Suite | Max Pt Rec (%) | | Max Pd Rec (%) | | Rate Constant ($min^{-1}$) | |
|---|---|---|---|---|---|---|
| **2.00E-04 mole/kg D200 + *x*** | **Actual** | **$R_{inf}$** | **Actual** | **$R_{inf}$** | **Pt** | **Pd** |
| *x* = 4.09E-04 mole/kg SIBX | 61.8 | 65.4 | 75.9 | 85.6 | 0.70 | 0.47 |
| *x* = 4.09E-04 mole/kg diethyl DTP | 42.6 | 48.8 | 48.6 | 55.1 | 0.37 | 0.39 |
| *x* = 4.09E-04 mole/kg [SIBX + di-E-DTP], 76 % SIBX; 24 % di-E-DTP; pre-mixed | 64.4 | 68.5 | 83.7 | 88.6 | 0.65 | 0.81 |
| *x* = 4.09E-04 mole/kg [SIBX + di-E-DTP], 76% SIBX; 24% di-E-DTP; SIBX first, diethyl DTP after | 57.7 | 64.4 | 76.3 | 89.7 | 0.47 | 0.38 |
| *x* = 3.82E-04 mole/kg [SIBX + diethyl DTP], 76 % SIBX; 24 % diethyl DTP; DTP first, SIBX after | 59.7 | 67.1 | 73.8 | 91.9 | 0.41 | 0.28 |

### 4.6.7 Froth Imagining for Batch Flotation Test where the Collectors SIBX and diethyl DTP were added at the Same Time and at a Total Collector Dosage of 4.09E-04 mole/kg

Figures 4.69 to 4.72 show pictures of the froth which were obtained when the collectors SIBX and diethyl DTP were used at a total dosage of 4.09E-04 mole/kg and in a 76 % SIBX, 24 % diethyl DTP mixture, i.e. the dosage of collectors was 3.07E-04 mole/kg SIBX and 1.02E-04 mole/kg diethyl DTP. The collectors were added to the flotation pulp at the same time.

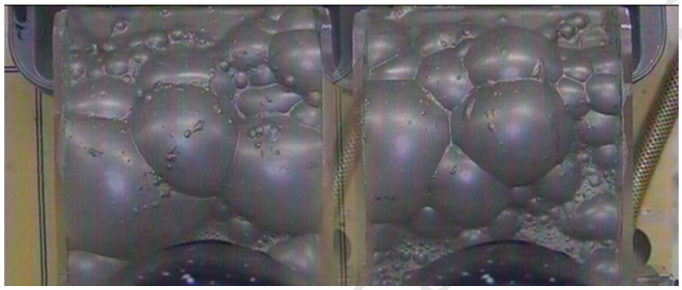

**Figure 4.69: Pictures of the froth from the first concentrate for the test where the collectors used were SIBX and diethyl DTP at the total dosage of 4.09E-04 mole/kg**

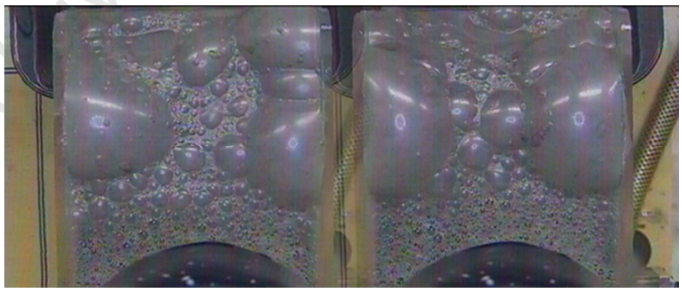

**Figure 4.70: Pictures of the froth from the second concentrate for the test where the collectors used were SIBX and diethyl DTP at the total dosage of 4.09E-04 mole/kg**

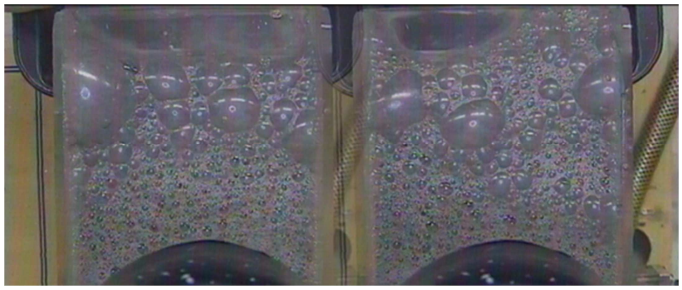

**Figure 4.71: Pictures of the froth from the third concentrate for the test where the collectors used were SIBX and diethyl DTP at the total dosage of 4.09E-04 mole/kg**

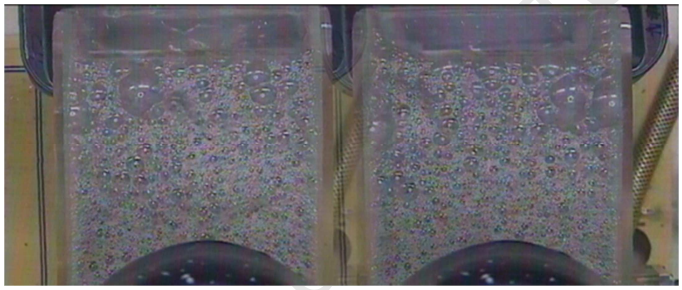

**Figure 4.72: Pictures of the froth from the fourth concentrate for the test where the collectors used were SIBX and diethyl DTP at the total dosage of 4.09E-04 mole/kg**

## 4.7 Recovery by Particle Size Batch Flotation Test Results

The particle size distributions of the feed, concentrate and tailings samples from selected tests were determined and the size fractions were assayed for copper and nickel which were then used to calculate the copper and nickel recoveries by particle size. This was done in order to establish if the use of diethyl DTP as a collector resulted in enhanced fine particle recovery. The results obtained from these experiments are presented here.

### 4.7.1 SIBX compared to di-E-DTP

Figure 4.73 shows the percentage of copper recovered from specific size fractions obtained when SIBX and diethyl DTP were, respectively, used as collectors. This figure shows that a significant drop in recovery occurred in the -25 µm size range when SIBX was the collector whilst, with diethyl DTP as collector, this did not happen. Figure 4.74, on the other hand, shows the percentage of nickel recovered from specific size fractions which were obtained when SIBX and diethyl DTP were used as collectors. This figure shows, firstly, that the use of diethyl DTP did not lead to any significant recovery of nickel-containing minerals above 38 µm. Secondly, Figure 4.74 also shows that the inability of diethyl DTP to recover the nickel-containing minerals above 38 µm cannot be attributed to poor liberation or other mechanical reasons because the SIBX was able to recover those nickel-containing minerals which were present in the coarser size fractions in significant amounts.



Figures 4.75 and 4.76 show, respectively, the copper and nickel recoveries obtained per particle size fraction when equimolar amounts of SIBX and diethyl DTP were used. A comparison of the nickel recovery obtained per size fraction when the diethyl DTP dosage was increased from 9.62E-05 mole/kg (cf. Figure 4.73) to 4.09E-04 mole/kg (cf. Figure 4.76) indicate that the use of diethyl DTP, at both lower and higher dosages, did not result in significant recovery of those nickel-containing minerals which were present as particles larger than 38 µm. Figure 4.75 however shows that diethyl DTP is an excellent copper collector and that it performed as well as the SIBX with regards to recovery per particle size.

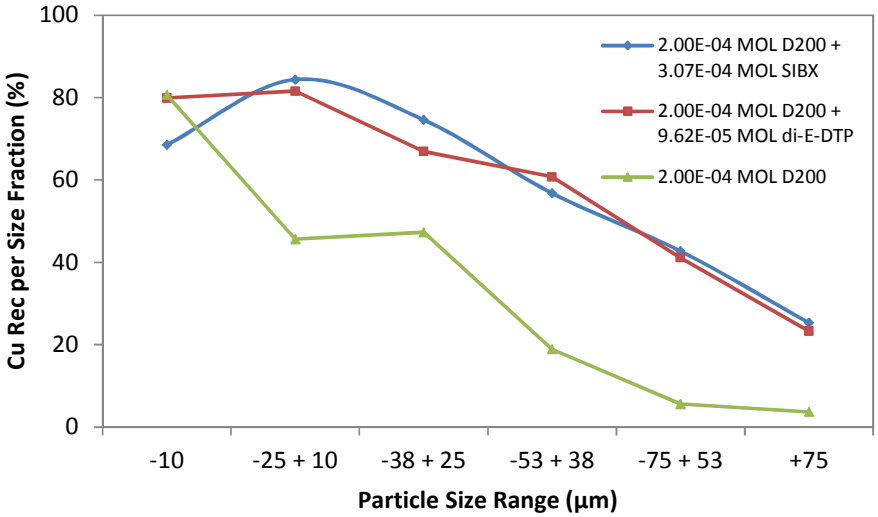


**Figure 4.73: The effect of the collectors SIBX and diethyl DTP, at respective dosages of 3.07E-04 mole/kg and 9.62E-05 mole/kg, and in the presence of 2.00E-04 mole/kg Dowfroth 200, on copper recovery as a function of particle size**

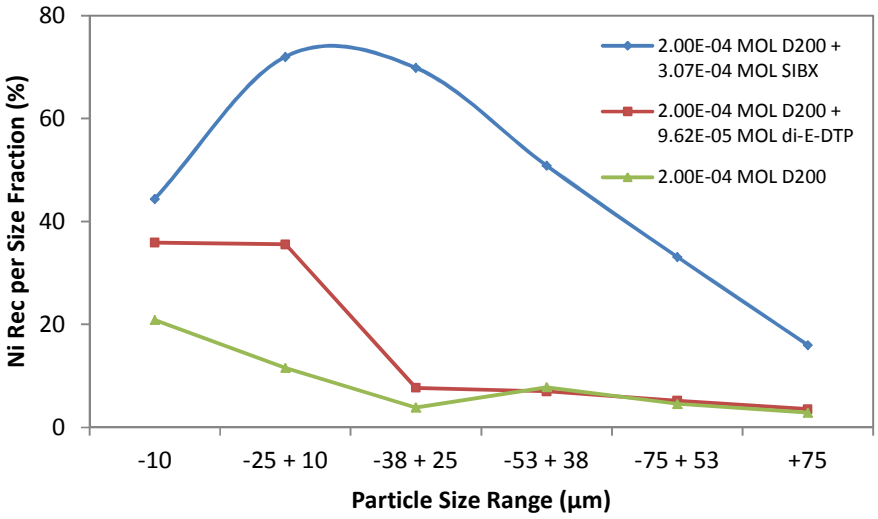


**Figure 4.74: The effect of the collectors SIBX and diethyl DTP, at respective dosages of 3.07E-04 mole/kg and 9.62E-05 mole/kg, and in the presence of 2.00E-04 mole/kg Dowfroth 200, on nickel recovery as a function of particle size**

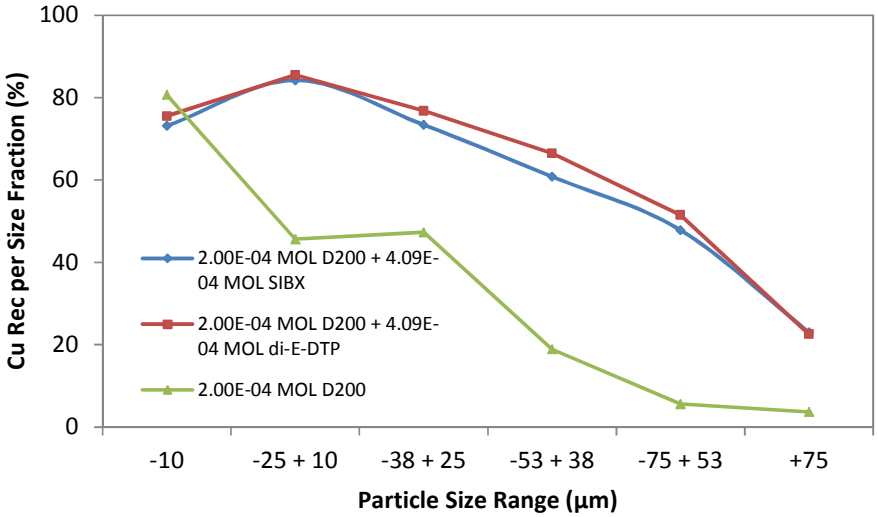


**Figure 4.75: A comparison of copper recovered from specified size fractions which were obtained with either SIBX or diethyl DTP as collectors at a collector concentration of 4.09E-04 mole/kg**

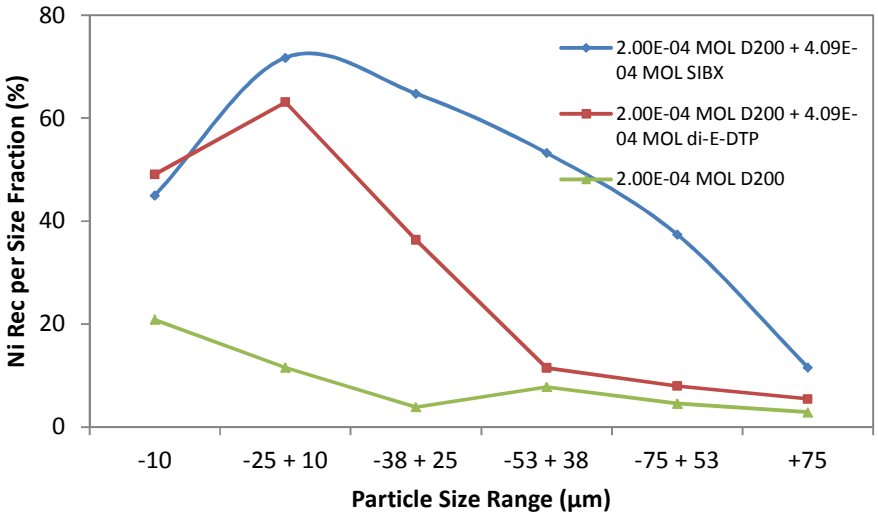


**Figure 4.76: A comparison of nickel recovered from specified size fractions which were obtained with either SIBX or diethyl DTP as collectors at a collector concentration of 4.09E-04 mole/kg**

### 4.7.2 Collector Mixtures

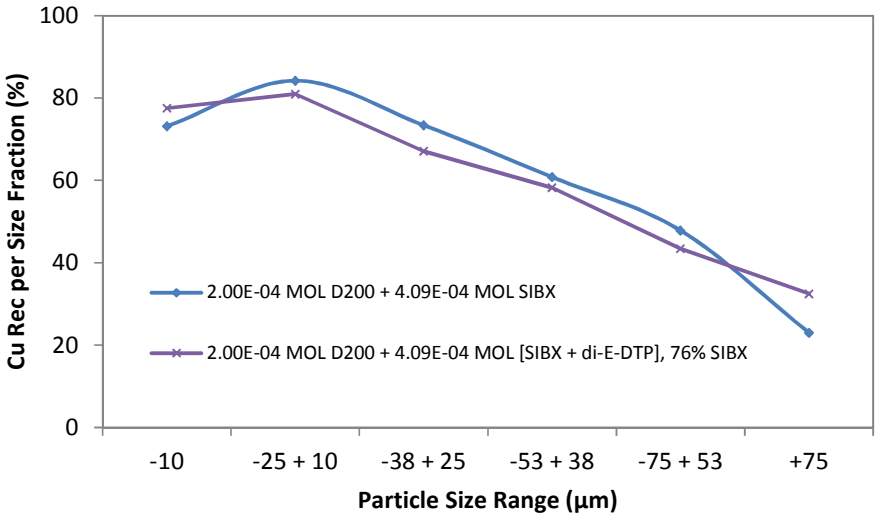


**Figure 4.77: Copper recovery as function of particle size for the collector mixture versus SIBX only tests at the standard dosage of 4.09E-04 mole/kg total collector**

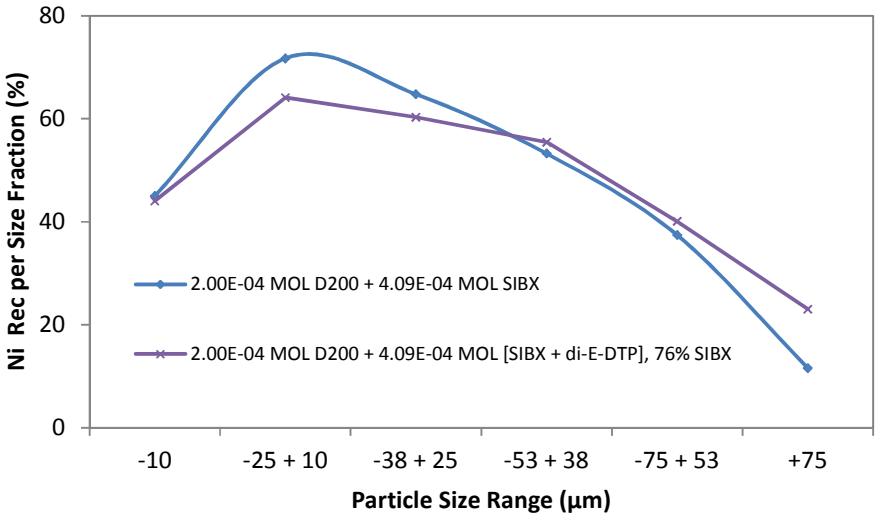


**Figure 4.78: Nickel recovery as function of particle size for the collector mixture versus SIBX only tests at the standard dosage of 4.09E-04 mole/kg total collector**

Figures 4.77 and 4.78 show, respectively, the percentage copper and nickel recovered from various particle size fractions using SIBX and mixtures of SIBX and diethyl DTP at a dosage of 4.09E-04 mole/kg. The figures show that the collector mixture, when compared to the "SIBX only" case, performed better with respect to the recovery of the coarse fractions but slightly worse in the intermediate size fractions.

### 4.7.3 Total Mass Recovery per Size Fraction

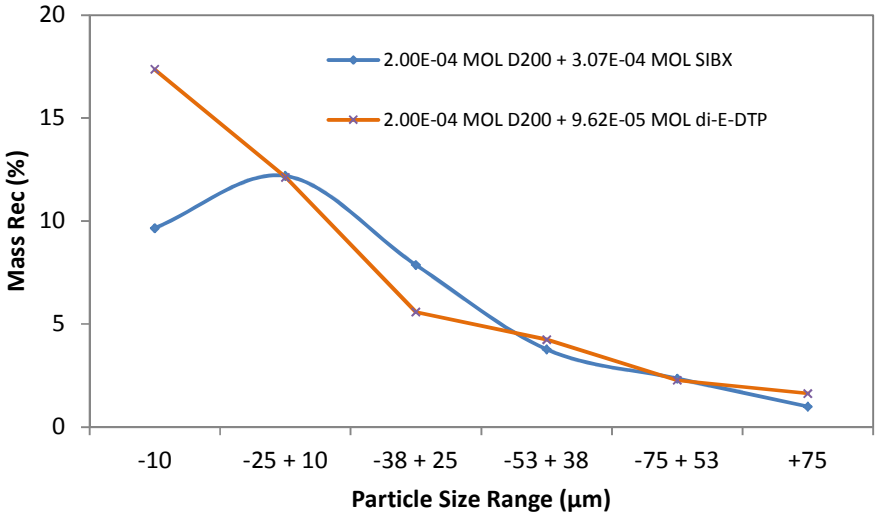


**Figure 4.79: The effect of the collectors SIBX and diethyl DTP, at respective dosages of 3.07E-04 mole/kg and 9.62E-05 mole/kg, and in the presence of 2.00E-04 mole/kg Dowfroth 200, on mass recovery as a function of particle size**

Figure 4.79 shows the effect of the collectors SIBX and diethyl DTP, at the dosages 3.07E-04 mole/kg and 9.62E-05 mole/kg, on the mass recovery per size fraction. This figure shows that the use of diethyl DTP has resulted in a significant increase in mass recovery from the -25 µm fraction when compared to SIBX. Figure 4.80 also shows that the use of diethyl DTP, at a higher dosage compared to that used to obtain the data represented in Figure 4.79, resulted in a significant increase in fines recovery when compared to SIBX. When a mixture of SIBX and diethyl DTP was used, as is shown in Figure 4.80, significantly more

amounts of fines were recovered when compared to the "SIBX only" case but less when compared to the "diethyl DTP" case.

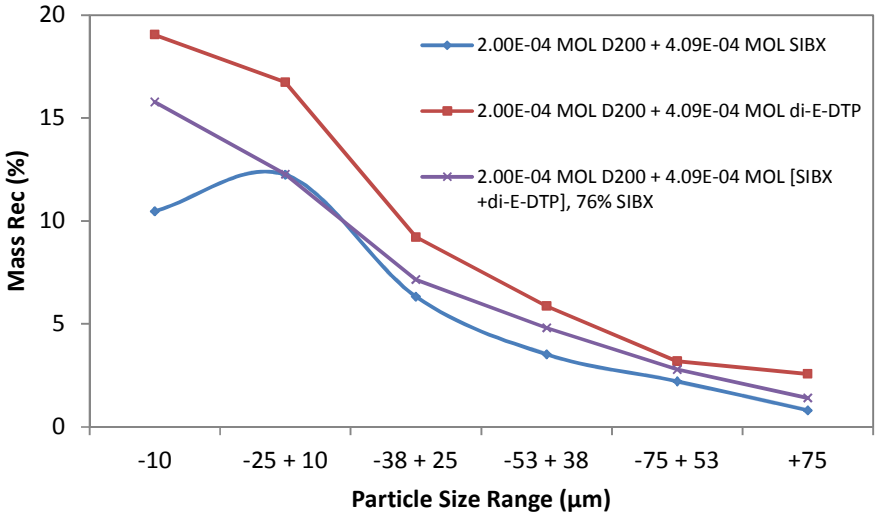


**Figure 4.80: A comparison of the mass recovery as a function of particle size obtained when the collectors SIBX and diethyl were added individually and when they were combined**

Figure 4.80 shows that the highest mass recovery was obtained with pure diethyl DTP for all particle size fractions. Similarly, Figure 4.81, which shows the effect of collector reagent suite on non-sulphide gangue recovery, shows that the highest non-sulphide gangue recovery was obtained with pure diethyl DTP for all particle size fractions. Furthermore, Figures 4.80 and 4.81 show that pure diethyl DTP significantly enhanced mass and non-sulphide gangue recovery from the finest size fractions whilst there was a decrease in mass and non-sulphide gangue recovery with pure SIBX at a finest size fractions. These figures (4.79, 4.80 and 4.81) may have important consequences for PGE recovery because, if the PGE minerals are mainly locked with the non-sulphide gangue, then the use of diethyl DTP should result in a significantly enhanced PGE recovery compared to a pure SIBX collector regime. However, as is shown in Figure 4.64 and 4.67, the worst palladium and platinum recoveries were obtained with a pure diethyl DTP collector reagent regime.

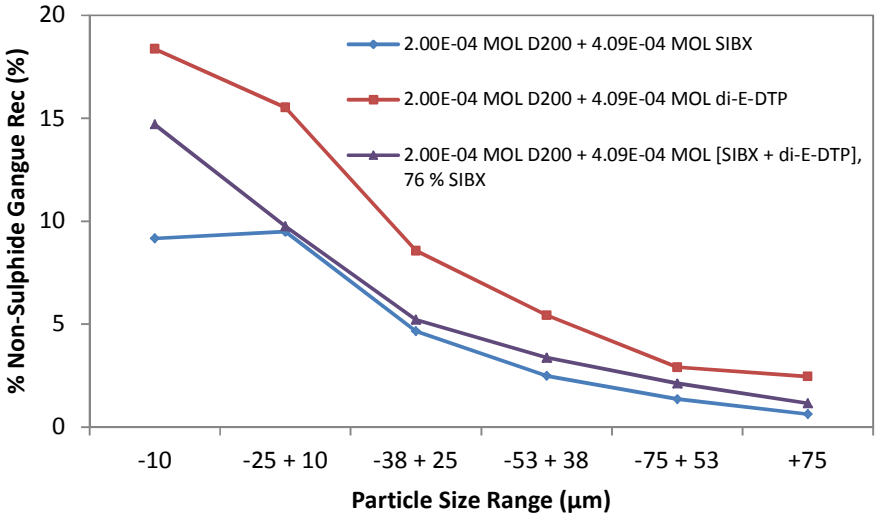


**Figure 4.81: A comparison of the non-sulphide gangue recovery as a function of particle size obtained when the collectors SIBX and diethyl DTP were added individually and when they were combined**

## 4.8 ToF-SIMS

A number of tests were completed in order to investigate the adsorption of the collectors SIBX and diethyl DTP, individually and when added sequentially, on sulphide minerals present in the ore using ToF-SIMS. The results which were obtained from these experiments are summarised in Figures 4.82 and 4.83. Figure 4.82 shows that the SIBX ions were adsorbed onto the sulphide mineral surfaces whilst Figure 4.83 shows that the diethyl DTP (labelled "Senkol 3" in this figure) only adsorbed onto the mineral surfaces once SIBX had adsorbed.

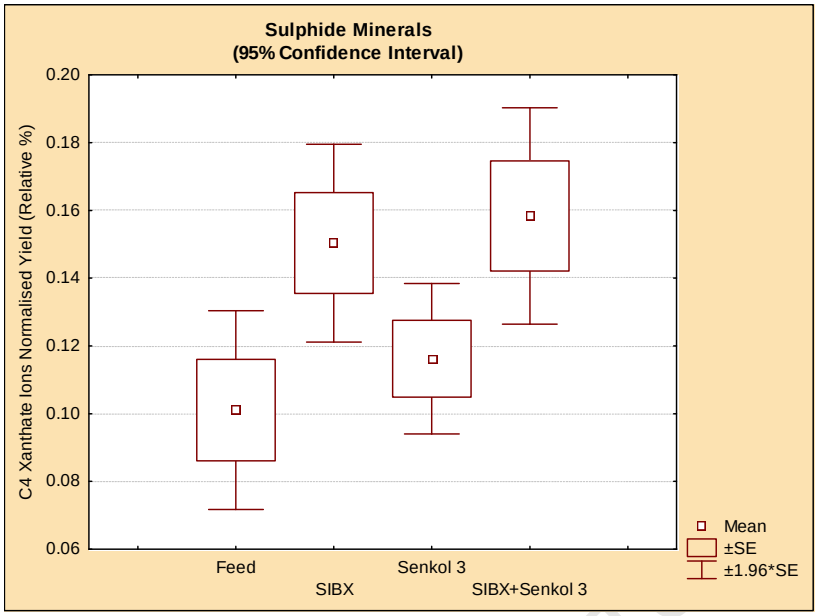


**Figure 4.82: The relative SIBX ions normalised yield obtained for the sulphide minerals**

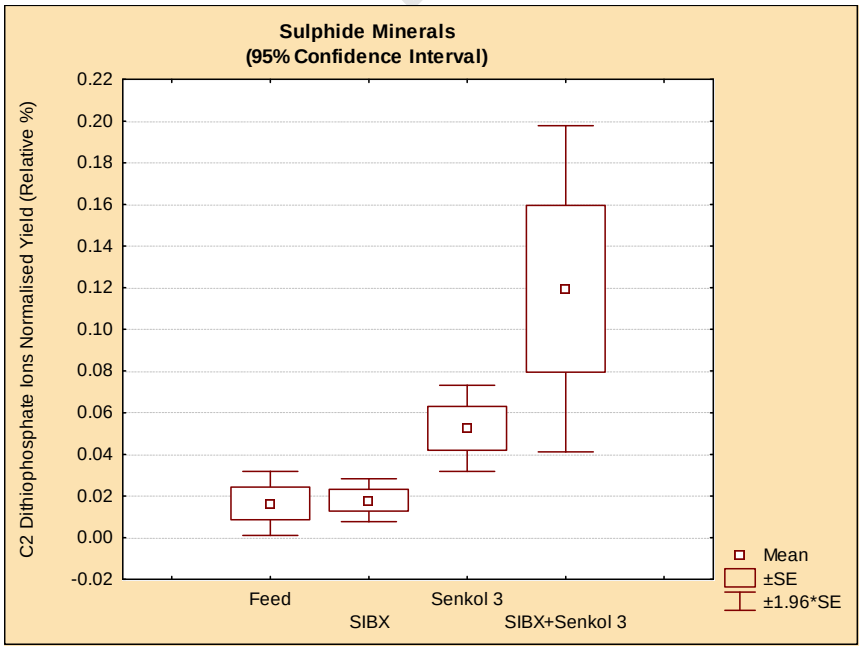


**Figure 4.83: Adsorption of diethyl DTP (labelled "Senkol 3" in figure) onto sulphide surfaces in the presence and absence of SIBX**

# Chapter 5: Discussion

The aim of this study was to investigate the effect of diethyl DTP, both in the presence and absence of SIBX, on copper, nickel, non-sulphide gangue and PGE recovery from a South African PGE-bearing ore. In this chapter batch flotation test results will be analysed with a view to establishing whether these results indicate that:

i. DTP possesses copper, nickel and PGE collecting properties equivalent to that of xanthate
ii. DTP, in the presence of xanthate, enhances recovery due a synergistic interaction between the collectors compared to the performance of the single collectors
iii. Mixtures of xanthates and DTP modify copper and nickel flotation rates compared to the single collectors
iv. DTP significantly increases non-sulphide gangue recovery as compared to SIBX, and
v. DTP modifies the froth phase behaviour and in doing so changes the recovery by particle size distributions



This chapter begins with a discussion of the results obtained from conducting collectorless flotation tests. These tests were carried out as it was considered important to establish whether the frother used in this investigation, viz. Dowfroth 200, possessed collecting properties. This is followed by a discussion on the flotation test results obtained with two different frothers in the presence of collector. The effects of pure collector and collector mixture reagent suites on copper, nickel, PGE and gangue recoveries are discussed next. This chapter ends with a discussion of the ToF-SIMS data presented in Section 4.9.

## 5.1 Role of the Frother

Collectorless batch flotation tests were conducted in order to ascertain whether the frother used in this investigation, viz. Dowfroth 200, possessed chalcopyrite and pentlandite collecting properties. A second frother, MIBC, was tested as an alternative. Further test work was carried out in which flotation performance, as indicated by copper and nickel recovery and grades, was investigated in the presence of collector. These tests were conducted as it was considered important that the role of the frother in this investigation should be, as far as possible, one which is to provide a stable froth phase only. The frothers Dowfroth 200 and MIBC were chosen because they:

i. are low molecular weight frothers and thus are not associated with excessive frothing when used at appropriate dosages
ii. are relatively pure chemicals and
iii. do not, as far as could be established from the literature, possess collecting properties.



### 5.1.1 Collecting Properties of the Frothers

Figure 4.12 showed that there was no difference in the observed mass pull between the two frothers whilst Figure 4.13 showed that the copper and nickel recovery patterns obtained are not significantly different. Furthermore, Figure 4.14 showed that approximately 80 % of the chalcopyrite particles present in the feed in the size range -10 µm were recovered whilst approximately 50 % of the chalcopyrite particles present in the feed in the size range -25 µm + 10 µm were recovered. These three graphs therefore suggest that, firstly, there was no difference in the hydrophobic character of the minerals floated with these two frothers and, secondly, the relatively high amount of copper recovered in the absence of any collector was due to the naturally hydrophobic character of chalcopyrite or due to entrainment or both but not due to any inherent collecting properties of the frothers. The latter conclusion is shown to be true by Figures 5.1 and 5.2 which show that the copper and nickel recoveries obtained with a collector which exhibited significant frothing behaviour in a two-phase frothing column test rig, di-iso-butyl DTP, were significantly higher compared to those which were obtained with the

frothers Dowfroth 200 and MIBC. Figure 5.2 also shows that the nickel recovery obtained when only frothers were used was directly proportional to water recovery. This suggests that nickel was recovered through an entrainment mechanism in the collectorless batch flotation tests.

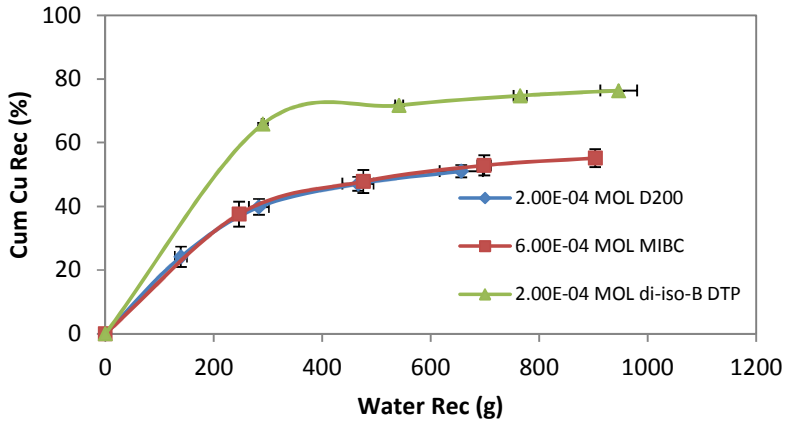


**Figure 5.1: A comparison of copper recovery as a function of water recovery obtained when frothers MIBC and Dowfroth 200 and the collector di-iso-butyl DTP were used in batch flotation tests**

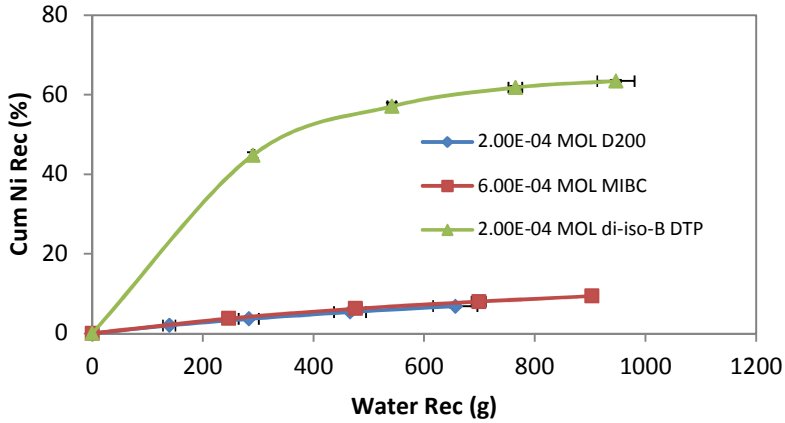


**Figure 5.2: A comparison of nickel recovery obtained as a function of water recovery when frothers MIBC and Dowfroth 200 and the collector di-iso-butyl DTP were used in batch flotation tests**

### 5.1.2 Interaction between Frothers and Collectors

Figure 4.15 showed that there was no difference in both the final copper and nickel recoveries obtained as well as the copper and nickel recovery as a function of water recovery patterns when the frothers MIBC and Dowfroth 200 were tested in the presence of a mixture of both SIBX and diethyl DTP. The collectors were added simultaneously to the flotation pulp and the total collector dosage was 4.09E-04 mole/kg which was the standard collector dosage used in this investigation. Interestingly however, when the two frothers were tested in the presence of only SIBX, as is shown in Figure 4.16, the copper and nickel recovery as a function of water recovery patterns were different although the final recoveries were not significantly different. For example, at a water recovery of 200 g, significantly higher nickel was recovered with Dowfroth 200 when compared to MIBC whilst the difference in copper recovery was not significant at the same water recovery. This is an interesting result which may suggest that, at the collector and frother dosages used in Figure 4.16, SIBX and Dowfroth 200 molecules have interacted on the mineral surface through a frother-collector interaction mechanism. This result is consistent with the work done by Hadler et al. (2005) who showed by measuring the adsorption of SIBX and Dowfroth 200 onto chalcopyrite-containing ore particles using UV spectrometry and total organic carbon (TOC) analysis, that the presence of frother resulted in a greater consumption of SIBX. However, as stated above, in the presence of diethyl DTP, there is no indication of an interaction between SIBX and Dowfroth 200.

In conclusion therefore, the solids and water recovery plots in Figure 4.12 as well as the copper and nickel versus water recovery plots in Figures 4.13, 4.15, 4.16, 5.1 and 5.2 have demonstrated that the choice of frother was not significant and that batch flotation tests may have been done using either frother. The decision was made to use Dowfroth 200 because this frother has frequently been used in batch flotation tests involving South African PGM ores. The frother concentration was set at 2.00E-04 mole/kg ore unless specifically stated otherwise. This frother concentration was decided on only after both two-phase and three-phase batch flotation tests had revealed that this is the minimum concentration of frother required in order to form a stable froth.

## 5.2 The Effect of the Single Collectors on Copper Recovery

### 5.2.1 The Effect of SIBX Dosage on Copper Recovery

Figure 4.22, which showed the copper grade-recovery curves obtained with increasing SIBX collector dosages, indicated that copper recovery:

i. was optimal at an intermediate SIBX concentration (3.07E-04 mole/kg) , and
ii. was reduced when the SIBX concentration increased from 3.07E-04 to 4.09E-04 mole/kg.

Fuerstenau (2007) has shown that increased collector addition in a galena float resulted in increased particle-bubble contact angle whilst Ata at el. (2002) reported higher mineral recoveries for moderately hydrophobic particles (contact angle ≈ 63$^{o}$) compared to strongly hydrophobic particles (contact angle ≈ 82$^{o}$). The reduced copper recovery observed at higher collector dosages (cf. Figure 4.22) may thus have occurred as a consequence of the action of highly hydrophobic particles on the flotation froth. These particles, because of their ability to bridge and thus dewater bubble-water films, increase bubble collapse rate and thus reduce overall froth stability (cf. Sections 2.3.3 and 2.4.1.5).

This explanation is however contradicted by Figure 4.25 which showed that water recovery was not significantly influenced by guar dosage. In addition, Figure 4.28 showed that nearly all of the floating gangue was depressed at a dosage of 500 g/t guar. Thus the only particles which could have been present in the froth when the guar dosage was increased to 500 g/t were the valuable sulphides and essentially only the entrained gangue. The entrained gangue is generally not expected to influence froth stability – however they may be present as fines which may in fact influence froth phase behaviour. In this case however a comparison is made between two different SIBX dosages with all other parameters constant. In this instance therefore, the froth influencing behaviour of the fines are not expected to be different. In summary therefore, the froth stability probably could only have been influenced by the hydrophobic sulphide minerals (cf. section 2.4.1.4). This result therefore indicates that the valuable

sulphide minerals, because they did not reduce water recovery in the presence of a high dosage of guar, may only have been of intermediate hydrophobicity (cf. sections 2.3.3 and 2.4.1.4). The decrease in copper recovery at an SIBX dosage of 4.09E-04 mole/kg thus cannot be attributed to an increase in the bubble collapse rate caused by the presence of highly hydrophobic particles. This conclusion is supported by the images of the froth phase in Figure 4.29. This figure showed two randomly selected images of the froth from the first concentrate when the SIBX dosage was 3.07E-04 mole/kg. Similarly, Figure 4.33 showed two randomly selected images of the froth from the first concentrate when the SIBX dosage was 4.09E-04 mole/kg. A visual comparison of these figures revealed that the froth in Figure 4.29 appeared to be richer in chalcopyrite minerals compared to the froth in Figure 4.33. However, the parameters which indicate froth stability, which are bubble diameter, froth mobility, bubble shape, etc., did not appear to be significantly different.

Wills and Napier-Munn (2006) reported that sulphide mineral depression, which occurs at high collector concentrations, may be a consequence of the adsorption of a second layer of collector molecules with an opposite orientation to the first layer of collector molecules (cf. end of section 2.4.2.2). The hydrophilic heads of the second layer of collector molecules are thus orientated outwards and render the mineral hydrophilic. Work done by Smar et al. (1994) has shown that the rate and recovery of copper sulphide minerals decreased once the collector dosage was increased beyond a certain optimum value. Somasundaran (1975) stated that "*excess collector will reduce mineral recovery*" whilst Taggart (1951) reported a decrease in the particle-bubble contact angle at high collector dosage. It is therefore more likely that the reduced copper recovery attained at a collector dosage of 4.09E-04 mol/kg compared to 3.07E-04 mole/kg was not due to froth destabilisation effects but rather due to the effects of excess collector.



### 5.2.2 The Effect of DTP Type and Dosage on Copper Recovery

Table 4.16 and Figure 4.38 showed that the DTP collectors tested are good chalcopyrite collectors. In fact, a comparison of the final copper recoveries obtained with equivalent molar dosages of diethyl DTP (cf. Table 4.16) and SIBX (cf. Table 4.13) showed that diethyl DTP has equivalent chalcopyrite collecting properties. This is illustrated in Figure 5.3 which shows the final copper and water recoveries obtained

with equivalent dosages of SIBX and diethyl DTP. Figure 5.3 shows that approximately a 50 % copper recovery was achieved without addition of any collector. This natural floatability complicates data interpretation as it becomes very difficult to isolate the effect of the collector which, in turn, makes it especially difficult to compare the flotation performance obtained with two different collectors. This effect is clearly illustrated in Figure 5.3 which shows that the differences in copper recovery obtained with equivalent molar concentrations of SIBX and diethyl DTP were negligible except at the highest collector dosages (see also Table 5.1). Figure 5.4 however shows that the increased copper recovery achieved with diethyl DTP and di-iso-butyl DTP was essentially due to increased water recovery. It is noticeable also that the longer chain DTP collector, di-iso-butyl DTP, was able to achieve a copper recovery comparable to that which was obtained with diethyl DTP and SIBX but at a significantly lower collector concentration.

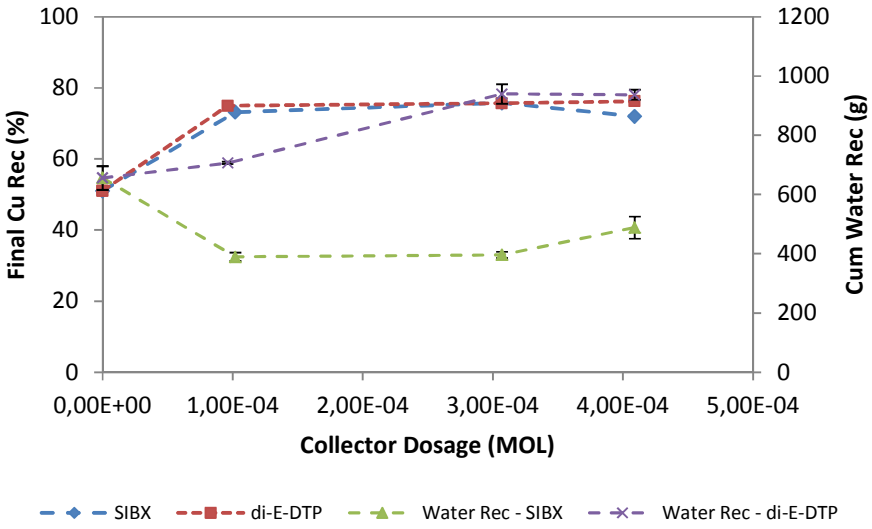


**Figure 5.3: A comparison of equimolar dosages of the collectors SIBX and diethyl DTP on copper and water recovery**

The most noteworthy trend in Figure 5.3 is however that, while increased copper recovery is associated with a decrease in water recovery for SIBX, the opposite is true for diethyl DTP. This is significant because generally one would expect, as is the case with SIBX, a decrease in water recovery as collector

concentration is increased because of the presence of increasingly hydrophobic particles which will result in an increase in bubble coalescence (cf. Sections 2.3.3 and 2.4.1.5). The result shown in Figure 5.3 may therefore indicate that the collecting action of diethyl DTP is not only related to it making the sulphide surface hydrophobic but also having an effect on the behaviour of the froth phase due to some collector-frother interaction. Alternatively, DTP may result in the creation of moderately hydrophobic particles which will result in an increase in water recovery.

**Table 5.1: A comparison of the final copper recoveries and grades obtained with SIBX, SEX and diethyl DTP at equivalent molar concentrations**

| Reagent Suite | Copper | |
|---|---|---|
| **2.00E-04 mole/kg D200 + 4.09E-04 mole/kg collector** | **Final Recovery (%)** | **Final Grade (%)** |
| Collector = SIBX | 72.0 ± 0.1 | 1.50 ± 0.04 |
| Collector = SEX | 72.8 ± 0.1 | 1.26 ± 0.04 |
| Collector = diethyl DTP | 76.2 ± 0.4 | 1.26 ± 0.04 |
| 2.00E-04 mole/kg D200 + 7.52E-05 mole/kg di-iso-B-DTP | 76.5 ± 0.1 | 1.06 ± 0.02 |



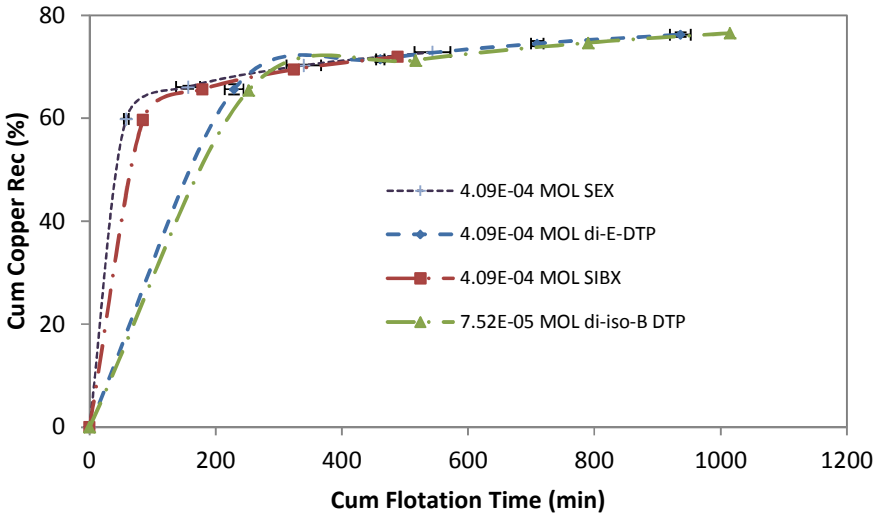


**Figure 5.4: A comparison of the cumulative copper recovery as a function of cumulative water recovery patterns obtained with SEX, diethyl DTP, SIBX and di-iso-butyl DTP**

## 5.3 The Effect of the Single Collectors on Nickel Recovery

### 5.3.1 The Effect of Xanthate Type and Dosage on Nickel Recovery

Figure 4.23, which showed the nickel grade-recovery curves obtained with different xanthate collector types and dosages, indicated that the final nickel recovery obtained was largely unaffected by changes in the variables tested. Table 4.14 however showed that the nickel first-order rate constant for SEX was approximately double that obtained with SIBX at equivalent molar dosages whilst the infinite time nickel recovery obtained with SEX was significantly lower than SIBX at the same collector concentration. This suggested that with SEX recovery was strongly kinetically controlled but not with SIBX.

The overall nickel recovery is poor when compared to copper recovery. Malysiak et al. (2004) attributed the poor nickel recovery experienced in industrial flotation plants to the effects of surface oxidation, slime coatings and the formation of passivating layers of metal ions present in the process water. The effect of process water on pentlandite recovery was highlighted by Hodgson and Agar (1989) who showed that $Ca^{2+}$ and $S_2O_3^{2-}$ ions compete with xanthate for adsorption onto the pentlandite surface. In this study the concentration of $Ca^{2+}$ ions in the process water was 80 ppm whilst the concentration of $SO_4^{2-}$ ions was 250 ppm. Furthermore, pentlandite, once oxidised, forms a range of iron oxides and hydroxides, nickel oxides and iron sulphates on its surface which will impair recovery significantly (Richardson and Vaughan, 1989; Legrand et al., 1997). In addition, the presence of gangue minerals such as the serpentine minerals lizardite and chrysotile in the ore has also been shown to significantly reduce nickel recovery (Edwards et al., 1989). The serpentine minerals made up approximately 7 %, by mass, of all the minerals present in the ore used in this investigation (cf. Table 4.1).

### 5.3.2 The Effect of DTP Type and Dosage on Nickel Recovery

Figure 4.38 showed that the nickel grade-recovery profiles using diethyl DTP were substantially different to those for copper. In Figure 4.38 the copper grade decreased approximately linearly with an increase

in copper recovery whilst the nickel grade remained approximately constant with increasing nickel recoveries. In addition, Figure 4.39 and Figure 5.5 showed that, at a concentration of 9.62E-05 mole/kg diethyl DTP, the nickel recovery varied approximately linearly with water recovery. Furthermore, Figure 4.74 showed that the nickel recovery obtained with diethyl DTP, at a dosage of 9.62E-05 mole/kg, did not exceed the recovery obtained with only frother except in the -25 µm particle size range. In other words, the difference in recovery obtained with reagent suite [2.00E-04 mole/kg Dowfroth 200] compared to [2.00E-04 mole/kg Dowfroth 200 + 9.62E-05 mole/kg diethyl DTP] can be attributed only to the difference in recovery in the fine size fractions. This suggests that DTP may have some froth modifying effect which enables fines to report to the launder.

The final nickel recovery obtained increased from 28 % to 46 % when the diethyl DTP dosage was increased from 9.62E-05 to 4.09E-04 mole/kg (cf. Figure 4.38). At the same time however, the total water recovered also increased from approximately 707 g to 936 g when the diethyl DTP dosage was increased from 9.62E-05 to 4.09E-04 mole/kg (cf. Figure 4.39). Furthermore Figure 4.76 showed that the increased nickel recovery obtained at the higher diethyl DTP dosage was accompanied by a significant increase in nickel recovery of -38 µm particle size range. It is significant however that the nickel recoveries obtained in the coarser fractions, i.e. the +38 µm size fractions, were not significantly higher than that which was obtained with the "frother only" reagent suite (cf. Figure 4.76). This is in contrast to SIBX which by comparison, as was shown in Figure 4.76, was able to achieve good nickel recoveries in the coarser particle size fractions as well as the fine fractions. Therefore, if true flotation extends to all particle size fractions, then this result can only mean that the diethyl DTP did not significantly enhance the hydrophobicity of the nickel-containing minerals in order to induce recovery via true flotation and that the increased recovery obtained at the higher diethyl DTP dosage occurred because of increased non-selective mass pull of fine particles.

The graphs of nickel recovery as a function of water recovery obtained with diethyl DTP as collector, which is shown in Figure 5.5, show that nickel recovery was directly proportional to the water recovery. This is clearly demonstrated by the high $R^2$ values which were obtained when a linear relationship was fitted to the nickel recovery versus water recovery at the various diethyl DTP dosages curves. This, together with the fact that increased nickel recovery appeared to be due to the non-selective increase in

fine particles as shown in Figure 4.76, clearly demonstrates that the nickel recovery obtained with diethyl DTP was probably due to an entrainment mechanism and not due to true flotation.

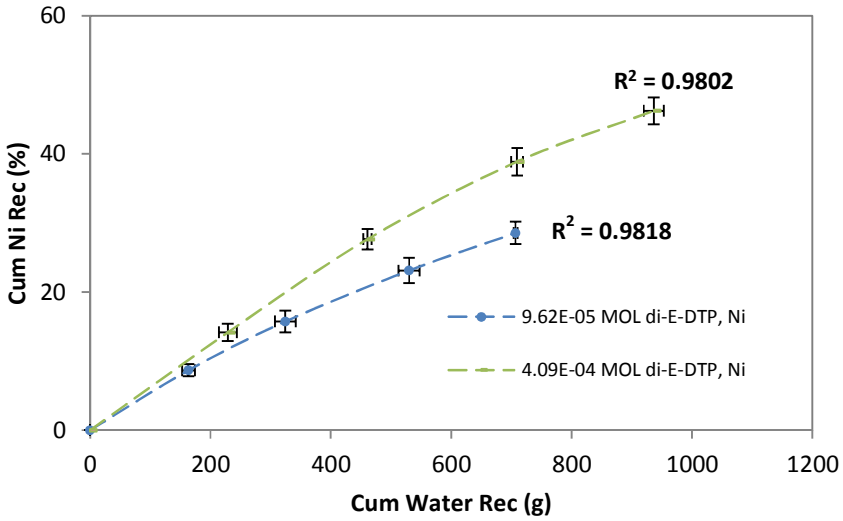


**Figure 5.5: Nickel recovery as a function of water recovery for different dosages of diethyl DTP**

In Figures 4.38 and 4.39, the effect of DTP collector chain length on nickel recovery is shown. The figures, as well as Table 4.16, clearly demonstrated that a significantly improved nickel recovery was obtained with di-iso-butyl DTP compared to diethyl DTP. In addition the nickel grade-recovery curve pattern obtained with di-iso-butyl DTP as collector is significantly different than those which were obtained when diethyl DTP was used as collector. The nickel grade-recovery curve obtained with di-isobutyl DTP is, in fact, one which is associated with true flotation, i.e. grade decreased linearly with an increase in recovery.

The experimental flotation test results therefore show that the effect of chain length in DTP collectors on flotation performance is particularly complex. This may be due, firstly, as was reported by Lovell (1982) and Mingione (1984), the long chain dialkyl DTPs, defined as those with more than four carbon atoms in their structure, exhibited both frothing and collecting properties whilst the short chain DTPs

are essentially non-frothing. Secondly, as was shown by Chander (1999), DTP offers greater resistance to oxidation and hydrolysis than the corresponding xanthate, i.e. the oxidation to its corresponding dithiolate is much more difficult for DTP compared to an equivalent chain length xanthate for example. This effectively means that if the dithiolate is responsible for flotation activity, then the xanthates will produce more dithiolates on mineral surfaces at lower oxidation potentials compared to DTP (du Plessis, 2003). This also means that, as was shown in Figure 2.15, if the dithiolate of DTP is responsible for inducing hydrophobicity to a specific mineral, then this will be much more easily achieved with di-iso-butyl DTP rather than diethyl DTP. The third reason for this contrast in flotation performance may also be attributed to the fact that DTP has a double hydrophobic group arrangement in its molecular structure. This double hydrophobic group molecular structure means that a modest increase in chain length will result in a significant increase in particle hydrophobicity (Mingione, 1984). In summary therefore, the contrast in flotation performance obtained with diethyl and di-iso-butyl DTP may have occurred if the species responsible for pentlandite hydrophobicity is the dithiolate species of DTP because (i) di-iso-butyl DTP will more readily form dithiolates according to Chander (1999) and (ii) di-iso-butyl DTP will induce a significantly higher hydrophobic character to the mineral due to the double hydrophobic group molecular structure of DTP.

It is interesting to note however that ToF-SIMS surface analysis on pyrite particles conditioned with di-iso-butyl DTP at pH 9.2 revealed that molecular DTP ions were indeed absorbed onto pyrite surfaces but, significantly, that no peaks which could be attributed to the collector dimer were identified (Nagaraj and Brinen, 2001). The authors in fact attributed DTP collector adsorption onto pyrite surfaces to both chemisorption of the DTP anion and the formation of an iron-collector complex. This result was explained on the basis of Chander's (1999) work, i.e. the iron-DTP complex is favoured for DTP adsorption on pyrite because the collector is less readily oxidised to its dimer. The inability of diethyl DTP to recover pentlandite via true flotation may therefore be related to the inability to form either the collector dimer or an iron-collector complex (diethyl DTP is known to be highly selective against iron compounds).

## 5.4 The Effects of Single Collectors and Guar Dosage on Copper and Nickel Recoveries

### 5.4.1 The Effects of SIBX and Guar Dosage on Water, Copper and Nickel Recoveries

Figure 4.26 showed that the final copper and nickel recoveries obtained were reduced at a guar dosage of 500 g/t whilst Figure 4.25 showed that water recovery was not reduced at the 500 g/t guar dosage. This means that the reduced copper and nickel recoveries obtained at a dosage of 500 g/t guar cannot be attributed to froth destabilisation effects (cf. Section 2.4.1.4). Furthermore, the guar molecules could not have been competing with SIBX molecules for adsorption sites on the surface of the valuable minerals because SIBX was added two minutes ahead of the guar. Wiese (2009) proposed that the surface of a mineral particle is composed of high-energy sites and low-energy sites and that SIBX will generally only adsorb onto the high energy sites, i.e. SIBX adsorbs in patches only. Therefore, if the guar molecules are able to adsorb onto low-energy surface sites, then mineral depression will occur once the balance of hydrophilic forces caused by guar molecules exceeds the action of the hydrophobic forces caused by the SIBX molecules. This is likely to occur at high guar dosages.

An alternative explanation for the depressant effect of guar molecules on chalcopyrite specifically was given by Rath et al. (2001). The experimental procedure involved measuring the adsorption of KEX onto a 0.5 g pure chalcopyrite sample in the presence of $10^{-2}$ M $KNO_3$, pH 9.5 to 9.8 and increasing amounts of guar. The authors reported that the amount of xanthate adsorbed increased as the concentration of guar gum in the solution increased. This, it was argued, is evidence of an association between the xanthate molecules and the guar molecules similar in nature to that which was proposed for starch and surfactants by Pugh (1989) and Somasundaran (1969). Rath et al. (2001) therefore proposed that the guar molecules effectively wrap up the xanthate molecules and that this is the reason why both xanthate molecules and guar gum molecules were adsorbed onto the chalcopyrite surface. They suggested that this wrapping up mechanism can also account for the loss of hydrophobicity of the chalcopyrite surface leading to its depression.

### 5.4.2 The Effects of diethyl DTP and Guar Dosage on Water, Copper and Nickel Recoveries

Table 4.18 showed that water recovery increased with increasing diethyl DTP dosage in the absence of guar. At 100 g/t guar dosage however, as was shown in Table 4.18, the frother-diethyl DTP-guar mixture has resulted in a significant increase in water recovery as compared to the 0 g/t guar test. The reasons for this peculiar behaviour are not known. It has however been proposed that guar molecules may remove from the froth those particles which destabilise the froth phase; this may therefore account for the higher water recovery which was achieved at 100 g/t guar dosage (Bradshaw et al., 2005). Interestingly, Mingione (1984) argued that DTP collectors, in contrast to xanthates, are highly susceptible to depressants because of the higher water solubility of heavy metal DTPs compared to xanthates. At the high guar dosage however, 500 g/t, the depressive action of guar has led to a significant reduction in both concentrate mass and water recovery. This suggests, as was shown in Table 4.19, that nearly all of the floatable gangue has been rendered hydrophilic at the 500 g/t guar dosage.

Figure 4.42 showed that, as with SIBX, copper recovery decreased at the high guar dosage. Similarly, Figure 4.43 showed that nickel recovery also decreased at the higher guar dosage. Interestingly, at a dosage of 4.09E-04 mole/kg diethyl DTP and an intermediate dosage of guar, which was 100 g/t, the nickel recovery increased significantly compared to the case where no guar was added. In contrast, at a dosage of 9.62E-05 mole/kg diethyl DTP and an intermediate dosage of guar, the nickel recovery decreased compared to the test where no was added. The reasons for the reduction in copper and nickel recovery in the presence of high dosages of guar are probably similar to those which were postulated for SIBX, i.e. either the guar molecules are able to adsorb onto low-energy sites on the surface of the mineral and thus cause depression at high guar gum dosage or the guar molecules are able to wrap up the DTP species which induce hydrophobicity and thus cause their depression (cf. Section 5.4.1).

## 5.5 The Effect Single Collectors and their Mixtures on Non-Sulphide Gangue Recovery

Table 5.2 shows the mass of total non-sulphide gangue, entrained gangue and floating gangue recovered at equivalent dosages of SIBX and diethyl DTP as well as their mixtures. The procedure used to separate entrained gangue and floating gangue was described in Section 3.3.3.3. The table shows that, with respect to single collectors, the mass of entrained gangue recovered increased with an increase in collector dosage for both SIBX and diethyl DTP and that a significantly higher mass of water and entrained gangue were recovered by diethyl DTP compared to SIBX. Table 5.2 also shows that, with respect to the collector mixtures, water and entrained gangue recovery increased with an increase in the diethyl DTP component of the [SIBX + diethyl DTP] collector mixtures.



**Table 5.2: The effect of collector type and dosage on water recovered as well as the mass of floating and entrained gangue recovered**

| Reagent Suite | Water Recovered (g) | Mass and type of Gangue Recovered | | |
|---|---|---|---|---|
| 2.00E-04 mole/kg D200 + collector | | Non-Sulphide Gangue (g) | Floating Gangue† (g) | Entrained Gangue (g) |
| Collector = 9.62E-05 mole/kg di-E-DTP | 707 | 78 | 31 | 47 |
| Collector = 3.07E-04 mole/kg SIBX | 397 | 58 | 31 | 27 |
| Collector = 3.07E-04 mole/kg di-E-DTP | 940 | 97 | 31 | 66 |
| Collector = 4.09E-04 mole/kg SIBX | 460 | 62 | 31 | 31 |
| Collector = 4.09E-04 mole/kg di-E-DTP | 936 | 96 | 31 | 65 |
| Collector = 4.09E-04 mole/kg [76 % SIBX + 24 % di-E-DTP] | 595 | 73 | 31 | 42 |
| Collector = 4.09E-04 mole/kg [85 % SIBX + 15 % di-E-DTP] | 506 | 68 | 31 | 37 |

† the mass of naturally floating gangue recovered was determined to be approximately 31 g (cf. Sections 4.5.4.3, 4.6.5.3 and 4.7.5.3) for all collector + guar tests done in this investigation. The mass of entrained gangue can then be calculated as the difference between floating gangue and total gangue.

In addition to the increased water and entrained gangue recovery that was achieved with pure diethyl DTP compared to equivalent molar concentrations of pure SIBX, as is shown in Table 5.2, Figure 4.81 showed that significantly higher masses of non-sulphide gangue were recovered in the fine and ultrafine particle size fractions especially (i.e. < 25 µm) in the case of pure DTP compared to pure SIBX. Figure 4.81 also showed that, in the case of pure SIBX versus a particular [SIBX + diethyl DTP] collector mixture, at equivalent molar concentrations, a significantly higher recovery of ultrafine (-10 µm) non-sulphide gangue was achieved with the mixture compared to pure SIBX. The combination of Table 5.2 and Figure 4.81 therefore showed that the use of [SIBX + diethyl DTP] mixtures compared to pure SIBX not only resulted in a significant increase in the entrained gangue recovered but that this additional entrained gangue recovery was achieved by increasing the recovery of the ultra-finely sized particles. Furthermore, two-phase bubble size test work conducted using the UCT bubble sizer has shown that a mixture of [Dowfroth 200 + diethyl DTP] did not reduce pulp bubble diameter significantly compared to Dowfroth 200 only. This was an important result as it proved that the increased ultrafine recovery was due to a froth phase effect and not due to a decrease in bubble diameter in the pulp phase. This highlights the important froth modifying effect of DTP, i.e. the character of the froth was modified in a manner such that fine and ultra-fine particles specifically were recovered.

In summary therefore, the use of pure diethyl DTP, as compared to pure SIBX, has led to a more stable froth phase which is able to successfully carry significantly higher masses of particles. This is clearly visible in the froth pictures (cf. Figures 4.46 to 4.49). Furthermore, as is shown in Figure 4.80 (cf. Section 4.8.3), which showed the total mass recovered using diethyl DTP and SIBX as collectors, at a concentration of 4.09E-04 mole/kg, the use of pure diethyl DTP, when compared to pure SIBX, has led to a significantly enhanced mass recovery in the fine and ultrafine fractions especially. The use of [SIBX + diethyl DTP] collector mixtures, compared to pure SIBX, is therefore expected to significantly dilute the concentrate grade because of the strong influence of DTP on the froth phase. This is because the concentrate grade is largely determined by the ability of the depressant to prevent floatable gangue particles from entering the froth zone and by the ability of the froth phase to facilitate removal of entrained gangue by a drainage mechanism (cf. sections 2.4.1.3 and 2.4.1.4).

## 5.6 The Effect of Mixtures of Collectors on Copper and Nickel Recovery

### 5.6.1 A Comparison of Flotation Performance obtained with Collector Mixtures versus Pure Collectors

Figure 4.50 showed that there was no significant difference in the slopes of the solids versus water recovery curves obtained with pure SIBX and a mixture of SIBX and diethyl DTP. The collector concentration for both tests was 4.09E-04 mole/kg and, in the case of the mixture, the molar composition was 76 % SIBX and 24 % diethyl DTP. It is noticeable however that a higher mass of solids and water was recovered with the collector mixture test compared to the pure SIBX test. This means therefore that, since the slopes were not significantly different, the solid versus water recovery plot for the collector mixture was simply an extension of the pure SIBX plot. This is a significant result as it implies that the collector mixture simply enhanced froth stability compared to the pure SIBX case.

Figure 4.51, which compared recoveries and grades obtained with a total collector dosage of 1.02E-04 mole/kg [76 % SIBX + 24 % diethyl DTP] and the individual collectors at equivalent dosages, showed that the final copper recovery was not affected by using different collectors. The nickel recovery obtained with 9.62E-05 mole/kg diethyl DTP was however significantly less than that which was obtained with either an equivalent SIBX dosage or the collector mixture. Figure 4.52, which compared copper recoveries and grades obtained with various mixtures of SIBX and diethyl DTP, added at a total collector dosage of 4.09E-04 mole/kg, as well as for individual collectors, also showed that the final copper recovery was not affected by collector type. This is confirmed by Figure 4.57 which showed that any recovery difference was due to increased, non-selective, mass pull only. Similarly, Figure 4.53 showed that the final nickel recovery obtained with mixtures of SIBX and diethyl DTP was not significantly different to that which was obtained with pure SIBX.

Furthermore, the equivalent chain length collector mixture tests, viz. SIBX + di-iso-butyl DTP and SEX + diethyl DTP, (cf. Figure 4.54 and Figure 4.55) showed that any difference in the copper and nickel recoveries between the mixtures and the pure collectors, at equivalent collector dosages, was due to

increased water recovery and therefore due to an increase in non-selective mass pull but not due to a true flotation effect.

In summary therefore, the batch flotation test results have shown that mixtures of diethyl DTP and SIBX, when added simultaneously, did not result in a significantly increased copper or nickel recovery and that a synergistic interaction between the collectors was not observed. Bradshaw (1997) had suggested, in a study using a mixture of PNBX and DTC in the flotation of pyrite, that the DTC may adsorb first and that layers of dixanthogen may form a secondary layer thus enhancing hydrophobicity. This increased hydrophobicity, if present, will be reflected as an increase in both grade and recovery in a batch flotation test. This was not observed in the present study where SIBX-DTP mixtures were used. This apparent lack of collector-collector synergism in the case of SIBX and diethyl DTP mixtures cannot be attributed to a dominant or even overpowering effect of the more powerful xanthate collector (SIBX) because tests completed using a weaker xanthate collector (SEX) or a stronger DTP collector (di-iso-butyl DTP) did not result in a collector-collector synergism interaction either. In addition, the collector mixture tests completed at different mole ratios of SIBX and diethyl DTP compared to that which was used in the standard, also showed that the apparent lack of collector-collector synergism cannot be attributed to the mole ratio of SIBX and diethyl DTP used in this study, viz. 4.09E-04 mole/kg [SIBX + diethyl DTP], 76 % SIBX and 24 % diethyl DTP.



### 5.6.2 The Effect of Sequence of Addition on Flotation Performance

A number of tests were done in which the collectors were added sequentially. This was done in order to investigate whether valuable mineral recovery can be increased if the mineral surface, which has a heterogenous distribution of energetically different sites, is exposed to the collectors sequentially. Sequential addition of collectors may enable the weakly adsorbing collector to occupy the highly energetic sites and the strongly adsorbing collector to occupy the residual sites. The reverse order of addition will not result in increased hydrophobicity since the weakly adsorbing collector would hardly adsorb on the energetically weaker surface sites. The results of these tests, shown in Figures 4.61 and 4.62, illustrated that the order of addition did not influence copper or nickel recovery. There was therefore no apparent preferential adsorption of collector onto the different surface sites. Alternatively,

the DTP is so weakly adsorbing that the xanthate will always dominate when there is competition for access to the surface sites. This will explain the similarity in flotation performance with respect to the overall copper and nickel recoveries between the use of pure xanthate and the mixture of xanthate and DTP.

### 5.6.3 The Effect of Collector Mixtures on Copper and Nickel Recovery as a function of Particle Size

The copper and nickel recovery as a function size of particle size plots (cf. Figure 4.77 and 4.78) has shown that the use of a collector mixture, viz. 4.09E-04 mole kg [76 % SIBX + 24 % diethyl DTP], has resulted in a significant increase in recovery at the extreme ends of the recovery by particle size curves when compared to pure SIBX at a dosage of 4.09E-04 mole/kg, i.e. +75 µm and -25 µm size fractions. It is interesting to note however that the pure SIBX test resulted in an increase in the recovery of middling size fractions. This behaviour perhaps explains why, even though the mixture resulted in increased recovery of the coarse and fine fractions, the final copper or nickel recovery obtained with the mixture was not significantly different to that which was obtained with pure SIBX.



### 5.6.4 ToF-SIMS Results

The test results obtained from the ToF-SIMS experiments showed that, compared to the pure diethyl DTP test, diethyl DTP adsorption onto sulphide minerals was significantly enhanced when SIBX was added ahead of diethyl DTP. Furthermore, the ToF-SIMS test results showed that the increased diethyl DTP adsorption onto the sulphide ore minerals appeared to increase in a synergistic manner. The abovementioned results are intriguing because they suggest that increased adsorption of diethyl DTP does not correlate to increased mineral recovery. This suggests perhaps that DTP results in a modification, even a reduction perhaps, in mineral hydrophobicity and that this will result in a change in froth phase behaviour but not a significant change in mineral recovery.

## 5.7 The Effect of Mixtures of Collectors on Palladium and Platinum Recoveries and Grades

### 5.7.1 PGE Mineralogy and Mineral Associations

Table 4.2 showed that palladium was present as palladium tellurides, palladium alloys and palladium-platinum-sulphide composites whilst platinum was present as platinum sulphides, palladium-platinum-sulphide composites, platinum-rhodium composites, platinum-tellurides, platinum arsenides and platinum alloys. Table 4.2 also showed that the major palladium-containing minerals present in the ore were palladium tellurides and palladium alloys whilst the major platinum-containing minerals were platinum tellurides and platinum arsenides. The associations of the PGEs with the sulphide copper and nickel or gangue minerals were however not established. It must be emphasised here that a final definitive interpretation of the relationship between mineralogical associations and recoveries can only be made after an in-depth mineralogical investigation of the feed, concentrate and tails from each batch flotation test. Hence, the following discussion is inevitably speculative in many respects.

Holwell and McDonald (2007) conducted mineralogical investigations on drill core ore samples from Overysel and concluded that: (i) PGE content is directly proportional to BMS content and (ii) pentlandite is the major carrier of rhodium and palladium. It is however interesting to note that Holwell and McDonald (2006b) stated that the direct relationship between PGE and BMS at Overysel is unusual for Platreef as other researchers found little or no correlation between sulphur grades and PGM grades for areas north and south of Overysel. Kinloch (1982) noted that only 31 % of the platinoid minerals were associated with the BMS in Platreef. The remaining 69 %, which were mostly tellurides and arsenides, were associated with the silicate gangue. It is also interesting to note that Vermaak (2005) and Penberthy et al. (2000) argued that copper and nickel recoveries are not reliable indicators for PGM or PGE recovery because most of these minerals will be liberated from their hosts after milling.

Figure 4.80 showed that, when the individual collectors are compared at equivalent molar dosages, pure diethyl DTP increased fines recovery significantly compared to pure SIBX. Similarly, Figure 4.80 also

showed that the pre-mixed mixture of SIBX and diethyl DTP resulted in significantly enhanced fine particle recovery when compared to the pure SIBX case. The implication of the pure diethyl DTP plot compared to the pure SIBX plot in Figure 4.80 is that, if the platinum and/or palladium-containing minerals were locked with the gangue then the pure diethyl DTP case must have resulted in the highest platinum and/or palladium recoveries. This is consistent with Table 4.19 which showed that approximately 96 g of gangue was recovered with pure diethyl DTP whilst only 62 g was recovered with pure SIBX. Figures 4.63 and 4.64 showed however that the pure diethyl DTP collector reagent suite did not result in the highest platinum and/or palladium recoveries. The opposite was true in fact, i.e. the pure diethyl DTP collector reagent suite resulted in the lowest platinum and/or palladium recoveries. This result can therefore only mean that the platinum and palladium-containing minerals were not associated with the silicate gangue after milling. However, when the composite [copper + nickel] recoveries are plotted against the composite [platinum + palladium] recovery, as is done in Figures 5.6, then it is clear that there was significant correlation between BMS recovery and PGE recovery when pure SIBX was used or when the collectors SIBX and diethyl DTP were added simultaneously.



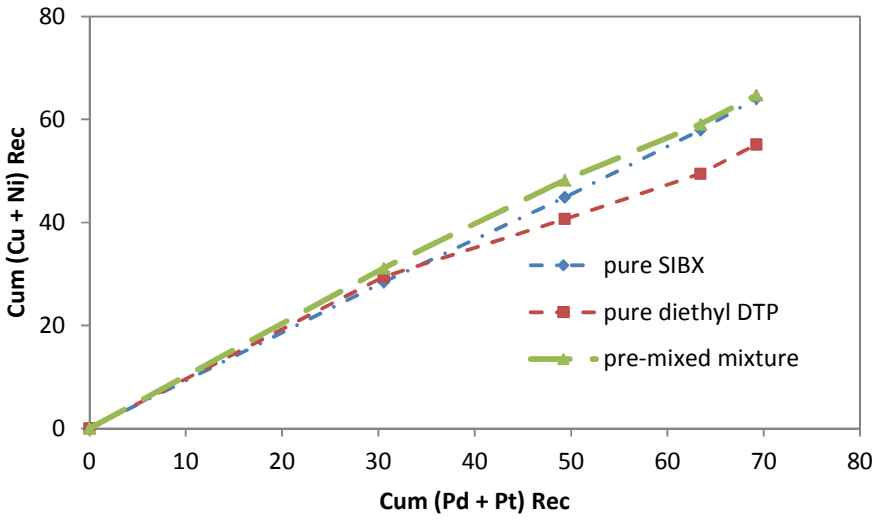


**Figure 5.6: The relationship between composite [copper + nickel] recovery as a function of composite [palladium + platinum] recovery**

The pure diethyl DTP plot in Figure 5.6 deviated significantly from the pure SIBX plot at higher recoveries. This suggests that the reduced nickel recovery obtained with pure diethyl DTP, compared to that which was obtained with pure SIBX, resulted in a lower PGE recovery. This therefore suggests, in agreement with Holwell and McDonald (2007), that PGE recovery was principally dictated by BMS recovery. Figure 5.6 does not however give any information with respect to any particular associations of the platinum and palladium-containing minerals with either chalcopyrite or pentlandite. It is perhaps also important to note that the slopes of the pure SIBX plot and the pre-mixed mixture of [SIBX + diethyl DTP] plot in Figure 5.6 was approximately 0.9, i.e. it is less than 1. This effectively means that, for example, a 60 % [Cu + Ni] recovery was approximately equal to 67 % [Pt + Pd] recovery. This can only therefore mean that additional PGE recovery was obtained from sources other than BMS/PGE associations.

### 5.7.2 Effect of Collector Mixtures on Platinum Recoveries and Grades

Figure 4.67 and Table 4.25 showed that a slightly higher platinum recovery was obtained with the pre-mixed mixture of SIBX and diethyl DTP (± 64 %) compared to pure SIBX (± 62 %). Platinum recovery however decreased slightly when the collectors were added in sequence in the case of mixtures of collectors (cf. Figure 4.67, Table 4.25). Furthermore, Figure 4.68 showed that the platinum grade-recovery profile obtained with pure diethyl DTP is horizontal. This suggest perhaps that either pure diethyl DTP is a poor platinum collector or that platinum was locked with pentlandite as it was shown that diethyl DTP recovered pentlandite via entrainment largely and not via a true flotation mechanism.

Figures 4.67 and 4.68 also showed that an acceptable platinum recovery was obtained with pure SIBX whilst Table 4.25 showed that the highest first order rate constant was obtained with pure SIBX. This is in agreement with the work done by Shackleton et al. (2007b) who showed that synthetic sperrylite ($PtAs_2$) responded well to SIBX. The authors obtained excellent platinum recovery with SIBX and ascribed this to either the effect of xanthate being covalently bonded to the surface or because of the formation of dixanthogen. The fact that recovery was slightly reduced when the collectors were added in sequence may suggest that the role of the two collectors were different, i.e. SIBX was responsible for inducing hydrophobicity in the pulp phase and diethyl DTP, because its function is related to froth

stability, ensured that drop-back from froth phase to the pulp phase was limited. Furthermore, the increased non-selective increase in fines recovery when diethyl DTP was used in combination with SIBX, i.e. pre-mixed condition, may have resulted in additional platinum recovery compared to pure SIBX.

### 5.7.3 Effect of Collector Mixtures on Palladium Recoveries and Grades

Figure 4.64 showed that good palladium recoveries (± 76 %) were obtained when pure SIBX was used as collector whist Table 4.2 (cf. Section 5.7.1) showed that the major palladium-containing minerals present in the ore were palladium tellurides and palladium alloys. This result is in agreement with Vermaak (2005) who showed that both chemisorbed xanthate and dixanthogen formed readily on the surfaces of synthetic palladium-bismuth tellurides when the minerals were exposed to ethyl xanthate (cf. Section 2.4.2.5). The author reported that the chemisorbed xanthate and dixanthogen co-existed and therefore concluded that palladium-bismuth-tellurides can be recovered economically using xanthate collectors.

Figure 4.64 also showed the effect of the individual collectors SIBX and diethyl DTP, at a total dosage of 4.09E-04 mole/kg, as well as their mixtures, which were added in particular sequences, on cumulative palladium recovery as a function of time. This figure and Table 4.25 showed that: (i) using pure diethyl DTP resulted in the poorest palladium recovery (± 49 %), (ii) the palladium recovery obtained when SIBX was added ahead of diethyl DTP (76 %) was not different to the pure SIBX case (76 %), (iii) palladium recovery was slightly reduced when the order of addition was reversed, i.e. diethyl DTP added ahead of SIBX (± 74 %) and, finally, (iv) a significantly enhanced palladium recovery (84 %) was obtained when the collectors SIBX and diethyl DTP were added simultaneously, i.e. pre-mixed before addition to the flotation cell. The increased recovery obtained when the collectors were pre-mixed, as can be seen from Figure 4.63, corresponded to an increase in palladium grades. This is significant because it suggests that the increased palladium recovery obtained when the collectors SIBX and diethyl DTP were added simultaneously was not simply due to increased mass pull. This result suggests that the collectors SIBX and diethyl DTP may have interacted in a synergistic manner which has resulted in a significantly enhanced palladium recovery. This is however contradicted by the fact that palladium recovery was not significantly improved beyond that which was obtained with pure SIBX when the collectors were added

in sequence. It is therefore more likely that the increased palladium recovery obtained when a pre-mixed mixture of SIBX and diethyl DTP was utilised occurred as a consequence of the ability of diethyl DTP to modify the froth phase to increase fine particle recovery.

# Chapter 6: Conclusions and Recommendations

This thesis investigated the flotation performance obtained when mixtures of thiol collectors, viz. SIBX and diethyl DTP, are used in the flotation of a PGM containing ore. The flotation performance obtained with the collector mixtures was then compared to that which was achieved with the individual collectors at equivalent molar collector dosages. The scope of reagents used in batch flotation tests was limited to collectors, i.e. reagents such as copper sulphate as activator and lime for pH control were not utilized. The batch flotation tests however necessitated the use of a frother. In addition, a number of tests were carried out in the presence of guar in order to investigate the effect of the collector reagent suite on gangue recovery using the method developed by Wiese (2009). In this investigation, the relative concentrations of collectors used in the mixture tests were generally at a molar ratio 76 %: 24 % of SIBX and diethyl DTP respectively, whilst the total collector dosage was set at 4.09E-04 mole/kg. A number of additional tests were however carried out in which the mole ratios as well as the collector dosage were varied. In addition, further tests were done in which the effect of chain length, viz. SEX plus diethyl DTP, and SIBX plus di-iso-butyl DTP, on flotation performance was investigated.



## 6.1 Conclusions

The batch flotation results presented in this thesis clearly showed that collector-collector synergism, which is generally defined in flotation as a phenomenon in which the combined effect of more than one reagent exceeds the sum of the individual reagent contributions, did not occur for copper, nickel or platinum when mixtures of collectors, viz. SIBX and diethyl DTP, were used in the study of the ore used in this investigation, i.e. recoveries and grades obtained with the collector mixtures were not significantly different to that which was obtained with the pure collector. Similarly, the batch flotation experiments carried out using collectors of equivalent chain lengths also showed that the apparent lack of collector-collector synergism in the case of SIBX and diethyl DTP collector mixtures cannot be attributed to a dominant effect of the more powerful xanthate collector (SIBX). In addition, batch flotation test results also showed that the lack of collector-collector synergism cannot be attributed to the particular mole ratio of SIBX and diethyl DTP used in this study. Furthermore, batch flotation experiments also showed that sequential addition of the collectors SIBX and diethyl DTP did not result in

collector-collector synergism as indicated by copper, nickel and platinum recoveries and grades. In summary therefore, the use of mixtures of diethyl DTP and SIBX, added in different molar mixtures as well as in different sequences, did not result in enhanced copper, nickel or platinum recovery relative to the individual contributions observed for the individual reagents.

The use of diethyl DTP in [SIBX + diethyl DTP] mixtures did however result in increased water recovery and a decrease in concentrate grade compared to pure SIBX. In addition, the mass of water recovered increased when the relative concentration of diethyl DTP in the [SIBX + diethyl DTP] mixture was increased whilst batch flotation tests conducted with high dosages of guar showed that the use of diethyl DTP resulted in increased gangue recovery via entrainment. Furthermore, an analysis of the particle size distributions of the feed, concentrate and tailings samples showed that the use of diethyl DTP resulted in a significant increase in recovery of the < 25 µm sized particles. This increase in recovery in the fine size fractions was shown to be non-selective.

In contrast to batch flotation experiments, the ToF-SIMS results showed that diethyl DTP adsorption onto selected sulphide minerals significantly increased in the presence of SIBX. In the ToF-SIMS experiments, the secondary collector (diethyl DTP) was added after the primary collector (SIBX). It was however not possible to conduct tests involving simultaneous addition of the collectors because of time and equipment availability constraints. The combination of batch flotation and ToF-SIMS results are interesting because they suggest that increased adsorption of diethyl DTP probably did not result in increased sulphide mineral recovery. This suggest perhaps that dixanthogen may form first on the surface of the sulphide mineral and that the diethyl DTP molecules therefore may anchor onto the previously adsorbed dixanthogen. Alternatively, DTP results in a modification, even a reduction perhaps, in mineral hydrophobicity and that this will result in a change in froth phase behaviour but not a significant change in mineral recovery.

In contrast to the results for the recoveries of base metal sulphides and platinum, palladium recovery increased significantly when mixtures of SIBX and diethyl DTP were added simultaneously compared to what was obtained with the single collectors. Palladium recovery did not however increase when the

collectors were added sequentially. Significantly, the increased recovery obtained with simultaneous addition of collectors was also accompanied by a significant increase in concentrate grade. This suggests that collector-collector synergism may have occurred in the case of palladium. The recovery by particle size results have however also shown that the use of diethyl DTP resulted in a significant increase in the recovery of the fine and ultra-fine sized particles. It is thus possible that the increase in palladium flotation performance observed with the mixture of collectors may be a result of the ability of the froth phase to selectively recover finely sized and liberated palladium particles. This is similar to what was proposed by Vermaak (2005) who found that a typical industrial flotation plant which treated a PGM ore and which operated on a SIBX only collector regime was not able to recover the fully liberated -5 µm sized palladium-bismuth-telluride particles. Whether or not the increased palladium recovery was due to collector-collector synergism or a froth phase modifying effect can probably only be established through further studies including detailed analysis of PGE recoveries on a size-by-size basis as well as detailed mineralogical and chemical analysis.

## 6.2 List of Recommendations

The following recommendations for future test work, based on the findings from this investigation, are listed below:

1. Microflotation test work must be conducted using the collectors SIBX and diethyl DTP and their mixtures in order to investigate the effect of collector type on the floatability of pure minerals such as chalcopyrite, pentlandite and various synthetic platinum and palladium-containing minerals.
2. The microflotation test work should be conducted in conjunction with collector adsorption tests in order to investigate the relationship between collector, with respect to type and adsorption, and floatability.
3. The batch flotation test work should be repeated in a pilot-plant trial environment. This will allow the experimenter to collect enough feed, concentrate and tailings samples in order to determine PGE recovery as a function of particle size. These sized samples can then be sent for

mineralogy analysis in order to determine mineralogical associations with gangue or base metal sulphides.

# References

Abramov, A. (1966). Character of the adsorption of butyl xanthate and dixanthogen and the flotation of chalcopyrite. *Obogashch Rud*, *11*, 6.

Ackerman, P., Harris, G., Klimpel, R. and Aplan, F. (1897). Evaluation of flotation collectors for copper sulphides and pyrite III Effect of xanthate chain length and branching. *International Journal of Mineral Processing*, *21*, 141 – 156

Adamson, A. (1960). Physical chemistry of surfaces. London: InterScience Publishers

Adkins, S. and Pearse, M. (1992). The influence of collector chemistry on the kinetics and selectivity in base metal sulphide flotation. *Minerals Engineering*, *5*, 295 – 310

Agar, G. (1985). The optimisation of flotation circuit data from laboratory rate data. *15th International Mineral Processing Congress*, pages 100 – 111. Cannes, France

Ahmed, N. and Jameson, G. (1985). The effect of bubble size on the rate of flotation of fine particles. *International Journal of Mineral Processing*, 14, 195 – 215

Ahmed, N., and Jameson, G. (1989). Flotation kinetics. *Mineral Processing and Extractive Metallurgy Review*, 5, 77 – 99

Allison, S., Goold, L., Nicol, M. and Granville, A. (1972). A determination of the products of reaction between various sulphide minerals and aqueous xanthate solution and a correlation of the products with electrode rest potentials. *Metallurgical Transactions*, *3*, 2613 – 2618

Armitage, P., McDonald, I., Edwards, S. and Manby, G. (2002). Platinum group element mineralisation in the Platreef and calc-silicate footwall at Sandsloot, Potgietersrus district, South Africa. Transactions *of the Institute of Mining and Metallurgy, Section B: Applied Earth Science*, *11*, B36 – B45

Ata, S., Ahmed, N. and Jameson, G. (2002). Collection of hydrophobic particles in the froth phase. *International Journal of Mineral Processing*, *64*, 101 – 122

Ata, S., Ahmed, N. and Jameson, G. (2004). The effect of hydrophobicity on the drainage of gangue minerals in flotation froths. *Minerals Engineering*, *17*, 897 – 901

Bagci, E., Ekmekci, Z., Gokagac, G. and Bradshaw, D.J. (2006). The synergistic effect of mixture of collectors on adsorption behaviour of chalcopyrite. *International Minerals Processing Conference*, 625 – 630, Istanbul

Bradshaw, D. and O'Connor, C.T. (1994). The flotation of pyrite using mixtures of dithiocarbamates and other thiol collectors. *Minerals Engineering*, *7*, 681 – 690

Bradshaw, D. (1997). *Synergism between thiol collectors* (PhD thesis). Cape Town: University of Cape Town

Bradshaw, D., Harris, P. and O'Connor, C.T. (1998). Synergistic interactions between reagents in sulphide flotation. *Journal of South African Institute of Mining and Metallurgy*, 187 – 192

Bradshaw, D., Harris, P. and O'Connor, C.T. (2005). Effect of collectors and their interactions with depressants on the behaviour of the froth phase in flotation. *Centenary of Flotation Symposium*, pages 329 – 333. Brisbane, Australia: AusIMM

Bradshaw, D., Oostendorp, B. and Harris, P. (2005). Development of methodologies to improve the assessment of reagent behaviour in flotation with particular references to collectors and depressants. *Minerals Engineering*, 18, 239 – 246

Breytenbach, W., Vermaak, M. and Davidtz, J. (2003). Synergistic effects among DTC, DTP and TTC in the flotation of a Merensky ore. *South African Institute of Mining and Metallurgy*, 667 – 670

Cawthorn, R. (1999). The platinum and palladium resources of the Bushveld complex. *South African Journal of Science*, *95*, 481 – 489

Chander, S. (1999). Fundamentals of sulphide mineral flotation. In. J. Miller and B. Parekh, *Advances in Flotation Technology*, pages 129 – 165

Chapman, N.J. (2010). *A study of the effect of different comminution procedures on the recovery of platinum group elements* (MSc Thesis). Cape Town, South Africa: University of Cape Town

Cho, Y. and Laskowski, J. (2002). Effect of flotation frothers on bubble size and foam stability. *International Journal of Mineral Processing*, *64*, 69 – 80

Cramer, L. (2001). The extractive metallurgy of South Africa's platinum ores. *Platinum Group Metals Overview*, pages 14 – 18

Cramer, L. (2008). What is your concentrate worth? *Third International Platinum Conference – Platinum in Transformation* (pages 387 – 394). Pretoria, South Africa: South African Institute of Mining and Metallurgy (SAIMM)

Crozier, R. and Klimpel, R. (1989). Frother: Plant Practice. *Minerals Processing and Extractive Metallurgy Review*, 275 – 279

Crozier, R. (1992). *Flotation: Theory, Reagents and Ore Testing*. New York: Pergamon Press

Dai, Z., Dukhin, S., Fornasiero, D. and Ralston, J. (1998). The inertial hydrodynamic interaction of particles and rising bubbles with mobile surfaces. *Journal of Colloid and Interfacial Science*, 197, 275 – 292

Dai, Z., Fornasiero, D. and Ralston, J. (2000). Particle-bubble collision models – a review. *Adv. Colloid Interfac.*, 85, 231 – 256

Dhilwayo, E. (2005). The interactive effect of depressant type and dosage with frother dosage in the flotation of a PGE ore (MSc thesis). Cape Town, South Africa: University of Cape Town

Dippenaar, A. (1982). The effects of particles on the stability of flotation froths. *National Institute for Metallurgy*

du Plessis, R. (2003). *The thiocarbonate flotation chemistry of auriferous pyrite* (PhD thesis), Salt Lake City, Utah: University of Utah

Dunne, R. (2007). Plant Practice: Sulphide Minerals and Precious Metals. In M. Fuerstenau, H. Jameson and R. Yoon, *Froth Flotation – A Century of Innovation* (pages 832 – 835). Littleton, Colorado: Society for Mining, Metallurgy and Exploration (SME)

Edwards, C., Kipkie, W and Agar, G. (1989). The effect of slime coating of the serpentine minerals chrysotile and lizardite on pentlandite flotation. *International Journal of Mineral Processing*, *7*, 33 – 42

Exerowa, D. and Kruglyakov, P. (1998). Foam and foam films: theory, experiment and application. In D. Mobus and R. Miller, Studies in Interface Science, Volume 5. Amsterdam: Elsevier

Finch, E. and Riggs, W. (1986). Fatty acids – a selection guide. In D. Malhotra and W. Riggs, *Chemical Reagents in the Minerals Industry*, page 95. Littleton, Colorado: SME

Finch, J., Xiao, J., Hardie, C. and Gomez, C. (2000). Gas dispersion properties: bubble surface area flux and gas holdup. *Minerals Engineering*, *13*, 365 – 372

Finch, J., Nesset, J. and Acuna, C. (2008). Role of frother on bubble production and behaviour in flotation. *Minerals Engineering*, *21*, 949 – 957

Finkelstein, N. and Goold, L. (1972). *The reaction of sulphide minerals with thiol compounds*. Durban, South Africa: Mintek (Report No 1439)

Fuerstenau, M. (1982). Chemistry of collectors in solution. In R. King, *Principles of Flotation*, pages 1 – 16. Johannesburg, South Africa: South African Institute of Mining and Metallurgy

Fuerstenau, M., Chander, S. and Woods, R. (2007). Sulphide Mineral Flotation. In M. Fuerstenau, G. Jameson and R. Yoon, *Froth Flotation – A Century of Innovation*, pages 445 – 453. Littleton, Colorado: Society for Mining, Metallurgy and Exploration (SME)

Gain, S. and Mostert A. (1982). The geological setting of the platinoid and base metal sulphide mineralisation in the Platreef of the Bushveld Complex in Drenthe, north of Potgietersrus. *Econ. Geol.*, *77*, 1395 – 1404

Garcia-Gonzales, R., Monnereau, C., Thovert, J., Adler, P. and Vignes-Adler, M. (1999). Conductivity of real foams. *Colloids and Surfaces A: Physicochemical and Engineering Aspects*, *151*, 497 – 503

Glembotskii, V., Klassen, V. and Plaksin, I. (1972). *Flotation*. New York: Primary Sources

Goodall, C. (1992). *The effect of flotation variables on the bubble size, mixing characteristics and froth behaviour in column flotation cells* (PhD thesis). Cape Town, South Africa: University of Cape Town

Grau, A., Laskowski, J., Heiskanen, K. (2005). Effects of frothers on bubble size. *International Journal of Mineral Processing*, *76*, 225 – 233

Hadler, K., Aktas, Z. and Cilliers, J. (2005). The effects of frother and collector distribution on flotation performance. *Minerals Engineering*, *18*, 171 – 177

Harris, P. (1982). Frothing phenomena and frothers. In R. King, *Principles of Flotation*, pages 237 – 250. Johannesburg, South Africa: South African Institute of Mining and Metallurgy (SAIMM)

Harris, P., Mapasa, K., Canham, A. and Bradshaw, D. (1999). The effect of power input on the efficiency of guar depressants in flotation. *Proceedings of the 3rd UBC-McGill International Symposium in Fundamentals of Mineral Processing – The Use of Polymers in Mineral Processing*. Quebec City: CIM

Heilbig, C., Bradshaw, D., Harris, P., O'Connor, C.T. and Baldauf, H. (2000). The synergistic interactions of mixtures of thiol collectors in the flotation of sulphide minerals. *Proceedings of the XXI International Mineral Processing Congress*. Rome, Italy

Hodgson, M. and Agar, G. (1989). Electrochemical investigations into the flotation chemistry of pentlandite and pyrrhotite: Process water and xanthate interactions. *Canadian Metallurgical Quarterly*, *28*, 189 – 198

Holwell, D., McDonald, I. and Armitage, P. (2005). Geochemistry and mineralogy of the Platreef and the "critical" zone of the northern lobe of the Bushveld Complex, South Africa: implications for the Bushveld stratigraphy and the development of PGE mineralisation. *Mineralium Deposita*, *40*, 526 – 549

Holwell, D., McDonald, I. and Armitage, P. (2006a). Platinum-group mineral assemblages in the Platreef at the Sandsloot Mine, northern Bushveld complex, South Africa. *Mineralogical Magazine*, *70*, 83 – 101

Holwell, D. and McDonald, I. (2006b). Petrology, geochemistry and the mechanisms determining the distribution of platinum group element and base metal sulphide mineralisation in the Platreef at Overysel, northern Bushveld Complex, South Africa. *Miner Deposita*, *41*, 575 – 598

Holwell, D. and McDonald, I. (2007). Distribution of platinum-group elements in the Platreef at Overysel, northern Bushveld Complex: a combined PGM and LA-ICP-MS study. *Contributions to Mineralogy and Petrology*, *154*, 171 – 190

Holwell, D. and McDonald, I. (2010). A review of the behaviour of platinum group elements within natural magmatic sulphide ore systems. *Platinum Metals Review*, *54*, 26 – 36

Johnson, N., McKee, D. and Lynch, A. (1974). Flotation rates of non-sulphide minerals in chalcopyrite flotation processes. *Trans. A.I.M.E.*, *256*, 204 – 209

Jowett, A. (1966). Gangue mineral contamination of froth. *British Chemical Engineering*, *2*, 330 – 333

Jowett, A. (1979). The formation and disruption particle-bubble aggregates in flotation. In P. Somarsundaran, *Fine Particle Processing*, pages 720 – 753

King, R. (1982). *Principles of Flotation – South African Institute of Mining and Metallurgy (SAIMM) Monograph Series No 3*. Johannesburg, South Africa: SAIMM

Kinloch, E. (1982). Regional trends in platinum-group mineralogy of the critical zone of the Bushveld Complex, South Africa. *Economic Geology*, *77*, 1326 – 1347

Kirjavainen, V. (1996). Review and analysis of factors controlling the mechanical flotation of gangue minerals. *International Journal of Mineral Processing*, *46*, 21 – 34

Klein, R., Proctor, S., Boudreault, M. and Turczyn, K. (2010). Criteria for data suppression, *Healthy People 2010*

Klimpel, R. (1984). *Froth Flotation: The Kinetic Approach*. Johannesburg, South Africa: Proceedings of Mintek 50

Klimpel, R., Fee, B. and Leonard, D. (1994). Some new chemical reagents to expand the capabilities of froth flotation processes. *Proceedings of the IV Meeting of the Southern Hemisphere on Mineral Technology and III Latin-American Congress on Froth Flotation*, *2*, pages 47 – 81. Concepcion, Chile: Concepcion, Chile

Langevin, D. (2000). Influence of interfacial rheology on foam and emulsion properties. *Advances in Colloid and Interface Science*, *88*, 209 – 222

Lascelles, D. and Finch, J. (2005). A technique for quantification of adsorbed collectors: xanthate. *Minerals Engineering*, *18*, 257 – 262

Laskowski, J. and Pugh, R. (1992). Dispersing stability and dispersing agents. In J. Laskowski and J. Ralston, *Colloid Chem. Miner. Process*, pages 115 – 171. Elsevier

Laskowski, J. (1993). Frothers and flotation froth. *Mineral Processing and Extractive Metallurgy Review*, *12*, 61 – 89

Laskowski, J. (1998). *Frothing in Flotation*. Amsterdam: Gordon and Breach Science Publishers

Laskowski, J. (2005). *Flotation Fundamentals and Applications*. Randburg, South Africa: University of Cape Town

Legrand, D., Bancroft, G. and Nesbitt, H. (1997). Surface characterisation of pentlandite by X-ray photo-electron spectroscopy, *International Journal of Mineral Processing*, *51*, 217 - 228

Leja, J. and Schulman, J. (1954). Flotation theory: molecular interactions between frothers and collectors as solid-liquid-air interfaces. *Trans. AIME*, *199*, 221 – 228

Livshits, A. and Dudenkov, S. (1965). Some factors in flotation froth stability. *Proceedings of VII International Mineral Processing Congress*, pages 367 – 371, New York

Lotter, N. (2010). *Private Communication*

Lotter, N. and Bradshaw, D.J. (2009). The formulation and use of mixed collectors in sulphide flotation. *Flotation 2009*. Cape Town, South Africa: Minerals Engineering

Lovell, V. (1982). Industrial flotation reagents. In R. King, *Principles of Flotation*, pages 73 – 89, Johannesburg, South Africa: South African Institute of Mining and Metallurgy

Mackenzie, M. (1986). Organic polymers as depressants. In D. Malhotra and W. Riggs, *Chemical Reagents in the Minerals Industry*, page 139. Littleton, Colorado: Society for Mining, Metallurgy and Exploration (SME)

Maier, W. (2005). Platinum-group element (PGE) deposits and occurrences: mineralisation styles, genetic concepts and exploration criteria. *Journal of African Sciences*, *41*, 165 – 191

Malysiak, V., Shackleton, N. and O'Connor, C.T. (2004). An investigation into the floatability of a pentlandite-pyroxene system. *International Journal of Mineral Processing*, *74*, 251 - 262

Malysa, E., Malysa, K. and Garnecki, J. (1987). A method of comparison of the frothing and collecting properties of frother. *Colloids and Surface*, *23*, 29 – 39

Manyeruke, T., Maier, W. and Barnes, S. (2005). Major and trace element geochemistry of the Platreef on the farm Townlands, northern Bushveld Complex. *South African Journal of Geology*, *108*, 381 – 396

Matveeva, T. and Gromova, N. (2007). Sorption of mercaptanbenzothiazol and dithiophosphate on Pt-Cu-Ni minerals at flotation process. *Journal of Mining Science*, *43*, 680 – 685

Merkle, R. and Harney, D. (1990). Pt-Pd minerals from the upper zone of the eastern Bushveld complex. *Canadian Mineralogist*, *28*, 619 – 628

Mingione, P. (1984). Use of dialkyl and diaryl dithiosulphate promoters as mineral flotation reagents. In M. Jones and R. Oblatt, *Reagents in the Minerals Industry*, page 19. London: IMM

Mitrofanov, S., Kuz'kin, A. and Filimonov, V. (1985). Theoretical and practical aspects of using combinations of collectors and frothing agents for sulphide flotation. *Proceedings of 15th Congr. Int. Metall.*, *2*, pages 65 – 73. St. Ettienne, France: SME

Moolman, D., Aldrich, C. and Bradshaw, D. (1995). The interpretation of flotation froth surfaces by using digital image analysis and neural networks. *Chemical Engineering Science*, *50*, 3501 – 3513

Moudgil, B. (1992). Enhanced recovery of coarse particles during phosphate flotation. Florida, USA: *Florida Institute of Phosphate Research*

Mukai, S., Wakamatsu, T. and Takahashi, K. (1972). Mutual interaction between collectors and frothers in flotation. *Mem. Fac. Eng. Kyoto Univ. III*, *34*, 279 – 288

Nagaraj, D. (1988). The chemistry and application of chelating or complexing agents in minerals separations. In P. Somasundaran and B. Moudgil, *Reagents in Mineral Technology*, pages 387 – 409. New York: Marcel Dekker Inc.

Nagaraj, D and Brinen, J. (2001). SIMS study of adsorption of collectors on pyrite, *International Journal of Mineral Processing*, *63*, 45 – 57

Nagaraj, D. and Ravishankar, S. (2007). Flotation Reagents – A Critical Overview from an Industry Perspective. In M. Fuerstenau, G. Jameson and R. Yoon. *Froth Flotation – A Century of Innovation*, pages 375 – 421. Littleton, Colorado: Society for Mining, Metallurgy and Exploration (SME)

Naldrett, T., Kinnaird, J., Wilson, A. and Chunnet, G. (2008). Concentration of PGE in the earth's crust with special reference to the Bushveld complex. *Earth Science Frontiers*, *15* (5), 264 – 297

Nashwa, V. (2007). *The flotation of high-talc containing ore from the Great Dyke of Zimbabwe* (MSc thesis). Pretoria, South Africa: University of Pretoria

Newell, R. and Grano, S. (2007). Hydrodynamics and scale up in Rushton turbine flotation systems: Part 1 – cell hydrodynamics. *International Journal of Mineral Processing*, *81*, 224 – 236

Newell, A. (2008). *The processing of PGM – part 1*. Lakewood, Colorado: Pincock Perspectives

Nguyen, A. and Schulze, H. (2004). Colloidal Science of Flotation. New York: Marcel Dekker

O'Connor, C.T., Botha, C., Walls, M. and Dunne, R. (1998). The role of copper sulphate in pyrite flotation. *Minerals Engineering*, *1*, 203 – 212

Oostendorp, B. (2003). *Reagent interactions and froth stability* (BTech thesis). Cape Town, South Africa: University of Technology

Pearce, C., Pattrick, R. and Vaughan, D (2006). Electrical and magnetic properties of sulphides. In D. Vaughan, *Sulphide Mineralogy and Geochemistry* (Volume 61). Chantilly, Virginia: Mineralogical Society of America

Pearse, M. (2005). An overview of the use of chemical reagents in mineral processing. *Minerals Engineering*, *18*, 139 – 149

Pease, J., Curry, D. and Young M. (2006). Designing flotation circuits for high fines recovery. *Minerals Engineering*, *19*, 831 – 840

Penberthy, C., Oosthuyzen, E. and Merkle, R. (2000). The recovery of platinum-group elements from the UG-2 chromitite Bushveld Complex – a mineralogical perspective. *Mineralogy and Petrology*, *68*, 213 – 222

Plaskin, I., Glembotskii, V. and Okolovich, A. (1954). Investigations of the possible intensification of the flotation process using combinations of collectors. *Naachnye Soobshcheniya Institut Gonnogo del Imeni AA Skochinskogo Akademiya Nauk SSRM (Mintek Translation February 1989)*, 213 - 224

Plaskin, I. and Zaitseva, S. (1988). Effect of the combined action of certain collectors on their distribution between galena particles in a flotation pulp. *Mintek Translation nr 1295*

Poling, G. (1976). Reactions between thiol reagents and sulphide minerals. In M. Fuerstenau, *Flotation: A.M. Gaudin Memorial Volume (Volume 1, pages 334 – 363)*. New York, USA: AIME

Pugh, R. (1989). Flotation depressant action of poly(oxyethylene) alkyl ethers on talc. *International Journal of Mineral Processing*, *25*, 131

Pugh, R. and Johannson, G. (1992). The influence of particle size and hydrophobicity on the stability of mineralised froths. *International Journal of Mineral Processing*, *34*, 1 – 21

Pugh, R. (1996). Foaming, foam films, antifoaming and defoaming. *Advances in Colloid and Interface Science*, *64*, 67 – 142

Pugh, R. (2005). Experimental techniques for studying the structure of foams and froths. *Advances in Colloid and Interface Science*, *114*, 239 – 251

Randall, E. (2009). The UCT bubble sizer (an inhouse presentation). Cape Town, South Africa: *Centre for Minerals Research*

Rath, R., Subramanian, S., Sivanandam, V. and Pradeep, T. (2001). Studies on the interaction of guar gum with chalcopyrite. *Canadian Mining Quarterly*, *40*, 1 – 12

Richardson, S. and Vaughan, D. (1989). Surface alteration of pentlandite and spectroscopic evidence for secondary violarite formation. *Mineralogical Magazine*, *53*, 213 – 222

Robertson, C., Bradshaw, D. and Harris, P. (2003). Decoupling the effects of depression and dispersion in the batch flotation of a platinum bearing ore. XXII International Mineral Processing Congress, pages 920 – 928. Cape Town, South Africa

Rodel, K. (1981). Proof of boundary surface water and its effect on colloidal-chemical properties – IR spectroscopy of foam films. *Tenside Detergents*, 18, 141 – 148

Ross, V. (1991). An investigation of sub-processes in equilibrium froths (1): the mechanisms of detachment and drainage. *International Journal of Mineral Processing*, *31*, 37 – 50

Savissi, O., Alexander, D., Franzidis, J. and Manlapig, E. (1998). An empirical model for entrainment in industrial flotation plants. *Minerals Engineering*, *11*, 243 – 256

Savassi, O. (2005). A compartment model for the mass transfer inside a conventional flotation cell. *International Journal of Mineral Processing*, *77*, 65 – 79

Schwarz, S. (2004). *The relationship between froth recovery and froth structure* (PhD thesis). Adelaide, Australia: Ian Wark Research Institute

Shackleton, N. (2003). *The role of complexing agents in the flotation of pentlandite-pyroxene mixtures* (MSc thesis). Cape Town, South Africa: University of Cape Town

Shackleton, N., Malysiak, V. and O'Connor, C.T. (2007a). Surface characteristics and flotation behaviour of platinum and palladium tellurides. *Minerals Engineering*, *20*, 1232 – 1245

Shackleton, N., Malysiak, V. and O'Connor, C.T. (2007b). Surface characteristics and flotation behaviour of platinum and palladium arsenides. *International Journal of Mineral Processing*, *85*, 25 – 40

Shackleton, N. (2007c). *Surface characterisation and flotation behaviour of the platinum and palladium arsenide, telluride and sulphide mineral species* (PhD thesis). Cape Town, South Africa: University of Cape Town

Shackleton, N. (2009). *Private Communication*

Shamaila, S. and O'Connor, C.T. (2008). The role of synthetic minerals in determining the relative flotation behaviour of Platreef PGE tellurides and arsenides. *Minerals Engineering*, *21*, 899 – 904

Sharman-Harris, E., Kinnaird, J., Harris, C. and Horstmann, U. (2005). A new look at the sulphide mineralisation of the northern limb, Bushveld Complex: a stable isotope study. *Transactions of the Institution of Mining and Metallurgy (Section B)*, 114, B252 – B263

Shortridge, P., Harris, P. and Bradshaw, D. (2003). The influence of ions on the effectiveness of polysaccharide depressants in the flotation of talc. *Proceedings of the third UBC-McGill International Symposium "Polymers in Mineral Processing"*, pages 155 – 170

Smar, V., Klimpel, R. and Aplan, F. (1994). Evaluation of chemical and operational variables for the flotation of a copper ore. Part I – Collector concentration, frother concentration and air flow rate. *International Journal of Mineral Processing*, *42*, 225 - 240

Somasundaran, P. (1969). Adsorption of starch and oleate and interaction between on calcite in aqueous solutions. *Journal of Colloid and Interface Science*, *31*, 557

Somasundaran, P. and Moudgil, B. (1988). *Reagents in Mineral Technology*. New York: Marcel Dekker

Somasundaran, P. (1975). Interfacial chemistry of particulate flotation. *AICHE Symposium Series*, *71*

Stamboliadis, E. (1976). *The surface chemistry of the flotation of millerite, pyrrhotite and pentlandite with dialkyl-dithiophosphates (PhD thesis)*. Montreal, Quebec: McGill University

Subrahmanyam, T. and Forssberg, E. (1988). Froth stability, particle entrainment and drainage in flotation – a review. *International Journal of Mineral Processing*, *23*, 33- 53

Sweet, J. (1999). *Investigation of a methodology to decouple physical and chemical effects for flotation circuit performance evaluation* (Masters thesis). Cape Town, South Africa: University of Cape Town

Szatkowski, M. and Freyburger, W. (1985). Kinetics of flotation with fine bubbles. *Transactions of the Institute of Mining and Metallurgy (Section C)*, 94, C61 – C70

Taggart, A. (1950). Handbook of mineral processing. New York: Wiley

Taggart, A. (1951). Elements of ore processing. New York: Wiley

Tambe, D. and Sharman, M. (1993). Factors controlling the stability of colloid-stabilised emulsions II. A model for the rheological properties of the colloid-laden interfaces. *Journal of Colloid and Interface Science*, *162*, 1 – 10

Tao, D. (2004). Role of bubble size in flotation of coarse and fine particles. *Separation Science and Technology*, *39*, 741 – 760

Trahar, W. (1981). Rational interpretation of the role of particle size in flotation. *International Journal of Mineral Processing*, *8*, 289 – 327

*University of Witwatersrand – School of Geosciences.* (2009). Retrieved 22 February 2010 from Virtual Tour of the Bushveld Complex:

http://web.wits.ac.za/Academic/Science/GeoSciences/Research/bushveld/bushvfthome.htm

Velikov, K., Durst, F. and Velev, O. (1998). Direct observation of the dynamics of latex particles confined inside thinning water-air films. *Langmuir*, 14, 1148 – 1155

Ventura-Medina, E. and Cilliers, J. (2002). A model to describe flotation performance based on physics of foams and froth image analysis. *International Journal of Mineral Processing*, *67*, 79 – 99

Vermaak, M. (2005). *Fundamentals of the flotation behaviour of palladium bismuth tellurides* (PhD thesis). Pretoria, South Africa: University of Pretoria

Warren, L. (1985). Determination of the contributions of true flotation and entrainment in batch flotation tests. *International Journal of Mineral Processing*, *14*, 33 – 44

Weaire, D. and Hutzler, S. (1999). *The physics of foams*. Oxford, Clarendon Press

Whitworth, F. (1926). *Patent No. 2404*. Australia

Wiese, J., Harris, P. and Bradshaw, D. (2005). Investigation of the role and interactions of a dithiophosphate collector in the flotation of sulphides from the Merensky reef. *Minerals Engineering*, *18*, 675 – 686

Wiese, J. (2009). *Investigating depressant behaviour in the flotation of selected Merensky ores* (MSc thesis). Cape Town, South Africa: University of Cape Town

Wills, B. and Napier-Munn, T. (2006). *Wills' Mineral Processing Technology (7th Edition)*. Oxford, UK: Butterworth-Heinemann

Woodcock, J., Sparrow, G. and Bruckard, W. (2007). Flotation of precious metals and their minerals. In M. Fuerstenau, G. Jameson and R. Yoon., *Froth Flotation – A Century of Innovation*, pages 586 – 696. Littleton, Colorado: Society for Mining, Metallurgy and Exploration (SME)

Xia, Y. (2000). *Dynamic property evaluation of frothers* (MSc thesis). Morgantown, West-Virginia: University of West Virginia

Xiao, Z. and Laplante, A. (2004). Characterising and recovering the platinum group minerals – a review. *Minerals Engineering*, *17*, 961 – 979

Yoon, R. and Basilio, C.I. (1993). Adsorption of thiol collectors on sulphide minerals and precious metals – a new perspective. XVII International Mineral Processing Congress, Volume 3, pages 611 – 617. Sydney, Australia

# List of Appendices

# Appendix A – Determination of the parameters of the flotation rate equation

The flotation first order rate constant ($k$) and the infinite time recovery ($R_{inf}$) were calculated using Klimpel's equation (Klimpel, 1984) and Excel's solver function. The Klimpel equation is given as:

$$R = R_{inf}[1- 1/(kt)\{1 - exp^{-kt}\}]$$

where $R_{inf}$ is the recovery achieved at infinite flotation time and $k$ is the first order rate constant. The procedure followed is explained below.



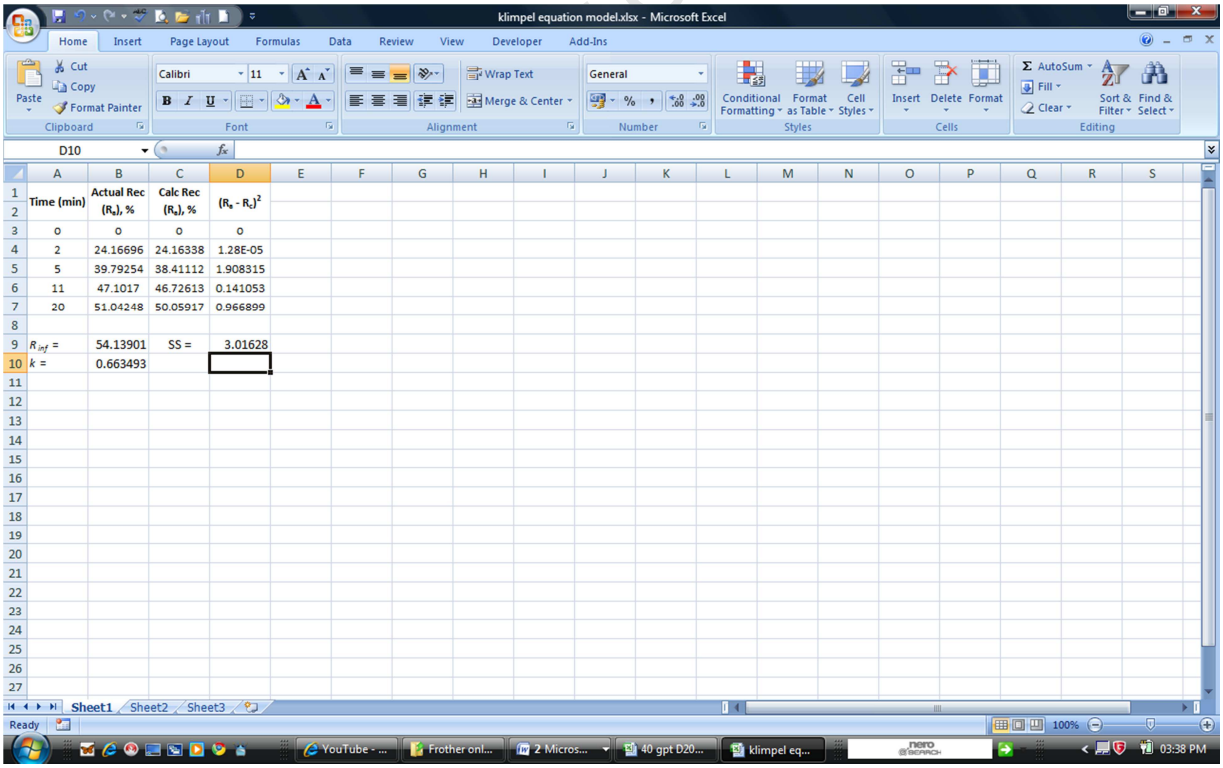


**Figure A1: An example of recovery modelling using the Klimpel model and Excel's solver function**

The procedure was as follows:

1. Enter the values for cumulative time and cumulative recovery in columns A and B respectively.
2. Enter the Klimpel equation labels $R_{inf}$ and $k$ in cells A9 and A10 respectively.
3. Rename Cell B9 to Rinf, i.e. position cursor in cell B9 and click the tab "Formulas"; click the tab "Define Name" and rename Cell B9 to Rinf.
4. Similarly, rename cell B10 to "k".
5. Guess initial values of $R_{inf}$ and $k$.
6. Enter the Klimpel recovery equation in column C using the guessed values of $R_{inf}$ and $k$.
7. In column D, calculate the difference between the actual recovery and the calculated recovery and square the difference.
8. Sum the square of the differences between the actual recovery and the calculated recovery in cell D9. The ultimate aim of this exercise is to minimise the value in cell D9.
9. Rename cell D9 as "SS".
10. Activate the Solver function in Excel
11. In the "Set Target Cell" box, enter SS or choose cell D9 (this is the cell that needs to be minimised).
12. Select the "Min" option box where it says "Equal To"
13. Select cells B9 and B10 in the "By Changing Cells" box; alternatively type Rinf, k in the box "By Changing Cells".
14. Select the "Solve" button

The optimisation program in Excel will now change the values $R_{inf}$ and $k$ until the minimum value of SS is obtained.

# Appendix B: Froth Column Test Results

## B1: Test Rig Description and Experimental Procedure Validation

A number of experiments were completed in order to validate the test rig and experimental procedure. Malysa et al. (1987) and Xia (2000) showed that, for the same frother, the attained froth height (*H*) increased with both dosage and air flow rate. The authors furthermore showed that the froth height also increased when higher molecular weight frothers were utilised. Other parameters which influenced frothability, which essentially is the froth height attained in the froth column, are frother chemical structure and chemical impurities present in the water used for test work. Figure B1, which shows the effect of Dowfroth 200 dosage on froth height as a function of air flow rate, shows that froth height increased with an increase in both air flow rate and frother dosage. Furthermore, the error bars, which show the standard error obtained from two independent tests, are minimal which indicates that the tests were repeatable.



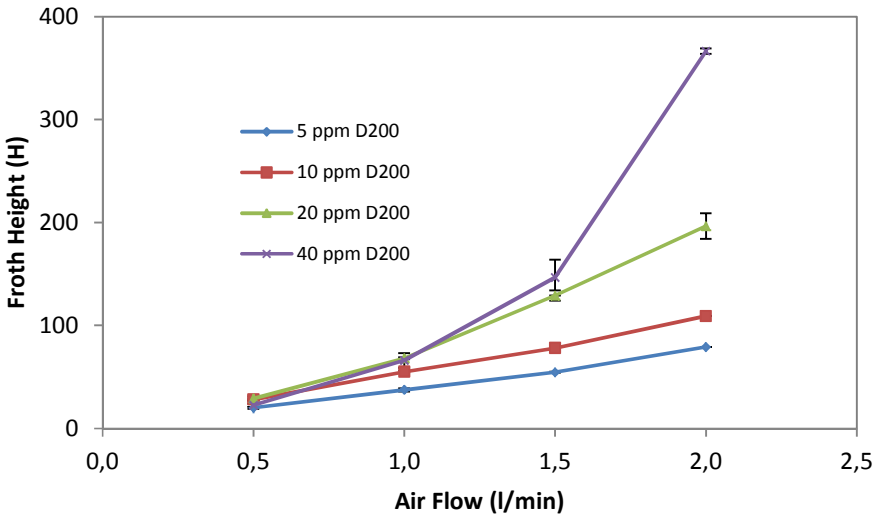


**Figure B1: The effect of Dowfroth 200 concentration on froth height**

It is interesting to note that the slopes of the curves in Figure B1 are constant until the frother dosage is increased to 40 ppm. Figure B1 also shows that the slope was dependent on frother concentration, i.e. slope increased with an increase in frother concentration. In addition to frother dosage, the effect of molecular weight on frothability was investigated by comparing the froth height attained with different frothers (but at equivalent molecular concentrations). The results obtained are shown in Figure B2 which shows, as expected, increased molecular weight resulted in increased froth height. Figure B2 also shows that very similar froth height growth patterns were obtained for Dowfroth 200 and Betafroth 206. This was an important result, for these frothers have similar molecular structures and weights. The error bars given indicate that the data obtained were repeatable and reliable.



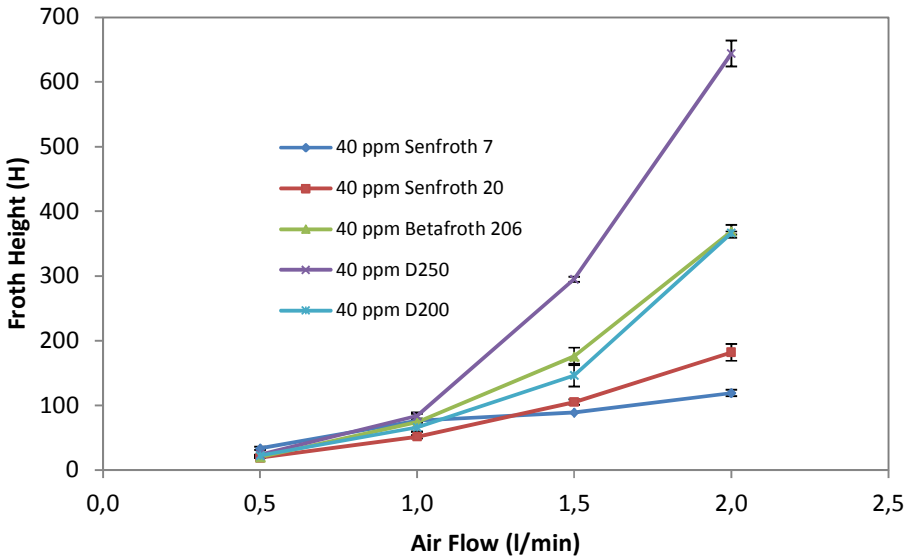


**Figure B2: The effect of frother type on froth height at a dosage of 40 ppm**

The results presented in Figures B1 and B2 clearly demonstrate that the results obtained with the froth column were experimentally repeatable and the trends are consistent with the findings obtained by Malysa et al. (1987) and Xia (2000).

## B2: Frothability Experiments Conducted with SIBX and Mixtures of Frother and SIBX as the Control Experiments

Further preliminary tests, in addition to those shown in Figures B1 and B2, were completed whereby the effect of addition of a non-frothing chemical, SIBX in this case, on froth height was investigated. It was considered critical that either a measurable froth phase should not form when SIBX was added to distilled water or that the froth height obtained with Dowfroth 200 and SIBX should not be significantly different to that obtained with only Dowfroth 200. Experiments with only SIBX did indeed show that a measurable froth did not form and are omitted from Figure B3 for clarity whilst the SIBX-Dowfroth 200 mixtures, as is shown in Figure B3, did not enhance froth height significantly above that which was obtained with only Dowfroth 200. The experiments with SIBX were thus considered the control experiments.



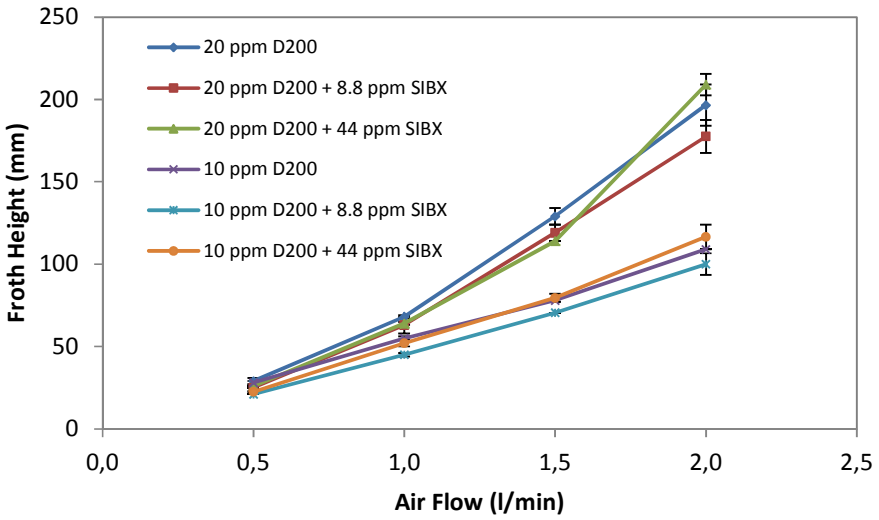


**Figure B3: A comparison of froth height formed with Dowfroth 200 and mixtures of Dowfroth 200 and SIBX**

## B3: Frothability Experiments Conducted with DTP and Mixtures of Frother and DTP

Figure B4, which shows the effect of increasing diethyl DTP concentration and air flow rate on froth height, shows that a very large concentration of diethyl DTP was needed in order to form a measurable froth in the absence of frother. Figure B4 also shows that between 500 and 1000 ppm diethyl DTP was required in order to form a froth similar in height to that which was obtained with 5 ppm Dowfroth 200. In other words, in a two-phase froth column, the frothing power of diethyl DTP is at least 100 times less than Dowfroth 200. Furthermore, as is shown in Figure B5, the froth obtained with a mixture of frother and diethyl DTP did not result in a significantly enhanced froth height compared to that which was obtained with frother only. This is a significant result and it shows that the main requirement of the test program was met, i.e. the DTP collector used in this investigation, which was diethyl DTP, does not possess frothing properties unless used at extremely high dosages. However, in contrast to the diethyl DTP, tests conducted with di-iso-butyl DTP showed that significantly increased froth heights were obtained with mixtures of frother and di-iso-butyl DTP compared to frother only (cf. Figure B6).



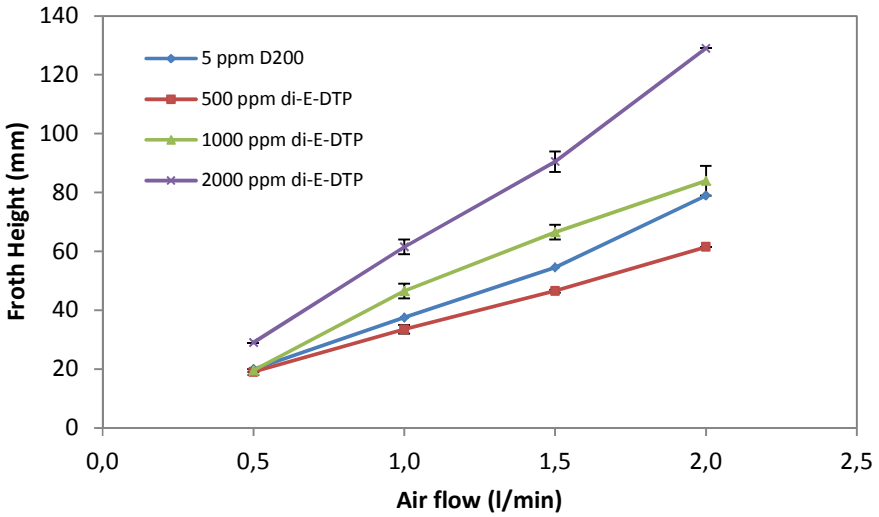


**Figure B4: The effect of increasing diethyl DTP concentration on froth height as a function of increasing air flow rate**

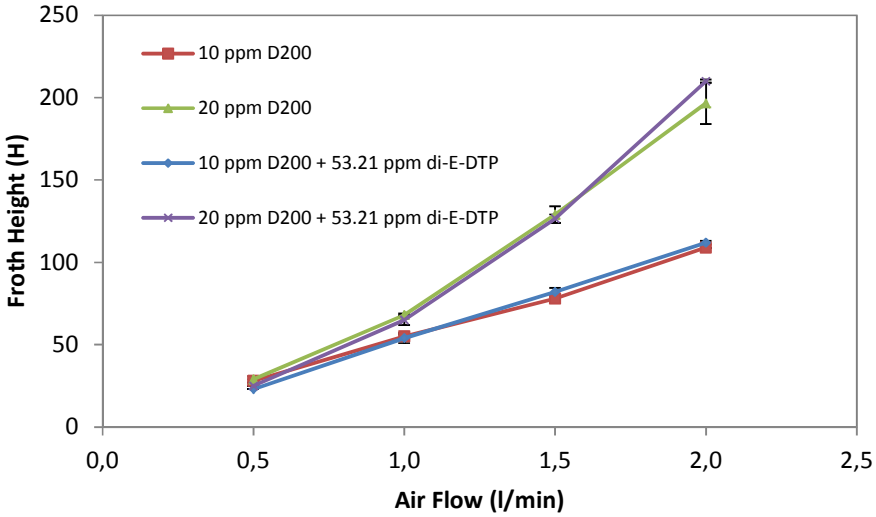


**Figure B5: Comparison of froth height obtained with mixtures of frother and diethyl DTP compared to frother only**

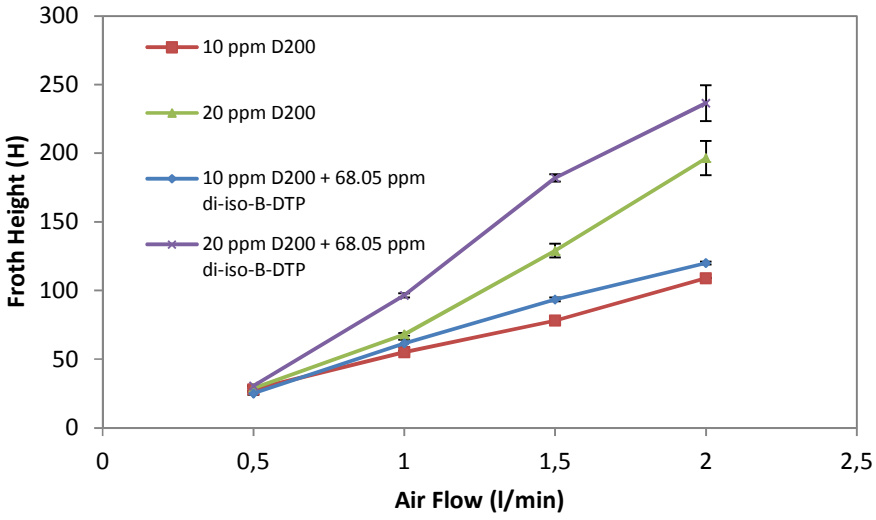


**Figure B6: Comparison of froth height obtained with mixtures of frother and di-iso-butyl DTP compared to frother only**

# Appendix C: Bubble Sizing Test Results and Discussion

A number of experiments were conducted using the UCT bubble sizer in order to establish if the use of diethyl DTP resulted in a significant reduction in pulp phase bubble diameter. A number of additional tests were completed whereby the effect of combinations of frother and diethyl DTP on bubble diameter were investigated. The experimental set-up, as is shown in Figure C1, consists of a capillary which is placed inside an aerated water reservoir, a detector head which contains two optical detectors mounted at right angles to each other, detector electronics, a microprocessor, a computer, a peristaltic pump and a gas burette.

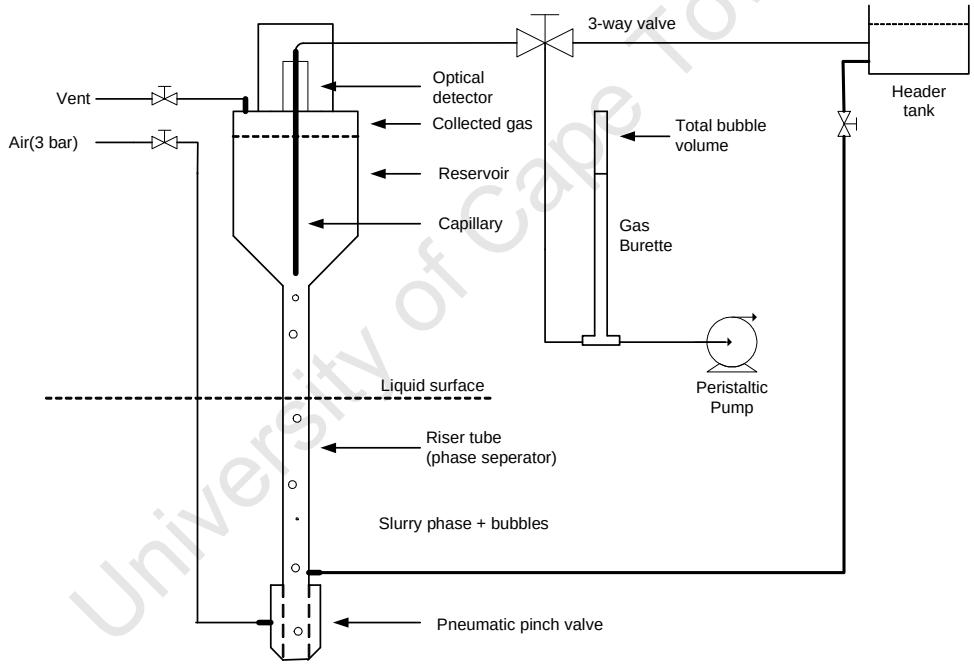




**Figure C1: The main components of the UCT bubble-sizing device (Randall, 2009)**

The basic principle of operation is that (i) the shape of the gas bubbles are transformed from near-spheres into cylinders once they are sucked into the capillary and (ii) their lengths and velocities are measured by optical detectors which monitor changes in light intensity when the bubbles pass between the detectors (Goodall, 1992). The function of the detector electronics is to amplify the light intensity

signal whilst the function of the microprocessor is to time and store the pulses in memory and, at the end of the measurement cycle, transfer the data to the computer (Goodall, 1992). Software stored on the computer then uses the bubble velocity and length data to calculate the volume of each individual bubble captured during the test cycle. The gas bubbles, once they pass the detectors, are collected in the gas burette in order that the total gas volume can be determined. The calculated bubble volumes are then normalised with respect to the total volume collected. This is necessary because a thin film of water, which is a function of bubble size and slurry viscosity, coats the inside of the capillary and thus makes it difficult to calculate the effective capillary diameter.

A number of preliminary tests were conducted using various frothers. The results obtained, shown in Figure C2, indicate that bubble diameter was reduced significantly when relatively small amounts of frother was added to distilled water. Further addition of frother did not however result in a significant reduction in bubble diameter. It is important to note that the error bars are smaller than the icons in Figure C2 and thus may not be visible.



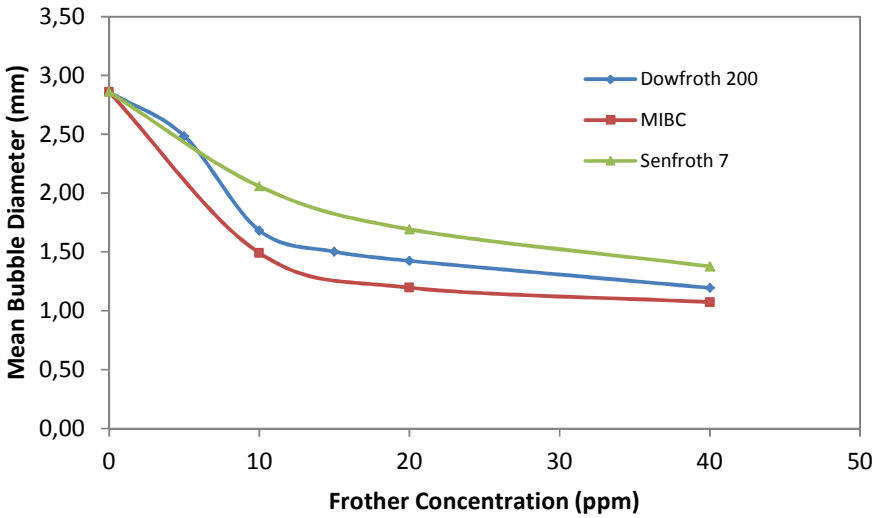


**Figure C2: The effect of frother type and concentration on the average diameter of bubbles generated in a laboratory bubble sizing column cell**

The effect of the collector's diethyl DTP and SIBX on bubble diameter was also investigated and the results obtained are shown in Figure C3. This figure shows that, compared to frother, significantly higher amounts of collector are required to reduce bubble diameter. Figure C3 does however show that diethyl DTP was able to reduce bubble diameter much more effectively than SIBX was.

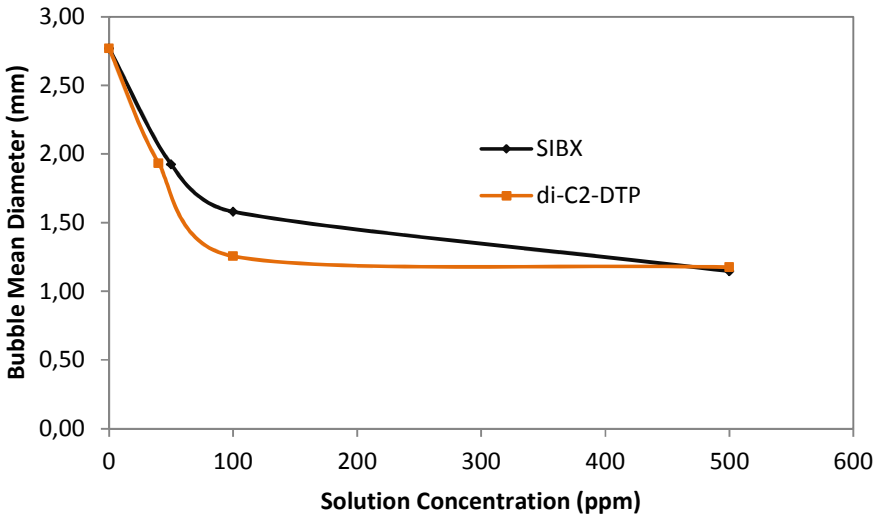


**Figure C3: The effect of collector type and dosage on the average diameter of bubbles generated in a laboratory bubble sizing column cell**

Finally, a number of tests were conducted whereby the effect of combinations of frother and diethyl DTP on bubble diameter was measured. The results obtained from these tests are shown in Table C1. This table shows that the addition of diethyl DTP, at a dosage of 20 ppm, to a 10 ppm frother solution significantly reduced the bubble diameter which was obtained with frother only. In addition, the bubble diameter was decreased further when the diethyl DTP was increased from 20 ppm to 60 ppm. Addition of diethyl DTP did not result in a measurable reduction in bubble diameter when the frother concentration was increased from 10 ppm to 40 ppm. This result is consistent with Figure C2 which showed that, for MIBC certainly and to some extent also for Dowfroth 200, bubble diameter was not reduced significantly when frother concentration was increased beyond 20 ppm. This is termed the CCC or the critical coalescence concentration (Grau et al., 2005), which is the frother concentration at which

coalescence of bubbles is prevented. This result is significant as it suggests that at the frother concentration used in the froth flotation test work, which was 2.00E-04 mole/kg or 40 ppm, the use of diethyl DTP did not result in an additional reduction in pulp phase bubble diameter. This is important because it can thus be concluded that the fact that diethyl DTP resulted in a significant increase in especially the recovery of finely sized particles was not due to a bubble size effect in the pulp phase but rather a froth phase effect.

**Table C1: The effect of [Dowfroth 200; di-iso-butyl DTP] mixtures on the average diameter of bubble which were generated in a laboratory bubble sizing column cell**

| Reagent Mixture | Mean Bubble Diameter (mm) | Standard Deviation | Standard Error |
|---|---|---|---|
| 10 ppm Dowfroth 200 | 1.66 | 0.06274 | ±0.01 |
| 10 ppm Dowfroth 200 + 20 ppm di-E-DTP | 1.25 | 0.01465 | ±0.01 |
| 10 ppm Dowfroth 200 + 60 ppm di-E-DTP | 1.19 | 0.01261 | ±0.01 |
| 40 ppm Dowfroth 200 | 1.11 | 0.09264 | ±0.05 |
| 40 ppm Dowfroth 200 + 20 ppm di-C2-DTP | 1.08 | 0.04151 | ±0.02 |
| 40 ppm Dowfroth 200 + 60 ppm di-E-DTP | 1.08 | 0.04540 | ±0.02 |

# Appendix D – Summary of Flotation Results

| Flotation Conditions | Sample ID | Time (min) | Cum Mass (g) | Cum Water(g) | Concentrate Grade | | | Recovery (%) | | |
|---|---|---|---|---|---|---|---|---|---|---|
| | | | | | % Cu | % Ni | % S | % Cu | % Ni | % S |
| 2.00E-04 mole/kg D200 | C1 | 2 | 22.21 | 139.31 | 1.68 | 0.34 | 1.76 | 24.17 | 2.00 | 6.97 |
| | C2 | 5 | 39.72 | 283.16 | 1.55 | 0.34 | 1.60 | 39.79 | 3.65 | 11.35 |
| | C3 | 11 | 57.50 | 466.14 | 1.27 | 0.35 | 1.44 | 47.10 | 5.38 | 14.78 |
| | C4 | 20 | 71.93 | 656.19 | 1.10 | 0.36 | 1.33 | 51.04 | 6.85 | 17.06 |
| 6.00E-04 mole/kg MIBC | C1 | 2 | 37.54 | 246.61 | 1.57 | 0.39 | | 37.57 | 3.75 | |
| | C2 | 5 | 61.52 | 475.73 | 1.22 | 0.40 | | 47.81 | 6.23 | |
| | C3 | 11 | 78.63 | 698.53 | 1.05 | 0.40 | | 52.86 | 8.00 | |
| | C4 | 20 | 91.56 | 903.31 | 0.94 | 0.40 | | 55.14 | 9.40 | |
| 2.00E-04 mole/kg D200 + 1.02E-04 mole/kg SIBX | C1 | 2 | 14.87 | 37.31 | 6.60 | 5.48 | | 60.17 | 19.45 | |
| | C2 | 5 | 32.32 | 115.92 | 3.38 | 5.78 | | 66.99 | 44.58 | |
| | C3 | 11 | 52.88 | 242.77 | 2.19 | 4.47 | | 70.90 | 56.41 | |
| | C4 | 20 | 71.14 | 389.85 | 1.68 | 3.53 | | 73.16 | 59.90 | |
| 2.00E-04 mole/kg D200 + 3.07E-04 mole/kg SIBX | C1 | 2 | 17.65 | 64.28 | 6.29 | 3.10 | 9.88 | 62.32 | 13.32 | 28.97 |
| | C2 | 5 | 33.88 | 142.88 | 3.68 | 4.23 | 8.69 | 69.93 | 34.83 | 48.89 |
| | C3 | 11 | 52.26 | 252.33 | 2.50 | 4.06 | 7.61 | 73.42 | 51.63 | 66.06 |
| | C4 | 20 | 70.40 | 396.59 | 1.92 | 3.48 | 6.44 | 75.76 | 59.56 | 75.25 |
| 2.00E-04 mole/kg D200 + 4.09E-04 mole/kg SIBX | C1 | 2 | 20.29 | 84.85 | 4.63 | 3.14 | 10.01 | 59.66 | 16.02 | 32.82 |
| | C2 | 5 | 37.00 | 178.87 | 2.79 | 3.95 | 9.17 | 65.58 | 36.72 | 54.82 |
| | C3 | 11 | 57.34 | 324.13 | 1.91 | 3.70 | 7.76 | 69.47 | 53.38 | 71.93 |
| | C4 | 20 | 75.56 | 488.35 | 1.50 | 3.21 | 6.59 | 71.98 | 60.99 | 80.53 |
| 2.00E-04 mole/kg D200 + 5.12E-04 mole/kg SIBX | C1 | 2 | 22.42 | 100.22 | 4.51 | 2.97 | 7.85 | 61.06 | 16.49 | 29.84 |
| | C2 | 5 | 41.55 | 210.75 | 2.68 | 3.68 | 7.81 | 67.25 | 37.84 | 54.97 |
| | C3 | 11 | 61.72 | 355.50 | 1.90 | 3.61 | 6.85 | 70.82 | 55.07 | 71.66 |
| | C4 | 20 | 81.09 | 532.45 | 1.50 | 3.15 | 5.79 | 73.31 | 63.17 | 79.53 |
| 2.00E-04 mole/kg D200 + 4.09E-04 mole/kg SEX | C1 | 2 | 19.63 | 58.20 | 4.72 | 5.98 | | 59.87 | 28.37 | |
| | C2 | 5 | 38.55 | 156.40 | 2.65 | 5.07 | | 66.05 | 47.24 | |
| | C3 | 11 | 65.49 | 339.51 | 1.66 | 3.71 | | 70.27 | 58.73 | |
| | C4 | 20 | 89.17 | 543.30 | 1.26 | 2.89 | | 72.82 | 62.21 | |

| Flotation Conditions | Sample ID | Time (min) | Cum Mass (g) | Cum Water (g) | Concentrate Grade | | | Recovery (%) | | |
|---|---|---|---|---|---|---|---|---|---|---|
| | | | | | % Cu | % Ni | % S | % Cu | % Ni | % S |
| 6.00E-04 mole/kg D200 + 4.09E-04 mole/kg SIBX | C1 | 2 | 27.71 | 132.51 | 4.09 | 2.93 | | 65.73 | 19.38 | |
| | C2 | 5 | 49.90 | 282.60 | 2.44 | 3.59 | | 70.69 | 42.85 | |
| | C3 | 11 | 70.87 | 463.97 | 1.79 | 3.30 | | 73.53 | 55.87 | |
| | C4 | 20 | 86.83 | 642.96 | 1.49 | 2.96 | | 75.12 | 61.38 | |
| 2.00E-04 mole/kg D200 + 4.09E-04 mole/kg SIBX + 50 g/t Guar | C1 | 2 | 17.34 | 77.56 | 5.31 | 3.10 | 10.20 | 58.57 | 13.32 | 33.24 |
| | C2 | 5 | 33.80 | 173.03 | 3.07 | 4.22 | 8.38 | 66.10 | 35.36 | 53.21 |
| | C3 | 11 | 53.58 | 316.76 | 2.05 | 3.91 | 7.08 | 70.06 | 51.96 | 71.24 |
| | C4 | 20 | 71.62 | 480.60 | 1.59 | 3.34 | 5.92 | 72.61 | 59.33 | 79.70 |
| 2.00E-04 mole/kg D200 + 4.09E-04 mole/kg SIBX + 100 g/t Guar | C1 | 2 | 14.55 | 68.45 | 6.44 | 3.31 | 12.31 | 57.39 | 11.77 | 32.76 |
| | C2 | 5 | 30.33 | 162.83 | 3.60 | 4.56 | 9.44 | 66.82 | 33.77 | 52.37 |
| | C3 | 11 | 50.60 | 311.54 | 2.29 | 4.15 | 7.61 | 71.03 | 51.30 | 70.48 |
| | C4 | 20 | 70.06 | 490.27 | 1.72 | 3.44 | 6.15 | 73.57 | 58.94 | 78.86 |
| 2.00E-04 mole/kg D200 + 4.09E-04 mole/kg SIBX + 500 g/t Guar | C1 | 2 | 21.15 | 142.95 | 3.89 | 5.49 | 12.74 | 55.89 | 28.96 | 48.06 |
| | C2 | 5 | 30.91 | 244.37 | 3.03 | 5.61 | 11.07 | 63.74 | 43.24 | 61.03 |
| | C3 | 11 | 41.38 | 388.21 | 2.40 | 5.04 | 9.67 | 67.62 | 51.99 | 71.42 |
| | C4 | 20 | 50.35 | 533.88 | 2.04 | 4.51 | 8.47 | 69.92 | 56.68 | 76.06 |
| 2.00E-04 mole/kg D200 + 9.62E-05 mole/kg di-E-DTP | C1 | 2 | 28.29 | 163.53 | 3.88 | 1.27 | 5.24 | 63.67 | 8.68 | 24.42 |
| | C2 | 5 | 48.41 | 324.29 | 2.49 | 1.35 | 3.83 | 69.78 | 15.75 | 30.60 |
| | C3 | 11 | 69.72 | 529.96 | 1.81 | 1.37 | 3.17 | 73.20 | 23.12 | 36.49 |
| | C4 | 20 | 85.52 | 706.89 | 1.51 | 1.38 | 2.90 | 74.96 | 28.56 | 40.88 |
| 2.00E-04 mole/kg D200 + 3.07E-04 mole/kg di-E-DTP | C1 | 2 | 37.10 | 231.84 | 3.03 | 1.70 | 4.76 | 65.46 | 15.09 | 28.26 |
| | C2 | 5 | 64.91 | 465.93 | 1.88 | 1.85 | 3.72 | 71.09 | 28.70 | 38.59 |
| | C3 | 11 | 87.90 | 708.02 | 1.45 | 1.86 | 3.34 | 74.03 | 39.23 | 47.03 |
| | C4 | 20 | 105.62 | 939.55 | 1.23 | 1.83 | 3.16 | 75.69 | 46.22 | 53.45 |
| 2.00E-04 mole/kg D200 + 4.09E-04 mole/kg di-E-DTP | C1 | 2 | 36.85 | 229.02 | 3.09 | 1.58 | 4.67 | 65.60 | 14.17 | 27.73 |
| | C2 | 5 | 64.05 | 460.84 | 1.94 | 1.77 | 3.66 | 71.45 | 27.65 | 37.83 |
| | C3 | 11 | 87.75 | 709.41 | 1.47 | 1.82 | 3.29 | 74.49 | 38.87 | 46.49 |
| | C4 | 20 | 105.34 | 936.47 | 1.26 | 1.80 | 3.13 | 76.22 | 46.25 | 53.13 |
| 2.00E-04 mole/kg D200 + 9.62E-05 mole/kg di-E-DTP + 100 g/t Guar | C1 | 2 | 34.41 | 243.96 | 3.18 | 1.26 | 4.06 | 55.05 | 10.27 | 24.26 |
| | C2 | 5 | 52.74 | 418.44 | 2.75 | 1.29 | 3.15 | 72.93 | 16.15 | 28.81 |
| | C3 | 11 | 68.10 | 583.34 | 2.20 | 1.30 | 2.74 | 75.53 | 21.06 | 32.33 |
| | C4 | 20 | 81.01 | 745.73 | 1.89 | 1.31 | 2.52 | 77.10 | 25.16 | 35.48 |

| Flotation Conditions | Sample ID | Time (min) | Cum Mass (g) | Cum Water (g) | Concentrate Grade | | | Recovery (%) | | |
|---|---|---|---|---|---|---|---|---|---|---|
| | | | | | % Cu | % Ni | % S | % Cu | % Ni | % S |
| 2.00E-04 mole/kg D200 + 9.62E-05 mole/kg di-E-DTP + 500 g/t Guar | C1 | 2 | 12.38 | 130.39 | 6.49 | 1.40 | 7.38 | 47.59 | 4.33 | 15.78 |
| | C2 | 5 | 21.02 | 246.20 | 4.78 | 1.58 | 5.99 | 59.40 | 8.27 | 21.72 |
| | C3 | 11 | 30.03 | 389.33 | 3.71 | 1.78 | 5.18 | 65.88 | 13.32 | 26.85 |
| | C4 | 20 | 39.05 | 539.25 | 2.98 | 1.93 | 4.76 | 68.95 | 18.75 | 32.06 |
| 2.00E-04 mole/kg D200 + 3.07E-04 mole/kg di-E-DTP + 100 g/t Guar | C1 | 2 | 49.82 | 322.18 | 2.31 | 1.80 | 4.19 | 66.33 | 21.03 | 33.67 |
| | C2 | 5 | 76.30 | 568.87 | 1.63 | 1.87 | 3.54 | 71.47 | 33.33 | 43.51 |
| | C3 | 11 | 95.95 | 794.45 | 1.34 | 1.86 | 3.27 | 74.33 | 41.82 | 50.61 |
| | C4 | 20 | 110.32 | 985.67 | 1.19 | 1.84 | 3.15 | 75.94 | 47.47 | 56.11 |
| 2.00E-04 mole/kg D200 + 3.07E-04 mole/kg di-E-DTP + 500 g/t Guar | C1 | 2 | 26.93 | 235.64 | 3.21 | 1.48 | 4.80 | 54.05 | 9.90 | 21.56 |
| | C2 | 5 | 41.47 | 425.01 | 2.44 | 1.81 | 4.44 | 63.25 | 18.69 | 30.70 |
| | C3 | 11 | 53.20 | 621.88 | 2.03 | 2.11 | 4.34 | 67.47 | 27.85 | 38.54 |
| | C4 | 20 | 64.00 | 816.59 | 1.75 | 2.23 | 4.28 | 70.16 | 35.46 | 45.72 |
| 2.00E-04 mole/kg D200 + 4.09E-04 mole/kg di-E-DTP + 100 g/t Guar | C1 | 2 | 66.16 | 376.00 | 1.83 | 1.77 | 3.41 | 68.23 | 26.71 | 35.11 |
| | C2 | 5 | 97.94 | 668.21 | 1.33 | 1.81 | 2.91 | 73.48 | 40.36 | 44.42 |
| | C3 | 11 | 120.09 | 927.98 | 1.13 | 1.79 | 2.66 | 76.32 | 48.83 | 49.66 |
| | C4 | 20 | 135.55 | 1137.42 | 1.02 | 1.76 | 2.61 | 77.93 | 54.26 | 55.04 |
| 2.00E-04 mole/kg D200 + 4.09E-04 mole/kg di-E-DTP + 500 g/t Guar | C1 | 2 | 26.20 | 221.73 | 3.53 | 1.38 | 4.65 | 55.00 | 8.74 | 21.31 |
| | C2 | 5 | 38.95 | 393.32 | 2.79 | 1.70 | 3.98 | 64.64 | 15.95 | 27.08 |
| | C3 | 11 | 52.88 | 587.06 | 2.21 | 2.04 | 3.74 | 69.32 | 26.04 | 34.57 |
| | C4 | 20 | 64.36 | 779.12 | 1.88 | 2.16 | 3.66 | 71.82 | 33.62 | 41.15 |
| 2.00E-04 mole/kg di-iso-B-DTP | C1 | 2 | 56.64 | 290.52 | 1.99 | 3.27 | 5.77 | 65.87 | 44.80 | 58.23 |
| | C2 | 5 | 88.18 | 541.73 | 1.39 | 2.68 | 4.70 | 71.71 | 57.06 | 73.89 |
| | C3 | 11 | 109.73 | 764.91 | 1.17 | 2.33 | 4.18 | 74.76 | 61.78 | 81.77 |
| | C4 | 20 | 123.24 | 946.71 | 1.06 | 2.13 | 3.87 | 76.37 | 63.41 | 84.90 |
| 2.00E-04 mole/kg D200 + 7.52E-05 mole/kg di-iso-B-DTP | C1 | 2 | 43.62 | 251.91 | 2.54 | 3.91 | 7.47 | 65.40 | 39.37 | 51.31 |
| | C2 | 5 | 77.22 | 516.83 | 1.57 | 2.99 | 5.63 | 71.25 | 53.31 | 68.48 |
| | C3 | 11 | 104.54 | 790.33 | 1.21 | 2.52 | 4.66 | 74.64 | 60.91 | 76.62 |
| | C4 | 20 | 122.16 | 1014.57 | 1.06 | 2.30 | 4.21 | 76.53 | 65.00 | 81.04 |
| 2.00E-04 mole/kg D200 + 1.02E-04 mole/kg [SIBX + di-E-DTP]; 76 % SIBX, 24 % di-E-DTP | C1 | 2 | 22.31 | 78.46 | 4.41 | 5.65 | | 62.11 | 30.35 | |
| | C2 | 5 | 43.06 | 199.99 | 2.51 | 4.85 | | 68.19 | 50.32 | |
| | C3 | 11 | 67.08 | 350.84 | 1.70 | 3.70 | | 71.84 | 59.81 | |
| | C4 | 20 | 88.20 | 577.19 | 1.33 | 2.95 | | 74.00 | 62.71 | |

| Flotation Conditions | Sample ID | Time (min) | Cum Mass (g) | Cum Water (g) | Concentrate Grade | | | Recovery (%) | | |
|---|---|---|---|---|---|---|---|---|---|---|
| | | | | | % Cu | % Ni | % S | % Cu | % Ni | % S |
| 2.00E-04 mole/kg D200 + 4.09E-04 mole/kg [SIBX + di-E-DTP]; 90 % SIBX, 10 % di-E-DTP | C1 | 2 | 14.78 | 52.02 | 6.64 | 2.69 | 9.96 | 58.41 | 9.53 | 28.69 |
| | C2 | 5 | 31.01 | 131.32 | 3.64 | 4.24 | 7.73 | 67.14 | 31.56 | 46.69 |
| | C3 | 11 | 51.27 | 259.50 | 2.34 | 4.08 | 7.26 | 71.28 | 50.15 | 72.58 |
| | C4 | 20 | 69.38 | 409.53 | 1.79 | 3.48 | 6.10 | 73.74 | 57.92 | 82.46 |
| 1.60E-04 mole/kg D200 + 3.07E-04 mole/kg SIBX + 4.00E-05 mole/kg di-E-DTP | C1 | 2 | 11.57 | 29.92 | 8.53 | 2.50 | | 56.67 | 6.77 | |
| | C2 | 5 | 24.52 | 79.70 | 4.72 | 4.61 | | 66.42 | 26.40 | |
| | C3 | 11 | 41.80 | 163.23 | 2.95 | 4.97 | | 70.76 | 48.54 | |
| | C4 | 20 | 58.79 | 269.83 | 2.17 | 4.20 | | 73.43 | 57.61 | |
| 2.00E-04mole/kg D200 + 4.57E-04 mole/kg [SIBX + di-E-DTP]; 89 % SIBX, 11 % di-E-DTP | C1 | 2 | 18.05 | 67.74 | 5.68 | 2.91 | 8.91 | 61.50 | 12.80 | 30.76 |
| | C2 | 5 | 35.92 | 161.18 | 3.14 | 4.21 | 7.40 | 67.58 | 34.83 | 50.82 |
| | C3 | 11 | 57.56 | 305.76 | 2.07 | 3.99 | 6.19 | 71.44 | 51.78 | 68.21 |
| | C4 | 20 | 75.73 | 463.35 | 1.62 | 3.42 | 5.32 | 73.74 | 59.05 | 77.07 |
| 2.00E-04 mole/kg D200 + 4.09E-04 mole/kg [SIBX + di-E-DTP]; 85 % SIBX, 15 % di-E-DTP | C1 | 2 | 18.25 | 70.24 | 5.50 | 2.88 | 9.16 | 60.28 | 12.48 | 32.99 |
| | C2 | 5 | 37.28 | 173.08 | 3.04 | 4.05 | 7.22 | 68.07 | 35.86 | 53.15 |
| | C3 | 11 | 59.90 | 331.02 | 2.00 | 3.65 | 6.26 | 72.11 | 51.94 | 74.02 |
| | C4 | 20 | 79.31 | 506.40 | 1.56 | 3.13 | 5.27 | 74.20 | 59.10 | 82.54 |
| 2.00E-04 mole/kg D200 + 3.49E-04 mole/kg [SIBX + di-E-DTP]; 59 % SIBX, 41 % di-E-DTP | C1 | 2 | 18.76 | 70.83 | 5.92 | 3.07 | 9.29 | 64.47 | 13.99 | 31.54 |
| | C2 | 5 | 38.98 | 179.78 | 3.10 | 4.18 | 7.99 | 70.13 | 39.55 | 56.37 |
| | C3 | 11 | 62.80 | 349.59 | 2.03 | 3.53 | 6.38 | 74.04 | 53.88 | 72.50 |
| | C4 | 20 | 81.56 | 519.16 | 1.60 | 3.01 | 5.31 | 75.98 | 59.65 | 78.48 |
| 2.00E-05 mole/kg D200 + 4.09E-04 mole/kg [SEX + di-E-DTP]; 76 % SEX, 24 % di-E-DTP | C1 | 2 | 21.84 | 78.07 | 4.42 | 5.60 | 11.59 | 61.99 | 28.62 | 52.00 |
| | C2 | 5 | 44.01 | 176.62 | 2.37 | 4.20 | 6.94 | 66.87 | 43.29 | 62.74 |
| | C3 | 11 | 65.58 | 355.90 | 1.70 | 3.65 | 6.05 | 71.46 | 55.97 | 81.55 |
| | C4 | 20 | 89.12 | 566.07 | 1.29 | 2.98 | 4.87 | 73.76 | 62.21 | 89.11 |
| 2.00E-04 mole/kg D200 + 4.09E-04 mole/kg [SIBX + di-E-DTP]; 76 % SIBX, 24 % di-E-DTP | C1 | 2 | 23.89 | 109.11 | 4.19 | 3.16 | 8.62 | 62.52 | 18.66 | 33.61 |
| | C2 | 5 | 45.10 | 243.24 | 2.43 | 3.61 | 7.81 | 68.33 | 40.30 | 57.50 |
| | C3 | 11 | 66.67 | 413.08 | 1.72 | 3.28 | 6.55 | 71.77 | 54.07 | 71.36 |
| | C4 | 20 | 86.32 | 594.95 | 1.37 | 2.86 | 5.57 | 74.08 | 61.04 | 78.52 |
| 6.00E-04 mole/kg D200 + 4.09E-04 mole/kg [SIBX + di-E-DTP]; 76 % SIBX, 24 % di-E-DTP | C1 | 2 | 28.11 | 136.87 | 3.91 | 2.97 | | 64.83 | 19.71 | |
| | C2 | 5 | 49.76 | 282.05 | 2.38 | 3.69 | | 69.79 | 43.45 | |
| | C3 | 11 | 70.05 | 454.19 | 1.76 | 3.37 | | 72.68 | 55.78 | |
| | C4 | 20 | 85.62 | 625.89 | 1.47 | 3.02 | | 74.32 | 61.09 | |

| Flotation Conditions | Sample ID | Time (min) | Cum Mass (g) | Cum Water (g) | Concentrate Grade | | | Recovery (%) | | |
|---|---|---|---|---|---|---|---|---|---|---|
| | | | | | % Cu | % Ni | % S | % Cu | % Ni | % S |
| 2.00E-04 mole/kg D200 + 3.82E-04 mole/kg [SIBX + di-iso-B-DTP], 80 % SIBX, 20 % di-iso-B-DTP | C1 | 2 | 48.60 | 272.07 | 2.43 | 2.42 | 7.48 | 66.78 | 26.91 | 55.07 |
| | C2 | 5 | 81.36 | 511.77 | 1.57 | 2.59 | 6.48 | 72.10 | 48.06 | 79.89 |
| | C3 | 11 | 106.95 | 760.10 | 1.24 | 2.43 | 5.61 | 75.09 | 59.27 | 90.88 |
| | C4 | 20 | 125.23 | 980.97 | 1.09 | 2.26 | 5.01 | 76.95 | 64.53 | 95.18 |
| 2.00E-04 mole/kg D200 + 4.09E-04 mole/kg [SIBX + di-E-DTP] + 100 g/t Guar; 76 % SIBX, 24 % di-E-DTP | C1 | 2 | 16.88 | 71.86 | 5.11 | 3.59 | 11.91 | 57.53 | 15.05 | 37.49 |
| | C2 | 5 | 34.36 | 188.51 | 2.83 | 4.44 | 8.95 | 64.80 | 37.92 | 57.37 |
| | C3 | 11 | 56.68 | 365.18 | 1.83 | 3.76 | 7.08 | 69.28 | 52.99 | 74.88 |
| | C4 | 20 | 77.05 | 562.07 | 1.40 | 3.13 | 5.65 | 71.95 | 59.95 | 81.22 |
| 2.00E-04 mole/kg D200 + 4.09E-04 mole/kg [SIBX + di-E-DTP] + 500 g/t Guar; 76 % SIBX, 24 % di-E-DTP | C1 | 2 | 17.78 | 109.32 | 5.51 | 7.15 | 13.72 | 52.66 | 26.77 | 46.61 |
| | C2 | 5 | 29.21 | 217.15 | 3.96 | 7.29 | 11.62 | 62.12 | 44.83 | 64.85 |
| | C3 | 11 | 39.83 | 354.64 | 3.09 | 6.47 | 10.25 | 66.20 | 54.26 | 78.03 |
| | C4 | 20 | 49.81 | 506.96 | 2.56 | 5.67 | 8.77 | 68.65 | 59.51 | 83.47 |
| 2.00E-04 mole/kg D200 + 4.09E-04 mole/kg [SIBX + di-E-DTP]; 76 % SIBX, 24 % di-E-DTP; DTP added ahead of SIBX | C1 | 2 | 15.75 | 55.88 | 6.37 | 2.78 | 9.61 | 59.57 | 10.49 | 31.05 |
| | C2 | 5 | 32.79 | 141.50 | 3.48 | 4.20 | 7.53 | 67.74 | 32.98 | 50.64 |
| | C3 | 11 | 52.69 | 268.64 | 2.29 | 4.07 | 6.73 | 71.63 | 51.43 | 72.68 |
| | C4 | 20 | 71.71 | 428.57 | 1.74 | 3.45 | 5.63 | 74.17 | 59.26 | 82.85 |
| 2.00E-04 mole/kg D200 + 3.82E-04 mole/kg [SIBX + di-iso-B-DTP], 80 % SIBX, 20 % di-iso-B-DTP; DTP added ahead of SIBX | C1 | 2 | 47.42 | 272.17 | 2.27 | 2.15 | 2.93 | 65.17 | 24.87 | 31.78 |
| | C2 | 5 | 77.92 | 503.24 | 1.49 | 2.39 | 3.56 | 70.39 | 45.38 | 63.31 |
| | C3 | 11 | 100.86 | 734.10 | 1.20 | 2.35 | 3.40 | 73.22 | 57.75 | 78.34 |
| | C4 | 20 | 119.68 | 964.70 | 1.04 | 2.19 | 3.12 | 75.21 | 63.77 | 85.31 |

# Appendix E – The Effect of di-iso-butyl DTP/Dowfroth 200 Mixtures on Flotation Performance

## E1: Two-phase Froth Column Test Results

Two-phase froth column tests involving mixtures of di-iso-butyl DTP and Dowfroth 200, at a constant total dosage but different molar mixtures have shown that the froth stability parameter, i.e. froth height, was significantly influenced by the proportion of di-iso-butyl DTP in the mixture. In fact, the relationship between the proportion of di-iso-butyl DTP in the mixture and froth height, as is shown in Figure E1, appeared to be one which is typical of synergism. Figure E1 shows for example that a [60 % Dowfroth 200 + 40 % di-iso-butyl DTP] reagent mixture, at a fix total reagent dosage of 8.00E-05 mole per 400 ml of distilled water (or 2.00E-04 mole/l), resulted in significant reduction in froth height compared to pure frother.



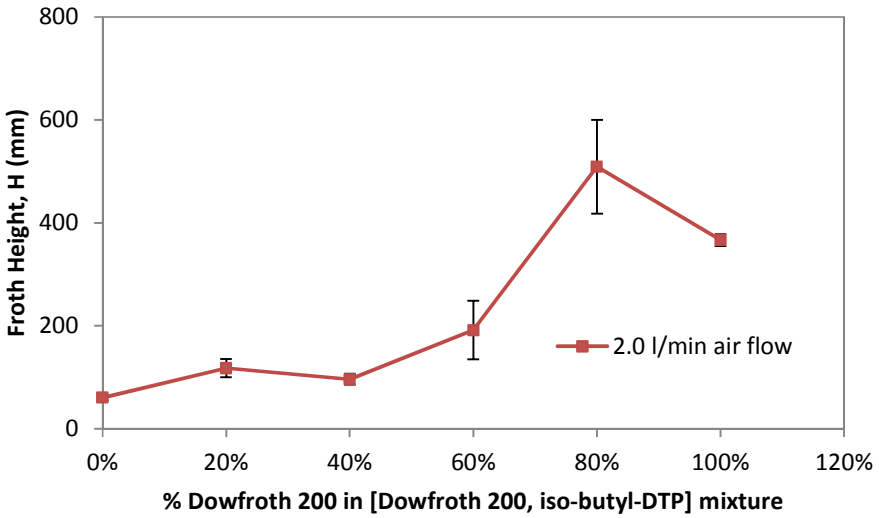


**Figure E1: The effect of the proportion of di-iso-butyl DTP in [Dowfroth 200 + di-iso-butyl DTP] mixtures on froth height in a two-phase froth column**

This was considered to be a significant result because one of the reasons for excluding di-iso-butyl DTP from the original scope of work in the first place was that excessive and uncontrollable froths are produced. However, if a stable froth can be produced by fine-tuning the di-iso-butyl DTP/frother mixture, then the di-iso-butyl DTP-frother mixture may result in enhanced flotation performance compared to diethyl DTP. Another reason however for excluding di-iso-butyl DTP from the original scope of work was that it contains a fair amount of unknown chemical components and thus it would be impossible to determine if the measured performance can be attributed to the DTP component or the unknown impurities of the reagent.

## E2: Batch Flotation Experiments

Batch flotation experiments were conducted using mixtures of di-iso-butyl DTP and Dowfroth 200 and the results are reported in this section. It is perhaps important to note here that, because di-iso-butyl DTP exhibits both collecting and frothing properties, designing a set of experiments to test a specific hypothesis was very difficult because both the pulp and froth phases are influenced simultaneously. The best experimental approach was considered to maintain the total molar concentration of Dow 200 frother and di-iso-butyl DTP constant and vary the contribution of each. The problem with this experimental approach is that, if you reduce the DTP component mixture for example, then you change both the frothing and collecting properties of the mixture. The tests are therefore, strictly speaking, not comparable. Nevertheless, the ultimate aim of the experiments conducted here was to establish if a controllable froth can be produced with di-iso-butyl DTP without sacrificing copper and nickel recoveries and grades.



### E2.1 Mass and Water Recovery

Figure E2 shows the water recovery obtained when various mixtures of Dowfroth 200 and di-iso-butyl DTP tested in batch flotation test results. This pattern is distinctly similar to that which was obtained with froth height experiments (cf. Figure E1). This indicates that perhaps a frother-collector interaction between DTP and Dowfroth 200 has resulted in significant variation in water recovery.

Figure E3 shows that very significant differences in mass pull and water recovery were obtained if the total dosage of frother and di-iso-butyl DTP is minimised, i.e. the frothing effect obtained in a flotation system involving di-iso-butyl DTP and frother cannot be attributed to the frother only. Figure E3 also shows that, if equivalent molar dosages are compared, then the di-iso-butyl DTP is in fact a much stronger frother than Dowfroth 200. This implies that one cannot view the two reagents as independent and mutually exclusive.

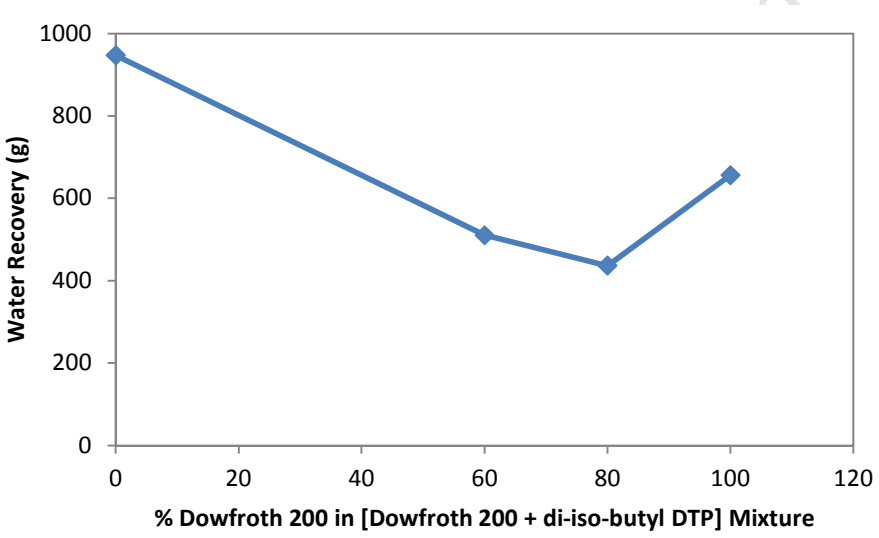


**Figure E2: The effect of the proportion of di-iso-butyl DTP in [Dowfroth 200 + di-iso-butyl DTP] mixtures on water recovery in batch flotation tests**

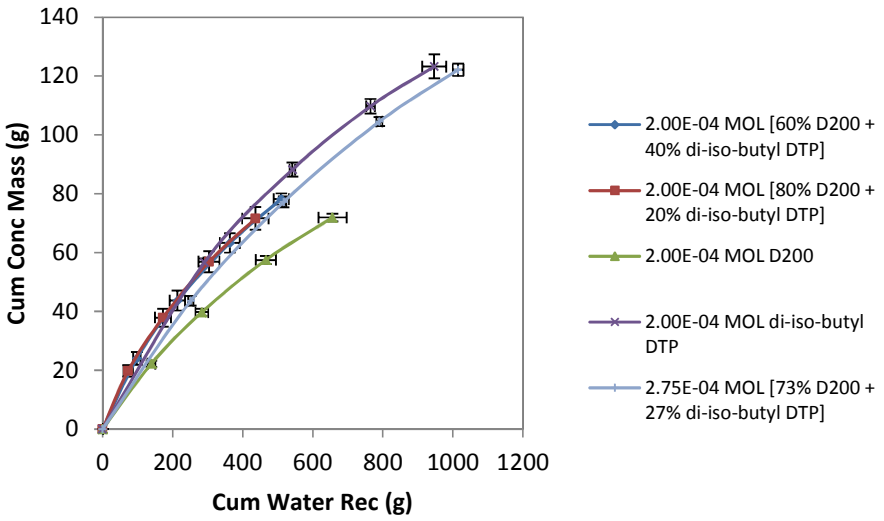


**Figure E3: Concentrate mass pull as a function of water recovery for the various mixtures of di-iso-butyl DTP and Dowfroth 200**



## E2.2 Copper & Nickel Recovery

Figure E4 shows the effect of various ratios of frother and DTP on copper recovery which is represented as a function of water recovery. This figure clearly shows that the final copper recovery which was obtained was essentially unaffected by reagent type or dosage; instead, the final copper recovery was principally determined by the extent of water recovered. It is however interesting to note that Figure E4 shows that, in the initial stages of flotation at least, much more copper per unit mass water was recovered for the conditions in which the total dosage of frother and di-iso-butyl DTP is minimised compared to the other conditions where the frother and DTP were viewed as independent and mutually exclusive reagents. Furthermore, when the frother was removed and only di-iso-butyl DTP was present, then a significantly less amount of copper was recovered per unit of mass water compared to when frother was present. This suggests that performance was optimal in the presence of frother.

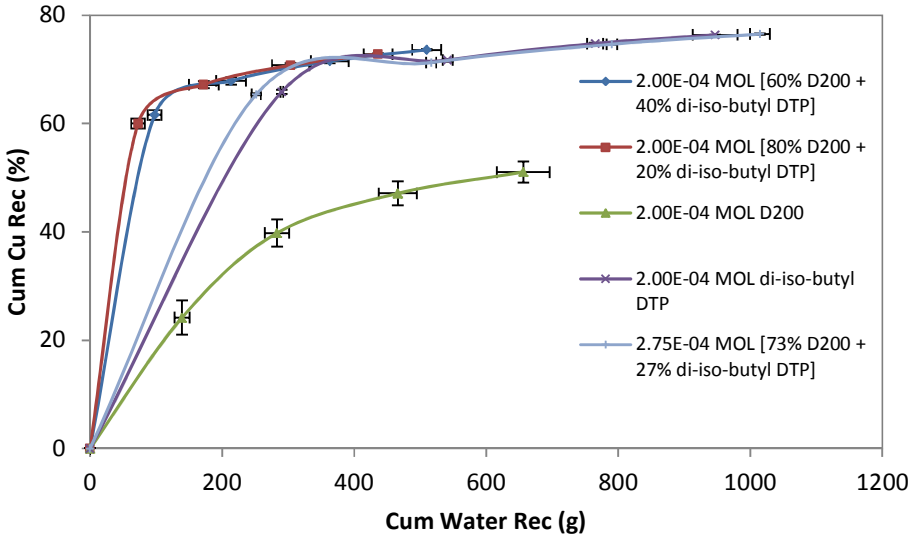


**Figure E4: The effect of water recovery on copper recovery for various mixtures of di-iso-butyl DTP and Dowfroth 200**

Figure E5 shows the effect of various ratios of frother and DTP on nickel recovery which is represented as a function of water recovery. This figure clearly shows that the nickel recovery was significantly affected by the ratio of Dow 200 frother to DTP as well as the total molar dosage of both reagents. The 2.00E-04 mole/kg mixtures of Dow 200 frother and di-iso-butyl DTP recovered a significantly higher amount of nickel per unit mass of water compared to all the other tests. Figure E5 also show that the ratio of frother to di-iso-butyl DTP is important – when the mixtures [80% frother, 20% di-iso-butyl DTP] and [60% frother, 40% di-iso-butyl DTP] are compared then it can be seen that the former mixture has resulted in a very sudden drop off in nickel recovered per unit mass of water at the end of the test which reduced total recovery, i.e. there was no enough froth present towards the end of the test in order to carry the minerals.

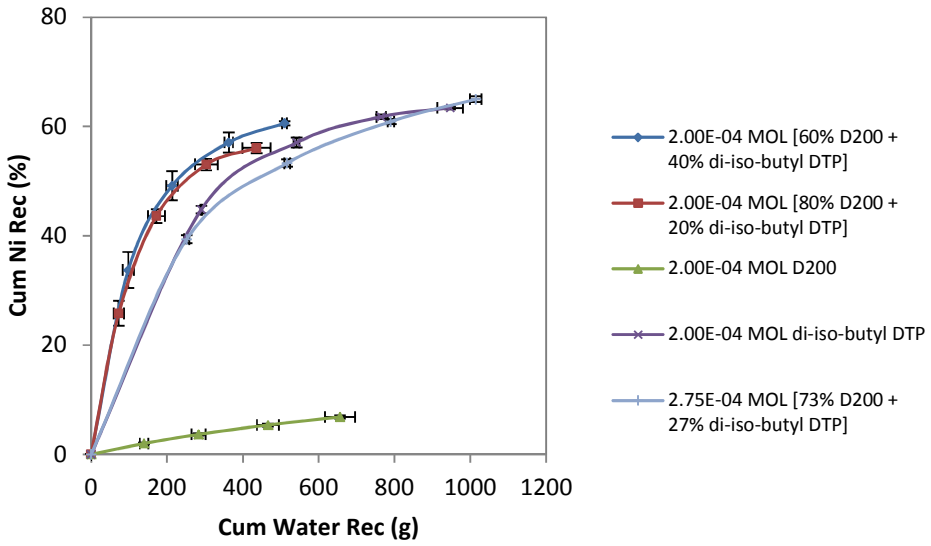


**Figure E5: The effect of water recovery on nickel recovery for various mixtures of di-iso-butyl DTP and Dowfroth 200**



## E2.3 Grade/Recovery Relationship

Figure E6 shows the effect of mixtures of frother and DTP on copper grade and recovery. This figure shows that copper recovery was essentially unaffected by reagent type or dosage. However, Figure E6 also shows that the different combination of frothers and DTP has resulted in significant differences in concentrate grade which is an important result. Figure E7 shows the effect of mixtures of frother and DTP on nickel grade and recovery. This figure shows that, unlike as was the case with copper, nickel performance was significantly influenced by the ratio of frother to DTP. A higher ratio of frother compared to di-iso-butyl dTP has resulted in higher concentrate grades.

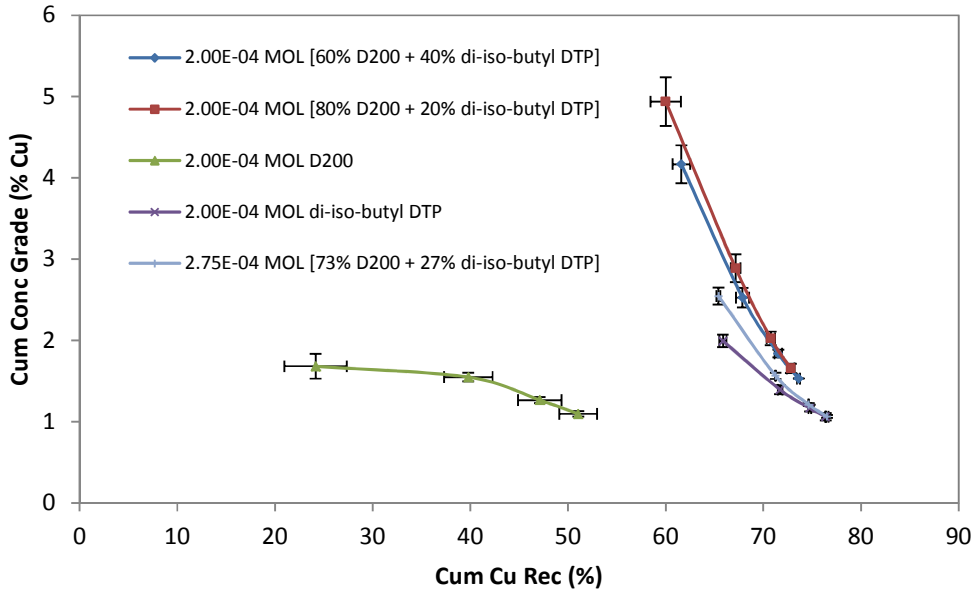


**Figure E6: The copper grade-recovery curves for [di-iso-butyl DTP; Dowfroth 200] mixture tests**

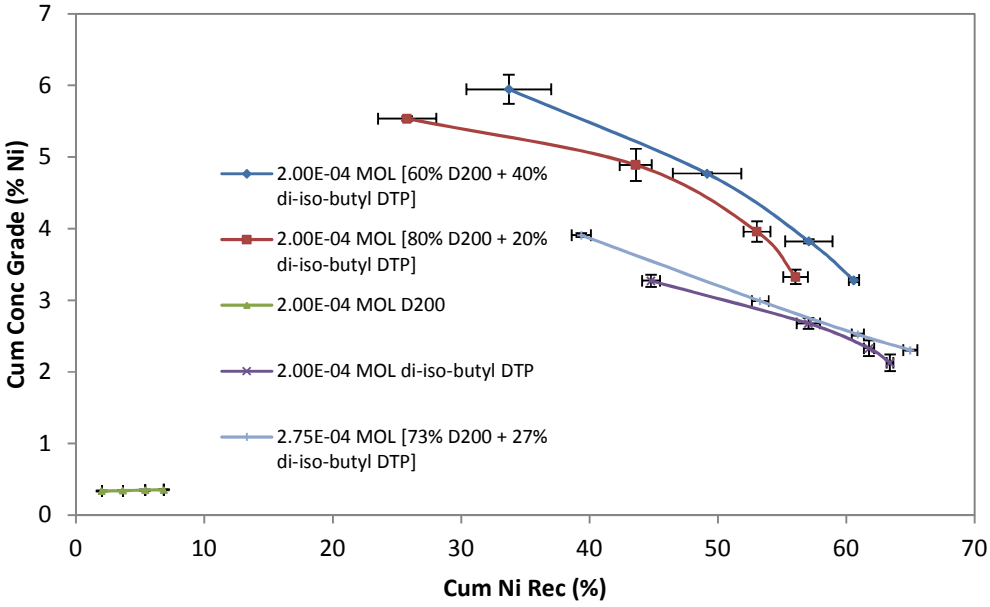


**Figure E7: The nickel grade-recovery curves for [di-iso-butyl DTP; Dowfroth 200] tests**

## E2.4 Kinetic Analysis of Flotation Results

Table E1, in combination with Figures E2 – E7, confirms that the di-iso-butyl DTP is a good flotation collector and, in fact, performed as well as the xanthates with regard to copper and nickel recovery. In addition, the reagent had the ability to interact with frother so that the total dosage of frother and collector was significantly less than was the case with the xanthates – without sacrificing froth stability that is. However, Table 4.19 also indicates that the xanthate tests have significantly higher nickel $R_{inf}$ values as compared to the frother-DTP tests. This may be an important finding which suggests that the best result may be obtained with mixtures of di-isobutyl DTP and xanthate rather than di-iso-butyl DTP alone.

**Table E1: The first order rate constant and infinite time recovery values for mixtures of di-iso-butyl DTP and Dowfroth 200**

| Reagent Suite | Max Cu Rec (%) | | Max Ni Rec (%) | | Rate Constant ($min^{-1}$) | |
|---|---|---|---|---|---|---|
| | Actual | $R_{inf}$ | Actual | $R_{inf}$ | Cu | Ni |
| 2.00E-04 mole/kg di-iso-B DTP | 76.4 ± 0.0 | 76.9 ± 0.1 | 63.4 ± 0.3 | 65.7 ± 0.3 | 3.4 ± 0.1 | 1.5 ± 0.1 |
| 2.00E-04 mole/kg [D200 + di-iso-B DTP], 80% D200 | 72.8 ± 0.4 | 73.5 ± 0.1 | 56.1 ± 1.0 | 61.5 ± 0.1 | 2.6 ± 0.3 | 0.6 ± 0.1 |
| 2.00E-04 mole/kg [D200 + di-iso-B DTP], 60% D200 | 73.6 ± 0.2 | 74.0 ± 0.2 | 60.6 ± 0.4 | 65.3 ± 0.4 | 2.9 ± 0.2 | 0.7 ± 0.2 |
| 2.00E-04 MOL D200 | 51.0 ± 1.9 | 55.1 ± 2.3 | 6.9 ± 0.3 | 8.3 ± 0.3 | 0.7 ± 0.2 | 0.3 ± 0.0 |
| 2.75E-05 mole/kg [D200 + di-iso-B- DTP], 73% D200 | 76.5 ± 0.1 | 77.0 ± 0.1 | 65.0 ± 0.6 | 67.4 ± 0.4 | 3.2 ± 0.0 | 1.0 ± 0.0 |